Harris, Christopher Mark

CHARACTERISTICS OF FIXATIONS IN HUMAN INFANTS

City University of New York PH.D. 1986

PLEASE NOTE:

In all cases this material has been filmed in the best possible way from the available copy. Problems encountered with this document have been identified here with a check mark __✓__.

1. Glossy photographs or pages _____
2. Colored illustrations, paper or print _____
3. Photographs with dark background _____
4. Illustrations are poor copy _____
5. Pages with black marks, not original copy _____
6. Print shows through as there is text on both sides of page _____
7. Indistinct, broken or small print on several pages ✓
8. Print exceeds margin requirements _____
9. Tightly bound copy with print lost in spine _____
10. Computer printout pages with indistinct print _____
11. Page(s) _____ lacking when material received, and not available from school or author.
12. Page(s) _____ seem to be missing in numbering only as text follows.
13. Two pages numbered _____. Text follows.
14. Curling and wrinkled pages _____
15. Dissertation contains pages with print at a slant, filmed as received ✓
16. Other _____

_____

_____

CHARACTERISTICS OF FIXATIONS IN HUMAN INFANTS

by

Christopher M. Harris

A dissertation submitted to the Graduate Faculty in Psychology in partial fulfillment of the requirements for the degree of Doctor of Philosophy, The City University of New York.

1986

This manuscript has been read and accepted for the Graduate Faculty in Psychology in satisfaction of the dissertation requirement for the degree of Doctor of Philosophy.

8/19/86
date

Louise Hainline
Chair of Examining Committee

August 21, 1986
date

Herbert D. Saltzstein
Executive Officer

Dr. Louise Hainline

Dr. Israel Abramov

Dr. David H. Raab

Dr. Josh Wallman

Dr. Larry Abel

Supervisory Committee

The City University of New York

Abstract

Characteristics of Fixations in Human Infants

by

Christopher M. Harris

Advisers: Professors Louise Hainline & Israel Abramov

When we freely view a scene, our eyes move in a sequence of saccades and fixations. Only during fixations, when the eyes are relatively stationary, is most (if not all) visual information acquired. Consequently, it is widely believed that fixations represent processing time and are driven by perceptual and/or cognitive processes. This view is disputed here, and instead, it is argued that visual scanning is basically a reflexive behavior.

Eye movements were recorded from 200 infants and 11 adults using a TV-based infrared corneal eye tracker. All records were manually parsed to isolate fixations and saccades.

It is shown that fixation duration is distributed exponentially for all subjects. The exponential is a basic waiting-time distribution and it is deduced that fixations are terminated by saccades triggered randomly in time by a memoryless mechanism. It is also found that the likelihood of a saccade increases with stimulus size. Thus, fixation termination is influenced by stimulating the peripheral retina rather than the fovea.

A "multiple target model" is proposed in which saccades are triggered by targets in the entire visual field with constant probability

per unit time. This exogenous process is Markovian and a theoretical treatment makes quantitative predictions which are corroborated by other studies.

It is then shown that the likelihood of a saccade increases with the rate of drift of the eye during a fixation. This is because of the increased saliency of visual targets when they drift across the retina. The occurrence of saccades also increases as arousal level of infants increases, as measured by the speed of saccades. The effect of state is incorporated into the model.

It is concluded that, while free-viewing, fixation duration is determined by the occurrence of saccades which are triggered by the stimulus at the level of the retina - not at higher levels of the brain.

Although this reflexive model is a radical departure from the current cognitive view, it is conceptually simple and testable. It makes a strong distinction between looking (directing gaze) and seeing (acquiring information). The ramifications of this distinction are discussed with respect to methodologies used to assess the infant visual system.

In Memory Of

Wilfred Harris

I acknowledge gratefully the following for providing assistance and the motivation to complete this work:

Larry Abel

Israel Abramov

Cheryl Camenzuli

Louise Hainline

Elizabeth Lemerise

Dave Raab

Henry Smith

Josh Wallman

Virginia & Cassandra

TABLE OF CONTENTS

1 INTRODUCTION 1
1.1 Adult Visual Scanning 1
1.2 Infant Visual Scanning 3
1.3 Basic Approach 6
1.4 Preview 12

2 METHOD AND METHODOLOGICAL ISSUES 15
2.1 Apparatus 15
Infrared Source 18
Video Camera 21
Subject Placement 21
Eye Tracker's Detection Algorithm 22
2.2 System Response 23
Linearity 24
Static Calibration 25
Dynamic Calibration 27
Noise 28
2.3 Subjects 28
2.4 Stimulus Conditions 28
2.5 Procedures 30
2.6 Analysis 31
Interactive Parsing Program 33

3 RESULTS AND DISCUSSIONS 37
3.1 Fixational and Drift Segments 37
3.2 Multiple Segments 42
3.3 Fixation Parameters 44

4 DURATION 46
4.1 Errors in Measuring Duration of Fixations 47
4.2 Stimulus Dependence 48
4.3 Distribution Identification by the Method of Moments 54
4.4 The Exponential Distribution 66
4.5 Departures From Exponentiality 71
4.6 Compound Exponential - Fluctuations in the B-period . . . 73
4.7 Fluctuations in the A-period 78
4.8 Discussion 78
The CPU Model 85
The Multiple Target Model 87
Spontaneous Saccade Model 88
Distinguishing Among Models 89

5 STIMULUS SIZE EFFECTS 90
5.1 Stimulus Size and FS Duration (Adults) 91
5.2 Stimulus Size, Breadth of Scan and Saccadic Amplitude (Adults) 92
5.3 The Multiple Target Model in Adults 95
Non-stationarity of Fixation Duration 103

Pre-emption and Eminency 105
Scanning Patterns and Markov Sequences 106
Scanning Homogenous Visual Scenes 112
Beyond Reflexive Scanning 125
5.4 Stimulus Size Effects with Infants 131

6 AMPLITUDE AND RATE OF DRIFT DURING FIXATIONS 139
Instrument Limitations in Measuring Drift Rate 140
6.1 Drift Amplitude and Bias 140
Drift Amplitude is the Product of Two Random Variables 144
Estimation of Drift Bias 153
6.2 Dependence Between Drift Rate and Duration 159
(i) Drift Rate Affected By Duration? 171
(ii) Duration Affected By Drift Rate? 171
(iii) Drift Rate and Duration are Determined By Other Variable(s)? 174
Summary 175

7 AROUSAL AND FIXATION DURATION IN INFANTS 179
7.1 The Main Sequence as a Measure of Arousal 180
Physiology of Peak Velocity 181
The Main Sequence in Infants 184
7.2 Dependence Between Fixation Duration and Main Sequence 185
Fatigue 191
Stimulus Effects on Arousal 194
7.3 Effects of Arousal on Fixation Duration 196
7.4 A Model of Infant Fixation Duration 198
a) Saccadic Trigger Level Modulated By Arousal 200
b) Overall Stimulus Saliency Modulated By Arousal . . . 203

8 SUMMARY AND DISCUSSION 205
8.1 Summary 205
8.2 Visual Scanning in Infants 208
8.3 Preferential Looking and Visual Perimetry 210
Preferential Looking in the Infant 210
The Visual Field in Infants 217
8.4 Conclusions 218

Appendices

A DIOPTRICS OF THE EYE TRACKER 221
A.1 First Purkinje Image 222
A.2 Position of the Centre of Pupil 228
A.3 Summary 232
A.4 References 232

B INSTRUMENT CONSIDERATIONS IN MEASURING FAST EYE MOVEMENTS 233

C ARTIFICIAL EYE FOR ASSESSING THE EYE TRACKER 243

D COMBINING SUBJECT MEANS 245
D.1 References 250

E MOMENTS 251
E.1 Definitions 251
E.2 Identifying a Distribution by its Moments 253
E.3 Estimating Moments 257
E.4 Moments of the Sum of Two Random Variables 258
E.5 Moments of the Product of Two Random Variables 259
E.6 References 260

F THE EXPONENTIAL WAITING-TIME DISTRIBUTION 261
F.1 Waiting-Time Distributions 261
F.2 The Exponential Distribution 263
F.3 Moments of the Exponential Distribution 263
F.4 Compound Exponential Distributions 265
The Gamma-Exponential Compound 267
The Rectangular-Exponential Compound 268
F.5 References 269

G STATISTICS OF VECTOR MAGNITUDE 270
G.1 References 273

H CHARACTERISTICS OF SACCADES IN THE HUMAN INFANT . 274

References

REFERENCES 284

LIST OF TABLES

1. Comparison of observed moments to moments of theoretical compound Exponential distributions. 77

LIST OF FIGURES

1. Arrangement of major components of the eye-tracker. 17

2. The optical components of the eye-tracker. 20

3. Example of a parsed eye movement record. 36

4. Examples of eye movement records showing drift. 39

5. Frequency histograms of durations of "Fixations" and "Drifts." 41

6. Mean fixation durations for different stimulus conditions. . . 50

7. Frequency distribution of mean durations of all infants. . . 53

8. Standard deviation vs. the mean of fixation duration for infants. 56

9. Third root moment vs. standard deviation of fixation duration for infants. 61

10. Fourth root moment vs. standard deviation of fixation duration for infants. 63

11. Plots of root moments of fixation duration for free-viewing adults. 65

12. The theoretical Exponential distribution. 70

13. A typical sequence of fixation durations showing non-stationarity as evidence for a compound Exponential. 75

14. The "Pareto" distribution - an example of a compound Exponential. 80

15. Effect of stimulus size on adult fixation duration. 94

16. Effect of stimulus size on mean saccade magnitude from adults. 97

17. Effect of stimulus size on the breadth of scan of adults. . . 99

18. Configuration of Markov matrices to describe free-viewing. 110

19. Comparison of distribution of saccade magnitude between model's prediction and other data. 117

20. Comparison of model's prediction of mean saccade magnitude with other data. 120

21. Model's prediction of fixation duration compared to other data. 124

22. Effect of stimulus size on infant fixation duration. 133

23. Effect of stimulus size on infant mean saccade magnitude. 135

24. Effect of stimulus size on infant breadth of scan. 137

25. Scatter plot of mean drift amplitude components (Cartesian) for infants. 143

26. Plot of the standard deviation against the mean of drift amplitude for infants. 146

27. Plot of the third root moment against the mean of drift amplitude for infants. 149

28. Plot of the third root moment against the standard deviation of drift amplitude for infants. 151

29. Plot of the standard deviation of drift amplitude against the mean of fixation duration for infants. 156

30. Plot of the third root moment of drift amplitude against the mean of fixation duration for infants. 158

31. Plot of mean drift magnitude grouped by fixation duration for textures and negative shape stimuli. 164

32. Plot of mean drift magnitude grouped by fixation duration for complex scenes and the single target stimuli. 166

33. Plot of mean drift magnitude grouped by fixation duration for the bar with sounds infant stimulus conditions. . . 168

34. Plot of mean drift magnitude grouped by fixation duration for free-viewing adults. 170

35. Plot of mean FS duration vs. Main Sequence slope for different infant stimulus conditions. 187

36. Plot of mean AISI duration vs. Main Sequence slope. . . 190

37. Plot of mean saccade magnitude vs. Main Sequence slope. 193

38. Hypothetical relationship among saliency, fixation

duration, and saccade trigger level. 202

INTRODUCTION

When we view an everyday scene, our eyes move haphazardly over the scene in a sequence of steady gazes ("fixations") and fast flicks ("saccades"). It is generally believed that information is gathered by the visual system during fixations, when the images on the retinas are stable; and little or no information is gathered during saccades when the images are blurred from their motion across the retinas. Saccades quickly redirect the central part of the retina, which has better resolution than the peripheral retina, to different features of the visual scene. It is as if the eye were taking a sequence of "snapshots" of different parts of the visual scene. This behaviour is called "visual scanning."

1.1 Adult Visual Scanning

We are very active in visually scanning our environment and we make about two saccades (or fixations) per second, or about 100,000 saccades per day. We can slow down this rate when we "pay attention" to an object, or we can speed it up when, for example, we read. Although in special circumstances, we can control our eye movements voluntarily, we are usually unaware of our eye movements and visual scanning seems to be an automatic process. As adults, we

are heavily dependent on vision and it is often thought that visual scanning plays an integral role in visual perception. Indeed, our everyday experience tells us that we point our eyes at an object in order to see it, and it takes considerable conscious effort to overcome this reflex when, for example, we have to look to the side of on an object in low illumination in order to see it. It is, therefore, understandable to consider "looking" and "seeing" as a unitary function of perception. However, we shall make the distinction between "looking" as an oculomotor process of directing the eye (usually by a saccade), and "seeing" as the acquisition of visual information (during fixations).

An early approach to understanding visual scanning was virtually to subjugate visual perception to motor behaviour, as embodied in the theories of Hebb (1949). It has been contended that the actual sequence of eye positions during visual scanning of an object is the neural representation of that object in the brain. This idea has had a few protagonists who have tried to show that the eye follows the same scanning pattern whenever the subject views the same stimulus (Noton and Stark, 1971). This is an extreme point of view and has not been readily demonstrable.

At the other extreme and more widely believed today, is that higher centres of the brain govern visual scanning behaviour; that is, "seeing" determines "looking." To support this, there is a large literature showing how scanning behaviour is affected by the subject's instructions, task, and expectations (Yarbus, 1967; Senders, Fisher, and Monty, 1978; Fisher, Monty, and Senders, 1981). Particular

emphasis has been directed towards the duration of fixations rather than eye position. This has been due to the inclination of the cognitive approach to employ the concept of "processing time" as an important variable of cognition. It is also due to the difficulty in characterising scanning patterns by a single useful quantity beyond simple statistical measures (such as dispersion). In spite of this large literature, no general model of fixation duration has emerged, and notwithstanding the lack of progress, the information processing approach still dominates this area of research (e.g., Groner, Menz, Fisher, and Monty, 1983). The prevalent view seems to be that fixations reflect both visual and higher-level processing time, and a fixation is only terminated by a saccade when processing is complete.

1.2 Infant Visual Scanning

The way we view infant behaviour is inevitably shaped by our understanding of the corresponding adult behaviour. If adult visual scanning is driven by high-level processing, then the developmentalist inherits the problem of either imbuing the infant with innate high-level processes, or finding a different and simpler mechanism for visual scanning in the infant which develops eventually into the fully integrated perceptual-motor organization attributed to adult visual scanning.

With the advent of corneal photography, it became possible to record eye position unobtrusively from the human infant (Salapatek and Kessen, 1966; Haith, 1969). This opened up the possibility of observing directly the development of perceptual-motor integration in

visual scanning. Most studies on infant scanning concentrated on where the infant looked when presented with a stimulus, in a similar way to the pioneering studies of Yarbus (1967) on adults. It was found that infants often only scanned parts of the stimulus and not the total stimulus as adults usually do (Salapatek and Kessen, 1966; Nelson and Kessen, 1969; Salapatek, 1969, 1975). In particular, it was claimed that infants preferred to look at the edges or vertices of geometric figures, which were often used for stimuli. With the discovery of complex cortical cells by Hubel and Wiesel (1968), the so-called "feature-detectors", the notion that only stimulus elements are scanned by the young infant had considerable appeal. It seemed to indicate a possible way perceptual learning could take place; the young infant attends those stimulus features that excite the tuned cortical cells. Visual scanning, therefore, was considered to have the function of exercising and stimulating the growth of the cortex (Haith, 1980). As the cortex matures, the infant would scan stimuli more broadly as the stimulus totality becomes more appreciated. Thus, as with adults, "looking" behaviour is controlled by the visual processing (although at a rudimentary level). However, there has been some controversy over this projected developmental trend: Salapatek (1969) has claimed to find more extensive scanning with age. However in his study, the experimenter simply watched the infants' eyes and drew an estimate of eye position by hand on a facsimile of the stimulus. By using more accurate and objective methods, Hainline and Lemerise (1982) have shown that there is no developmental trend for breadth of scan. They have shown that the infant does not adopt

any reliably identifiable scanning strategy - some infants will scan only a subset of stimulus features and other infants will scan the whole stimulus. No developmental change was detected, which casts doubt on any perceptual-motor development which might be manifest in visual scanning. They did observe an increase in the dispersion of fixation eye position with stimulus size, which indicated that the scanning in infants was at least visually sensitive to the stimulus.

Unfortunately, there is a methodological problem in interpreting infant scanning data. To be able to state precisely where a subject is looking, it is necessary to calibrate the subject's line of regard. This is true of any eye-tracker technology or subject. Calibration is easy with adults because they can be instructed to look at calibration targets. With infants, however, calibration is much more difficult and time-consuming (Harris, Hainline, and Abramov, 1981). No studies of infant visual scanning have individually calibrated their infant subjects and they have relied upon "average" calibration. Although average calibration is quite adequate for relative measures of eye position, such as dispersion of fixation eye positions, it is inadequate when eye position is to be related to the features of small stimuli (average calibration has an accuracy of about 3 - 4 degrees or worse, see Hainline and Lemerise (1985)). Thus, the claim by Haith (1980) and others that infants cross stimulus edges when scanning seems untenable considering the absence of any calibration.

In spite of its promising start, progress in understanding visual scanning in infants has been slow, not only because of the awkward problem of calibration, but also because of the difficulty in interpret-

ing scanning patterns. Quantifying the spatial patterns of fixations and then using such a quantity to relate the stimulus to perception has been a difficult undertaking. We will attempt to show that many aspects of visual scanning for the free-viewing subject can be explained at a sensorimotor level in both the adult and the infant as "looking" rather than "seeing."

1.3 Basic Approach

We shall be concerned mostly with the temporal aspects of visual scanning rather than with relating eye position to stimulus features. This avoids the difficulties of individual calibrations and interpreting scanning patterns. We shall also take a somewhat unusual perspective of visual scanning by concentrating on when fixations are terminated (usually by a saccade, but sometimes a head movement or blink). Fixation duration is then only the time between terminating events. Of course this is really only a shift in emphasis, but it makes no a priori asssumptions about any "processes" that may occur during fixations. We shall consider the "active" component of scanning to be the terminating event rather than the fixation; that is, we consider visual scanning to be a sequence of "looking" behaviours rather than as a "seeing" process.

To begin, we ask in a broad sense what can trigger a saccade. Four general classes of saccadic etiology can be identified, each requiring a different level of neural organization. In descending levels of neural organization:

(i) Saccades can be initiated voluntarily and consciously. We are

aware of these deliberate eye movements either through introspection or by the ability of others to follow instructions.

(ii) Saccades can be a learned behaviour. Reading is an example of a behaviour where years of practice result in sequences of saccades to move the eye in a specific pattern across a page. We are usually unaware of our eye movements during reading.

(iii) At a simpler level, a saccade can be a reflexive behaviour triggered by the sudden appearance of a visual target in the peripheral visual field. This reflex is often accompanied by a head movement and it occurs in all species with ocular motility.

(iv) We also include the possibility that saccades could occur spontaneously with no apparent external stimulus. Such ocular "twitches" would require no afferent visual system.

The most parsimonious approach is to attempt first to explain scanning at the lowest level of organization, namely, by postulating that saccades are spontaneous and are not triggered visually. Because we are aware that saccades can be triggered visually or voluntarily does not mean that this possibility should be discounted, especially in the infant. Only if sufficient evidence can be accumulated to reject this hypothesis should the next level of organization be entertained, and so on. Although this approach may be self-evident, it has not been adhered to, particulary in respect to visual scanning in the infant. As discussed earlier, the tendency has been to show that perceptual or cognitive influences on scanning entail that visual scanning is driven by these processes; or in our scheme, scanning saccades are a learned behaviour dependent on the completion of

high-level processes. The possibility that these saccades are only reflexes has not been thoroughly investigated, and the possibility that they are spontaneous has not even been considered in the literature.

The temporal aspects of scanning from other studies are difficult to compare because there has not been a consistent definition of "fixation." There seem to be two inter-related reasons for this.

First, what constitutes a fixation depends on whether scanning is considered to be a "seeing" or "looking" behaviour. If the former view is maintained then "fixations" are defined relative to the stimulus. Thus, while the eye remains pointing within a certain stimulus region, a fixation or fixation time is recorded (e.g. Maurer, 1983). This measure is also known as "looking time" or "dwell time." The rationale behind this definition is that the time spent by the subject looking at a region reflects some form of visual processing of that region. Depending on the size of the region, considerable detail of visual scanning can be lost.

If fixation is considered to be a motor behaviour, that is, eye position is held relatively stable as opposed to drifts or fast saccadic eye movements, then fixations are determined solely by the eye movement recording since different eye movements need to be separated (parsed) only in time. The position of the eye relative to the stimulus is irrelevant for this definition (although it may be of great interest as a dependent variable). This oculomotor definition is almost universally accepted for scoring eye movement recordings from adults, but it has not been applied often to recordings from infants. In part,

this has been because of the above-mentioned view of fixation but also because of the different technologies that have been used to record eye movements in infants and adults.

The second difficulty in defining fixation is methodological. Most studies of infant scanning have used corneal photography with poor temporal and spatial resolution (see Hainline and Lemerise, 1985 for a review). Typically, the sampling rate of eye position has been less than 4 samples/sec where each sample has an exposure of about 100 msecs. With this resolution it becomes impossible to draw any conclusions about the duration of fixations. Spatial resolution also affects the apparent fixation duration since detecting the termination of a fixation depends on the ability of the apparatus to resolve small saccades. This is a problem even when recording eye movements from adults (Karsh and Breitenbach, 1983). Poorer instrument resolution will yield, on average, longer fixation durations because small saccades go undetected. This probably explains the difference between the only two published studies with meaningful sampling rates that report on infant fixation duration (Bronson (1982) and Coles and Sigman (1986)).

Bronson's measurements yield distributions of fixation durations with a modal duration of about 500 msecs. His instrument resolution was about 1 - 2 degrees, which Bronson justifies to be adequate because of the immature infant macular region. Coles and Sigman found very short durations with a mode below 200 msecs. However, their instrument had a resolution of 0.5 - 1.0 degrees, which probably detected many small saccades that Bronson's apparatus could

not. It is of interest to note that Bronson interpreted his long duration measurements as signifying "suboptimal visual processing" - in contrast to the view that in adults, longer fixations indicate more processing. Although there is evidence that the infant fovea is immature (Abramov, Gordon, Hendrickson, Hainline, Dobson, and LaBossiere, 1982; Hendrickson and Yuodelis, 1984), it is an empirical question whether and how this affects fixation duration.

We shall use a TV-based corneal reflection system that has a sampling rate of 60 Hz and a spatial resolution of 0.5 degrees. This is an improvement over many other techniques but is still leaves problems in defining fixations. It must be borne in mind, therefore, that fixation duration has to be operationally defined, at least with the currently available techniques for recording eye movements from infants. This issue will be discussed further in Section 3.

We shall examine the duration of fixations of the infant under a variety of stimulus conditions for the following reasons. Most studies on infant visual scanning have concentrated on the spatial pattern of fixations. We know very little about the duration of fixations in the infant. It is difficult to assess the value or "valency" of a stimulus from an infant's viewpoint. Preferential looking[1] has shown that infants' preference is sensitive to the amount of contour in a stimulus (Karmel and Maisel, 1975). For simple stimuli, preference increases

---

[1] Data from preferential looking must be interpreted cautiously. It has not yet been shown whether this paradigm elicits true "preference" from the infant (in terms of centrally comparing the two stimuli) or it elicits an orienting reflex depending on the relative saliency of the two stimuli; preferential looking is a special case of visual scanning and so this issue will be returned to later (Section 8).

with the amount of contour up to a maximum and then declines with a further increase in the amount of contour. At least for checkerboard stimuli, an equally good and perhaps more sensible predictor of this preference is the spatial frequency content of the stimulus. Gayl, Roberts, and Werner (1983) have re-analysed Karmel and Maisel data to show that infants' preference can be predicted by the total power in a frequency band centred around the spatial frequency with the highest power after filtering by the infants' visual system. Banks and Salapatek (1981) have also shown that the change in preferred checkerboard size with age is in agreement with the development of the infants' most sensitive spatial frequency. However, it is not clear that the preferences of infants at all ages is based solely on the power of the spatial frequency content of the stimulus. Banks (personal communication) suggests that infants become sensitive to the phases of the spatial frequencies in a stimulus after about 3 months. Nevertheless, if different stimuli elicit different looking times, it would seem likely that fixation duration should also be affected by the stimuli.

Another reason for using different stimuli is that quite different and unexpected effects can occur. A study on infant saccades showed that the ratio of saccadic peak velocity to saccadic magnitude depended on which stimulus was viewed by the infants (Hainline, Turkel, Abramov, Lemerise, and Harris, 1984; see Appendix H). This ratio usually remains constant for alert adults. If only one stimulus had been used, quite different conclusions would have formed depending on which stimulus was used. This stimulus dependency

will be examined more closely in Section 7, but for now, it illustrates the advantages of using a variety stimulus conditions when recording eye movements from infants.

1.4 Preview

It will be shown that the use of different stimuli and many subjects elicits a wide range of mean fixation durations (Section 3). In Section 4, the method of moments will be used to show that there is a common distribution of fixation durations among infants. This distribution shape will be identified as basically the Exponential waiting-time distribution (actually a compound exponential), which has important implications for how fixations are terminated. Interestingly, the same basic distribution will be found in adults under the free-viewing condition. The identification of this distribution is an important clue to the underlying mechanism for fixation termination. Three models will be entertained in keeping with the classes of saccadic etiology as described earlier. These will be a spontaneous saccade model, a reflexive saccade model (the "multiple target model"), and a learned saccade model (the "CPU model").

In Section 5 the effect of stimulus size on mean fixation duration will be shown and discussed. This will lead to the acceptance of the reflexive model as the best fitting model. The simple logic of this model will be extended to make some predictions under special stimulus conditions which will be corroborated by other existing studies. It will then be shown that the effect of stimulus size on scanning is less pronounced in the infant. Sections 6 and 7 will attempt to

explain this.

In Section 6 an attempt to measure eye drift during fixations will be made. Because of instrument noise, it will only be shown that fixation duration and drift rate are approximately reciprocally related. This will open up the possibility that drift rate may play an important role in visual scanning.

The final analysis in Section 7 will examine the effect of arousal on fixation duration. It will be shown that lower levels of arousal are associated with shorter fixations. A simple modification of the model will be suggested to account for this influence.

In the summary (Section 8), the results will be reviewed and the model will be compared to the existing data on infant scanning. Because of the nature of existing data, this comparison will only be qualitative. Nevertheless, some of the early work on infant perimetry (P.Harris and MacFarlane, 1974; MacFarlane, P.Harris, and Barnes, 1976) will be explained, and an alternative description of preferential looking will be proposed.

Finally, two points need to be emphasised. First, a strictly empirical approach will be followed. Assumptions about the infant's oculomotor and visual abilities will be kept to a minimum. No assumptions on the existence of perception or high level processes in the infant will be made. This is not to imply that these processes do not exist in the infant, but rather, that they are not necessary to explain scanning (at least under our stimulus conditions). The analyses are not hypothetico-deductive and the model to be described is essentially data-driven.

Second, because this is a behavioural study, no physiological model will suggested. Although neurophysiological studies have given us considerable insight into the visual and oculomotor systems, the pathways between these systems is largely unknown. In spite of the clear findings to be shown here, it is felt that extrapolations to the neurophysiological level are premature. However, since we shall be concerned with visually triggered saccades, it will be necessary to consider the filtering action of the visual system, particularly its spatial inhomogeneity. To do this we shall make continual references to the retina and the receptive field organization of the retinal ganglion cells. We justify this on the grounds that any visual information must pass through the retina and, also, that we know much more about the retina than any other parts of the visual system. Nevertheless, it should not be construed that we are proposing a direct connection between the retina and the oculomotor system and that other parts of the visual sytem play only minor roles in visual scanning.

[2]

METHOD AND METHODOLOGICAL ISSUES

2.1 Apparatus

Eye movements were recorded from infants and adults using a TV-based infrared corneal reflection/bright pupil system. This was a commercially manufactured system (Applied Science Laboratories, model 1994), with extensive modifications to the optics. An overall schematic of the system is shown in Figure 1.

The basic mode of operation is as follows: A virtually invisible collimated infrared beam is projected onto the subject's eye. The anterior surface of the subject's cornea acts as a partially reflective convex mirror by reflecting some of the light back to a video camera. The remaining light is transmitted through the ocular media and impinges on the retina. Because the subject is accommodating a stimulus at about 2D, the transmitted light does not come to a focus at the retina but is diffusely reflected. A portion of the diffuse reflection back-illuminates the subject's pupil and re-emerges from the eye towards the video camera. An infrared sensitive video camera forms two images - an image of the corneal reflection (the first Purkinje image), and an image of the bright pupil. A considerable proportion

Figure 1

Arrangement of major components for recording eye movements from infants. Note: For the single target and bar stimuli the rear-projection screen is replaced by a CRT monitor.

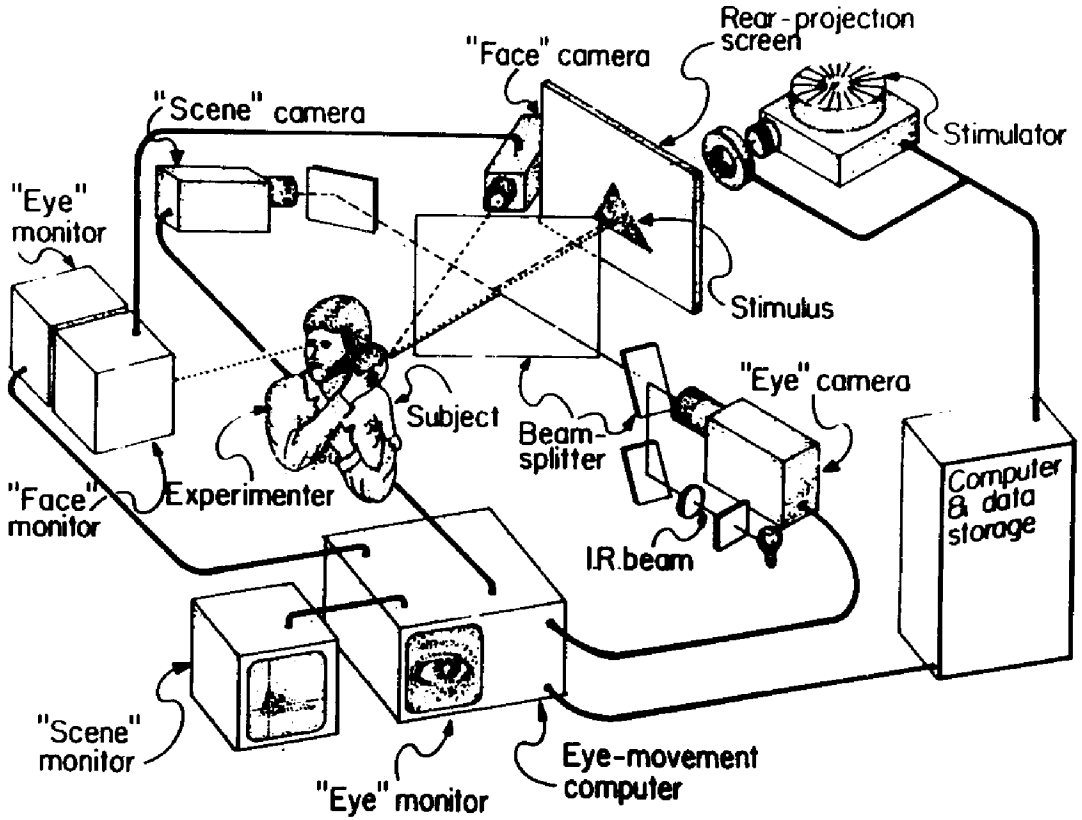
Rear-projection screen
"Face" camera
"Scene" camera
Stimulator
"Eye" monitor
Stimulus
"Eye" camera
Subject
Beam-splitter
"Face" monitor
Experimenter
Computer & data storage
I.R. beam
"Scene" monitor
"Eye" monitor
Eye-movement computer

of light is lost through scatter and absorption in the ocular media, depending on accomodative state and pigmentation. By means of beam splitters, the infrared source, the video camera, and the stimulus are coaxial with the subject's right eye when the eye is in its primary position. Thus, when the subject is looking straight ahead, the first Purkinje image (P1) will appear at the centre of the bright pupil image. As the eye rotates, both images move at different rates in the direction of rotation, and P1 no longer appears at the centre of the pupil image. The eccentricity of P1 from the centre of the pupil image is a measure of the amount and direction of eye movement (Figure 2). The advantage of using both images to measure eye position, rather than say just P1, is that the difference between P1 and the centre of the pupil image is independent of head motion. The separation between P1 and the pupil centre is calculated from the video image by a microprocessor-based (proprietary) algorithm, which estimates the horizontal and vertical components of the eye rotation. These estimates are then transmitted digitally to a host computer for storage on magnetic tape and later off-line analysis. The pupil diameter is also measured and transmitted to the host computer; this is useful since it allows the eye position data to be cross-checked for validity when blinks or poor pupil delimiters occur (see below). The major components of this system will now be described.

Infrared Source

A 150 watt tungsten filament lamp (24V) provided sufficient radiation in the near infrared for successful operation of the eye-tracker with most subjects. The lamp was driven by a constant DC current

Figure 2

Stylization of the optical components in the eye-tracker. Lower panel shows differential movement of bright pupil and first Purkinje image (dot).

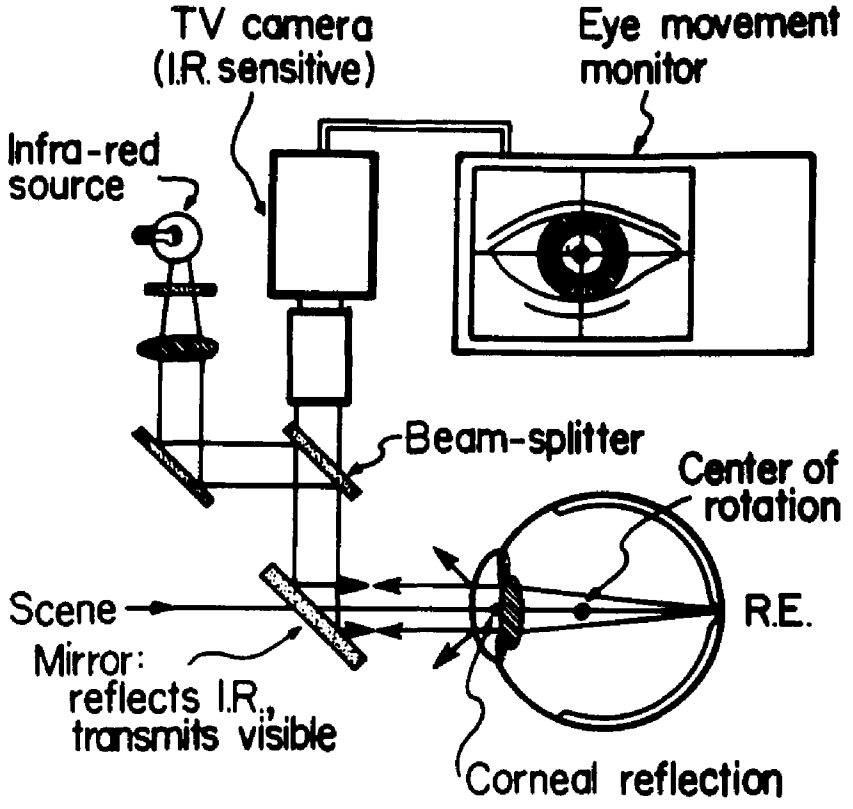
TV camera
(I.R. sensitive)
Eye movement
monitor
Infra-red
source
Beam-splitter
Center of
rotation
Scene
R.E.
Mirror:
reflects I.R.,
transmits visible
Corneal reflection

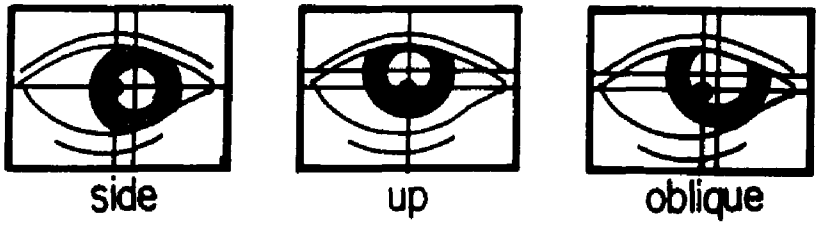
side
up
oblique

source at a current adjustable by the operator up to 6 amps - the processing electronics in the eye-tracker would not to operate properly if the IR beam were too weak or too intense, depending on how much light was reflected from a particular subject's retina. The visible and ultraviolet radiation was filtered out by two absorption filters (Corning 7-69 heat filter and crossed Polaroids, HN-7, for the visible). The resulting pass region peaked at 970 nm with 100 nm half-power bandwidth. This was invisible under any of the stimulus conditions (although a fully dark adapted adult subject could see a faint red glow when no stimulus was present). A lens with a focal length of 30 mm collimated the beam. Forced air was used to prevent overheating of the assembly. As a safeguard, two photodiodes were installed on the subject's side of the filters to switch off the filament current instantly if the light intensity suddenly rose. This hazard might have occurred (but never did) should a filter have cracked because of excessive heat absorption.

Video Camera

A Hitachi camera (model HV-16SU) was operated at standard television specification (60 Hz) with a one inch silicon vidicon. A telephoto lens was attached to provide the necessary magnification of the subject's pupil at 60 cm (effectively 270 mm f/3.5 - 4.0). The diameter of the image of the pupil usually took up about 1/3 of the full frame width.

Subject Placement

Infant subjects were held upright against the shoulder of an

assistant so that an infant's chin would rest immobile on the assistant's shoulder. The assistant's hand also held the infant's head laterally firmly against the crook of the assistant's neck. The assistant faced away from the stimulus and viewed a TV monitor which displayed the IR camera image of the pupil, which permitted the assistant to maintain the subject's eye in the field of view of the IR camera. The field of view was about 2.5 x 2.5 cms in which the whole pupil had to be maintained in order for the processing electronics to function. The depth of field of the IR camera telephoto lens was about 1 cm. Thus, this optical arrangment provided an excellent means of maintaining a constant eye position from subject to subject since data could not be collected if the subject's eye moved outside this volume. Adult subjects were stabilised by a chin rest.

Eye Tracker's Detection Algorithm

Provided the subject's eye maintained its position in the volume of view of the IR camera, a very bright first Purkinje image (P1) and a somewhat less bright pupil image were formed against a dark background. The pupil image was generally an ellipse with an eccentricity that depended on the angle of eye rotation. P1 was small and approximately circular with a size dependent on the amount of defocus. Defocus was always present since P1 and the pupil image are not coplanar, and a compromise plane of focus was necessary. The problem for the algorithm is to find the geometric centres of these two images. Although the details are proprietary, the basic algorithm functions in the following manner: Each raster line of the IR image is scanned for two intensity transitions - a dark to bright transition

indicating the beginning of the bright pupil against the dark background; and a bright to very bright transition indicating the beginning of the very bright first Purkinje image superimposed on the bright pupil image. Whenever these transitions occurred along a raster line, their coordinates were stored in memory and a small bright dot was superimposed on the image and displayed on the operator's and assistant's monitors in order to give feedback on the algorithm's performance. The thresholds for detecting these transitions were set by the operator via "delimiters" (potentiometers) for reliable identification of P1 and the bright pupil image. Occasionally, the intensity of the IR beam and/or the f/stop of the IR camera telephoto lens had to be adjusted (but never the focus). By identifying these transitions in the relevant raster lines, the loci of the left edge of the bright pupil and P1 were digitized. Firmware in the resident microprocessor then found the centres of the best-fitting ellipses to each of these boundaries. The horizontal and vertical separations of the two estimated centres were thus calculated every TV frame. Because of noise, estimates from every two consecutive frames were averaged before being transmitted to the host computer.

2.2 System Response

In order to interpret the eye movement data recorded by this instrument, it is essential to understand the details of its response to any eye movement. It should be noted that these details could not be provided by the manufacturer of the eye-tracker and so they were worked out for our particular instrument.

Linearity

As mentioned above, the microprocessor computes the coordinates of the centres of the first Purkinje image and the pupil image. The difference between these two centres is then an estimate of eye position. In fact this estimate is proportional to the sine of the angle through which the eye moves relative to the system's axis (Young and Sheena, 1975), assuming a spherical cornea. For small angles the sine of an angle is approximately equal to the angle itself (when specified in radians). The largest stimulus here subtended a total angle of 45 degrees at the subject so that we can expect, roughly, a maximum eye rotation of 22.5 degrees from the system's axis. This causes a departure from linearity of about 0.6 degrees (2%). Since the resolution of the eye-tracker is about 0.5 degrees and since the eye is much closer to the system's axis most of the time, we can ignore this relatively small departure from linearity.

A possibly more serious departure from linearity might be caused by the asphericity of the cornea. In infants and adults, the radius of curvature increases radially from the corneal pole. This increase can be as much as 10% at 3 mm from the pole (Mandell, 1967). Therefore, as the eye rotates, P1 and the bright pupil image are formed by different parts of the cornea that have different curvatures and powers. This problem is worked out in Appendix A using an ellipsoidal approximation of the corneal profile as suggested by Mandell and York (1969). It is found that the effect of ellipsoidal asphericity on the linearity of this eye-tracker is small (<2%).

Static Calibration

The output of the eye-tracker was two 8-bit digital numbers (0 - 255 machine units) which were proportional to the horizontal and vertical angles subtended by the *optical axis* of the cornea to the axis of the system. There are two unknown factors that ideally need to be known, namely, the constant of proportionality (Gain) and the DC-offset. The gain consists of an instrument component and a subject component. The instrument component depended on the optical magnification of the system and the distance from the subject's eye to the camera. Because of the small depth of field of the telephoto lens, the instrument component of gain remained effectively constant. The subject-dependent component depends on the optics of the particular subject, namely, the distance between the centre of curvature of the cornea and the centre of the entrance pupil (Young and Sheena, 1975; Appendix A). This optical distance, K, will vary among subjects since it depends on the corneal curvature and the depth of the anterior chamber; thus, each subject will have a slightly different gain. Anatomically small eyes (such as infants') have shallow anterior chambers but this is offset by corneas with small radii of curvature. The opposite occurs for large eyes. Bronson (1982) has calculated that the gain factor for infant eyes is only slightly different from adult eyes. Thus, an average gain factor describes both infant and adult populations equally well. An average gain factor for the complete instrument was based on 6 adults and applied to all adult and infant subjects. Calibration data from several infants (Harris, Hainline and Abramov, 1981) confirmed the appropriateness of its value.

This is quite adequate for our purposes, since we are only concerned with the "average" performance of subjects, and we are not concerned with how a specific subject performs in relation to other subjects. It should be noted that even a gain factor is not necessary for estimating some quantities; in particular, main sequence slope of saccades is the ratio of eye velocity to saccade amplitude, which is independent of gain.

The fovea in the typical adult retina lies about 5 degrees temporally from the optic axis of the eye (Millodot, 1982). In the infant, the fovea (or its anatomical precursor) appears to lie further eccentric (Slater and Findlay, 1972) and appears to move towards the adult location with age. It is unclear whether this movement is true migration or just apparent because of eyeball growth (Slater and Findlay, 1975). Thus, knowing where the optic axis of the eye intersects the visual scene does not tell us where the point of regard is in the visual scene. Each subject has an offset depending on the location of his fovea with respect to the optic axis of the eye; however, in the infant, this problem is exacerbated by the immaturity of the fovea (Bach and Seefelder, 1914; Mann, 1964; Abramov, Gordon, Hendrickson, Hainline, Dobson, and LaBossiere, 1982; Hollyfield, Frederick, and Rayborn, 1983; Hendrickson and Youdelis, 1984) which may not be functional. Perhaps the infant prefers some other retinal locus for line of regard, or even has no single consistent location. Notwithstanding the various calibration schemes that have been devised (Bullinger and Kaufmann, 1977; Carmody, Kundel, and Nodine, 1980; Harris, Hainline, and Abramov, 1981; Kliegl and Olson, 1981; Mendel-

son, Haith, and Goldman-Rakic, 1981), accurately relating the point of regard to a stimulus feature is still a major problem in infant eye movement recording.

For our purposes absolute calibration is not necessary, and the difficulties of individual infant calibrations can be avoided. We are not attempting to relate eye position to stimulus features because of the reasons outlined in the Introduction; our concern is with relative measures of eye position such as amplitude of movement (saccade amplitude) or standard deviation of eye position (breadth of scan). For these quantities the constant offset factor subtracts out and is not necessary. Of course, we are assuming that the infant uses a single retinal location or, at least, a closely packed array of retinal locations for the line of regard.

Dynamic Calibration

The dynamic properties of the eye-tracker need also to be understood for the correct interpretation of measured fast eye movements. Here we are concerned with bandwidth and sampling rate issues. Although this eye-tracker has a much higher bandwidth and sampling rate than most other instruments that have been used with infants, it is still low compared to the bandwidth of saccadic eye movements. The effect of low bandwidth is that the measured velocity of saccades will be lower than it really is because the instrument is unable to respond fast enough. This also causes saccades to appear to have longer durations than they really have. The effects of bandwidth and sampling rate is a complex problem and it is examined both generally and with reference to our instrument in Appendix

B. It is shown that peak velocity of saccades can be recovered from the eye movement records in spite of the suboptimal bandwidth. In order to accomplish this calibration it was necessary to present the eye-tracker with a controllable and known input. An artificial eye was constructed using a contact lens and rotated by a galvanometer motor. Saccades could then be simulated and the effect of the dynamic response of the eye-tracker was measured. Details of the artificial eye are given in Appendix C.

Noise

It was also necessary to measure the noise level of the eye-tracker. This was accomplished by placing the artificial eye at various angles to the system axis for periods of five seconds (300 samples). The standard deviation of the records was found to be about 0.5 degrees at all angles. The horizontal and vertical components were uncorrelated. The effects of noise are discussed extensively in Appendix B.

2.3 Subjects

Infant subjects were all healthy, full term, and ranged in age from 14 to 256 days. They were located through contacts with hospitals and physicians. Parents signed a consent form before data collection began. Adults were faculty, students and research assistants.

2.4 Stimulus Conditions

Two kinds of stimuli were used: static and operator-controlled.

The static stimuli were photographic slides rear-projected onto a viewing screen and advanced by the host computer. The screen was 50 cm from the subject's eye and subtended an angle of 45 degrees at the subject. Three subcategories of stimuli were used: (i) simple black and white geometric forms (circles, squares, and triangles) in sizes 5, 20, and 30 degrees (Hainline and Lemerise, 1982); geometric forms which were luminous with a dark background will be called "negative" shapes, and geometric forms with a dark interior and luminous background will be called "positive" shapes. (ii) textures consisting of black and white gradients of lines, and patterns created from juxtaposed checkerboards of different check sizes (e.g., see Gibson, 1950); (iii) Complex coloured scenes. The textures and complex scenes filled the entire screen.

For the operator-controlled stimuli, the rear projection screen was removed and replaced by a 19" CRT monitor (Hewlett-Packard, model 1310A). The CRT was situated 60 cm from the subject's eye and subtended 30 degrees horizontally and 22 degrees vertically. The phosphor was green (P31). The screen was maintained at a mean luminance of about 2 nits and a small bright spot (1 degree x 1 degree) was superimposed by a pattern generator (Rockefeller University optical stimulator model V2). The position of this spot could be controlled by a host computer. A pseudo-random sequence of positions for the spot was stored in the host computer and stepped through sequentially as requested by the operator via a remote switch. When the spot had remained at a new position for more than 2 seconds, it was automatically flashed on and off at 2 Hz with equal

duty cycle. This was done to attract the infant subject in case he/she had not noticed the change in stimulus position. As soon as the operator requested a new position in the pseudo-random sequence, the flashing was automatically stopped and the spot remained on for one second before being moved to the new position, where it remained for another two seconds before flashing again, etc..

For some sessions, the spot was replaced by a vertical or horizontal bar (1 degree wide) that traversed the screen. The bar was moved in a similar fashion to the spot except only along its orthogonal dimension. Bars were used because they possibly provided a more salient target for the infant.

In spite of the flashing, most infant subjects did not find these operator controlled stimuli particularly engaging. It is not clear whether these stimuli were never very salient or just very boring. In order to increase the likelihood of collecting eye movement data, a variety of sounds (rattles, whistles etc.) were generated from behind the CRT to attract and orient the infant subject.

2.5 Procedures

The subject placement (see above) and the small field of view of the camera demanded that infants were in a state of alert inactivity while eye movements were recorded. If an infant did not maintain this state because of sleepiness, fussiness, hunger, crying, or other untoward and vicissitudinous behaviour, the infant was removed from the apparatus. If the alert inactive state was regained, the infant was returned to the apparatus for further recording, otherwise the ses-

sion was terminated. For the static stimuli, each stimulus was presented for 10 seconds with an inter-stimulus-interval of 5 seconds. During the interval a slide of a human face was presented but no data were collected. For the operator-controlled stimuli, data were collected continuously while the infant was alert. Pacifiers were used only for some subjects viewing the complex scenes.

2.6 Analysis

The first and important aspect of data analysis was to segment the eye movement record into the categories of interest (saccades and fixations). Then a particular parameter of interest could be measured from each relevant segment (saccade amplitude, fixation duration, etc.) for further analysis. The problem was to decide how to parse a record into each category of eye movements - manually or by an automatic computer algorithm. A successful algorithm would be many times faster than by hand, and the huge amount of data here provided a strong incentive to use the computer. However, there are some serious problems to be considered which caused us to reject the automatic computer algorithm.

(i) Computer algorithms require rigid criteria in order to make decisions which must be set up ahead of time by the programmer; however, we were not sure what to expect from infant subjects. There was a strong possibility that subsequent analysis would be unwittingly biased either because of a poor choice of criteria, or, because of a side-effect of the algorithm itself. As Karsh and Breitenbach (1983) have demonstrated, this is a serious problem even in the automatic

analysis of adult data. For example, they show that by re-analysing the *same* adult eye movement record, a change in algorithm criteria yielded completely different scanning patterns, numbers of fixations, and mean fixation durations. Their effect was large: for example, by increasing the number of sample points that determined the onset of a fixation from 2 to 6, their algorithm yielded an increase in mean fixation duration from 96 msecs to 249 msecs.

(ii) Although a human operator could distinguish between, for example, a small saccade and machine noise, it was unclear how to program a computer to make the same distinction - humans are still much better at pattern recognition than computers.

(iii) Errors are inevitable in both manual and automatic procedures. However, systematic algorithms make systematic errors, while humans are more likely to make random errors. The latter are preferred when trends and populations are to be studied.

(iv) Even if an automatic algorithm is used, the final decision is by a human. This is either implicit when the performance of an algorithm is assessed at the testing stage; or explicit when an uncertainty arises. In other words, automatic parsing is not "better" than manual parsing, just faster.

(v) With an automatic procedure, one does not see or get a "feel" for the data; such impressions can be important in forming hypotheses.

It was felt that the disadvantages of computer algorithms outweighed their advantages of speed and reliability. Therefore, an

interactive program was developed which allowed the operator to parse but used the computer to compute rapidly all the necessary parameters. The program functioned as follows.

Interactive Parsing Program

A portion of an eye movement record (buffer) was displayed on a graphics oscilloscope as two traces for horizontal and vertical eye position components. By means of movable display cursors, the operator partitioned (parsed) consecutive segments of the record into various categories of eye movements. A menu of categories was available to the operator: "Fixation", "Drift", "Saccade", "Noise", and "Other." The "Fixation" category was reserved for segments in which the eye remained stationary, that is, both the traces on the oscilloscope were flat within machine noise. The "Drift" category was used when the eye was not stationary and had no accelerative component. On the oscilloscope, "Drifts" appeared as inclines on one or both traces. If an accelerative component was discernible by the operator, the "Saccade" category was used. The judgement of acceleration was left to the operator and no absolute criterion was used. Usually there was no difficulty in identifying saccades with a magnitude greater than one degree. Few saccades below about one degree were identified because of machine noise, and sometimes, the operator was forced to make a choice between a slow saccade and a drift. The "Noise" category was used for unscorable episodes, which were either head movements that placed the eye out of the field of view of the camera, poor delimiter settings which would result in non-scorable data whenever the subject made a saccade, blinks (which occurred rarely in

infants), or occasionally the contrast of the pupil image would fall too low for detection. It is important to note that, most of the time, the termination of a fixation by a "Noise" segment still reflected a true termination by the subject in some form or other, and did not reflect an artificial termination by the instrument. The "Other" category was reserved for any unusual movement and the operator specified the label - this occurred rarely. If a mistake was made, the operator could correct all parses still visible on the screen. Once the operator was satisfied, parameters from each parsed segment were computed and written to an output file preserving the original sequence, and a new buffer of data was displayed. In this manual manner, each eye movement record was exhaustively (and exhaustingly) parsed. A log book was kept for unusual eye movements or impressions. Figure 3 shows an example of how a record was parsed.

Many parameters were computed from each parsed segment. However, only a few were eventually used. The most important parameters were the eye position and time at the beginning and end of each parse. This allowed the amplitude vector and duration to be calculated. For saccades, peak velocity was measured. For "Fixations" and "Drifts" eye position was linearly regressed against time separately for the horizontal and vertical components. This was intended to yield average drift rate, but as discussed later (Results) proved to be inadequate because of noise.

Parsing and all subsequent analysis was carried out on a PDP8/E with 28K of memory and a floating point processor. Programs were written in Fortran IV, PDP8 assembler, Ralf and Basic.

Figure 3

Example of how an eye movement record was parsed. The upper trace represents the horizontal component of eye position in time (abscissa), and the lower trace represents the vertical component. Vertical lines indicate the boundaries between consecutive parsed segments: "F" - Fixation; "D" - Drift; "S" - Saccade; "N" - Noise. These boundaries were determined by the operator.

Parsing an Eye Movement Record

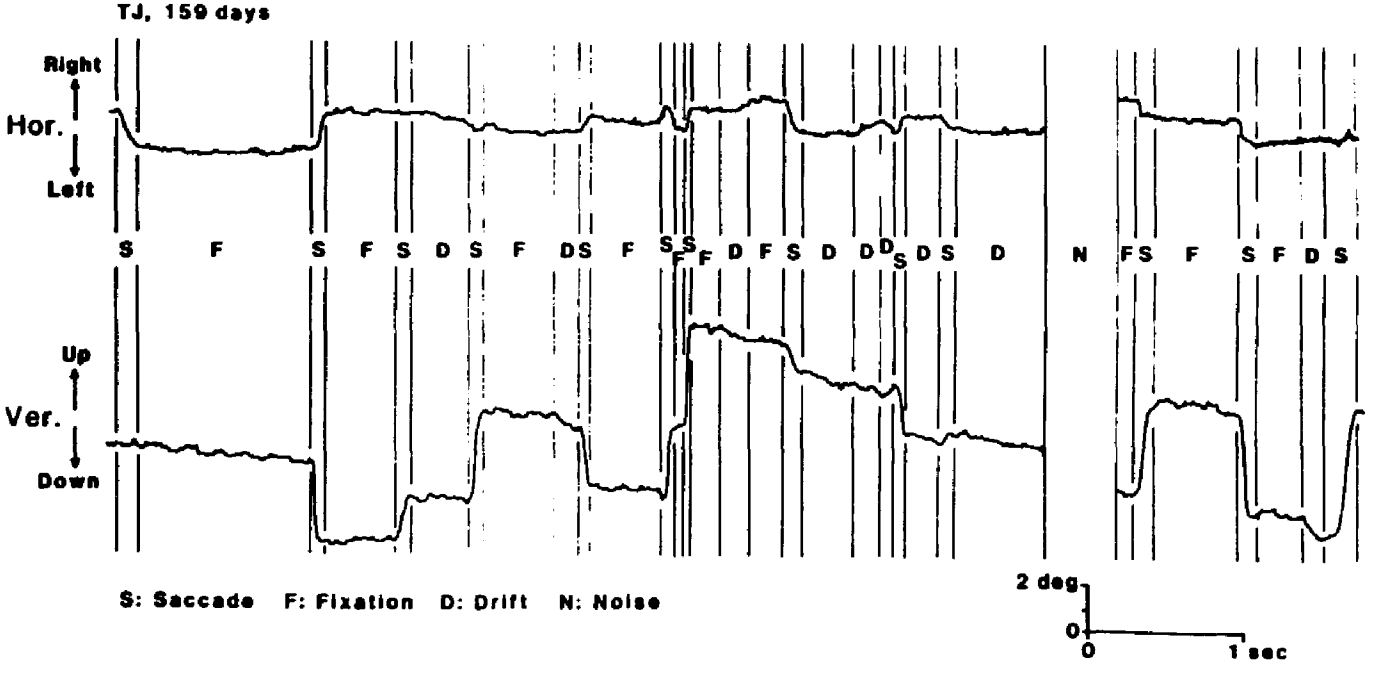

[3]
RESULTS AND DISCUSSIONS

3.1 Fixational and Drift Segments

As mentioned earlier (Methods), non-saccadic eye movements were parsed as either "Fixations" or "Drifts." These categories were made available to the parse operator since it was quite obvious from eye movement records that the eye did not always remain stationary between saccades (Figure 4). It was possible that "Drifts" did not belong to the category of "Fixation" but represented some other distinct oculomotor behaviour - such a possibility could not be excluded *a priori*.

However, no evidence was found to support the notion that "Drifts" were distinct from "Fixations." This is evident from the typical examples shown for four infant subjects in Figure 5. Each panel represents the grouped frequency of occurrence for "Drifts" (shaded), and "Fixations" (unshaded) at different durations. By adding the frequencies of these two categories, the envelope (heavy line) shows the total frequency distribution for each subject. As can be seen, there is considerable overlap between the "Drift" and "Fixation" distributions and there is no indication of bimodality in the envelope.

Figure 4

Typical examples of eye movement records from infants and adults. In each pair of traces, the upper trace represents the horizontal component of eye position, and the lower represents the vertical component. The upper four pairs show traces from subjects free-viewing and the lower three show traces from subjects viewing the single target. Examples of high and low drift are shown. No examples of high drift could be found for adults viewing the single target.

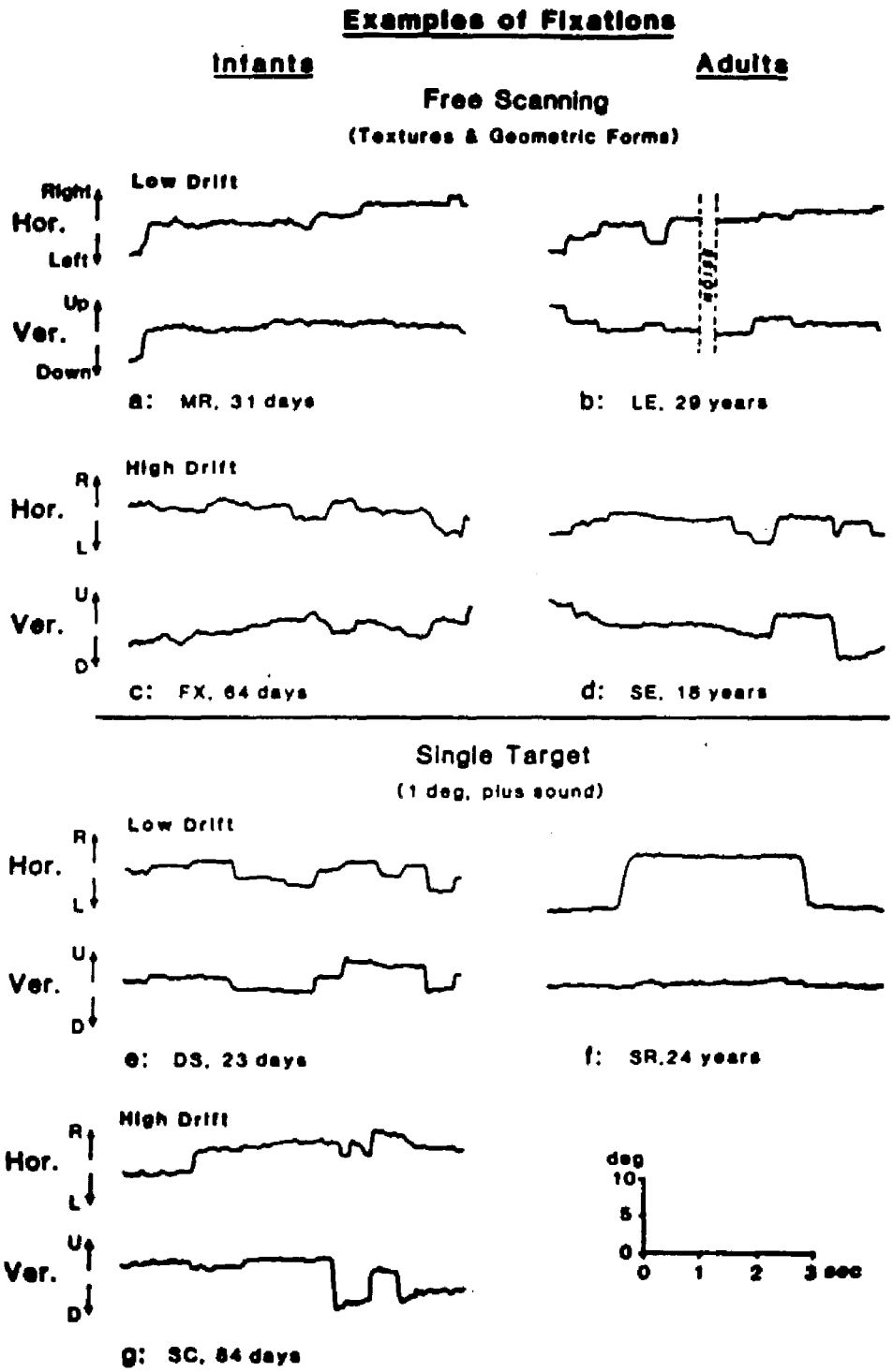
Examples of Fixations
Infants
Adults
Free Scanning
(Textures & Geometric Forms)
Low Drift
Right
Hor.
Left
Up
Ver.
Down
a: MR, 31 days
b: LE, 29 years
High Drift
R
Hor.
L
U
Ver.
D
c: FX, 64 days
d: SE, 18 years
Single Target
(1 deg, plus sound)
Low Drift
e: DS, 23 days
f: SR,24 years
High Drift
g: SC, 84 days
deg
10
5
0
0 1 2 3 sec

Figure 5

Frequency histograms of the durations of "Fixations" and "Drifts" for four typical infant subjects; free-viewing stimulus condition in the left panels and single target condition in the right panels. Each bar represents the frequency of "Drifts" (shaded portion) and "Fixations" (unshaded portion). Note the lack of bimodality indicating that "Drifts" and "Fixations" probably belong to the same category. Also note the similarity of the shapes of these histograms.

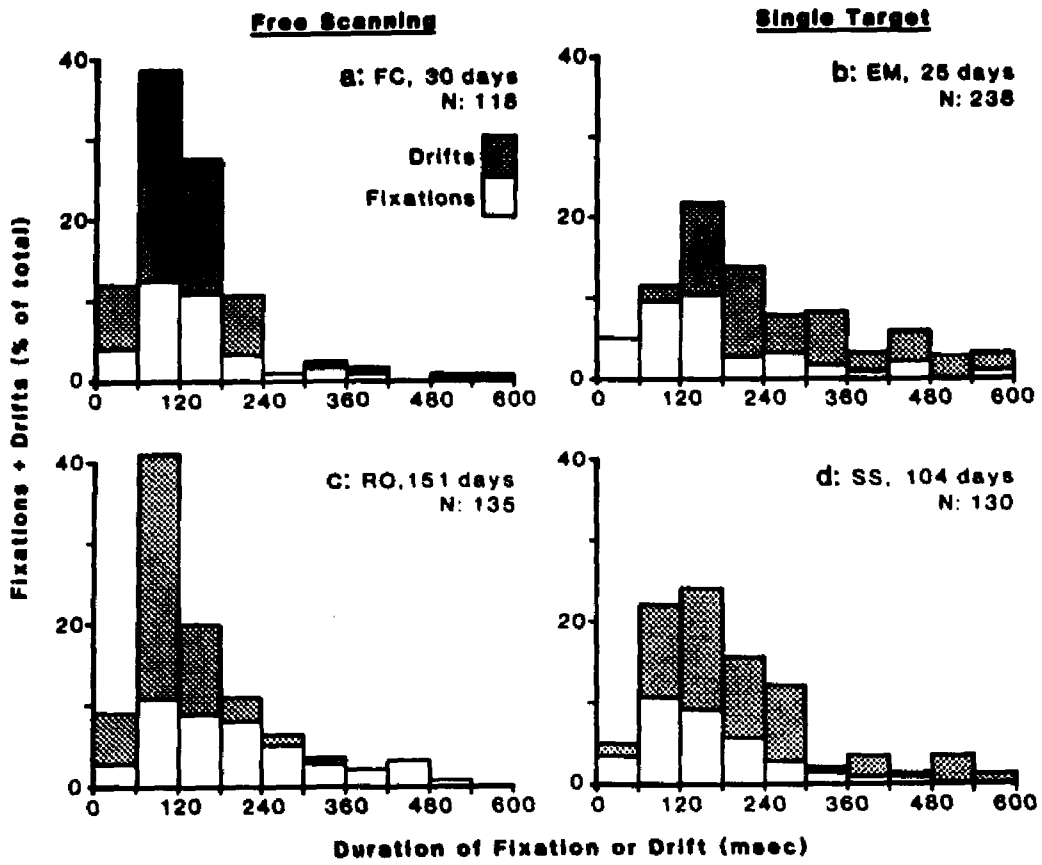
Free Scanning
Single Target
a: FC, 30 days
N: 118
Drifts
Fixations
b: EM, 25 days
N: 238
c: RO, 151 days
N: 135
d: SS, 104 days
N: 130
Fixations + Drifts (% of total)
Duration of Fixation or Drift (msec)
0
20
40
120
240
360
480
600

There is a similar lack of bimodality if, instead, the abscissa is drift magnitude or or drift rate. Although the lack of bimodality does not prove that there are not two populations of "Fixation" and "Drifts", it does show that they are not distinct and that there is a continuum from stationary to drifting segments and the parse operator was merely presented with a choice of two artificial categories for these non-saccadic segments. Henceforth, "Drifts" and "Fixations" will be combined into a single category called "Fixational segments" (FS).

3.2 Multiple Segments

It is apparent from Figure 4 for example, that an inter-saccadic interval (ISI) may sometimes contain more than one FS. This is even true for adults while free-viewing but occurs less often when adults view the single target. About 20% - 30% of ISI's which were uninterrupted by a "Noise" segment contained more than one FS. There are three plausible interpretations for this phenomenon:

a) Perhaps, multiple segments result from noise or artifact such that a single fixation becomes broken into more than one segment. Machine noise is unlikely since multiple segments do not appear so often when adults view the single spot, and as will be shown later, the amplitude of the segments is greater than would be expected from machine noise. The eye-tracker is not completely insensitive to head movements, which might account for some infant multiple segments. This does not explain why free-viewing adults exhibit these multiple segments since all adult subjects used the chin rest.

b) Multiple segments are not artifact but indicate that the eye actually changes direction during an ISI. Indeed, eye position during fixations is not perfectly stable even under the ideal conditions when a well-motivated and practised subject using a bite-bar is instructed to fixate a small high contrast target (e.g., Kowler and Steinman, 1979). Under these conditions, the standard deviation of eye position is about 10 minarc, and the mean speed of the eye is about 1/4 degree/sec (Skavenski, Hansen, Steinman, and Winterson, 1979). It seems quite plausible that instability of eye position could increase if the subjects are not instructed (and hence not motivated to give their best performance) and are not given a small high contrast fixation target, but rather, are given a large stimulus with a range of fine and coarse details and contrasts. Unfortunately, the stability of the eye during uninstructed free-viewing has not been studied quantitatively.

Another possibility is that eye drift might reflect the vestibular ocular reflex (VOR) in the infant. However, as stated in the Methods, only small amounts of eye translation are permitted before the eye-tracker's electronics fail. Moreover, the head compensation circuitry removes most of the parallax caused by eye translation whether this is caused by head translation or head rotation. There might be some residual uncorrected VOR drift, but the infant holder did not detect any head movement. Therefore, the contribution of VOR responses (if any) can only be small.[2]

---

[2] In any case, Skavenski et al. (1979) report only low VOR gains for small head rotations.

Thus, eye drift due to fixation instability may be a facet of free-viewing. Clearly, if the eye is stationary such direction changes cannot occur and would not appear in a typical adult fixation task (viz. the single target paradigm).

c) Because of the instrument resolution of about 0.5 degrees, it was difficult for the parse operator to detect saccadic eye movements with an amplitude under 1 degree. Multiple segments may actually be separated by small saccades, in which case ISI's with multiple segments could really be multiple ISI's.

We are unable to distinguish among these possibilities; indeed all three may be occurring to some extent. It follows, therefore, that the intervals between those saccades that are detected by the parse operator may be too long some of the time by argument (c) and so henceforth this interval will be called an "apparent inter-saccadic interval" (AISI). Where necessary, results will be shown for both FS's and AISI's so that conclusions will not be predicated on the validity of any of the above arguments. When no distinction is warranted, both FS's and AISI's will be called "fixations."

3.3 Fixation Parameters

Most eye movement records from infants conform to the general adult behaviour in that the eye passes through a usually alternating sequence of saccades and fixations. This behaviour is present at an early age and probably exists at birth. However, the stability of the eye between saccades is usually worse than adult fixational stability,

although even adults are far from stable under the free-viewing condition. In order to quantitatively examine infant and adult fixations, three paramaters were calculated from each parsed FS: duration (T), average drift rate (R), and amplitude (A). These measured quantities are related for any given fixation by:

$$A = RT. \qquad (1)$$

However, it is important to note that this equation may only hold in the algebraic sense and not necessarily in the mechanistic sense.[3] Thus, the amplitude of drift may indeed be the product of drift rate and duration; on the other hand, amplitude may be fixed and the eye drifts for a specific distance regardless of the rate of drift. Duration would then be mechanistically the ratio of amplitude to drift rate. By further contradistinction, amplitude might be mostly noise and drift would therefore be spurious. In this case there would be no detectable mechanism. Nevertheless, we can be sure that there is at least one degree of freedom since fixations do terminate, and no more than two degrees of freedom for Equation 1 to be true even algebraically (although there may be more than two mechanisms involved).

---

[3] By "mechanistic" we mean representing a physical process. Thus, A=BC indicates that quantity A physically occurs as a result of the process B times C. On the other hand, B=A/C indicates B is the result of the process A divided by C. Thus "=" indicates the direction of causality.

[4]
DURATION

Little is known about the durations of infant fixations. Most studies have concentrated on the direction of infants' gaze rather than the duration (see Introduction). Undoubtedly, a major reason for this has been the lack of temporal resolution in most of the previous techniques used for recording eye movements from infants. Therefore, the initial purpose of this Section is simply to describe the typical durations of fixations for infant subjects under different stimulus conditions and to compare the durations to those of adults. A more ambitious purpose here, and in subsequent Sections, is to begin to infer the mechanism that determines fixation duration, that is, the mechanism by which saccades are triggered. This Section will lay the foundation for a hypothesis which, it will be argued, can be extended to adults and possibly other species. If this extension is valid, the hypothesis will start to explain why fixation duration can appear, on the one hand, to be random, and on the other, to be quite deterministic in adults.

The anticipated errors in measuring duration will be outlined first. The difference between infant and adult mean duration as well as how duration depends on the stimulus conditions will then be reported. It will then be shown that the frequency distribution of

durations remains essentially invariant in shape across subjects and stimuli in spite of the large variations in the mean. The shape will then be identified to be close to the Exponential waiting time distribution. Finally, the findings will be compared to other studies and three classes of models will be discussed.

4.1 Errors in Measuring Duration of Fixations

The problems in identifying a fixation have already been discussed. Results for both FS's (fixational segments) and AISI's (apparent inter-saccadic intervals) will be shown. The temporal resolution of the instrument is 16.7 msecs (60 Hz). If we assume that an event has an equal probability of falling anytime within a 16.7 msec sampling window, then a rectangular probability distribution of error and the standard deviation of measuring the time between two events will be 6.8 msces. This error has no bias - there is an equal chance of underestimating or overestimating duration. For our purposes this error presents only a minor problem since it can be compensated for (Sheppard's correction) when estimating moments.

A more serious problem arises from the bandwidth limitations of the recording instrument. As explained in Appendix B, the measured durations of saccades will be increased by the poor response time of the eye-tracker. This extra response time will encroach on the subsequent ISI, and so on average, fixations will appear shorter than they really are. The underestimation on any particular fixation will depend on the amplitude and speed of the immediately preceeding saccade (if there was one). The worst underestimation will occur for

fixations that follow small amplitude saccades because small saccades have greater bandwidth (see Appendix B). We estimate this error to be about two sampling intervals (34 msecs) at worst. The underestimation for fixations following large saccades will be negligible. It is difficult to apply a correction factor since it will be stimulus-dependent because different stimuli will evoke saccades with different distributions of amplitude and speed (Hainline et al., 1984).

4.2 Stimulus Dependence

The mean duration of each infant's FS or AISI showed no developmental trend over the age range 7 to 169 days. The mean duration for all infants viewing a specific stimulus type was calculated for each stimulus type and is shown for FS's and AISI's in Figure 6. Because there was considerable variability in the duration of fixations for each subject, it was necessary to combine subject means to take both within subject and between subject variances into account. This is explained in Appendix D. For the free-viewing stimulus conditions, the average FS duration (open bars) is very brief (<200 msecs), which is about half the duration of the average adult FS. The shaded bars in Figure 6 show the mean durations for AISI's. These are obviously longer than FS's because, for some fixations, multiple segments are now concatenated. Nevertheless, AISI's are also very brief, 200-300 msecs, and are much shorter than adult AISI's which last about 400-500 msecs. Clearly, infants make many more saccades (about 4 per second) than adults (about 2 per second) under our free-viewing condition.

Figure 6

Mean fixation durations for different stimulus conditions. Means and standard errors were computed from each subject's mean and standard error using the scheme in Appendix D. Open bars depict Fixational segments (FS's) and shaded bars depict apparent inter-saccadic intervals (AISI's). Adults viewing the single target are not shown because of contamination from the target being moved by the experimenter; their durations would be off the ordinate scale.

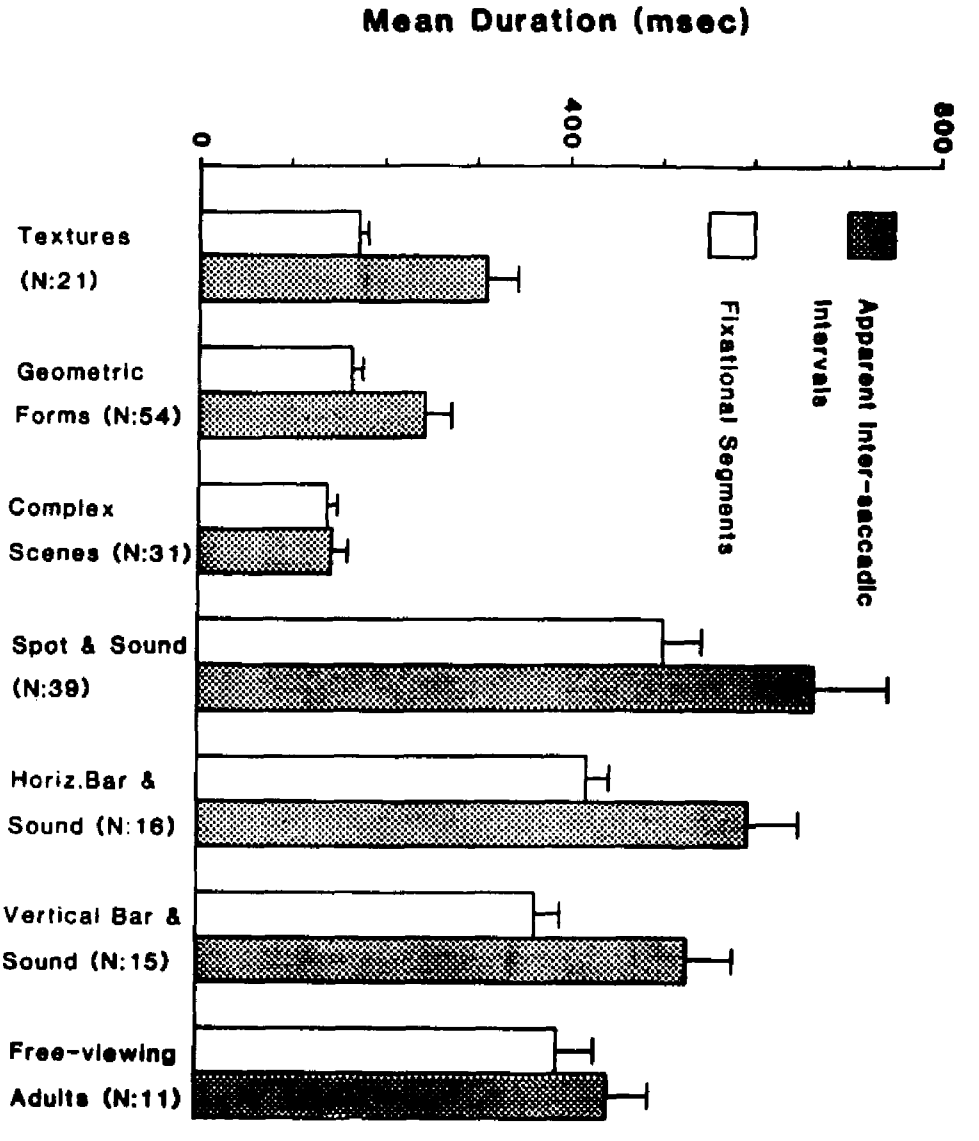
Mean Duration (msec)
0
400
800
Textures (N:21)
Geometric Forms (N:54)
Complex Scenes (N:31)
Spot & Sound (N:39)
Horiz.Bar & Sound (N:16)
Vertical Bar & Sound (N:15)
Free-viewing Adults (N:11)
Fixational Segments
Apparent Inter-saccadic Intervals

When infants viewed the single spot or bars with sound, the durations of FS's and AISI's were much longer, in excess of 500 msecs for the spot. Adults typically made saccades only when the stimulus was shifted to a new position, even though there were no explicit instructions to do so. Thus, mean duration for adults does not reflect any spontaneous activity but only the experimental conditions. Infants still produce spontaneous saccades even when viewing this rather sparse stimulus, although it must be remembered, of course, that infants cannot be instructed to fixate the small spot or bar. Although adults were not instructed, they were aware of their participation and probably formed an implicit task to follow the spot. (From an adult viewpoint, there was nothing else to look at.)

Thus, the average infant's fixation duration is not only shorter than the adult's but is also stimulus-dependent.

While the group means in Figure 6 illustrate the different central tendencies of fixation duration under different stimulus conditions, they conceal the considerable range of means among infants. This range is shown by the histogram in Figure 7. This histogram shows the distribution of mean fixation duration for all infant subjects regardless of stimulus conditions (similar distributions of means but with narrower ranges are obtained for each stimulus condition separately). The histogram in Figure 7 is positively skewed and far from Normal and suggests that the sampling variance, associated with each mean, increases with the mean in some systematic way. This prompts a closer examination of the distributions of durations for each subject.

Figure 7

Frequency histogram of the mean durations of all infant subjects. Fixational segments (FS's) are shown in the upper panel and apparent inter-saccadic intervals (AISI's) in the lower panel. Note the range in mean durations.

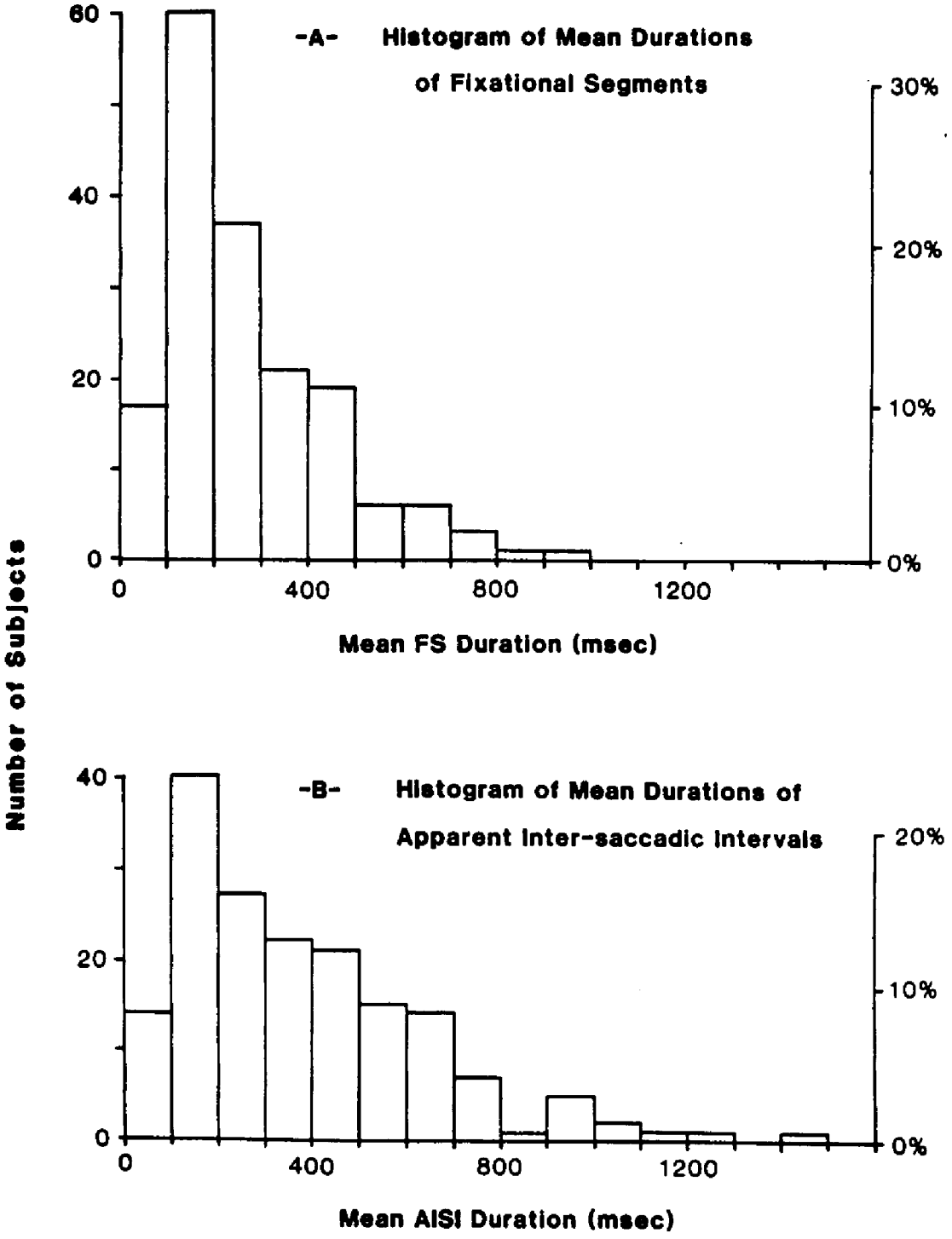
-A- Histogram of Mean Durations of Fixational Segments
60
40
20
0
30%
20%
10%
0%
0
400
800
1200
Mean FS Duration (msec)
Number of Subjects
-B- Histogram of Mean Durations of Apparent Inter-saccadic Intervals
40
20
0
20%
10%
0%
0
400
800
1200
Mean AISI Duration (msec)

4.3 Distribution Identification by the Method of Moments

The large body of data accumulated here together with the wide range of means provides an opportunity to examine the distributions by the method of moments. Moments are very efficient descriptors[4] of distributions since only a few numbers (in our case - 4) are needed to convey the shape rather than the customary frequency polygon. This is particularly worthy when there are so many distributions to describe. Moments also have inferential value provided enough moments are taken and estimated with sufficient precision. This is a powerful technique if many distributions can be obtained with wide ranging values for their moments (as in our case) since the relationships among moments can then be readily seen as trends. Therefore, for each subject the mean, the standard deviation, the third root moment (cube root of the third central moment), and the fourth root moment (fourth root of the the fourth central moment) were computed separately for FS's and AISI's. These moments were then corrected for sampling bias and plotted against each other. Root moments were preferred since the units then become the same (msecs rather than $msecs^2$, $msecs^3$, and $msecs^4$); sampling errors take on approximately the same order of magnitude, and so plotting is made easier. Details of moments are given in Appendix E.

In Figure 8 the sample standard deviation and mean of fixation duration are plotted against each other for each subject session, each

---

[4] But inefficient estimators (see Kendall and Stuart, 1979).

Figure 8

Plot of standard deviation against the mean of fixation duration for infant subjects. Each point represents one subject and each symbol represents one stimulus condition. Fixational segments are shown in the left panel and apparent inter-saccadic intervals (AISI's) in the right panel. Only subjects who produce 10 or more AISI's are shown. Bivariate regression for FS's: $Y = 1.23 (X - 40)$; $r = 0.96$; for AISI's: $Y = 1.28 (X - 60)$; $r = 0.93$. Standard errors of slopes = 0.03 and 0.04, and of intercepts = 7 and 18 msecs. The solid line depicts Exponential distributions: $Y = X - 50$.

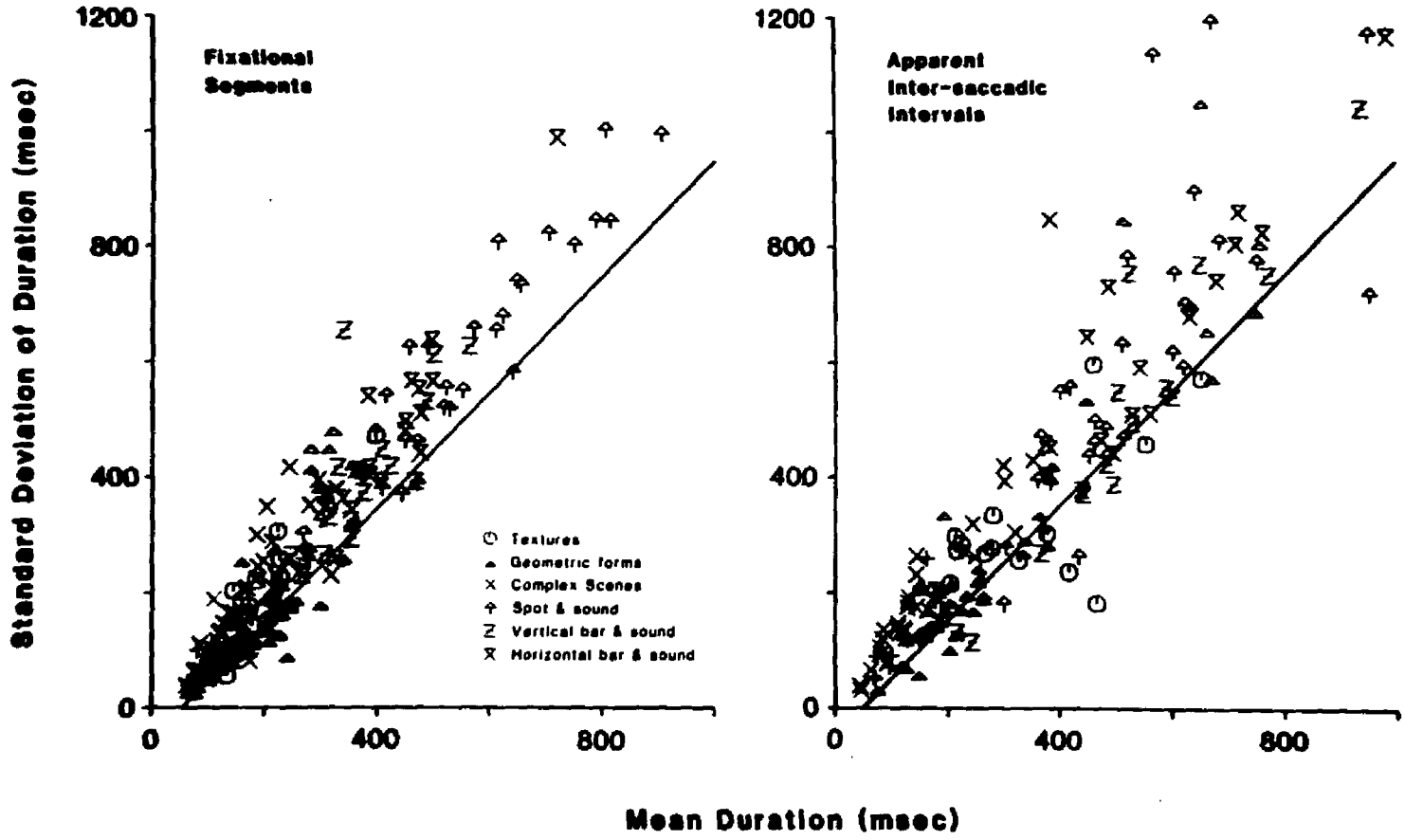
Fixational Segments
Apparent inter-saccadic intervals
Standard Deviation of Duration (msec)
Mean Duration (msec)
1200
800
400
0
0
400
800
Textures
Geometric forms
Complex Scenes
Spot & sound
Vertical bar & sound
Horizontal bar & sound

point representing one subject session. Different symbols correspond to different stimuli and all ages are included. Those sessions with less than 10 AISI's were excluded in order to maintain a reasonable sampling error. As can be seen, in spite of the variability, there is a linear relationship between the standard deviation and the mean with a slope of 1.23 ± 0.03 for FS's (r=0.96) and 1.28 ± 0.04 for AISI's (r=0.93), using bivariate regression.[5] The intercepts on the abscissa were 40 ± 7 msecs for FS's and 60 ± 18 msecs for AISI's. (We shall take a value of 50 msecs for the abscissa intercept for future discussions.) This shows that there exists a commonality among the distributions obtained from different subjects viewing different stimuli, that is, a similar mechanism or stochastic process is involved in all subjects.

Any kind of systematic relationship between mean and standard deviation indicates that the distributions are not Normal. The linearity of the trend in Figure 8 eliminates some other possibilities. For example, although the Poisson distribution has a similar shape to the duration distributions, it has a square root relationship between its mean and standard deviation - clearly distinguishable from a linear trend. Other distributions can be discounted on similar grounds. Table E1 in Appendix E shows the relationship between the mean and standard deviation for a variety of "classical" distributions. As can be seen, some distributions do have a linear relationship between

---

[5] For bivariate regression both variables are considered to be random rather than just one as in standard regression. The "best" straight line was found which had the least square error for both variables. This line was found by the "steepest descent" iterative procedure.

their mean and standard deviation. However, only the Exponential and Gamma distributions could exhibit a slope of unity or more. Both of these distributions are degenerate cases of the Pearson Type III class of distributions and are uniquely determined by, at most, the first four moments (Kendall and Stuart, 1977). In fact, the Exponential distribution can be considered as a special case of the Gamma distribution (where the latter has an index of unity), but the Exponential is an important and basic reference distribution in the study of "waiting-time" theory (sometimes called "queuing theory" or "survival analysis"), (Trivedi, 1982; Cox and Oakes, 1984).

The probability density of the Exponential distribution is given by:

$$\frac{1}{B} e^{(x-A)/B} \tag{2}$$

with mean and variance:

$$\begin{aligned} \mu &= A + B \\ \sigma^2 &= B^2 \end{aligned} \tag{3}$$

and hence:

$$\sigma = \mu - A. \tag{4}$$

Thus, the standard deviation of the Exponential distribution is a linear function of the mean with unit slope and intercept -A. The Exponential distribution is depicted by the solid line in Figure 8 with

an intercept of -50 msecs and unit slope. As can be seen, the data have a slightly higher slope. This difference will be returned to later.

In Figures 9 and 10, the third and fourth root moments (see Appendix E) are plotted against the standard deviation. The solid line represents the theoretical slope for the Exponential distribution. Central moments are independent of any offset parameter and show no intercept when plotted against each other. For the third root moment against the standard deviation, bivariate regression constrained to pass through the origin yields a slope of 1.30 ± 0.02 ($r=0.99$) for FS's and 1.23 ± 0.03 ($r=0.98$) for AISI's; the Exponential distribution has a slope of 1.26. For the fourth root moments, the slopes were 1.79 ± 0.03 ($r=0.98$) for FS's and 1.73 ± 0.03 ($r=0.98$) for AISI's; the Exponential has a slope of 1.73.

It should be noted that trends similar to those in Figures 8, 9, and 10 also appear if each stimulus condition is plotted separately. However, because each condition has fewer subjects and a narrower range of mean durations, they produce lower correlations.

In Figure 11, the moments of duration for 11 naive adults under free-viewing conditions are shown. These adults were given no instructions and viewed the "texture" and "geometric form" stimuli. The trends are quite similar to those obtained from the infant. The correlation between the standard deviation and the mean is weaker for the adults than the infants: for FS's $r=0.80$ and for AISI's $r=0.79$ (compared to 0.99 and 0.98 for the infants). However, these correlations are still significant ($p<0.01$) and are lower than for the infants

Figure 9

Plot of the third root moment (cube root of the third central moment) against the standard deviation of fixation duration for infant subjects. Each point represents one subject and each symbol represents one stimulus condition. Fixational segments are shown in the left panel and apparent inter-saccadic intervals (AISI's) in the right panel. Only subjects who produce 10 or more AISI's are shown. Bivariate regression through the origin for FS's: $Y = 1.30\ X$; $r = 0.99$; for AISI's: $Y = 1.23\ X$; $r = 0.98$. Standard errors of slopes = 0.02 and 0.03. The solid line depicts Exponential distributions: $Y = 1.26\ X$.

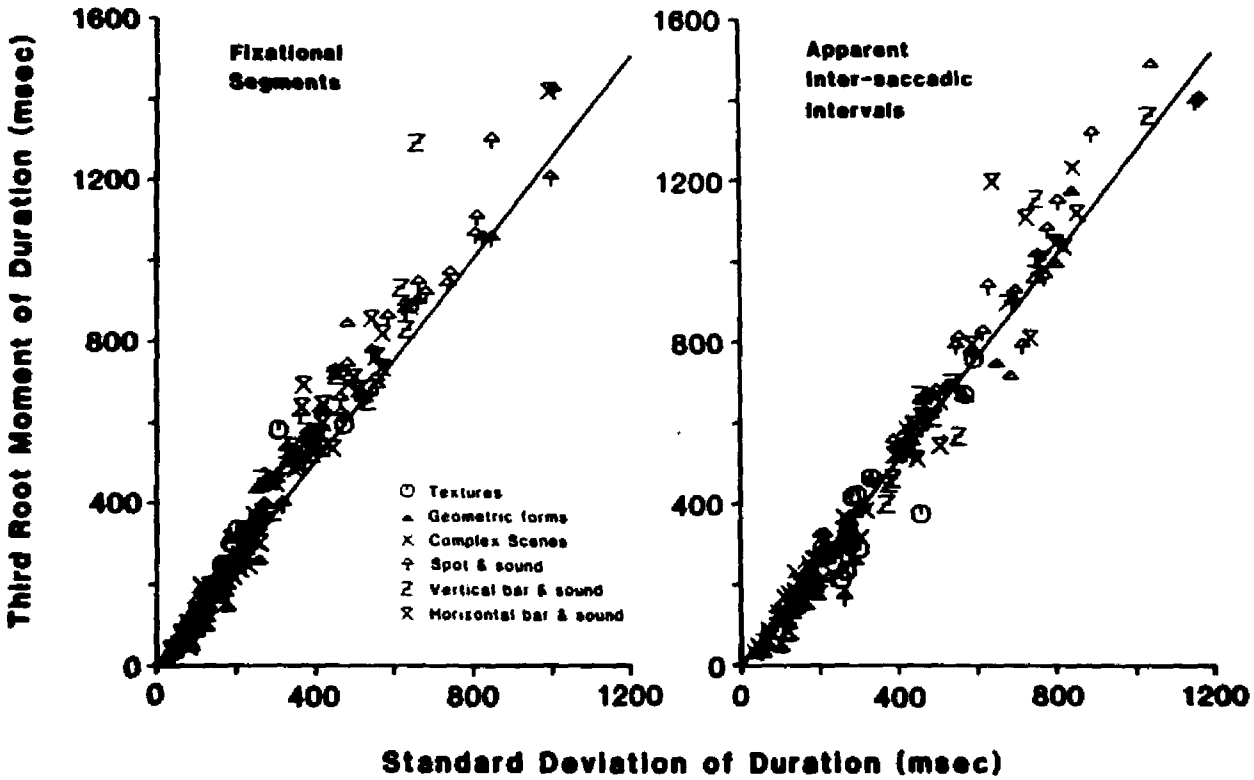
Fixational Segments
Apparent inter-saccadic intervals
Third Root Moment of Duration (msec)
Standard Deviation of Duration (msec)
0
400
800
1200
1600
Textures
Geometric forms
Complex Scenes
Spot & sound
Vertical bar & sound
Horizontal bar & sound

Figure 10

Plot of the fourth root moment (fourth root of the fourth central moment) against the standard deviation of fixation duration for infant subjects. Each point represents one subject and each symbol represents one stimulus condition. Fixational segments are shown in the left panel and apparent inter-saccadic intervals (AISI's) in the right panel. Only subjects who produce 10 or more AISI's are shown. Bivariate regression through the origin for FS's: $Y = 1.79\ X$; $r = 0.98$; for AISI's: $Y = 1.73\ X$; $r = 0.98$. Standard errors of slopes = 0.03. The solid line depicts Exponential distributions: $Y = 1.73\ X$.

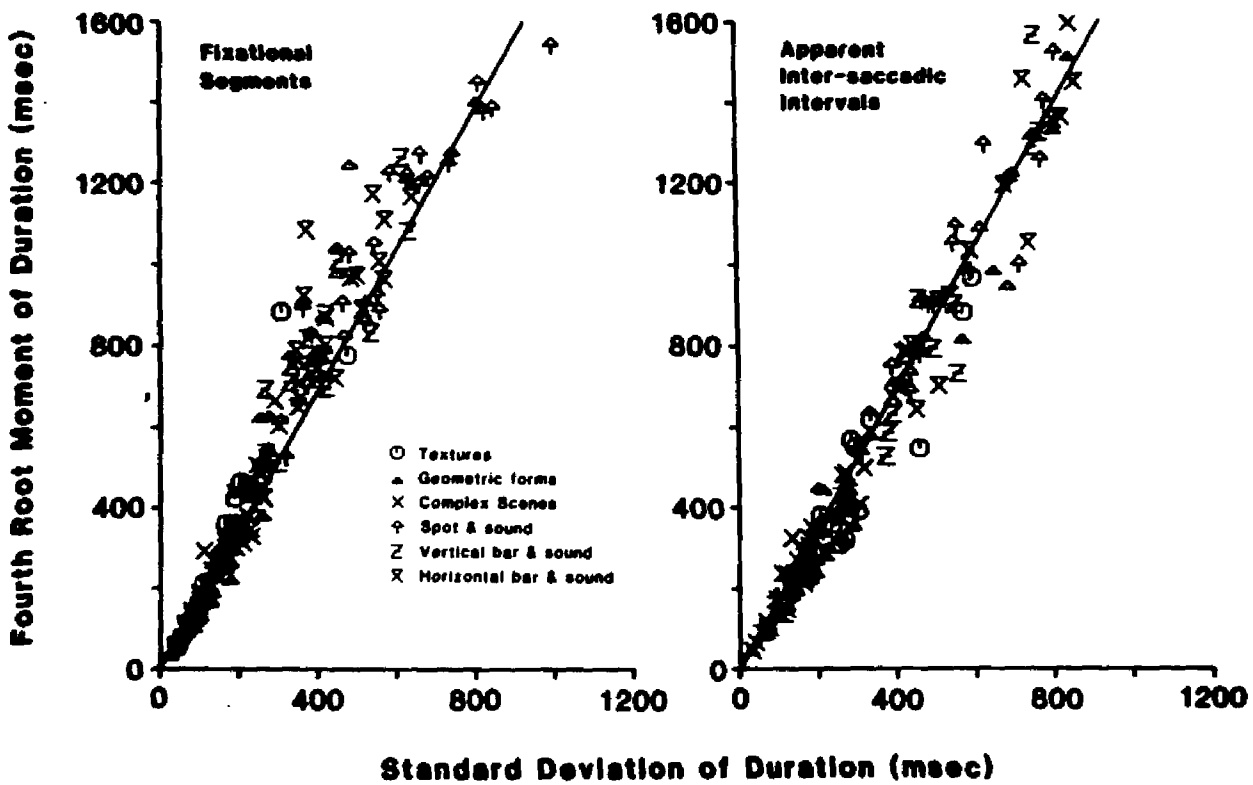
Fixational Segments
Apparent Inter-saccadic Intervals
Fourth Root Moment of Duration (msec)
Standard Deviation of Duration (msec)
0
400
800
1200
1600
Textures
Geometric forms
Complex Scenes
Spot & sound
Vertical bar & sound
Horizontal bar & sound

Figure 11

Plots of root moments of fixation duration for 11 free-viewing adults. Left panels show fixational segments (FS's) and right panels show apparent inter-saccadic intervals (AISI's). Upper panels show the standard deviation vs. the mean. Bivariate regression for FS's: $Y = 1.60 (X - 170)$; $r = 0.80$; for AISI's: $Y = 1.04 (X - 50)$; $r = 0.79$; standard error of slopes = 0.4, of intercepts = 100 msecs. Middle panels show third root moment vs. standard deviation. For FS's: $Y = 1.43 X$; $r = 0.98$; for AISI's: $Y = 1.37$; $r = 0.92$; standard errors of slopes = 0.1 and 0.2. Lower panels show fourth root moment vs. standard deviation. For FS's: $Y = 2.0 X$; $r = 0.97$; for AISI's: $Y = 1.84 X$; $r = 0.88$; standard errors of slopes = 0.2. The solid line in all panels shows the Exponential distribution with slopes of 1.0, 1.26, and 1.73 in the upper, middle, and lower panels. The intercept on the abscissa for the Exponential in the upper panels is 100 msecs.

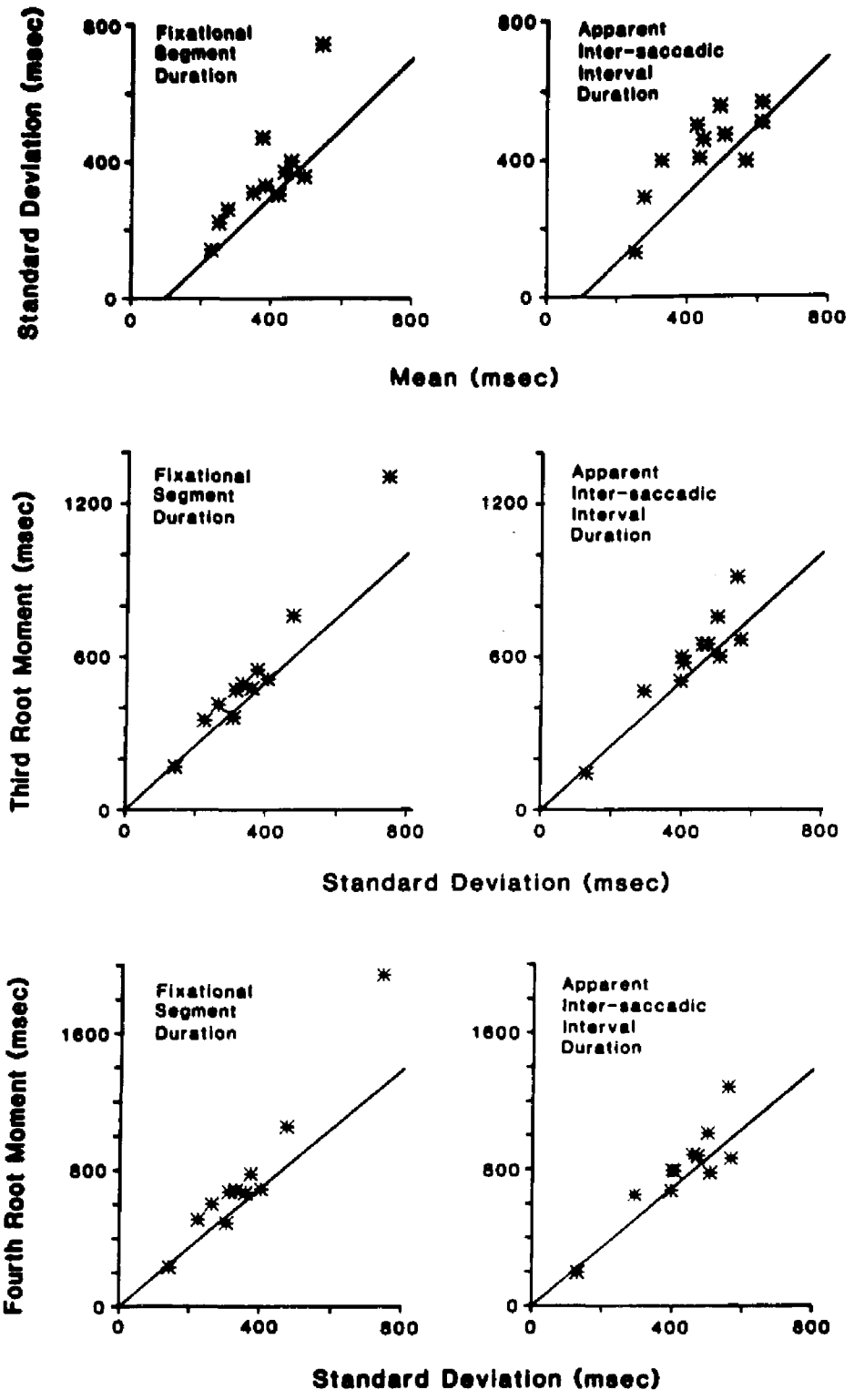
Standard Deviation (msec)
Fixational Segment Duration
Apparent Inter-saccadic Interval Duration
800
400
0
0
400
800
Mean (msec)
Third Root Moment (msec)
1200
600
Standard Deviation (msec)
Fourth Root Moment (msec)
1600
800
Standard Deviation (msec)

probably because of the reduced sample size and range. Bivariate regression yields slopes of 1.60 for FS's and 1.04 for AISI's with a standard error of about 0.4, and intercepts on the abscissa of 170 msecs for FS's and 50 msecs for AISI's with a standard error of about 100 msecs. Our confidence in the intercept is poor but it appears to be greater than for infants (50 msecs). We shall take a value of 100 msecs as a rough estimate for future discussions. For the third root moment plotted against the standard deviation, bivariate regression yields slopes of 1.43 ± 0.1 (r=0.98) for FS's and 1.37 ± 0.2 (r=0.92) for AISI's; the Exponential has a slope of 1.26. For the fourth root moment against standard deviation, the slopes are 2.0 ± 0.2 (r=0.97) for FS's and 1.84 ± 0.2 (r=0.88); the Exponential has a slope of 1.73. There is a similarity between the observed moments and the theoretical moments of the Exponential distribution (solid line in 11), especially when alternative classical distributions are considered. However, there are differences between the observed moments and the moments expected from the pure Exponential distribution for infants and adults. These differences will be discussed later after an appropriate context has been developed.

4.4 The Exponential Distribution

We will now attempt to explain why fixation durations might have an Exponential (or close to) distribution. The Exponential distribution belongs to a class of probability distributions that have well known mechanisms associated with them; the Exponential is the basic "waiting-time" distribution. To illustrate this, first consider time to

be in discrete units of, say, δt, so that time proceeds δt, $2\delta t$, $3\delta t$....etc.. Also, let the oculomotor system be in a state of fixation to begin with, at t=0. We now define p_i as the probability that an event which will terminate the current fixation (usually a saccade), will occur at time $t=i\delta t$. We now wish to find the probability that the *first* terminating event will occur after $t=n\delta t$, that is, the probability that a fixation will have a duration, T, of at least $n\delta t$. Clearly, this is given by the probability that no terminating events occur in the first n time units, which will be given by:

$$P(T>n\delta t) = (1 - p_1)\ (1 - p_2)\ \ldots\ (1 - p_n) = \prod^{n} (1 - p_i) \qquad (5)$$

The probability that the duration will be exactly $n\delta t$ is then simply:

$$P(T=n\delta t) = P_{n+1} \prod^{n} (1 - p_i) \qquad (6)$$

If we now make the crucial assumption that the probability of a terminating event is *Independent* of time, that is, it has an equal chance of occurring at any time then $p_1 = p_2 = \ldots = p_n = p$. The probability of a fixation duration equalling $n\delta t$ then becomes:

$$P(T=n\delta t) = p(1 - p)^n \qquad (7)$$

This is the Geometric probability distribution and it describes the probability of the first "success" in a sequence of independent Bernoulli trials. If δt is allowed to become arbitrarily small in such a way

that the probability per unit time of a terminating event, np/t, remains at a constant value, λ, the discrete Geometric distribution becomes, in the limit, the continuous Exponential distribution:

$$P(T>n\delta t) = (1 - \lambda t/n)^n \tag{8}$$

From the above equation and assumptions:

$$P(T<t) = 1 - \lim_{n\to\infty} [(1 - \lambda t/n)^n] = 1 - e^{-\lambda t} \tag{9}$$

which has a probability density of:

$$f(t) = \frac{d}{dt}[P(T<t)] = \lambda e^{-\lambda t} \tag{10}$$

Thus the Exponential distribution describes the probability density of the "waiting-time" for the first event given that the probability of an event remains constant throughout time. The Exponential distribution has the important property of being the *only* waiting-time distribution that requires no memory. (Conversely, any other waiting-time distribution must have memory.) A more general version of the Exponential can be obtained by shifting the time origin by A (location parameter):

$$f(t) = \lambda e^{-\lambda(t-A)}, \quad t \geq A \tag{11}$$

In this case no event occurs during the time A and outside this time window an event occurs with constant probability per unit time. Fig-

Figure 12

The pure Exponential distribution with different means but with the same location parameter, A. The top distribution has a mean = 0 and a standard deviation = 1; the middle distribution has a mean = 1 and a standard deviation = 2; the lower distribution has a mean = 3 and a standard deviation = 4.

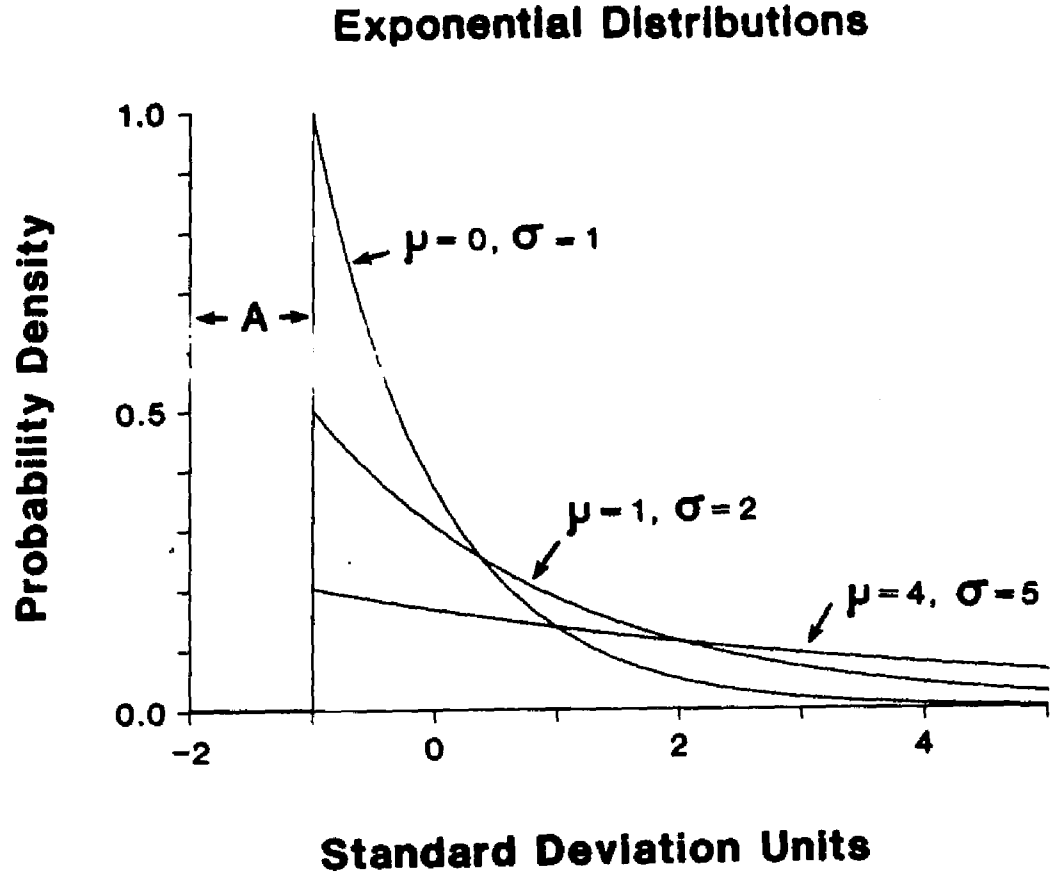
Exponential Distributions
Probability Density
1.0
0.5
0.0
A
μ = 0, σ = 1
μ = 1, σ = 2
μ = 4, σ = 5
−2
0
2
4
Standard Deviation Units

ure 12 illustrates the general Exponential distribution with examples having different means but the same location parameter.

Therefore, the general Exponential is a waiting-time distribution with two-distinct time regimes. It is important to note that the actual sequence of these regimes cannot be determined from the probability distribution.

The finding that infant and adult fixations (at least under free-viewing conditions) can be closely described by an Exponential distribution together with the above discussion allow fixations to be recast in a different perspective. Fixations have two components: There is a minimum period of time in which, on average, fixations are not terminated. The intercepts in Figures 8 and 11 indicate that this period lasts about 50 msecs for infants and about 100 msecs for adults, although there is considerable variability between subjects. Besides this period, there is a waiting-time during which there is a constant probability per unit time of a fixation being terminated. We shall call these two periods the A-period and the B-period to allow easy reference and to avoid any implied or accidental connotations.

4.5 Departures From Exponentiality

Although the representation of the infant and adult data by the Exponential distribution is reasonable, it is not perfect. There are two salient departures from Exponentiality: First, the slopes of the plots in Figures 8, 9 and 10 are slightly higher than that expected from a pure Exponential distribution. Second, the general shape of the frequency distributions is more rounded at the transition from the

A-period to the B-period than the Exponential (see modes in Figure 5).

Two views on these departures can be taken. One possibility is that the underlying distribution is not Exponential at all and a completely different model is necessary. It is, of course, impossible to reject unequivocally such an hypothesis because of the infinity of possible probability distributions. The second possibility is that the fundamental distribution is indeed Exponential, and that the departures represent either some perturbation of the Exponential or some other waiting-time distribution closely allied to the Exponential. Because of the reasonably good fit to the Exponential (especially for the central moments) and because of the mechanistic underpinning to the Exponential, this second possibility will be pursued.

As discussed earlier, the Exponential is characterised by the fact that the probability of a terminating event remains constant throughout time. If this probability does change during a fixation, then the distribution is no longer Exponential but some other waiting-time distribution. A waiting-time distribution is completely determined by the time course of the probability of the terminating event (e.g., see Papoulis, 1965 and Appendix F), which we shall call the "termination rate" (also known as "failure rate", "conditional failure rate", "hazard function", "mortality curve"). If the termination rate increases in time, the waiting-time distribution is less dispersive than the Exponential, that is, it is "hypoexponential." Conversely, if the termination rate decreases in time the distribution becomes "hyperexponential." Among the hyperexponential waiting-time distributions,

the well documented are the Hyperexponential, Gamma, Weibull, Log Normal, Log Logistic, and the Compound Exponential (see Trivedi, 1982). Cox and Oakes (1984) have suggested that by plotting the third standardised moment (skewness, see Appendix E) against the coefficient of variability, waiting-time distributions can be distinguished. This was attempted. The observed relationships were so far away from the Log Logistic and Log Normal distributions that these distributions were immediately discounted as possible explanations for our data. However, our sample sizes (100 fixations or less) produced enough sampling error to obscure any differences among the Weibull, Gamma, and the Compound Exponential distributions.

4.6 Compound Exponential - Fluctuations in the B-period

The Weibull, like the Gamma distribution, has no clear mechanism for an index parameter that is less than unity (that is, hyperexponential distributions). The Compound Exponential distribution, on the other hand, is very simple to explain. Here, the termination rate remains constant during a fixation but takes on a new value for each new fixation. Each fixation is then purely Exponentially distributed but with a different mean (reciprocal of the termination rate). Thus, observing many fixations will give rise to an Exponential where the mean varies. Such a distribution is inevitably hyperexponential because of the extra variability associated with the mean. The Compound exponential distribution will depend on the distribution (or variations) of the termination rate (the "compounding distribution"). Figure 13 shows a plot of the sequence of fixations (FS's) for a typi-

Figure 13

A plot of the sequence of fixations (FS's) for an infant showing the duration of a fixation against its ordinal position in the sequence of fixations in time during the recording session. Fixation durations (ordinate) are shown in standard deviation units from the mean of all durations in the recording session. The modal duration is at approximately -0.5 standard deviations with the density of outliers falling off above the mean. The down-arrows and dashed lines point to sequences of short durations that have a significantly low probability of occurrence ($p<0.05$) assuming an Exponential parent distribution. These sequences are probably due to fluctuations in the standard deviation (the B-period) of the parent distribution. Similarly, the up-arrows and dashed lines point to fluctuations in the modal value (the A-period) of the parent distribution. These causes of non-stationarity indicate the existence of a compound Exponential (see text).

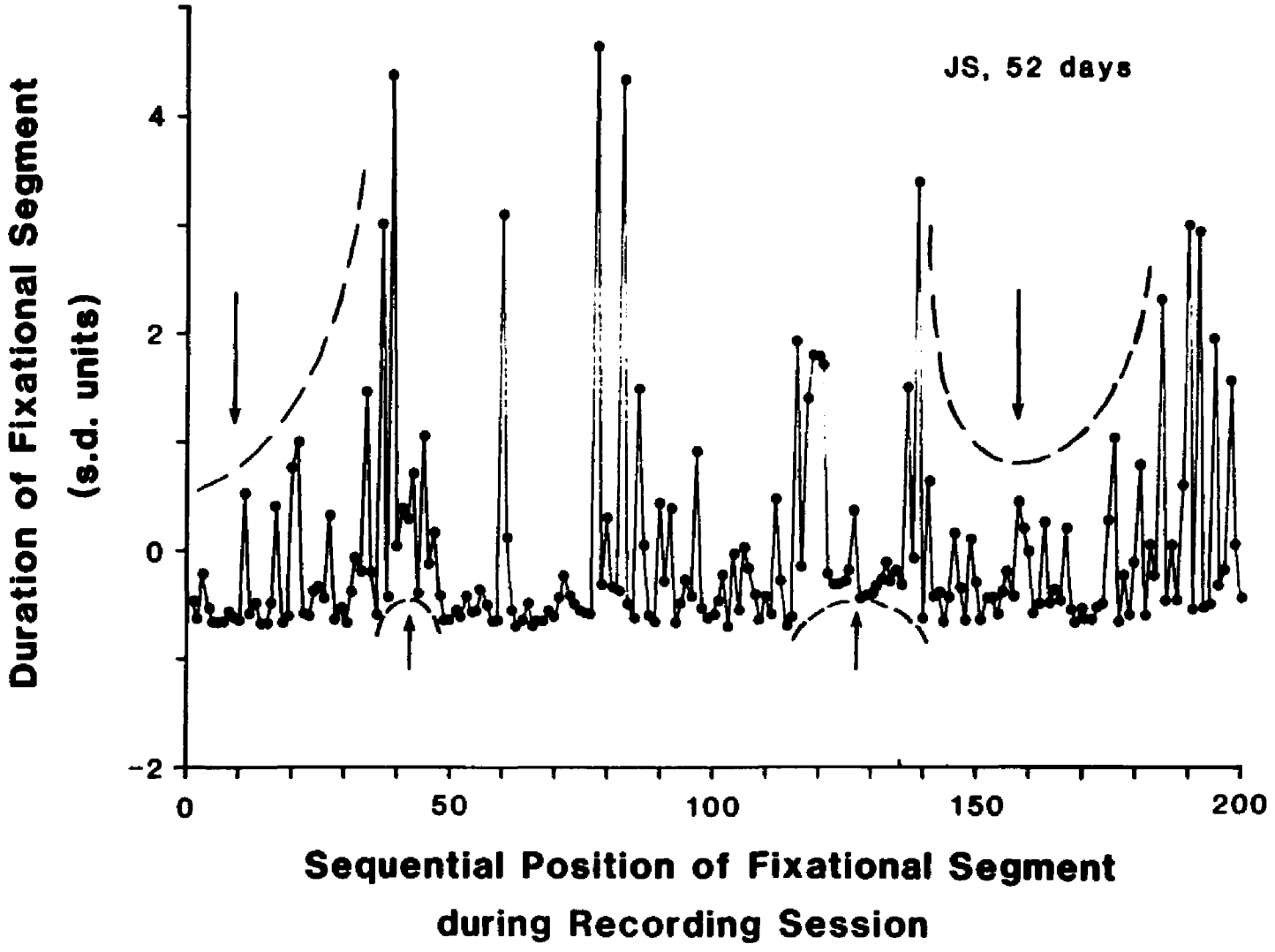
JS, 52 days
Duration of Fixational Segment
(s.d. units)
4
2
0
-2
0
50
100
150
200
Sequential Position of Fixational Segment
during Recording Session

cal infant subject viewing the spot with sound. The ordinate is the duration in standard deviation units from the mean and the abscissa is the sequential position of the fixation during the recording session. As can be seen there is no systematic change in fixation duration but there are sequences of brief FS's shown by the dashed lines and down-arrows. The probability of any one of these sequences of short durations occurring is less than 0.05, assuming an Exponential parent distribution. These fluctuations can be found in all subjects and corroborate the Compound Exponential model.

Different compounding distributions will give rise to different overall Compound Exponentials which will be reflected in their moments. Mathematical intractability prevents direct identification of the compounding distribution from the observed moments. However, for some special cases, the moments of theoretical Compound Exponentials can be calculated and compared to the observed moments to give, at least, a general idea of the shape of the compounding distribution for fixation duration. One special case is where the compounding distribution is the Gamma distribution. This yields the so-called "Pareto" Compound Exponential distribution (Cox and Oakes, 1984). The moments of the Pareto distribution were calculated for a variety of parameter values (see Appendix F). A parameter value of 7 produced the best fit for the first three moments but was far too high with respect to the fourth root moment, indicating that the Gamma is a too leptokurtic model. Another special case is the rectangular compounding distribution which yields a Compound Exponential (which we shall refer to as the "Rectangular Exponential") whose moments provide a

Table 1

Comparison of

Observed Moments to Theoretical Moments of Compound Exponentials

	Observed Regression Slopes*		Theoretical Slopes†				
	Constrained Through Origin	(Unconstrained)	Pure Exponential	Gamma Exponential		Rectangular Exponential	
	FS	AISI	‡ V_λ = 0%	20%	30%	20%	30%
$\frac{\sigma}{\mu - A}$	(1.23)	(1.28)	1.00	1.04	1.11	1.04	1.10
${}_3\mu^{1/3}/\sigma$	1.30 (1.38)	1.23 (1.46)	1.26	1.28	1.31	1.31	1.37
$\mu^{1/4}/\sigma$	1.79 (1.82)	1.73 (1.93)	1.73	1.84	2.01	1.83	1.95

* Standard errors of bivariate regression slopes $\sim$ 0.03.

‡ $V_\lambda = \sigma_\lambda / \mu_\lambda$

† $P(X=x) = \lambda e^{-\lambda x}$, where λ is the compounding random variable.

Pure Exponential: $P(\lambda=y) = \delta(y - \mu_\lambda)$

Gamma Exponential (Pareto): $P(\lambda=y) = \frac{1}{\Gamma(p)} y^{p-1} e^{-y}$

Rectangular Exponential: $P(\lambda=y) = 1/(b-a)$, $0<a<b$, $a<y<b$

better fit to the observed moments as summarised in Table 1. Clearly, if mathematical tractability were abandoned, perseverance with numerical techniques would yield a well fitting platykurtic compounding distribution. The difference in the shape of the Pareto distribution (solid line) and the pure Exponential distribution (dotted line) is shown by Figure 14 to be quite small (which illustrates the finesse of the method of moments).

4.7 Fluctuations in the A-period

The second departure from Exponentiality is the rounded transition between the A-period and the B-period (see the modes in Figure 5). The rounded transitions from the A-period to the B-period can be explained by fluctuations in the A-period from fixation to fixation. The up-arrows in Figure 13 show some possible variation in the A-period. Fluctuations in the A-period are also evident from the difference in the scatter between Figures 8, 9 and 10. There is more variability when the standard deviation is plotted against the mean than when the third or fourth root moments are plotted against the standard deviation. This is unusual since one would expect the reverse. However, the mean is much more sensitive to any changes in the A-period than the central moments. Central moments will be affected to some degree by A-period fluctuations and may account for some of the hyperexponentiality discussed above.

4.8 Discussion

We will now summarize these results and compare them to other

Figure 14

The "Pareto" distribution (solid line) is an example of a compound Exponential. The dotted line shows a pure Exponential distribution with the same mean and location parameter. Abscissa is shown in standard deviation units of the Pareto (mean = 0).

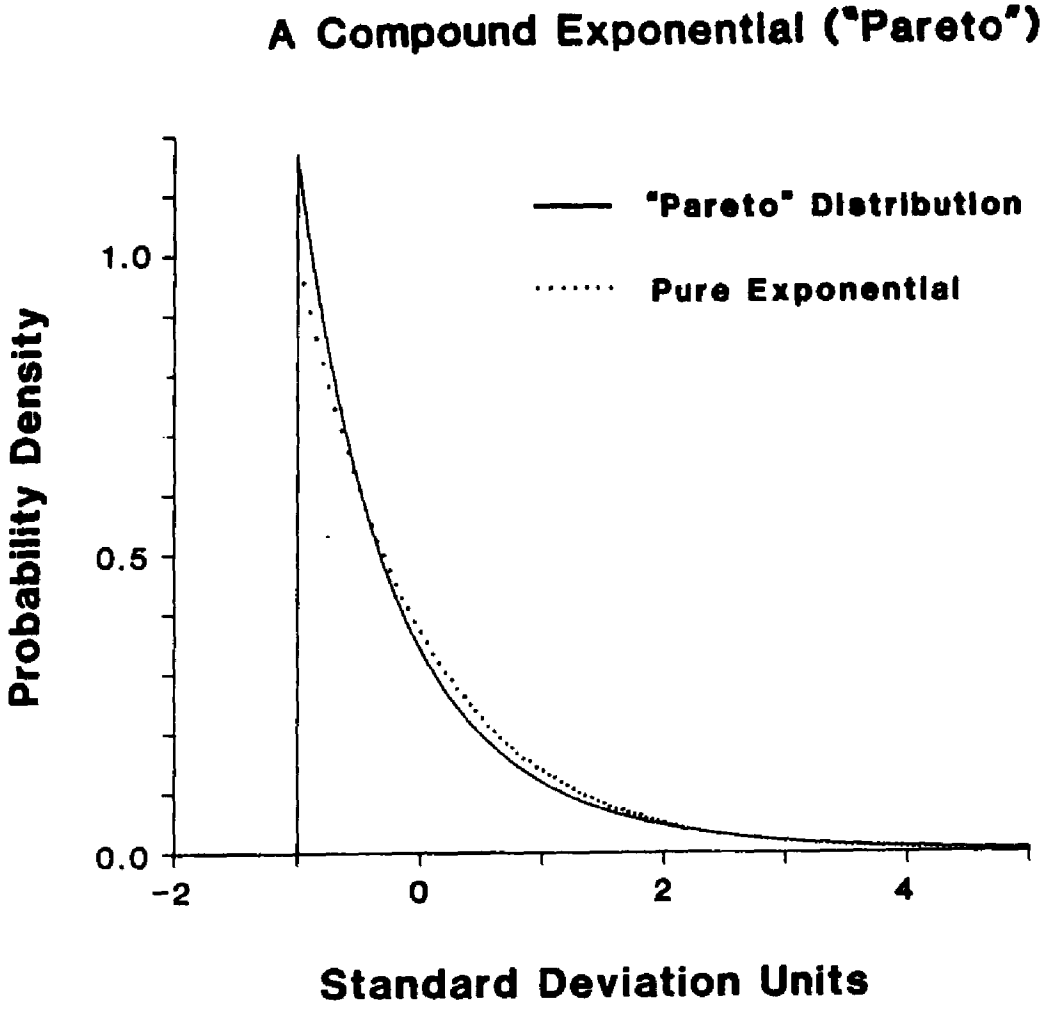
A Compound Exponential ("Pareto")
"Pareto" Distribution
Pure Exponential
Probability Density
1.0
0.5
0.0
-2
0
2
4
Standard Deviation Units

work. The implications for the oculomotor system will then be discussed with respect to alternative classes of models.

We have found that the distribution of fixation duration (FS's or AISI's) has the same form for all subjects, including adults, regardless of age or stimulus conditions. We conclude that the same mechanism or stochastic process underlies fixation termination for all subjects - at least under free-viewing conditions. The distribution shape is close to Exponential but slightly more dispersive (hyperexponential) which strongly suggests that fixation termination is a waiting-time process. We have emphasised the compound exponential model where each fixation is purely Exponential but has a different mean. It has been shown that, besides the waiting-time (B-period), there is a minimum period during which terminating events do not occur (A-period). We estimate this period to be about 50 msecs in the infant and about 100 msecs in the adult.

Fixation duration (or inter-saccadic interval) has also been fractionalised in other studies in an attempt to explain how saccades are triggered or "programmed" (Becker and Jurgens, 1979; Hallett and Adams, 1980). By using a double step target to elicit saccades from instructed subjects (Wheeless, Boynton, and Cohen, 1966), Becker and Jurgens (1979) have broken down an ISI into a sequence of subprocesses, each requiring an amount of time for completion. In particular, they isolate three subprocesses: an afferent delay for signalling a new target position, a central decision and computing stage, and an efferent delay to transmit the motor signal to the saccade generator. These stages are in a "pipeline" so that one stage can be

processing for one saccade while the earlier stage is processing for the next saccade. An inappropriate saccade at one stage can be cancelled depending on the outcome of a later stage. Becker and Jurgens set the whole process to take about 280 msecs, but of course, there can be considerable overlap between consecutive saccades because of the pre-programming capability of their model.

Hallett and Adams (1980) have taken a similar approach based on the "anti-saccade" paradigm (Hallett, 1978), where the subject is instructed to look in the opposite direction to a peripheral target. They term afferent, computational, and efferent delays as "low-level" processes which have more-or-less fixed durations, and they term the decision making process as a "high-level" process which is highly variable from one saccade to the next and idiosyncratic for subjects. It is tempting to draw parallels between Hallet and Adams' low-level process and our A-period, and their high-level process and our B-period. However, they set the minimum duration for their low-level process to be about 110 msecs, which is considerably more than the A-period for our infant subjects (50 msecs) but similar for our adults (100 msecs). Although we may have underestimated our A- and B-periods by one or two sampling intervals (17 - 34 msecs) because of bandwidth (see Section 4.1), both the models of Becker and Jurgens and Hallett and Adams require processes which are longer than our infant A-periods, even if we neglect the decision processes in their models.

More recently Fischer and Boch (1983) have elicited saccades from well-trained monkeys with very short latencies (70 - 80 msecs).

In their paradigm, the central fixation light was turned off 200 msecs before the peripheral target light was turned on. These extremely short latencies seem to show that saccades can be visually triggered without any decision process (Fischer and Boch, 1984) and probably do not involve cortical pathways (Boch, Fischer, and Ramsperger, 1984). Boch and Fischer (1983) suggest that the monkey learns to automate its responses at the subcortical level with training. Express saccades, per se, have not been identified in human subjects, but using a similar paradigm, Saslow (1967) measured quite short latencies (110 msecs). It is not known whether these are the homologue of the monkey express saccade, Nevertheless, it is difficult for the models of Becker and Jurgens (1979) and Hallett and Adams (1980) to account for these short latency saccades. If we can use results from the monkey as a model of human saccade triggering, then it seems that we ought to conclude from Fischer and Boch (1984) that there is more than one pathway for visually triggered saccades depending on the degree of cortical involvement in the task. Clearly, the degree of cortical involvement may become an important consideration in examining fixation duration, especially in the infant. We will return to this issue later in Section 5.

While the various variations of the Wheeless paradigm to elicit saccades may have some relevance to the A-period in terms of fixed processes, these models have less to say about the highly variable Exponential B-period which dominates most fixations in free-viewing. For this we must turn to studies which allow the subject more freedom of viewing targets.

Although fixation duration (or inter-saccadic interval) is commonly measured in eye movement studies, the actual distribution shape is seldom reported. Nevertheless, all of the studies surveyed depict a highly positively skewed distribution for duration. For example, Cohen (1977), reports a distribution with mean of 0.36 secs, a standard deviation of 0.22 secs, and a skewness of 2.18 (skewness = 2.0 for the Exponential), obtained from a subject under simulated automobile driving conditions; this is also slightly hyperexponential. Ellis and Smith (1985) found the distribution of fixation durations of airline pilots viewing dynamic displays of air traffic to have positive skew from 1.84 to 2.64 (which embraces the Exponential), means of 341 - 554 msecs, and standard deviations of 282 - 498 msecs. These data would suggest an A-period of about 60 msecs. Schoonard, Gould and Miller (1973) show positively skewed distributions for subjects under a variety of inspection tasks. Similar distributions are shown by McConkie, Zola and Wolverton (1985) in a perceptual span experiment in reading. Some studies show only composite distributions averaged across more than one subject (Enoch, 1959). These distributions are still positively skewed but more rounded than single subject distributions. However, this would be expected since averaged Exponentials result in Gamma-like distributions (e.g. see Papoulis, 1965).

Turning to other species, the distribution of intersaccadic intervals in the cat (Young, 1981) and the monkey (Fischer and Boch, 1984) are again positively skewed and appear to be exponential in shape. Perhaps the most striking is a report on two avian species, the Tawny Frogmouth and the Little Eagle (Wallman and Pettigrew,

1985). The Little Eagle produces saccades with a mean interval of 285 msecs and a standard deviation of 213 msecs. The Tawny Frogmouth has a much lower rate of saccade production with a mean ISI duration of 40.8 secs and standard deviation of 39.0 secs. This clearly shows the almost unit slope relationship between mean and standard deviation of the Exponential distribution.

Although we cannot prove that the distribution of fixation durations from these studies are Exponential, they do appear to be exponential in character regardless of the viewing task or even species. The only exception that could be found was for "express saccades" (Fischer and Boch, 1984) whose latency distributions are roughly symmetrical. However, it could be discerned from all of the above studies that there was a tendency for distributions with lower means to be more rounded. One would expect such a phenomenon if the variations in the A- period were independent of the B-period, since for very brief ISI's, the A-period fluctuations would dominate the overall distribution shape. Perhaps this is the explanation for the symmetry for express saccades which have extremely short latencies.

We will now outline three models: a visual processing model which we shall call the "Central Processing model" (or "CPU model"), an exogenous stimulus-dependent model, the "multiple target model", and an endogenous "spontaneous saccade model."

The CPU Model

During fixations "processing" of visual information takes place. The constitution of this information and the nature of the process are

rather vague, but nevertheless, whatever[6] is necessary for vision takes place during fixations - saccades are much too fast for any meaningful visual information to be transferred. Since the processing of information must take a finite time, a natural step is to postulate that fixations represent this visual processing time. Indeed, much evidence has been gathered to show that fixation time increases as task difficulty (among many other stimulus variables) increases. Thus, it can be argued that even though the actual retinal image does not change in complexity and hence probably does not require any more encoding time, the fixation time depends on higher levels of processing. The next step (or leap) in the argument is to postulate that fixation duration is actually determined by the visual processing. In other words, the eye does not move to a new target until processing of the current target is complete, in much the same way that "handshaking" is used to control the flow of information between a computer terminal and its host (hence "CPU model"). In this kind of model visual processing is serial and it is synchronous with eye movements. Rayner and McConkie (1976) would term this model as belonging to the class of "high-level control" or "process monitoring control" models.

It is difficult to reconcile this model with the Exponential waiting time distributions of fixation durations since it would mean that visual processing is terminated randomly - hardly an attribute of "process-

---

[6] For example Aslin (1985) uses processing to refer to the "transmission of information to a level of the central nervous system that can affect behavior (e.g., perception), but without any connotation that the information reached a conscious level."

ing." One might expect there to be a distribution of processing times dependent on the distribution of processing demand among the viewed targets. However, it seems very unlikely (but not impossible) that this distribution should be Exponential and invariant in shape across subjects and stimuli.

The Multiple Target Model

A much simpler model is that saccades are triggered by "targets" in the visual scene, in the same way that a peripheral flash of light will reflexively elicit a saccade. In this model a potential target for fixation triggers a saccade with a particular probability, and so sooner or later, a saccade will occur with the appropriate vector and thus terminate the current fixation. When the saccade is complete, the triggering target comes under central retinal scrutiny. A new potential target will eventually trigger another saccade, and so on. If the probability of the target triggering a saccade remains constant in time then the distribution of fixation durations will, of course, be Exponential. For most naturally occurring stimuli, there are many potential targets which are all vying for foveation. One target will eventually "win" and a new competition with different potential targets will begin after the saccade. This model does not require any high-level processing but only the saccadic reflex which most species with oculomotor ability possess. This is not to say that visual processing does not occur but rather, fixation duration is not determined by the processing.[7] In this model there is a shift in emphasis from saccades

---

[7] For an analogy, it is well known that the duration of telephone calls

being subordinate to processing to saccades being the determinant of duration. Any processing does not have to be serial and is asynchronous with eye movements.

Spontaneous Saccade Model

Another possibility is that saccades are the result of some random endogenous fixation terminator or saccade generator. The efficacy of such a generator would be that the eye is kept in a visual sampling mode even if there is no demand to fixate a target, and so be more likely to detect a far peripheral object. Such a generator would not directly depend on the stimulus although it could be affected by state (arousal, attention) which, in turn, could be affected by stimulus attributes (size, brightness, novelty etc.).

Rather than there being a specific endogenous generator, spontaneous saccades could be generated by a "noisy" trigger. For example, in the saccade generator, "pause" neurons fire tonically to keep the saccade generator switched off; stimulating these neurons will arrest a saccade in mid-flight (Keller, 1977). If the "latch" signal generated by these neurons were insufficient or incorrectly timed, then it is possible that random spontaneous saccades (opsoclonus) might occur because of the inherent high gain instability of the saccade generator (Zee and Robinson, 1979). Although these saccades would not occur to any visual targets, they could be dependent on

---

in the USA (at a constant tariff) also follow an Exponential distribution - indicating that a call is terminated by a random impulse (Feller, 1968). However, it would be an exercise in extreme cynicism to propose a lack of high-level processing during telephone calls.

the subject's state, which in turn, could be influenced by the visual stimulus.

Distinguishing Among Models

A distinctive feature among these models is their different dependence on the stimulus. Under the CPU model, fixation duration depends on the processing time of the current visual target but independent of the surrounding or peripheral visual scene. On the other hand, the multiple target model depends on the presence of potential peripheral targets and would be independent of the current fixation target. The spontaneous generator would be essentially independent of either the central or peripheral visual scene, inasmuch as state is not affected by the stimulus.

We will now pursue these distinctions by examining how fixation duration is affected by the stimulus conditions. It should be noted, however, that since duration is a random variable, we cannot expect to find "effects" at the level of the single fixation, but only at the level of the mean. We are dealing with a stochastic process whose average performance could be affected even though the process is "random." This point was missed* by Rayner and McConkie (1976), who reject a random model of fixation duration during reading on the basis that fixation duration means are affected by stimulus conditions.

---

*It is worth noting that "randomness" does not necessarily imply non-determinism. A process can appear random and yet be completely deterministic. This occurs when there are many degrees of freedom at play (e.g. classical Brownian motion). Alternatively, an apparent random process may be inherently non-deterministic (e.g., the Uncertainty principle).

[5]
STIMULUS SIZE EFFECTS

In this Section, evidence will be presented to support the multiple target model that was outlined at the end of the last Section. The evidence will be supplied by the adult data and the model will be discussed in more detail. It will be shown that infants do not fit the model as well as adults. Possible reasons for this will then be discussed.

First, we shall review a simple experiment by Enoch (1959) which showed a large change in mean fixation duration as stimulus size was varied. In this experiment, adult subjects were instructed to search for a 5 minarc target (Landholt "C") embedded in highly textured aerial contour maps. The visible area of the maps was changed by circular masks of approximately the same luminance as the median of the maps. For a 3 degree diameter stimulus the average fixation duration for six subjects was 578 msecs. As the stimulus size was increased to a maximum 51.3 degrees, the mean fixation monotonically decreased to a minimum of 307 msecs. This experiment provides a clear example of how fixation duration depends on the area of the stimulus being attended. Enoch (1959) mentions that it is as if the subject keeps his fixations brief in order to search more stimulus area, but, as Enoch himself points out, subjects were not aware of

any time limit.

In Enoch's experiment the visual content of the stimulus areas that were foveated did not change on average as the stimulus size was varied. It seems, therefore, that the change in duration depends on the area of the stimulus outside the immediate area under fixation. This is consistent with the multiple target model: As the stimulus size increases, more potential targets become available and terminate fixations, on average, earlier. A rather weaker argument could be made for the spontaneous saccade model if saccade rate were dependent on the area of retinal excitation. Thus, the effect of stimulus size on duration does not, *prima facie*, exclude the endogenous spontaneous saccade model. On the other hand, it is difficult to explain the stimulus size effect by the CPU model. One would have to posit that visual processing is affected by the contents of the visual scene as far as 50 degrees from the fovea.

The argument for the multiple target model is strengthened if it can be shown that fixation durations are dependent on stimulus size *and* distributed Exponentially. Since we have already shown that our adult subjects have Exponentially distributed fixation durations (see Section 4), we will now examine the effect of stimulus size for the same subjects.

5.1 Stimulus Size and FS Duration (Adults)

Eleven adults were each presented with stimuli of different sizes as a control group in a previously published experiment on form scanning (Hainline and Lemerise, 1982). These data were reanalysed

using the parsing technique (Methods) and compared to Enoch's (1959) results. The stimuli were rear-projected geometric forms (circles, squares, and triangles) whose major dimension varied in size; 5, 20, and 30 degrees. The luminance of the stimuli was approximately constant, and the stimuli were presented in a random sequence.

The mean FS duration is clearly affected by the stimulus size as shown in Figure 15a and is significant ($p<0.0005$, Friedman 2-way ANOVA by ranks, Siegel, 1956).[9] The solid line represents individuals and the dashed line represents the mean. As a post-hoc test, the Wilcoxon test showed no significant difference between the mean durations for the 20 and 30 degree stimuli. For comparison, Figure 15b shows Enoch's (1959) data. As can be seen, there is a similarity between these two sets of results which taken together show an hyperbolic relationship between stimulus size and mean fixation duration. It should be noted that changing the abscissa in Figure 15 to stimulus area rather than size would only further exaggerate the non-linearity.

5.2 Stimulus Size, Breadth of Scan and Saccadic Amplitude (Adults)

If the multiple target model is the explanation for the decrease in fixation duration when stimulus size increases, one would expect two other relationships to exist: As stimulus size increases, more eccentric potential targets become available and should increase the

---

[9] Parametric ANOVA cannot be employed because fixation durations are Exponentially distributed. Although mean durations approach Normality, the homogeneity of variance assumption in the parametric ANOVA is seriously violated.

Figure 15

Effect of stimulus size on fixation duration for free-viewing adults. (a) Mean FS duration for each subject viewing 5, 10, and 30 degree geometric figures. Each subject is connected by a solid line. The dashed line shows the mean of 11 adults. (b) Comparison of the means from above with results from Enoch (1959).

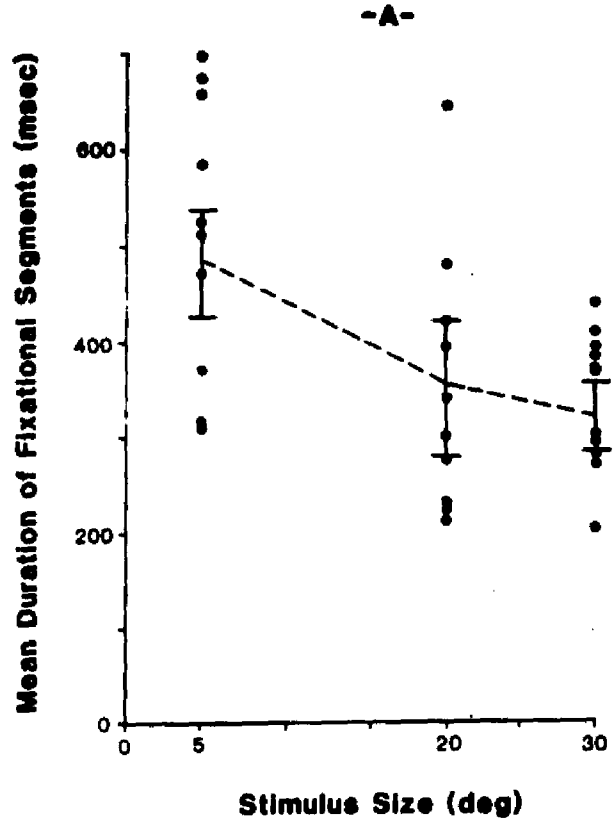
-A-
Mean Duration of Fixational Segments (msec)
600
400
200
0
0
5
20
30
Stimulus Size (deg)

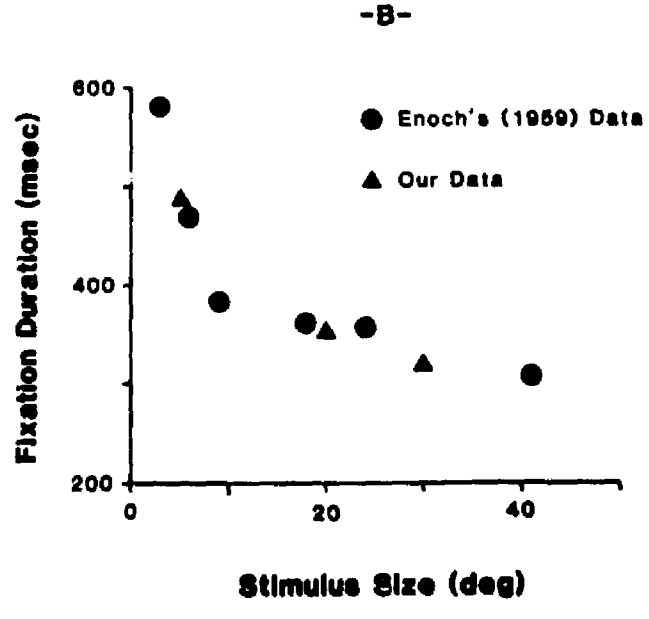
-B-
Fixation Duration (msec)
600
400
200
0
20
40
Enoch's (1959) Data
Our Data
Stimulus Size (deg)

average amplitude of saccades because, sometimes, these targets will "win" the "competition" for foveation. One would also expect the area of stimulus scanned by the eye ("breadth of scan") to increase for the same reason. These predictions were tested and confirmed (Figures 16 and 17). In these Figures, each solid line represents a different subject and the dashed line represents the mean. In Figure 17, breadth of scan was measured as the standard deviation of eye position at the end of every saccade. Breadth of scan and mean saccadic amplitude do not neccessarily have to be correlated, since a given breadth of scan could be maintained by either many small saccades or fewer but larger saccades.

In summary so far, the Exponential distribution of fixation duration, the decrease in mean duration with stimulus size increase, and the increase in mean saccadic amplitude and breadth of scan with stimulus size, taken together support the multiple target model - at least for adults. The CPU model can be rejected and only a very weak case can be made for the spontaneous saccade model. The multiple target model will now be examined more closely and some logical consequences will be discussed.

5.3 The Multiple Target Model in Adults

The multiple target model is conceptually quite simple but it predicts complex patterns of eye movements that are difficult to quantify. Under some conditions, however, quantitative predictions can be made; some of which will be corroborated by existing data, and others remain to be tested. A model or theory should be judged not only

Figure 16

Effect of stimulus size on mean magnitude of saccades from 11 adult subjects free-viewing geometric figures of different sizes. Each subject is connected by a solid line. The dashed line shows the mean.

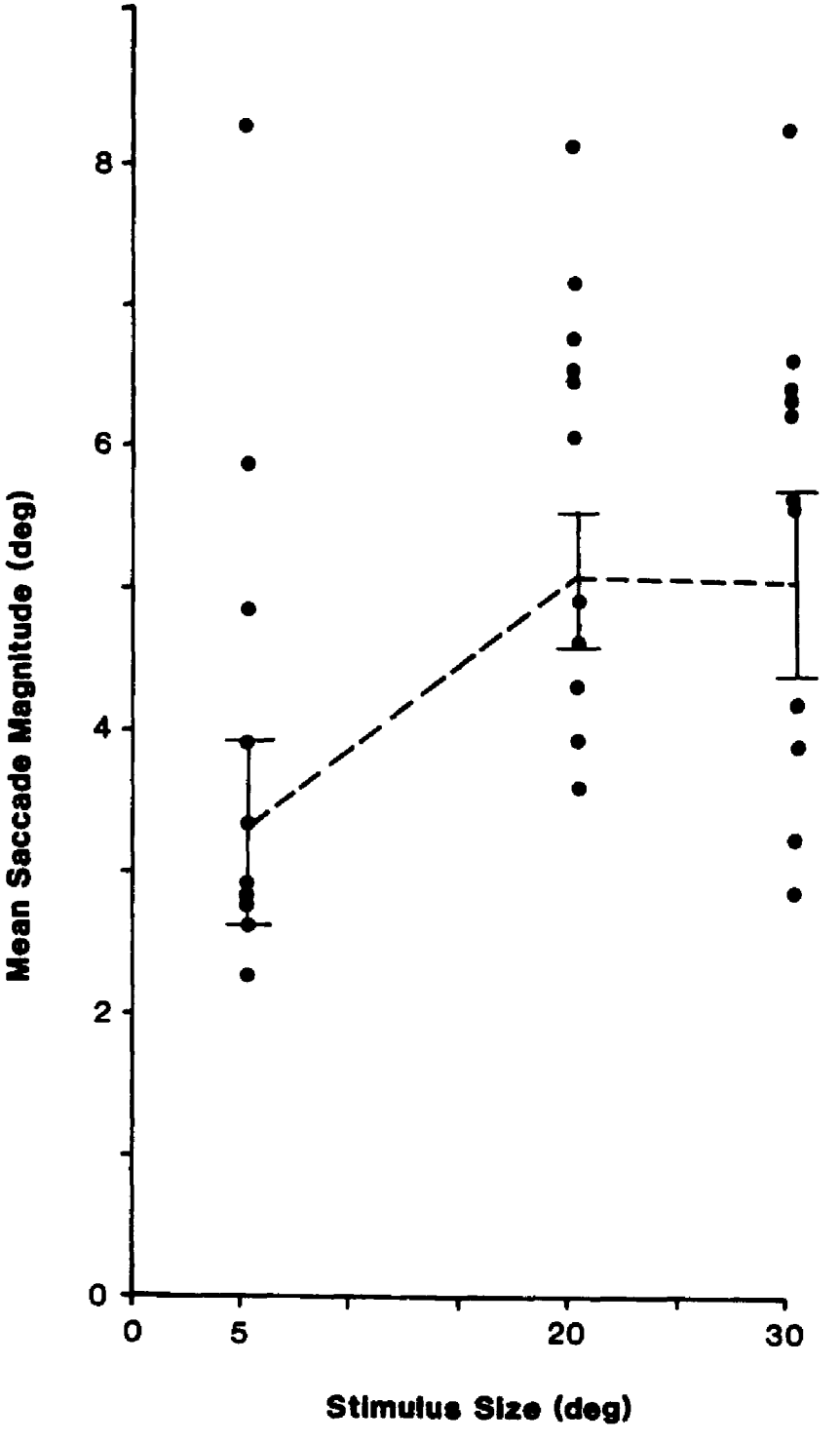
Mean Saccade Magnitude (deg)
0
2
4
6
8
0
5
20
30
Stimulus Size (deg)

Figure 17

Effect of stimulus size on the breadth of scan of 11 adult subjects free-viewing geometric figures of different sizes. Each subject is connected by a solid line. The dashed line shows the mean. Breadth of scan is calculated as the standard deviation of eye position at the end of each saccade.

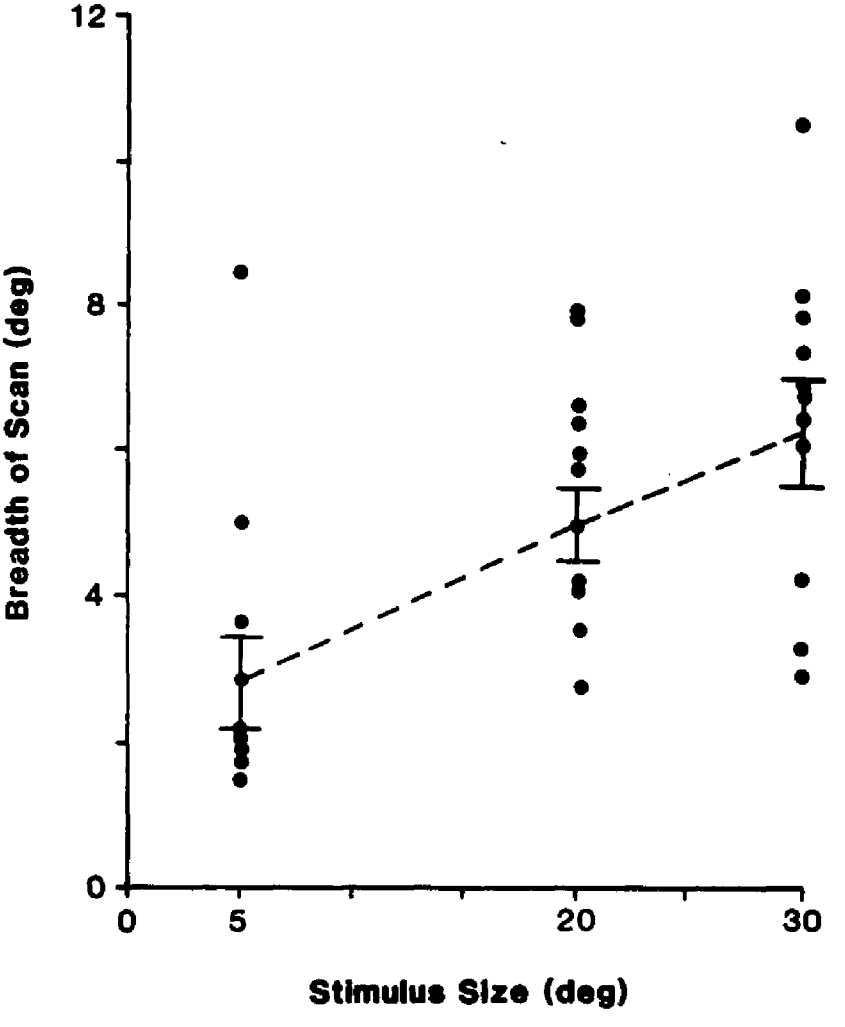
12
8
4
0
Breadth of Scan (deg)
0
5
20
30
Stimulus Size (deg)

by its explanatory power but also by its consequences. Therefore, we shall discuss the model quite thoroughly in terms of its consequences, which may not be apparent from a cursory examination. Mathematical rigour will be avoided since it adds nothing save obfuscation.

There are two basic mechanisms in this model: First, in free-viewing, saccades are triggered by visual targets in a similar fashion to the saccadic reflex but without the abrupt stimulus onset. Second, visual targets trigger saccades probabilistically rather than with certainty. We consider the specific case where the probability per unit time of target triggering a saccade, λ, does not change during the fixation. Such a mechanism can be illustrated easily by a target generating a stochastic signal (for example, the firing pattern of retinal ganglion cells) whose instantaneous level fluctuates randomly about some mean level. There is a constant probability per unit time that a fluctuation will exceed a threshold and trigger a saccade. Eventually a saccade will occur to this target, giving rise to the Exponential distribution for the waiting time for the saccade with mean, $1/\lambda$ (for the purpose of this discussion we shall ignore the A-period of fixation duration). In the multiple target model, we consider N visual targets simultaneously vying for foveation. Each target has a different but constant probability per unit time, λ_i, of triggering a saccade to itself. Although not crucial, we will make the simplifying assumption that the targets are independent of each other so that the probability per unit time of a saccade occurring to a target is independent of the presence and location of other targets. The probability per unit time

of a saccade being triggered by *any* target is then $\Sigma\lambda_i$, which is also constant. Thus, the distribution of waiting time is still Exponential but now has a mean of $1/\Sigma\lambda_i$. Hence, as the number of targets increases, the mean duration will decrease in reciprocal fashion. Obviously, the number of targets will increase as the stimulus area increases because more retina is being stimulated.

To facilitate further discussion, we shall define the quantity "saliency" of a target as the probability per unit time that the target will trigger a saccade. Thus, during any given fixation, each target will have an associated saliency, λ_i. For independent targets, saliencies are additive so that the total stimulus will have a total saliency equal to the sum of individual target saliencies, $\lambda_t = \Sigma\lambda_i$.

The problem, now, is to find what constitutes a target and what determines a target's saliency. When using the term "target" we have been implicitly referring to the stimulus, as if a target exists outside the subject. Although convenient, such usage is misleading. Any visual information, whether for triggering saccades or otherwise, must be filtered by the retinal nuclear layers before being transmitted via the optic nerve to other centres. Thus, the image of the visual scene that impinges on the retina will be filtered by the receptive field organization that emerges at the retinal ganglion level. It follows, therefore, that there are discrete channels (each ganglion cell) that transmit the information for triggering saccades. At the fovea the receptive fields are very small and densely packed. In the periphery the size of the receptive fields becomes much larger, and although receptive fields overlap, their density falls off. It is, therefore,

more appropriate to consider saccades as being triggered by "receptive fields" at the ganglion level rather than by the visual image per se. We shall continue to use the term "target", but to mean the target receptive field excited by the stimulus.

We can now look at saliency in terms of what stimulus parameters are needed to excite particular retinal ganglion cells. We will assert that a saccade is more likely to occur to a receptive field if the firing rate of the retinal ganglion cell for that receptive field increases (that is, ON cells). With this assumption it can be seen that a high luminance element of a stimulus will have more saliency (more likely to trigger a saccade) than a low luminance element. Also, the saliency of a luminance element will depend on its temporal component (due to motion or flashing), and greater temporal frequencies or speeds will increase saliency up to some maximum before blur sets in (this will be discussed later in Section 6). Furthermore, because of the centre/surround antagonism of most receptive fields, there will be some patterns of luminance that will have more salience than, say, a large high luminance stimulus element. This spatial frequency tuning will vary across the retina as the receptive fields change in diameter. Thus, very fine details will be more likely to trigger a saccade when they are perifoveal than when they are in the periphery. The effect of retinal inhomogeneity on saccades can be seen from a few studies: First, it is well known that saccadic accuracy decreases the larger the saccade (Becker, 1972; Henson, 1979). This is consistent with the notion that a peripheral target cannot be localised more accurately than the size of the receptive field which is stimulated. Acuity falls

off approximately linearly with foveal eccentricity (Alpern, 1962). Thus, error should be proportional to eccentricity and as Henson (1979) has shown, saccadic localization error is roughly a constant 10% of saccadic demand (or target eccentricity under our model).

Findlay (1980) has shown that the area of a peripheral stimulus must be much larger than the area of a less foveally eccentric stimulus to maintain the same probability of triggering a saccade. Findlay shows that the area increases with the sixth power of eccentricity, which is much more than would be expected by change in receptive field diameter alone, and also much more than that expected from the cortical magnification factor. Nevertheless, his result clearly shows that the retina is not homogenous in its probability of triggering saccades.

Non-stationarity of Fixation Duration

The inhomogeneity of the retinal triggering mechanism means that the saliency of a target in the visual scene will not only depend on the distribution of luminance and other visual parameters (colour and brightness contrast, temporal components, adaptation state), but also on the retinal locus of the target's image. Consequently, saliency cannot be considered as belonging solely to the stimulus domain but should be considered as a product of the interaction of the stimulus parameters and the current eye position. Since, according to our model, the mean fixation duration is dependent on the inverse of total saliency of a visual scene, we must conclude that the mean fixation duration will depend on where the eye is pointing in the visual scene; that is, mean duration will change from fixation to fixation according

to how total saliency changes across fixations. Some visual scenes will not evoke large changes in total saliency from fixation to fixation, because no matter where the eye points, the luminance pattern will remain roughly the same. Such stimuli would be homogenous in their contour patterns (for example, uniform fields, fine checkerboards, dense contour maps, etc.). However, for less homogenous stimuli one would expect large changes in total saliency from fixation to fixation, and hence fixation duration as the eye scans the stimulus.

From a statistical point of view fixation duration is a *non-stationary* random process according to this model, because the moments change in time. For any particular fixation, its duration will be Exponentially distributed because of the constant saliency (within a fixation). The next fixation will also be Exponentially distributed but it will have a different mean. Over many fixations the distribution of durations will appear to the experimenter as a Compound Exponential, which is indeed what is observed and has already been discussed in Section 4.[10]

---

[10] A legitimate concern arises over the validity of measuring moments of what now appears to be a non-stationary random process. There are two ways to look at this problem. First, the severity of the non-stationarity and its time course should be considered. Here, the change in the mean (and higher moments) of the underlying Exponential distribution is rapid (every observation) so that its main effect will be to inflate the variance - hence the hyperexponentiality. Clearly the change in mean duration from one fixation to another has not been so large as to prevent us from at least identifying the underlying distribution as Exponential. Second, if the changes in mean from fixation to fixation are themselves random, then the distribution is compound but stationary. Because total saliency is made of many individual (and independent) target saliencies, there are many degrees of freedom determining mean duration for most stimuli. The changes in total saliency from fixation to fixation will be deterministic but will be quasi-random.

Pre-emption and Eminency

Even though we have assumed the saliencies of targets to be independent of each other, we will now discuss how targets will appear to be strongly affected by each other. This is a logical consequence of the multiple target model and no other assumptions will be made.

First, consider a single target which is in the peripheral visual field and is stimulating a single retinal ganglion cell. Let this target (at this retinal locus) have a low saliency, say, $\lambda = 0.01$ sec^{-1}. If this arrangement could be repeated many times, we would have to wait, on average, $1/\lambda = 100$ seconds for the target to trigger a saccade - the distribution of waiting times would be Exponential, of course. Let us now add a second target at a different locus but with the same saliency. We would still have to wait, on average, 100 seconds for a saccade to a specific target because of the assumption of independence. But, now we would have to wait on average, only 50 seconds for *any* saccade; that is, to either target. Thus the addition of a target reduces the waiting time for a saccade by 50%. Now consider 100 targets, all with the same saliency, $\lambda = 0.01$ sec^{-1}. We would now have to wait, on average, only 1 second for the first saccade. If one more target were added, the waiting time would only be reduced by 1% to 0.99 seconds. From the point of view of a specific single target, the probability that the target will actually "win" foveation by triggering the first saccade will depend on the number of the other targets present. For these examples it will be reduced from 0.5 with two targets to 0.01 with 100 targets. In other words a

target is effectively pre-empted by other targets (even though the saliencies are independent of one another). More generally, the probability that a specific target will tigger a saccade on a given fixation will be given by the ratio of the target's saliency to the total saliency of all the targets. We shall refer to this (conditional) probability as the target's "Eminency" (relative importance). Thus, "saliency" refers to the absolute probability per unit time that a target will trigger a saccade given that it is not pre-empted by another target. "Eminency" is the probability that a target will trigger a saccade before the other targets do.

Scanning Patterns and Markov Sequences

Periodically, scanning patterns of eye movements for subjects viewing stimuli have become of interest in the literature (for example, Yarbus, 1967; Noton and Stark, 1971; Stark and Ellis, 1981). Therefore, even though we have made no attempt to relate eye position during fixation to actual stimulus features, we will pursue the statistical properties of the multiple target model a little further.

Conceptually, the model as outlined here is quite simple, yet it predicts complex patterns of eye movements which depend on the stimulus. The complexity arises from the sequential nature of eye movements. Although we might be able to predict which potential target is the most salient, and therefore, the most likely to be the target for the next fixation, we cannot predict which target will *actually* trigger the saccade - even a target with very low saliency could win foveation. Of course, once the eye is in a new position, all targets take on different saliencies because of their new retinal loci. Thus, a

target that had a high saliency on one fixation may have a low saliency on the next fixation, and vice versa. The spatial pattern of fixations, or scanning pattern, for a free-viewing adult subject will therefore appear quite haphazard yet still be inextricably linked to the stimulus.

According to the model, the probability that a saccade will terminate a fixation depends only on the saliencies of all the potential targets at their retinal loci, and does not depend on the current target being foveated. More important, the saccade probability is independent of *how* the eye reached its current position - there is no memory within or between fixations. Thus, if the eye should repeat a fixation (a rare occurrence), all potential targets will have the same saliency as they did on the last fixation. If this condition holds, then the eye position of current fixations can be described by a Markov process where each possible eye position corresponds to a state of the Markov process (for a description of Markov processes, see Feller, 1968). At any given instant in time, the probability that a saccade will move the eye from its current position to a specific new target will be given by the new target's saliency at its eccentricity from the current eye position (given no pre-emption). Thus, the eye position at any instant is given by a process whose transition probabilities are proportional to saliencies of all targets with respect to each other. In fact, the multiple target model can be succinctly restated as postulating that the development of eye position in time is a stationary, continuous general Markov process. Note, that this Markov process only describes the B-period of fixations. The A-period and saccade dura-

tion are not included. It is also important to note that the whole process is stimulus-dependent - each stimulus or visual scene creates a different set of Markov probability transitions. An illustration of this kind of Markov process is shown in Figure 18a. Each element in the matrix represents the transition probability of the eye moving from a specific position to another in the time interval, δt. The diagonal elements represent the probability that the eye will stay in its current position (ignoring drift) or, in other words, the probability that the eye will not make a saccade in a time interval. For constant transition probabilities in time, the probability distribution of duration at any given position will be Exponential. Since diagonal elements will be generally different, the mean duration will vary from one position to another. This model therefore describes the duration of fixations by a compound Exponential distribution (see Section 4 and Appendix F). It is necessary to add on the fixed A-period to each fixation in order to completely describe fixation duration. Saccade duration would also have to be added to obtain eye position in time.

This matrix representation can be simplified if the transitions represent a saccade rather than the eye position at every time interval, δt . In this case, a matrix element represents the probability that a saccade will occur to a position before a saccade occurs to another position, regardless of how long the eye stays in its current position. The fixation duration information is lost and only spatial information of eye position is described. In this matrix the leading diagonal becomes zero since the eye cannot make a saccade to its current position (by definition saccades move the eye). Each element

Figure 18

The multiple target model can be defined in terms of Markov matrices. (a) The full matrix: Each element contains the saliency of a potential target triggering a saccade from one eye position (row) to another position (column). A leading diagonal element describes the probability per unit time that the eye does *not* move and (for constant saliencies) describes an Exponential distribution for fixation duration at any position. This full matrix describes the probability of a transition at every instant of time, δt. (b) Simplified matrix: Same as the full matrix, except that each element is the probability that the eye will make a saccade from a row position to a column position *given* that a saccade does occur. The leading diagonal becomes zero since a saccade must move the eye (by definition). Duration information is lost in the simplified matrix. In both matrices the A-period of duration and saccade duration are not included.

-A-

	P_1	P_2	P_3	P_4		P_n
P_1	$\lambda_{11}\delta t$	$\lambda_{12}\delta t$	$\lambda_{13}\delta t$	$\lambda_{14}\delta t$		$\lambda_{1n}\delta t$
P_2	$\lambda_{21}\delta t$	$\lambda_{22}\delta t$	$\lambda_{23}\delta t$	$\lambda_{24}\delta t$		$\lambda_{2n}\delta t$
P_3	$\lambda_{31}\delta t$	$\lambda_{32}\delta t$	$\lambda_{33}\delta t$	$\lambda_{34}\delta t$		$\lambda_{3n}\delta t$
P_4	$\lambda_{41}\delta t$	$\lambda_{42}\delta t$	$\lambda_{43}\delta t$	$\lambda_{44}\delta t$		$\lambda_{4n}\delta t$
P_n	$\lambda_{n1}\delta t$	$\lambda_{n2}\delta t$	$\lambda_{n3}\delta t$	$\lambda_{n4}\delta t$		$\lambda_{nn}\delta t$

$$\lambda_{ii}\delta t = 1 - \sum_{j \neq i}^{N} \lambda_{ij}\delta t$$

-B-

	P_1	P_2	P_3	P_4		P_n
P_1	0	ε_{12}	ε_{13}	ε_{14}		ε_{1n}
P_2	ε_{21}	0	ε_{23}	ε_{24}		ε_{2n}
P_3	ε_{31}	ε_{32}	0	ε_{34}		ε_{3n}
P_4	ε_{41}	ε_{42}	ε_{43}	0		ε_{4n}
P_n	ε_{n1}	ε_{n2}	ε_{n3}	ε_{n4}		0

$$\varepsilon_{ij} = \lambda_{ij} / \sum_{k \neq i}^{N} \lambda_{ik}$$

now represents eminency - the probability that the eye will move from one position to another *given* that the eye moves somewhere (Figure 18b). The advantage of this simplified chain is that it may lead to a means of testing the model as follows: If the saliencies of targets are truly independent of each other, then elements in the Markov matrix can be collapsed into sub-areas and so create new elements. These elements will then represent the probabilities that the eye moves from one sub-area to another. Scanning patterns could be observed and fixation positions could be grouped into the sub-areas and tested for departures from a first order Markov chain.[11]

Noton and Stark (1971) and a few others (see Stark and Ellis, 1981) have shown that subjects sometimes repeat their idiosyncratic scanning pattern, "scanpath", when they repeatedly viewed the same stimulus. This finding has attracted much attention because of possible cognitive/perceptual implications (and probably because it is rare to find any stable pattern in visual scanning experiments). Close examination of the few published scanpaths reveals that the scanning patterns are not identical but have only a resemblance to each other.

---

[11] Ellis and Smith (1985) attempted this kind of analysis with adult subjects and found a significant departure from first order expected probabilities. However, it is difficult to interpret their result because of their unusual stimulus conditions, and because their analyses appear to be inappropriate: They used stimuli with features that moved linearly and/or rotated at 1 degree/sec. Moreover, their stimuli were not identical from one trial to the next. Thus, stimulus saliencies were not stationary (statistically) either within or between trials. They used an automatic parsing procedure which has known problems (Karsh and Breitenbach, 1983). They used the simplified matrix of eminencies (Figure 18b) with a non-zero leading diagonal, and they used a Chi-Square test even though many of their cells had very low frequencies - a well known problem (see Siegel, 1956).

According to the multiple target model, the probability of the eye passing through the same sequence of eye positions is remote (even if durations were ignored). If the targets were collapsed into sub-areas as mentioned above, the probability of a scan repeating itself may reach observable levels in some cases. The likelihood of scanpaths would be greater for stimuli that were sparse in contour (such as line drawings) since on any fixation there would be few alternative targets. It is possible that scanpaths are just unlikely events that attract much more attention from the experimenter than warranted by their probability of occurrence.

Scanning Homogenous Visual Scenes

Because of the Markovian character of this model of visual scanning, it is difficult to make any predictions of even average scanning behaviour unless we have very detailed knowledge of the stimulus and its distribution of saliencies at all eye positions. The "homogenous" stimulus is one exception to this problem. The homogenous stimulus has a uniform distribution of contour (or spatial frequency per unit area), so that wherever the eye points, there is a similar distribution of saliencies across the retina; such stimuli are everyday views, random patterns, contour maps (as used by Enoch, 1959), etc.. Many laboratory stimuli, such as geometric forms, scant line drawings, etc., are not homogenous because the distribution of saliency will depend non-trivially on where the eye is pointing (such as the centre of triangle as opposed to a vertex).

For the homogenous stimulus, then, we can treat each fixation and saccade as transitions from the same Markov chain because the

matrix of transition probabilities now remains approximately the same from fixation to fixation. We now need to estimate how saliency is influenced by retinal filtering; we can then make some predictions of the relationships between the distribution of saccades, mean saccade magnitude, and the B-period of fixation duration.

As discussed earlier, saccadic triggering is mediated by at least the retinal ganglion cells. The spatial information for triggering saccades probably passes through other retinotopic cellular laminae (such as the those in the superior colliculus or, possibly, the visual cortex). However, we will assume that the saccadic system cannot localise more accurately than permitted by the receptive field organization at the retina. Thus, we place the limitation that the density c′ targets can be no greater than the density of receptive fields. The diameter of receptive fields increases approximately linearly with foveal eccentricity up to about 25 degrees, as inferred by the change in acuity (for example, Alpern, 1962). At eccentricities beyond about 25 degrees, acuity decreases more rapidly than linearly (Woodhouse and Barlow, 1982). If we assume a constant degree of overlap between adjacent receptive fields, the density of receptive fields will be inversely proportional to the square of eccentricity. This is consistent with the anatomical assay of retinal ganglion cell density in the macaque monkey (Perry and Cowey, 1985), except for the foveal region where ganglion cells are displaced (the fibres of Henle). Approximately then, the density of potential targets will follow the inverse square of eccentricity from the fovea. However, care must be taken in estimating saliency near the fovea since the inverse

square approaches infinity as eccentricity becomes very small. A more accurate, but still linear, description of receptive field diameter, d, with eccentricity, r, is given by:

$$d = a + br \tag{12}$$

where a is the diameter of the most central foveal receptive field and b is the slope of the rate of diameter increase with eccentricity. Assuming a radially symmetric retina[12] with an homogenous stimulus, the saliency, $\lambda(r)$, at an eccentricity, r, will be given by:

$$\lambda(r) = 1/(a + br)^2. \tag{13}$$

For large eccentricities this relationship becomes the inverse square, but for small eccentricities the ratio, a/b, becomes quite significant. We shall call this ratio, $\Omega = a/b$, the "acuity ratio" which is the minimum foveal receptive field diameter divided by the rate of increase in receptive field diameter with eccentricity. There is some discrepancy on the value of this ratio. Probably the most accurate measure can be obtained from Jones and Higgins (1947) whose intra-foveal measurements yield a value of 0.5. This assumes that central foveal

---

[12] This assumption is really only for mathematical convenience. In fact the nasal hemiretina has a greater density of ganglion cells than the temporal hemiretina (Perry and Cowey, 1985). However, this asymmetry may be cancelled for binocular viewing if the two eyes trigger saccades independently. Binocular viewing increases the visual field horizontally rather than vertically; however, this asymmetry is in the far periphery and should have only a very small effect on total saliency.

receptive fields contain only one cone. Acuity measures yield an acuity ratio of about 1.0 (for an overview, see Jacobs, 1979), although some studies yield much higher ratios of 5 or more (for example, Millodot, Johnson, Lamont, and Leibowitz, 1975). These differences may be caused by different procedures, acuity targets, and levels of luminance. We will show predictions using the values, Ω = 0.5, 1.0, and 1.5; the lower values are probably more accurate.

For a radially symmetric and homogenous stimulus with radius, R, the probability density of saccade magnitude is given by:

$$f_s(r) = r\lambda(r) \Big/ \int_0^R x\lambda(x).dx. \qquad (14)$$

The denominator normalises the distribution by assuming that all saccades point the fovea somewhere inside the stimulus area. Substituting $\lambda(r)$ from Equation 13, this becomes:

$$f_s(r) = [R/(R+\Omega)^2]/[\Omega/(R+\Omega) + \log(R/\Omega + 1) - 1]. \qquad (15)$$

As can be seen, this distribution depends only on the acuity ratio and the stimulus size - there are no other free parameters. This theoretical distribution is compared to actual distributions obtained by Bahill, Adler, and Stark (1975) in Figure 19. Bahill et al. measured the distribution of saccade magnitude from three subjects freely viewing everyday scenes which we will assume to be approximately homogenous. Both the theoretical and obtained distributions show the same shape; there is a peak in the distributions around 1 degree with

Figure 19

Comparison of the distribution of saccade magnitude between the prediction of the multiple target model (Equation 15) and the data from Bahill et al. (1975). Note: Bahill et al.'s distributions were normalised over the range 1 - 30 degrees. The model's distributions are normalised over the range 0 - 30 degrees, with different acuity ratios, Ω.

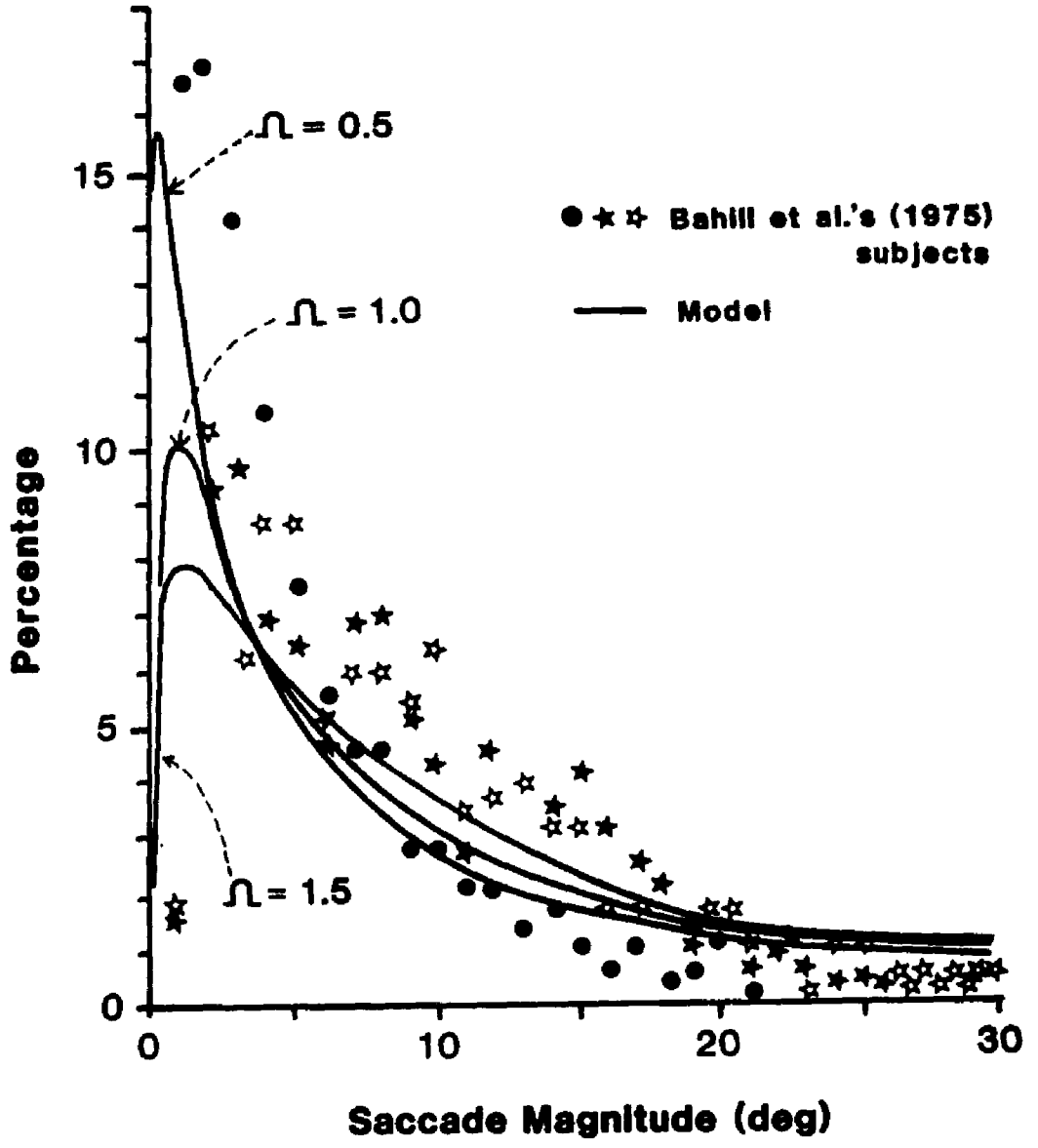
Percentage
15
10
5
0
0
10
20
30
Saccade Magnitude (deg)
Λ = 0.5
Λ = 1.0
Λ = 1.5
Bahill et al.'s (1975) subjects
Model

a hyperbolic fall-off for higher saccade magnitudes. It should be noted that the theoretical distributions were normalised over the range 0 - 30 degrees, while Bahill et al.'s data were normalised from about 1 to 30 degrees because of the one degree resolution of their EOG apparatus. This discrepancy in normalisation accounts for some of the difference between the theoretical and obtained distributions, especially for small saccades. This comparison between actual and theoretical distributions suggests that the different distributions among Bahill et al.'s subjects reflect different acuity ratios. Thus, subjects with high acuity (low a) will produce saccades with magnitude distributions having higher modal probabilities at lower magnitudes than subjects with poor acuity.

Since the multiple target model accurately predicts the distribution of saccade magnitude for homogenous visual scenes, we will examine the mean of this distribution. The mean is given by:

$$\bar{f}_s = \int_0^R r f_s(r).dr \qquad (16)$$

which becomes:

$$\bar{f}_s = \frac{R - 2\Omega\log(R/\Omega + 1) - \Omega^2/(R+\Omega) + \Omega}{\Omega/(R+\Omega) + \log(R/\Omega + 1) - 1}. \qquad (17)$$

Again, the only free parameter is the acuity ratio. In Figure 20 the mean saccade magnitude from Enoch's data is plotted against the diamater of a homogenous stimulus for different acuity ratios (solid lines). Mean saccade magnitude only becomes sensitive to the acuity ratio for

Figure 20

Comparison of mean saccade magnitude between the multiple target's model's prediction (Equation 17) (solid lines) and data from Enoch (1959) (dots) for different stimulus sizes. Different acuity ratios are shown.

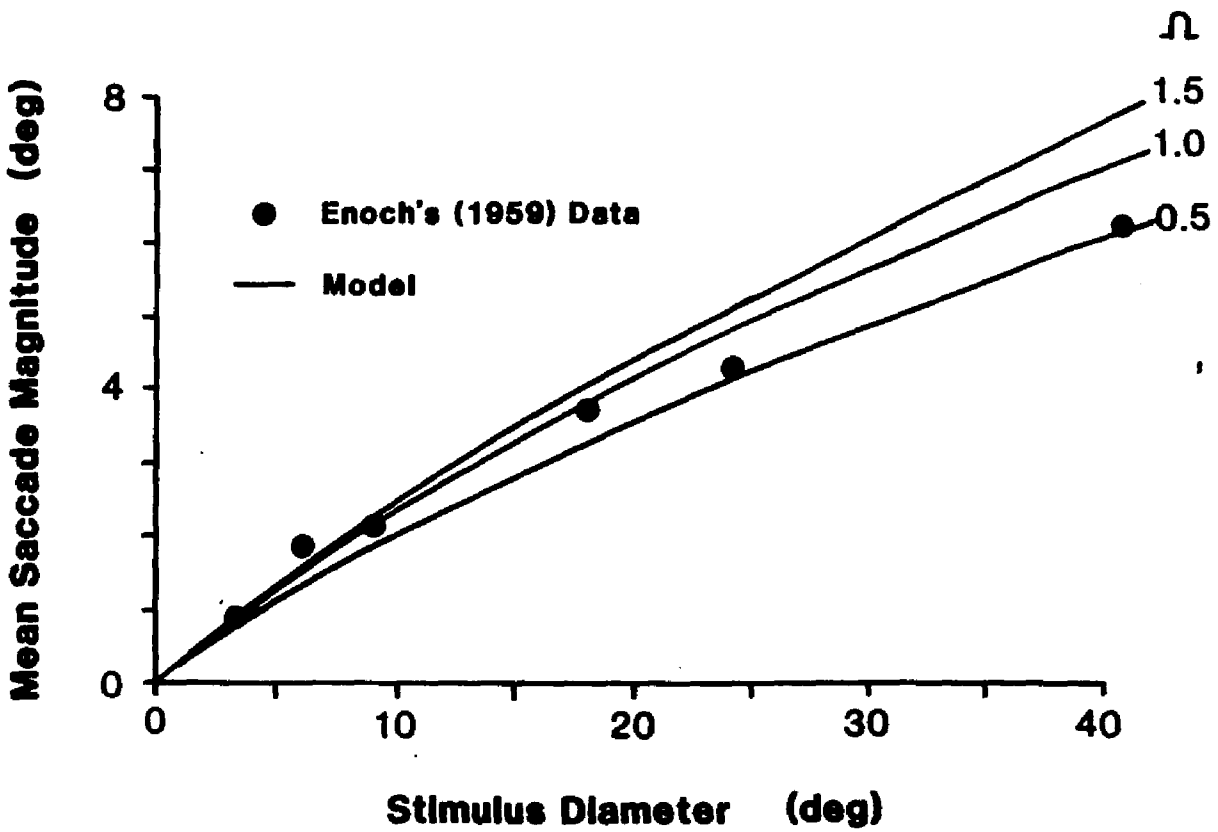
Mean Saccade Magnitude (deg)
8
4
0
0
10
20
30
40
Stimulus Diameter (deg)
Enoch's (1959) Data
Model
Ω
1.5
1.0
0.5

large stimuli. The dots in Figure 20 show the mean saccade magnitude obtained by Enoch (1959) from subjects viewing contour maps of different diameters. Although Enoch's stimuli were homogenous, the small stimuli must break the assumption that the Markov matrix remains constant from fixation to fixation since the overall retinal image and saliency should change considerably, depending on whether the eye is pointing towards the middle or the edge of the stimulus. Nevertheless, there is close agreement between Enoch's data and the theoretical model. This comes about, in part, because Enoch's subjects spent most of their trials viewing the centre of the stimuli (even the smallest 3 degree diameter stimulus).[13] It is emphasised that these comparisons are not the result of "curve fitting." Except for the acuity ratio, Ω, there are no free parameters. The agreement is even more remarkable considering the assumption of perfect homogeneity which can only be realised theoretically. We conclude that average saccade magnitude must be a rather stable parameter of visual scanning.

We shall now consider fixation duration. The B-period of fix-

---

[13] The multiple target model predicts that most fixations will occur in the middle of a small homogenous stimulus. This can be seen at least intuitively: If a fixation occurs away from the centre of the stimulus, there will be more potential targets triggering saccades back towards (or beyond) the stimulus centre, than away from the centre. Thus, the further a fixation is from the stimulus centre, the more likely the next fixation will be closer to the centre. On average, the eye will wander around the stimulus centre. Unfortunately, we have been unable to describe the statistics of eye position mathematically, so far.

In addition, there may be a small directional bias in eye movements which tends to keep the eye in the primary position (Wallman and Pettigrew, 1985).

ations is equal to the reciprocal of total saliency. However, for the homogenous stimulus, we only know the relative distribution of saliency, and not the absolute distribution. Thus, there is an unknown multiplicative constant, β, which cannot be eliminated by normalisation. Also, the multiple target model only describes the B-period of fixations, and so there is an unknown additive constant - the A-period, α. Assuming a constant A-period, the mean fixation duration, D, will be given by:

$$\bar{D} = \alpha + \beta \Big/ \int_0^R r\lambda(r).dr \qquad (18)$$

In Figure 21a, the reciprocal of total saliency is plotted against stimulus diameter for different acuity ratios. As expected, the B-period monotonically decreases with stimulus size, but it is quite sensitive to the acuity ratio for small stimuli. It was possible to fit these curves to Enoch's measurements of fixation duration by choosing appropriate constants, α and β. Such a fit is shown in Figure 21b for an acuity ratio of 0.5. In spite of the freedom provided by two unknown parameters, a reasonable fit could only be obtained if the A-period were assigned a duration of 230 msecs or more (dashed line in Figure 21b). Similar fits could be obtained for Ω = 1.0 and 1.5 but it was necessary to increase the duration of the A-period even more. These A-periods are far longer than the A-periods shown by our subjects (adults - 100 msecs, infants - 50 msecs; see Figures 8 and 11). This suggests that the A-period not only varies between infants and adults, but also between different stimuli or task conditions for the

Figure 21

Model's fit to fixation duration data. (a) Relative B-period duration plotted against stimulus diameter for an homogenous stimulus; parametric in acuity ratio. (b) Scaled B-period and A-period to fit Enoch's (1959) data (Equation 18) for acuity ratio = 0.5. Note: For a reasonable fit a minimum A-period of 230 msecs was required.

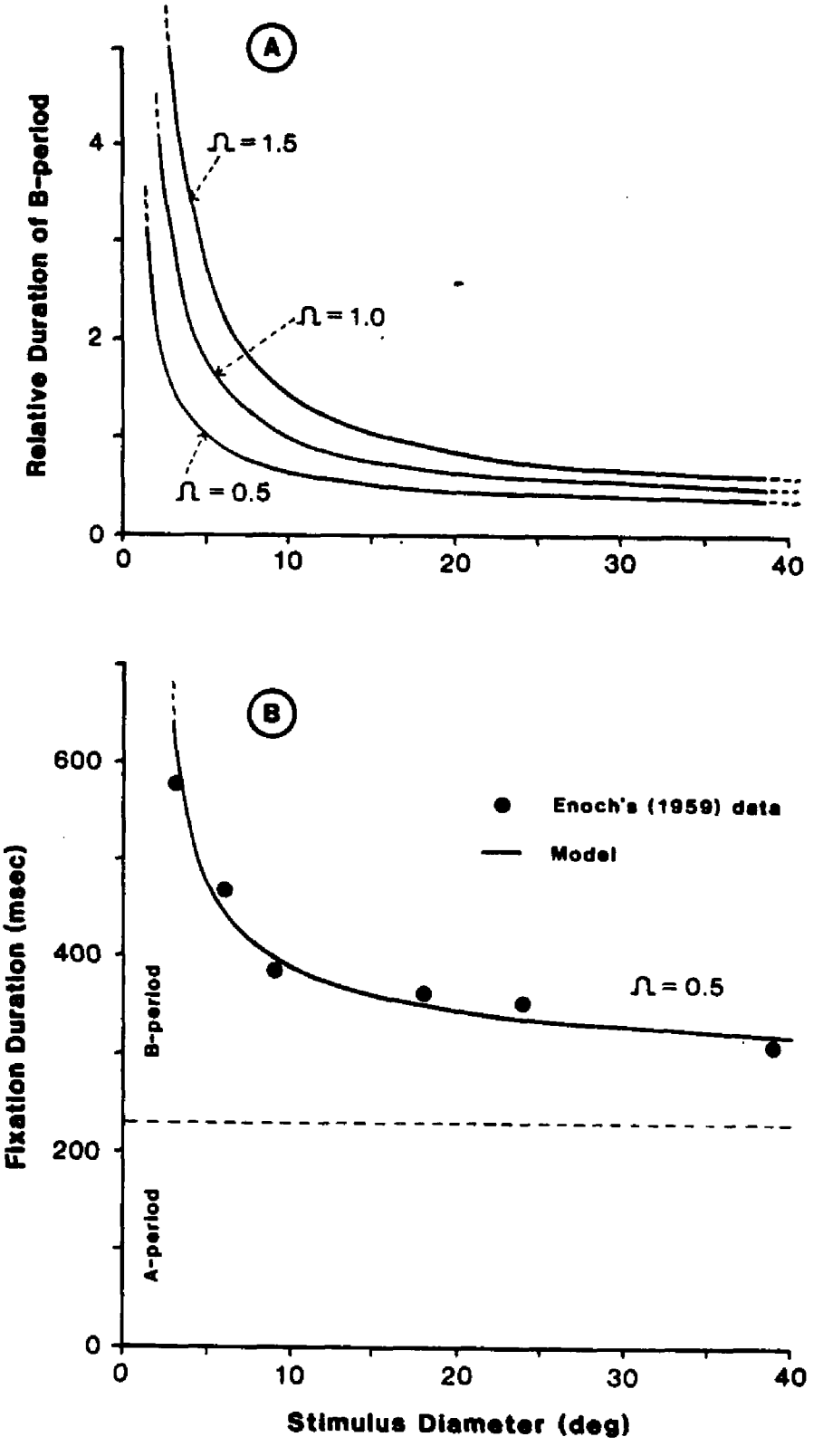
A
Relative Duration of B-period
4
2
0
0
10
20
30
40
Π = 1.5
Π = 1.0
Π = 0.5
B
Fixation Duration (msec)
600
400
200
0
Enoch's (1959) data
Model
Π = 0.5
B-period
A-period
0
10
20
30
40
Stimulus Diameter (deg)

adult. One would not expect such differences if the A-period were solely due to saccade preparation time or simple conduction delays. A possible explanation for these different A-periods will be discussed next.

Beyond Reflexive Scanning

The basic unit of the multiple target model of free-viewing is the saccadic reflex in which peripheral visual targets trigger the saccades. Although this process predicts complex scanning patterns, it also implies that visual scanning is completely stimulus driven. Even though most of the time we are not aware of our eye movements, there is a large literature which shows that fixation duration is affected by the task or "cognitive load" imposed on the subject (Senders, Fisher, and Monty, 1978; Fisher, Monty, and Senders, 1981; Rayner, 1983). More complex tasks induce longer fixation durations. This supports the CPU model, since it can be argued that more complex tasks require more processing than simple tasks.

In tasks which affect fixation duration, the reflexive scanning embodied in the multiple target model must either be overridden or adapted to the task. As discussed in Section 4, other studies suggest that fixation duration may be Exponentially distributed for a variety of tasks. It seems plausible, therefore, that the reflexive scanning is somehow adapted, rather than replaced, by higher levels of processing. Two possible ways are by modulating the A-period or modulating the B-period

It is helpful at this point to differentiate two kinds of processing, namely, *synchronous processing*, and *asynchronous processing*.

When they exist, synchronous processes are processes that must be completed before the fixation is terminated. Asynchronous processes can continue across fixations.

The most basic synchronous process is the transmission of the saccadic triggering signal from the retina to the saccade generator in the brainstem. The conduction time for this must exist for visually triggered saccades, and so it constitutes a minimum refractory period between saccades. However, we now postulate that there are other synchronous processes, depending on the fixation task. For example, some tasks are sequential in nature because each part of the task must be successfully completed before the next part can be attempted: In reading it is necessary to have understood (centrally processed) most of the current words before processing the next words simply because of memory limitations. Even the search experiment of Enoch's (1959) is probably a sequential task since the visual contents of each fixation must be compared to memory of the target (5 minarc Landholt "C"). Clearly then such tasks impose a delay on the subject's eye movements to the same extent as if the experimenter had instructed the subject explicitly, except that the delay seems to occur automatically. For these sequential tasks, it is important that visual information be acquired without a premature interruption by the next saccade. Therefore, because of the inherent uncertainty of when a saccade might be triggered during the B-period, it seems plausible that synchronous processes occur during the A-period and thereby extend it. Obviously then, those tasks which require more information per fixation will have longer A-periods.

The simplest way the A-period could be extended by a synchronous process is by inhibiting visually triggered saccades. It is of interest to note that for a constant probability per unit time for fixation termination, the statistics of the B-period remain unaltered for any extension of the A-period, and the overall probability distribution of duration will always be Exponential but with a different location parameter depending on the duration of the A-period. Thus we can envisage two interacting systems during visual scanning: At the simple level there is a stream of signals reflexively triggering saccades at a rate depending on the saliency of the visual scene at a given fixation. This system is stochastic and has an Exponential distribution. *Concurrently,* there is a higher-level system which is responsible for acquiring visual information during a fixation depending on the scanning task. This system can inhibit the reflexive system. Once all the necessary information has been acquired, this system "releases" the reflexive system which then waits for the next potential target to win the competition for foveation (presumably ignoring any triggering events that may have occurred during the extended A-period).[14] For this dual system to be effective, the inhibition must occur at a late stage of saccade generation (possibly the "pause" neurons), otherwise trigger signals already in the "pipe-

---

[14] The similarity between this approach and queuing theory (e.g., Trivedi, 1982) is quite compelling: The potential targets present a Poisson source of "jobs" for "service" by the high-level processor and the saccade generator. The interesting question is whether there is a queue with a service discipline. That is, are potential targets remembered for service after the next saccade, or are they lost during the current A-period processes? Whether queuing theory has any insights to offer in free-viewing or is only an analogy remains to be seen.

line" could still terminate a fixation prematurely.

The brevity of the A-period in infants (50 msecs) suggests that they have very little synchronous processing. It also suggests that the minimum transmission time (or refractory period between saccades) is only 50 msecs or therabouts. As mentioned earlier (Section 4.8), this is much less than most models of saccade programming but not inconsistent with latency of express saccades (Fischer and Boch, 1983). It is possible, therefore, that the infant A-periods represent no inhibition from higher levels of synchronous processing - similar to Boch et al.'s (1984) suggestion for monkey express saccades. Of course, we cannot argue whether this is because infants do not have high-level synchronous processes or whether there was no need for them to synchronously process with our stimulus conditions.

The other possibility is that asynchronous processing can take place during the B-period, even though this period is random and stimulus driven. Of course such processing cannot be strongly dependent on the current fixation, but much visual processing requires the integration of information from many fixations (such as object or face recognition). It is suggested here that this perceptual processing can take place asynchronously from fixations and does not require any extension of the A-period. Instead, the B-period is modulated by changing the overall saliency of the stimulus. This could be accomplished by changing the saliency of either all potential targets or a selected number of targets.

For example, the saliency of all targets could be increased or decreased depending on how fast the eye drifts during a fixation. If

a subject pays attention to a fine detail by keeping a very steady fixation (possibly by increased controller gain), potential peripheral targets will also become steady and their saliency will diminish. If on the other hand, the subject pays little attention and allows his fixations to wander, peripheral targets will acquire retinal slip and become more salient and so will terminate fixations sooner, on average. This possibility will be examined more closely in Section 7.

An example of how only selected targets are permitted to trigger saccades is found in reading. According to the multiple target model, a page of text would elicit saccades to any word or letter that "won" the competition for foveation. These targets could be above, below, or to the left of the current fixation as well as to the right as is normal in reading (left-to-right languages). Thus, the reader masks out all targets which are not in the narrow horizontal "window" to the right of the current fixated word. Only potential targets in this "window of attention" have sufficient saliency to actually trigger saccades. Fixation durations will still be Exponentially distributed because the saccade is triggered by a visual target in the window (presumably with constant saliency during the fixation). This windowing could be accomplished by decreasing the saliency of targets outside the window (target inhibition) and/or by increasing the saliencies within the window (target facilitation). The short fixation durations normally associated with reading tend to suggest target facilitation rather than target inhibition. The mean fixation durations obtained by the "perceptual span" experiment (e.g., Rayner, Inhoff, Morrison, Slowiaczek, and Bertera, 1981) are consistent with the

notion of attention windows. In these experiments, peripheral text is masked leaving a window of normal text around the current fixation letter. As the eye moves, the mask also moves so that there is always a window of normal text. It is found that as the window of normal text decreases, the mean fixation duration increases. The canonical explanation is that the mask prevents important peripheral processing from taking place and thereby increases the processing load for the central retina which, in turn, increases fixation duration. An alternative explanation is that the subject sets a window of attention around the normal text (probably after a brief learning period). As the window size decreases, the number of potential targets also decreases and so increases fixation duration.[15]

It is possible that different scanning strategies adopt different sized "windows of attention" and the reflexive scanning embodied in the multiple target model then operates within this window. Some tasks, such as Enoch's (1959), probably did not invoke any strategy and the window of attention encompasses the whole stimulus or visual field. If the creation of these windows were very fast and flexible a subject could control individual fixation durations and positions (provided visual targets exist to trigger saccades). However, it is dubious whether the model has any explanatory power when taken to this

---

[15] The fixation durations and saccade magnitudes reported in the perceptual span experiments by Rayner et al. (1981) can be fitted by the multiple target model with some assumptions about the saliency of the mask. It fits less well the reverse experiment where the central visual field is masked and only peripheral letters are visible. However, reading breaks down under these conditions and it is not clear what kind of scanning takes place. This is still under study and is somewhat tangential to our goals.

extreme.

5.4 Stimulus Size Effects with Infants

The evidence for the multiple target model is based on the Exponential distribution of fixation durations shown by both infants and adults, and the effect of size on fixation durations from adults. We will now look for similar stimulus size effects in the infant. Infant subjects viewed the same geometric forms (circles, squares and triangles) and sizes, 5, 20, and 30 degrees as the adults did. Only sessions where the infant produced at least three uninterrupted AISI's for each stimulus were included. In addition to this condition, each subject had to view at least one stimulus of each size. For other analyses, a session had to produce at least ten uninterrrupted AISI's; however this criterion had to be relaxed for this analysis in order to provide a reasonable sample size. Twenty three infants fulfilled these requirements. The mean FS duration for each of these subjects is shown in Figure 22. Each subject is represented by a point at 5, 20, and 30 degrees (which are disconnected for the sake of clarity). For each stimulus size, subject means were combined to give an overall weighted mean according to the scheme in Appendix D. These means are shown with ±1 standard error and they are connected by the solid line in Figure 22. There is a small decrease in FS duration with increasing stimulus size. However, this decrease did not reach significance using a Friedman 2-way ANOVA. As with the adults, breadth of scan and mean saccade magnitude were compared across the different stimulus sizes (Figures 23 and 24). Saccade magnitude increased

Figure 22

Effect of stimulus size on fixation duration for infants. Only 23 subjects who produced three or more AISI's when viewing each of 5, 20, and 30 degree geometric figures are included. The means are connected by the solid line.

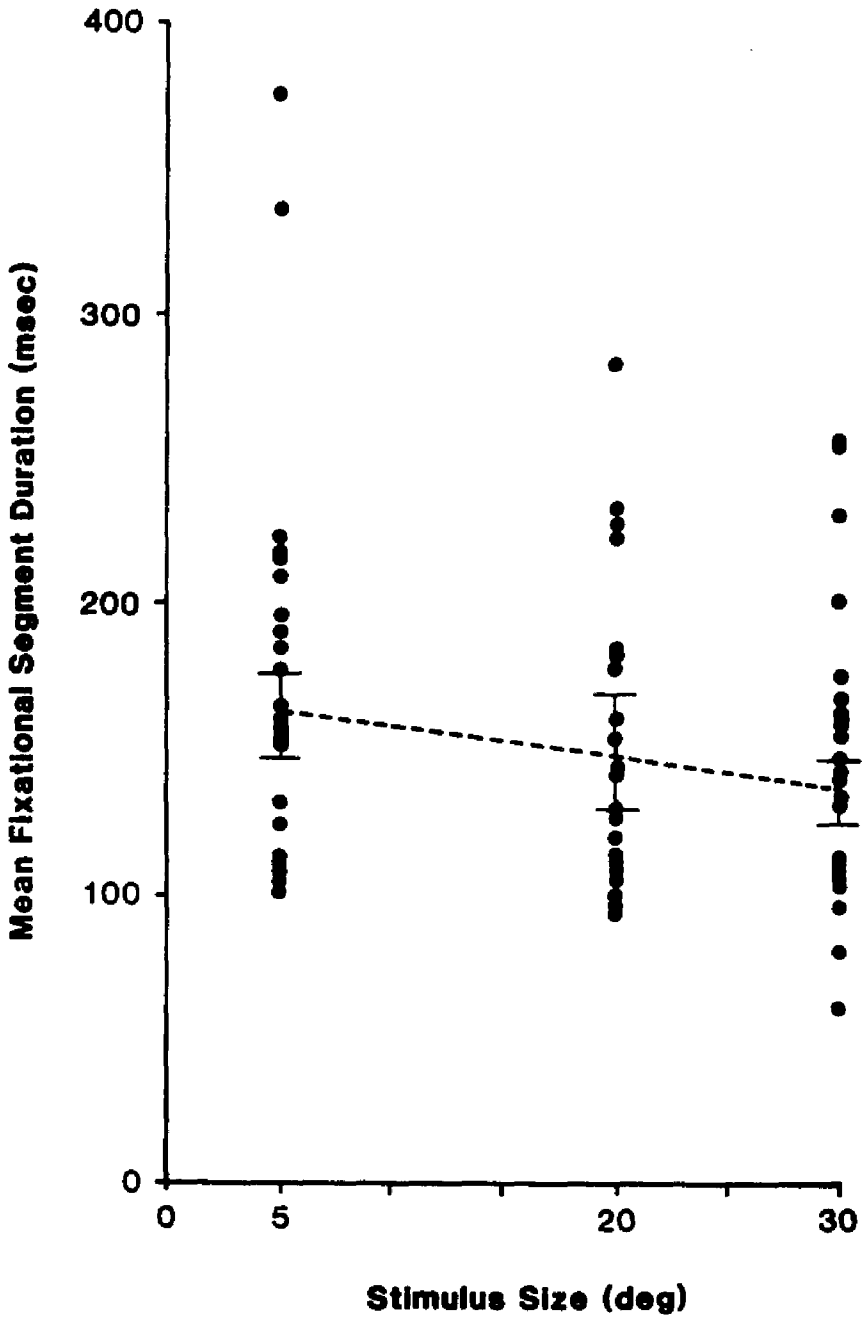
400
300
200
100
0
Mean Fixational Segment Duration (msec)
0
5
20
30
Stimulus Size (deg)

Figure 23

Effect of stimulus size on mean saccade magnitude for infants. Only 23 subjects who produced three or more AISI's when viewing each of 5, 20, and 30 degree geometric figures are included. The means are connected by the solid line.

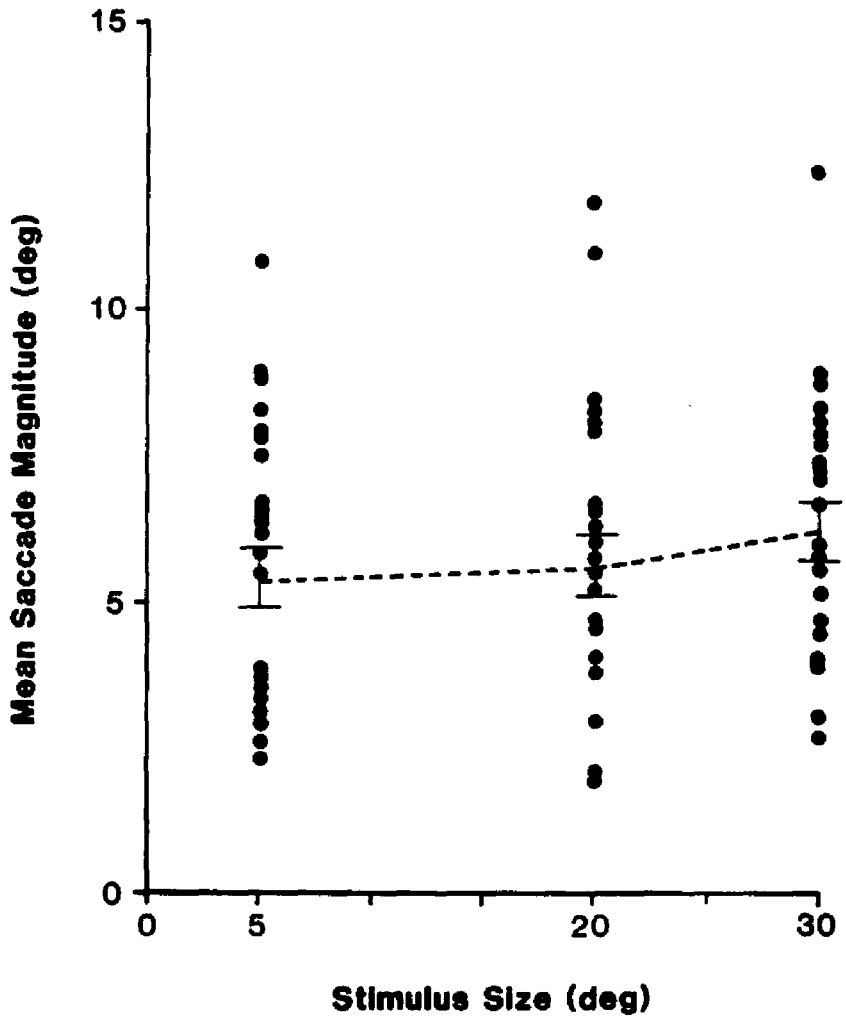
15
10
5
0
Mean Saccade Magnitude (deg)
0
5
20
30
Stimulus Size (deg)

Figure 24

Effect of stimulus size on the breadth of scan of infants. Breadth of scan is calculated as the standard deviation of eye position at the end of each saccade. Only 23 subjects who produced three or more AISI's when viewing each of 5, 20, and 30 degree geometric figures are included. The means are connected by the solid line.

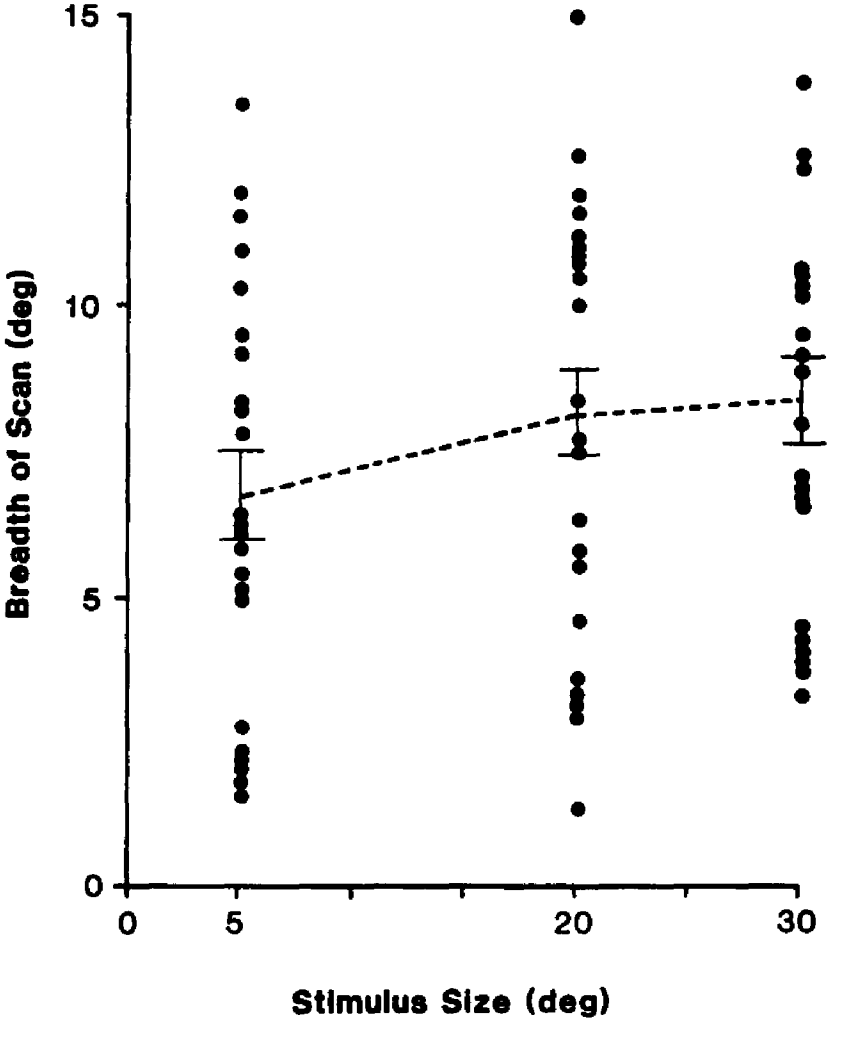
15
10
5
0
Breadth of Scan (deg)
0
5
20
30
Stimulus Size (deg)

with size but did not reach significance. Breadth of scan also increased with stimulus size and was significant ($p<0.05$).

By comparing these trends to the effect of stimulus size with adults (see Figures 15, 16, and 17), it can be seen that the overall effect of stimulus size is much weaker in the infants than the adults. However, all the trends have the same direction as the adults, and are consistent with the multiple target model. The other noticeable difference between the infant fixations and the adults is the brevity of the infant fixations (see also Section 4). Perhaps saccade rate is saturating in the infant so that stimulus size can have only a weak effect. The question is, therefore, why are infant fixations so short. According to the multiple target model, this can only come about if the total saliency of the stimulus is much higher in the infant than the adult, which could occur if there were either more targets for the infant, or some (or all) targets had more saliency for the infant than the adult. It seems unlikely that there should be more targets for the infant; indeed, one might expect the opposite from the immature infant retina. Therefore, in the next two Sections, we shall explore the possibility that visual targets have more saliency for the infant than the adult.

[6]

AMPLITUDE AND RATE OF DRIFT DURING FIXATIONS

We have found considerable drift rate in both adult and infant fixations (see Figure 4). This raises the possibility that fixation drift may play a role in fixation termination as follows: When the eye drifts during a fixation, the image of the visual scene slips across the retina. Because of the temporal tuning of the retina (or motion sensitivity), it seems plausible that the saliency of potential targets will increase as eye drift increases, at least for drift rates of a few degrees/sec. Consequently, according to the multiple target model, when the eye drifts, mean fixation duration should decrease because of the increased likelihood of a saccade being triggered.

The purpose of this Section, therefore, is to examine drift rate in infants and adults to see if it can be related to fixation duration. However, there are considerable technical problems which prevent any meaningful direct measurement of drift rate. We will have to resort to the measurement of drift amplitude and disentangle fixation duration as a confounding variable. This approach is unorthodox and requires some unusual applications of moments to separate different random variables. First, instrument limitations will be discussed.

Instrument Limitations in Measuring Drift Rate

Ideally, motion of the eye during fixations should be analysed by measuring eye velocity. Unfortunately, machine noise in this eye-tracker precludes measurement of instantaneous eye velocity (based on two consecutive samples of eye position). This is best seen by referring to Figure 4b in Appendix B: If we assume machine noise to be band-limited to about 15 Hz, then the r.m.s. velocity noise will be 45 times machine positional noise. This yields a machine velocity noise in excess of 15 deg/sec - completely dwarfing any small actual eye velocity.

An alternative to measuring eye velocity from two consecutive samples is to compute the "average" velocity over a period of time, say, the fixation duration. Although this reduces noise, the reduction is not sufficient to reveal actual average velocity, and furthermore, the amount of noise reduction depends on the fixation duration - a very undesirable contamination which will be discussed in detail later. In view of the severe noise levels, the serious question arises as to how much apparent eye drift is real. To answer this question we will first examine amplitude of drift in fixation segments. Here again moments and their properties will be used.

6.1 Drift Amplitude and Bias

The amplitude of a fixation is defined here as the net displacement of the eye during a fixation and is measured as the difference between the last and first sample of eye position during a FS. Amplitude is a vector quantity and has two components. These components

can be considered in the Cartesian sense with horizontal and vertical components, or in the polar sense with radial and angular components. Although it is simple to transform a vector from one coordinate system to another, the statistics of vectors do not transform so readily. For example, if a vector has horizontal and vertical components which are independent and Normally distributed random variables with zero means and identical variance, the radial component is always positive and has a Rayleigh distribution (see Papoulis, 1965) with a non-zero mean. A more general description is taken up in Appendix G, where an approximation for transforming non-Normal distributions from Cartesian to polar coordinates is shown. Thus, care has to be taken in choosing the more appropriate coordinate system when statistically analysing vectors. Since the instrument operates in Cartesian coordinates, we expect noise also to be in Cartesian coordinates. Therefore, we shall first examine the horizontal and vertical components of drift amplitude.

Figure 25a shows the mean drift amplitude of each Cartesian component for each infant subject (there were too few adult subjects to be shown). As can be seen most subjects exhibit a non-zero mean which might indicate a possible directional bias, since on average, rightward drifts would tend to cancel with leftward drifts if no directional preference existed, and similarly, upward drifts would cancel with downward drifts. However, each mean in Figure 25a is obtained from a finite sample of FS's from each subject ranging in size from 10 to 450 (samples with less than 10 FS's were excluded). There will be random fluctuations in subject means depending on the distribution of

Figure 25

Scatter plot of mean horizontal and vertical components of drift amplitude for each infant subject. Each point represents a subject and each symbol represents a stimulus condition. (a) Plot of means in degrees. (b) Plot of each standardised mean (mean / standard error). Circles represent the 95% confidence interval around zero drift amplitude (Hotelling's T); inner circle for infinite and outer circle for 8 degrees of freedom.

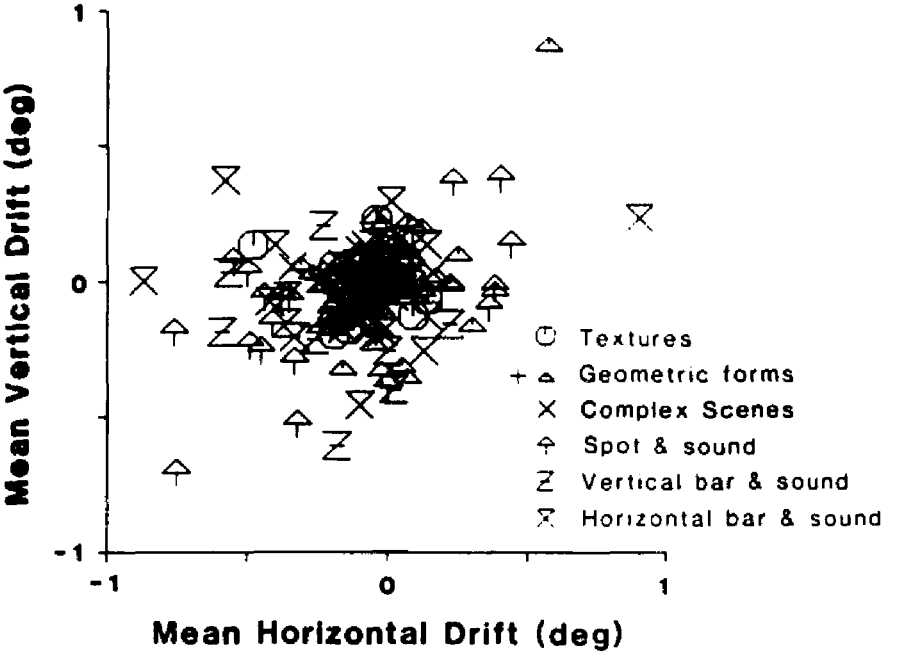
Mean Vertical Drift (deg)
1
0
-1
-1
0
1
Mean Horizontal Drift (deg)
Textures
Geometric forms
Complex Scenes
Spot & sound
Vertical bar & sound
Horizontal bar & sound

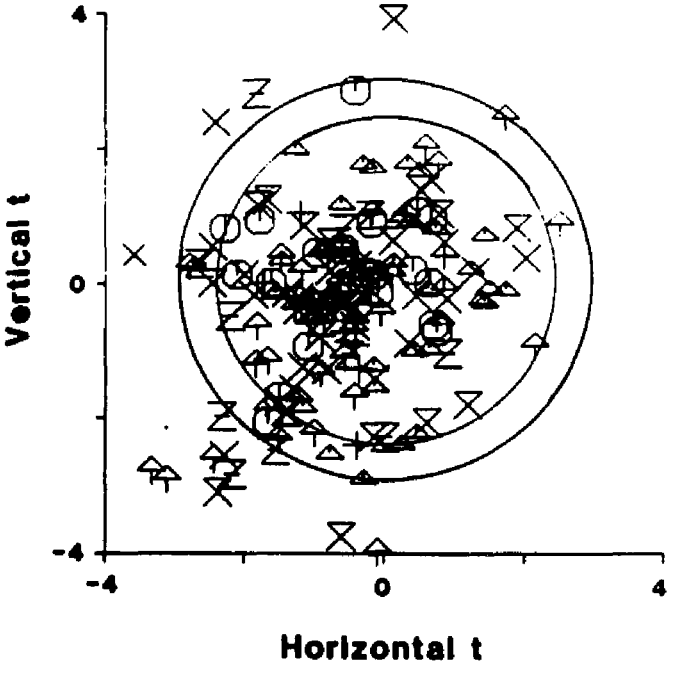
Vertical t
4
0
-4
-4
0
4
Horizontal t

FS amplitude and sample size. Therefore, to assess whether these drift amplitudes were significant, we plot "standardised" subject means: Each infant's mean is divided by the standard error of that component in order to produce a "student t" for each subject's mean component (Figure 25b). For statistical testing purposes both components must be considered simultaneously and the appropriate bivariate test, assuming bivariate normality, is Hotelling's T (see, for example, Batschelet, 1981). In Figure 25b the solid circles show the 95% confidence interval for a zero population mean, the inner circle for infinite sample size and the outer for a sample size of 10. The majority of means fall inside the circles and only a few subjects reach significance at this level (0.05) by falling outside the circles. Calculating each subject's Hotelling's T shows that 11% of 209 subjects reach significance at the 0.05 level, which is more than would be expected by chance. This is due to a small bias down and nasal. We have no explanation for this small effect. However, it is clear that with this level of noise, we cannot really measure drift amplitude or bias directly with any certainty.

Drift Amplitude is the Product of Two Random Variables

We will now examine higher moments of the Cartesian components of drift amplitude for infant subjects. The relationship among these moments is unusual and will allow us to deduce that drift amplitude is a product of two random variables and not a single primary random variable. That is, we will show that fixations are not terminated because the eye drifts a certain distance.

Figure 26 shows the standard deviation of each amplitude compo-

Figure 26

Plot of the standard deviation vs. mean of drift amplitude for infants. Left panel shows the horizontal component and the right panel shows the vertical component of drift amplitude. Note that there is more variability in the standard deviation than the mean. Also, there is more variability in drift amplitude horizontally than vertically.

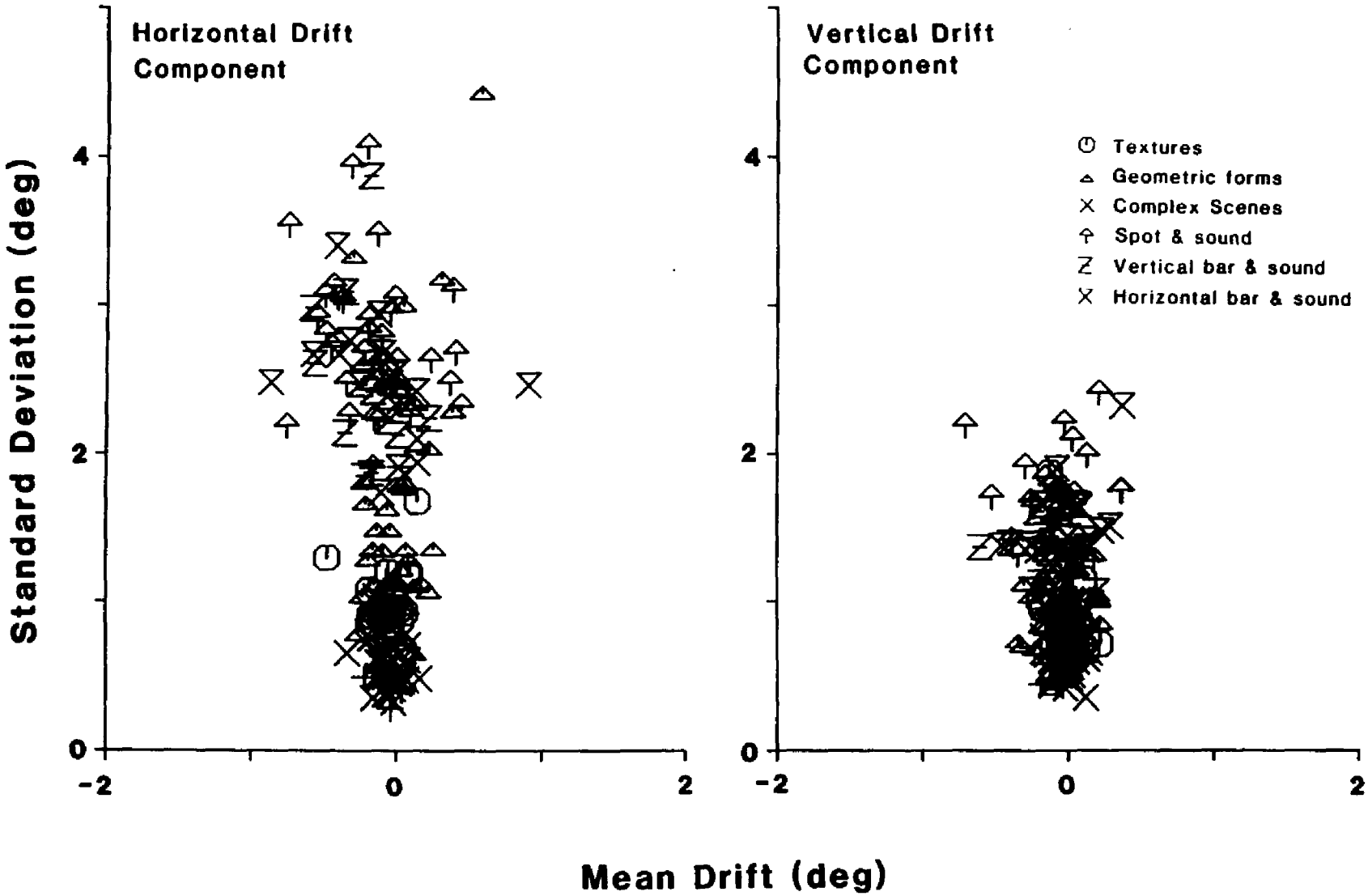
Horizontal Drift Component
Vertical Drift Component
Textures
Geometric forms
Complex Scenes
Spot & sound
Vertical bar & sound
Horizontal bar & sound
Standard Deviation (deg)
Mean Drift (deg)
0
2
4
-2
0
2

nent plotted against the mean for each subject. As would be expected from a roughly symmetrical distribution, there is no definite relationship between the standard deviation and the mean, and as discussed above, the non-zero means probably reflect sampling error. It seems from Figure 26 that the scatter for standard deviation is more than would be expected from sampling error alone. It is also noticeable that the horizontal component is more dispersive than the vertical component. This is common feature throughout and indicates a greater tendency for horizontal drift.

The third root moment is plotted against the mean for each component in Figure 27. The scatter for the third root moment is also much larger than would be expected from random sampling, indicating that some subjects exhibit skewed distributions while their means do not differ significantly from zero. This is rare since the third moment is usually related to the mean (especially the sign of the mean). In fact, although barely discernible from Figure 27, the mean is indeed proportional to the third root moment with a slope of about 0.05 ± 0.01 ($r=0.33$) for the horizontal component and 0.07 ± 0.01 ($r=0.47$) for the vertical component, as found by bivariate regression. Although these slopes are significantly different from zero, they still represent only a very small change in the mean for a corresponding large change in the third root moment.

Even more unusual and striking is the relationship between the third root moment and the standard deviation for each component (Figure 28). Here, as the standard deviation of a subject's amplitude distribution increases, the third root moment also increases - either

Figure 27

Plot of the third root moment (cube root of the third central moment) vs. mean of drift amplitude for infants. Left panel shows the horizontal component and the right panel shows the vertical component of drift amplitude. Note that there is more variability in the third root moment than the mean. Also, note that the third root moment splits into positive and negative lobes.

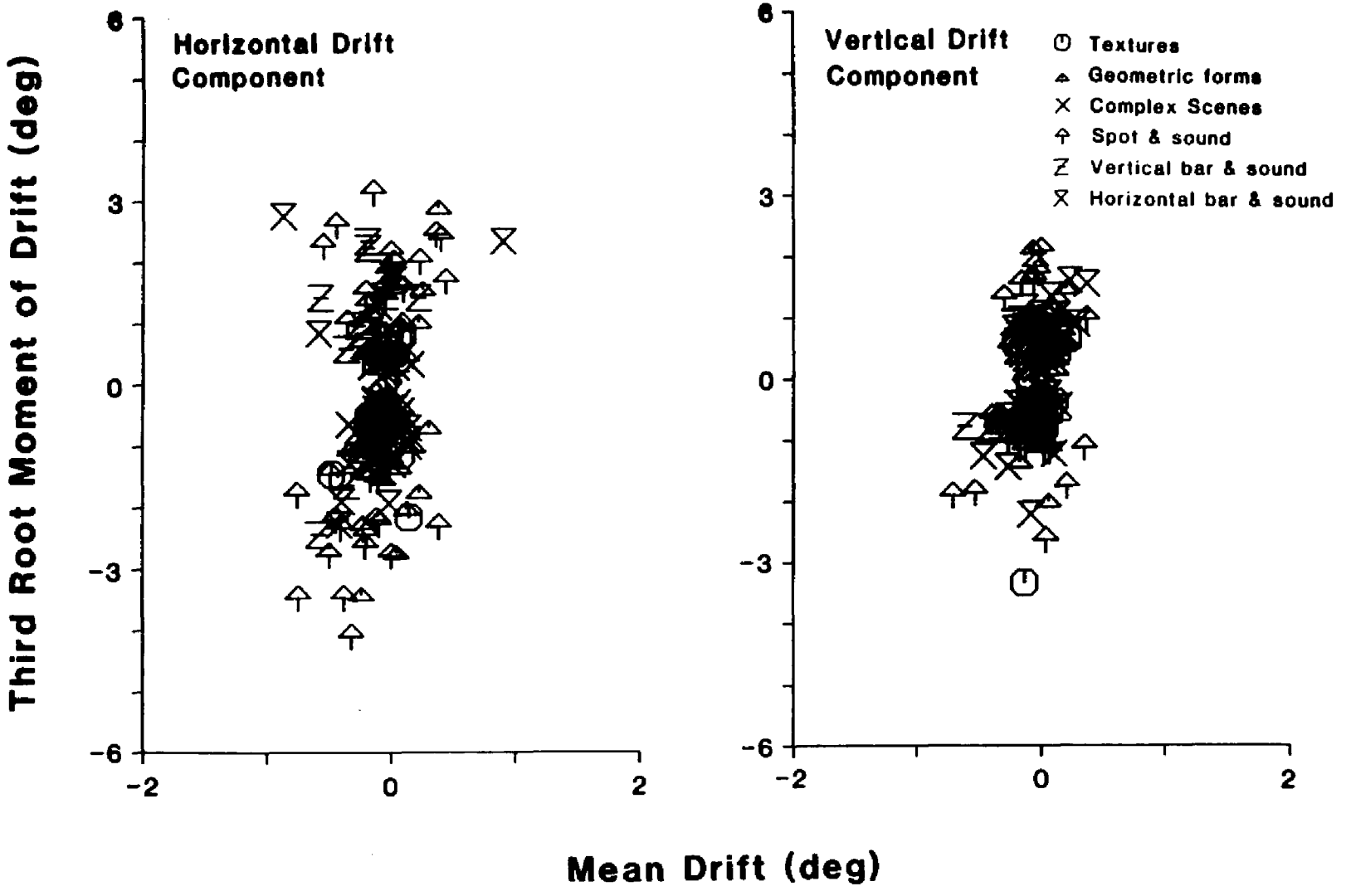
Horizontal Drift Component
Vertical Drift Component
Textures
Geometric forms
Complex Scenes
Spot & sound
Vertical bar & sound
Horizontal bar & sound
Third Root Moment of Drift (deg)
Mean Drift (deg)
6
3
0
-3
-6
-2
0
2

Figure 28

Plot of the third root moment (cube root of the third central moment) vs. the standard deviation of drift amplitude for infants. Left panel shows the horizontal component and the right panel shows the vertical component of drift amplitude. Note the bifurcation of the third root moment with increasing standard deviation.

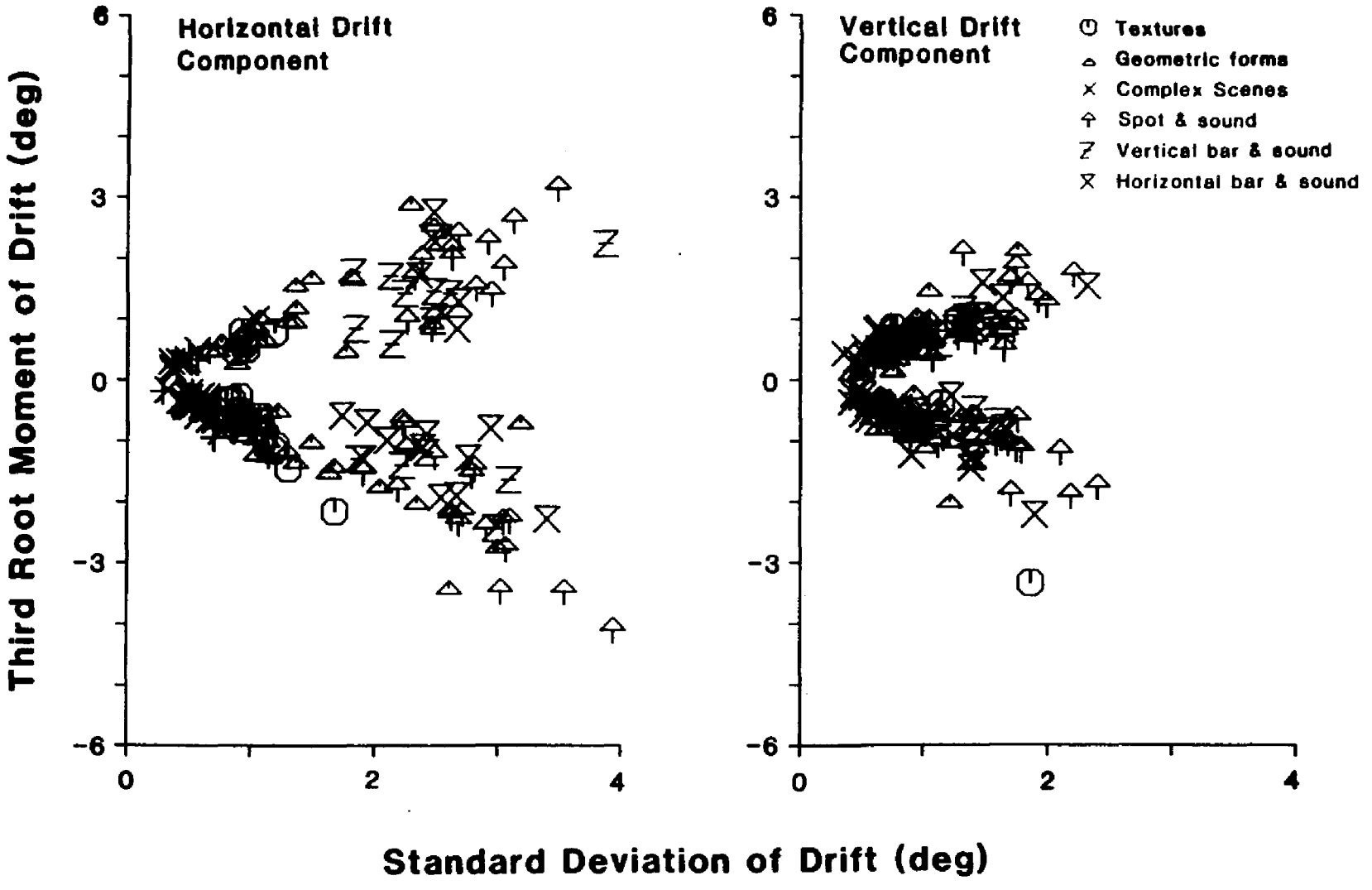
Horizontal Drift Component
Vertical Drift Component
Textures
Geometric forms
Complex Scenes
Spot & sound
Vertical bar & sound
Horizontal bar & sound
Third Root Moment of Drift (deg)
Standard Deviation of Drift (deg)
6
3
0
-3
-6
0
2
4

more positively *or* more negatively. It would appear that there are two populations, those subject sessions that have positively skewed amplitude distributions and those with negatively skewed distributions. The allocation of subject sessions to these two populations seems to be completely random. Postulating two populations is really more descriptive than explanatory and does not account for the trends in Figure 28. In fact the relationship among the moments in Figures 26, 27, and 28 can only occur under rather special circumstances, namely, that each component of amplitude is a product of two random variables. This is complex and is best shown by illustration.

For the sake of argument, consider drift amplitude to be indeed the product of two random variables, duration, D, and average drift rate (or eye velocity), R. For simplicity, we shall also assume that the two random variables are independent of each other in Cartesian coordinates, and that the distribution of drift rate is symmetrical. We shall now be considering the Cartesian components and it is important not to confuse the *amplitude* of each cartesian component with the *magnitude* or radial component of the drift rate and drift amplitude vectors. From Appendix G, the mean amplitude of each Cartesian component will be given by:

$$\bar{A}_{x,y} = \bar{R}_{x,y}\bar{D}. \qquad (19)$$

The variance of amplitude will be:

$$\sigma^2_{A_{x,y}} = \sigma^2_{R_{x,y}}\sigma^2_D + \bar{R}^2_{x,y}\sigma^2_D + \bar{D}^2\sigma^2_{R_{x,y}} \qquad (20)$$

and the third moment of amplitude will reduce to:

$${}_3\mu_{A_{x,y}} = \vec{R}_{x,y}[{}_3\mu_D(3\sigma^2_{R_{x,y}} + \bar{R}^2_{x,y}) + 6\bar{D}\sigma^2_{R_{x,y}}\sigma^2_D] . \qquad (21)$$

Now, if a subject exhibits a small bias in drift rate to one direction, then R is no longer zero and consequently from Equation 21 the third moment of amplitude will also not be zero. As the drift rate bias increases, both the second and third (and higher) moments of amplitude will also increase, but the third moment (and higher odd moments) will have the same sign as the drift rate bias, R, while the variance (and higher even moments) will always be positive. This explains the bifurcation in Figure 28 - those subjects who have a positive drift rate bias (upward and/or temporal for the right eye) will exhibit a positive third root moment (or skewness) and those with a negative bias (nasal or downward) will exhibit negative skewness. Because R is multiplied by quite large quantities in Equations 20 and 21, only a small bias is sufficient to yield large second and third moments. This is why the trends in Figure 26 are so shallow and barely detectable, the third root moment being about 20 times the bias.

Estimation of Drift Bias

Not only does this theory explain the observed moments of ampli-

tude, it also predicts, from Equations 20 and 21, that the amplitude moments should depend on the distribution of duration - which has already been shown to be close to Exponential (Section 4). By neglecting the A-period of fixations, the moments of duration can be approximately related by:

$$\sigma_D^2 \approx \bar{D}^2, \quad {}_3\mu_D \approx 3\bar{D}^2. \tag{22}$$

By substituting into Equations 20 and 21, we obtain the prediction that:

$$\sigma_{A_{x,y}} \approx (2\sigma^2_{R_{x,y}} + \bar{R}^2_{x,y})^{\frac{1}{2}}\,\bar{D} \tag{23}$$

$${}_3\mu^{1/3}_{A_{x,y}} \approx [\bar{R}_{x,y}(15\sigma^2_{Rx,y} + 3\bar{R}^2_{x,y})]^{1/3}\bar{D}. \tag{24}$$

Thus, the standard deviation and third root moment of drift amplitude should be proportional to the mean duration. These predicted relationships are confirmed in Figures 29 and 30. Since $\bar{R} << \sigma_R$, we can obtain from the slopes the rough estimates: $\bar{R}$ = 0.1 deg/sec; σ_R = 2 deg/sec. Despite the fact that these slopes may only be accurate to an order of magnitude because of the inherent assumptions and variability between subjects, it is now clear why any drift bias is difficult to measure with the current apparatus - a fixation of 200 msecs would, *on average,* drift by about 0.02 degrees which is a thirtieth of machine noise.

Figure 29

Plot of the standard deviation of drift amplitude vs. mean FS duration for infants. Left panel shows the horizontal component and the right panel shows the vertical component of drift amplitude.

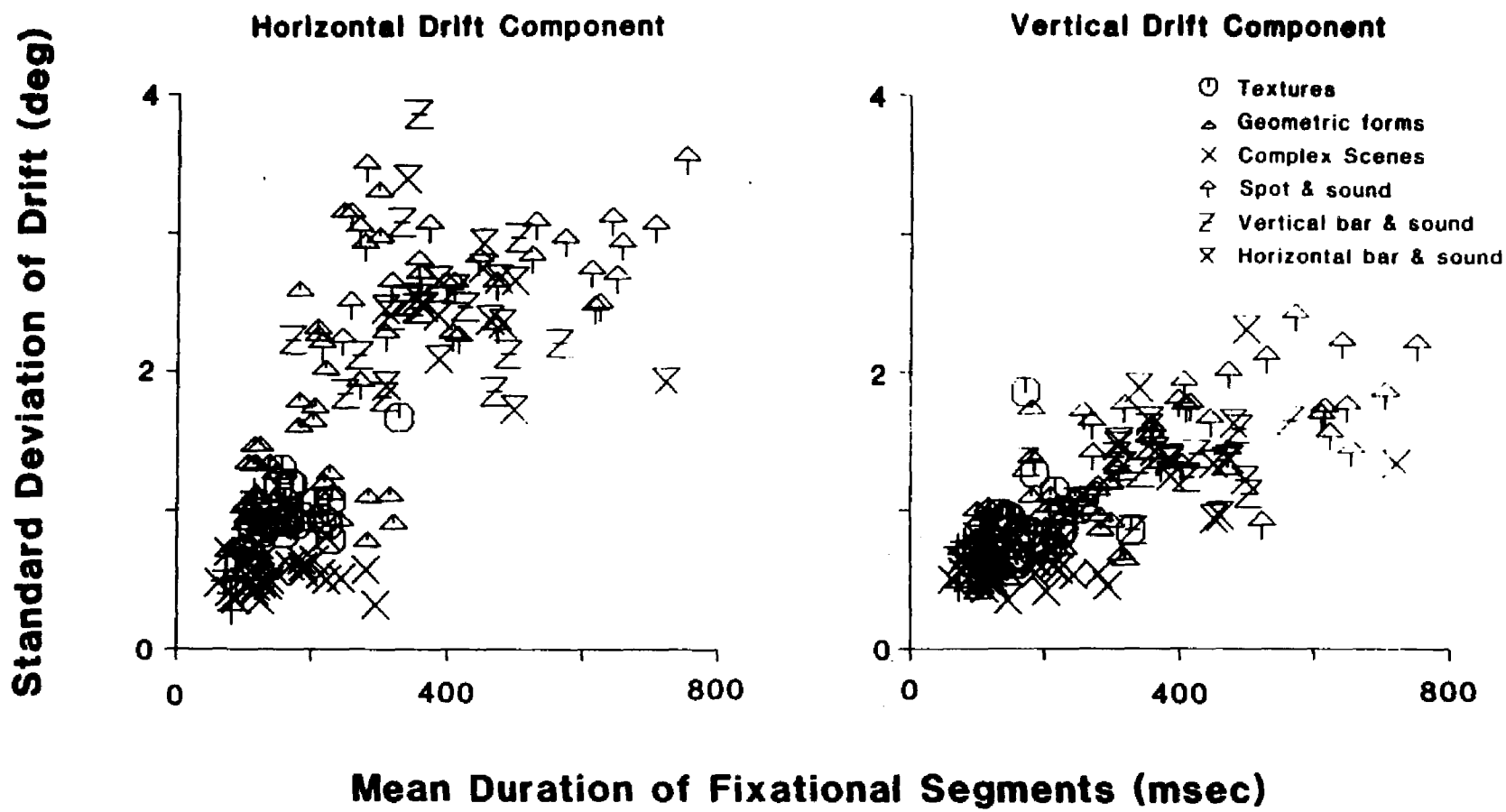
Horizontal Drift Component
Vertical Drift Component
Standard Deviation of Drift (deg)
Mean Duration of Fixational Segments (msec)
Textures
Geometric forms
Complex Scenes
Spot & sound
Vertical bar & sound
Horizontal bar & sound
0
2
4
0
400
800

Figure 30

Plot of the third root moment (cube root of the third central moment) of drift amplitude vs. mean FS duration for infants. Left panel shows the horizontal component and the right panel shows the vertical component of drift amplitude.

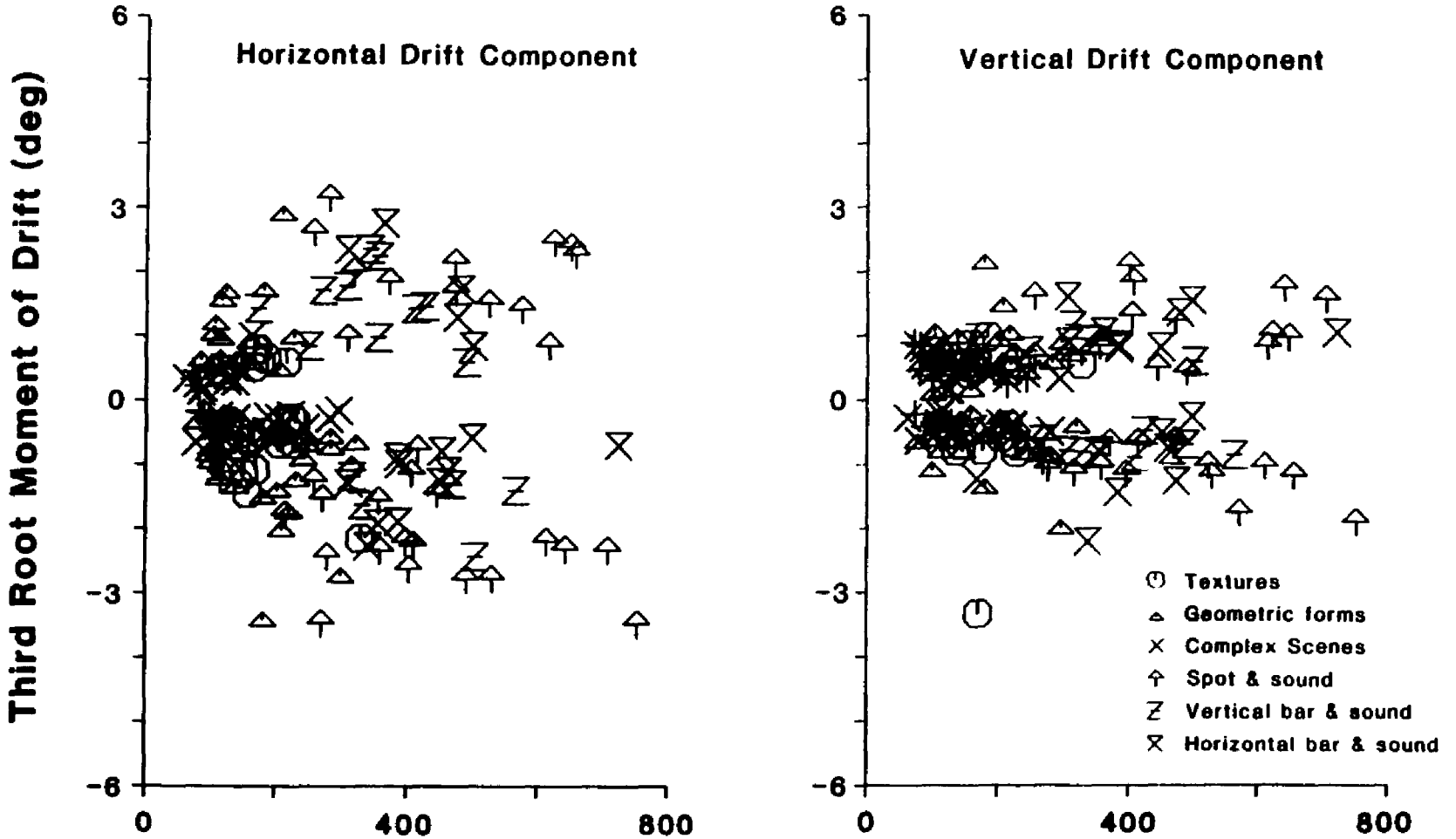
Horizontal Drift Component
Vertical Drift Component
Third Root Moment of Drift (deg)
6
3
0
-3
-6
0
400
800
Textures
Geometric forms
Complex Scenes
Spot & sound
Vertical bar & sound
Horizontal bar & sound
Mean Duration of Fixational Segments (msec)

The purpose of this analysis has been to establish that the apparent drifting in eye position is truly intrinsic to the subject and not an artifact or contribution from some unknown noise source. Examining the moments of drift amplitude has shown that amplitude is the product of two random variables, one of which is fixation duration. We are therefore led to conclude that the other variable is average drift rate. This means that the amplitude of drift is not a primary parameter; its distribution depends on the distributions of the drift rate and duration of fixations. Assuming the above analysis to be correct, the duration of a fixation does not depend on the eye drifting a pre-determined distance. Even if the distance varied from fixation to fixation, one would expect amplitude to be a single random variable - certainly not the product of two random variables. Nor would one expect this distance to depend on the duration of fixations. Such a theory must be discounted - amplitude of drift is not a primary factor in fixations but is only the distance the eye happens to drift during a fixation, that is, the product of drift rate and duration.

6.2 Dependence Between Drift Rate and Duration

Having established that drift rate is a meaningful parameter, we shall examine it more closely within the limitations of instrument noise. First, the reason why direct direct measurement of drift rate is precluded will be re-examined, and then an alternative way of deducing how drift rate changes with duration will be used.

For any fixation (FS or AISI) drift rate can be calculated either

by linear regression against time (as was originally done here) or by dividing the amplitude of drift by duration (ratio method). Since the measured eye position has noise associated with it, the computed drift rate will also have noise. However, drift rate noise will be *relatively* larger for short durations than for long durations. For example, machine noise has a standard deviation of about 0.5 degrees. If a fixation had a duration of 50 msecs, the drift rate would have a standard deviation of about 10 deg/sec by the ratio method and 7.5 deg/sec using regression. If, instead, the fixation were 500 msecs long, the standard deviation would be reduced to about 1 deg/sec by the ratio method and 0.3 deg/sec by regression. Although regression is obviously preferable to taking ratios, both methods result in an error that increases as duration decreases. Now, the magnitude of drift rate is obtained from its vector components. As shown in Appendix G, the mean magnitude of a vector depends mostly on the variance of the components. Thus, even if there were no actual eye drift, noise *alone* would give rise to an apparent drift rate magnitude of about 10 deg/sec for a 50 msec fixation and about 1 deg/sec for a 500 msec fixation. This inverse relationship is observed and it totally contaminates the measurement of any actual drift rate.

An alternative approach is to take means and thereby reduce error by the square root of sampling size. However, mean drift rate cannot be found by simply taking the ratio of mean amplitude to mean duration since it is not yet known whether drift rate and duration are correlated, viz:

$$\bar{A}_{x,y} = \bar{R}_{x,y}\bar{D} - 2\mathrm{cov}(R,D) \tag{25}$$

and so:

$$\bar{R}_{x,y} \neq \bar{A}_{x,y}/\bar{D}. \tag{26}$$

In fact, Equation 25 should be expressed in polar coordinates because any effect by duration will be on the radial component and not specific to the horizontal or vertical component. This adds another complication since statistical independence and dependence are not invariant when transforming from Cartesian to polar coordinates. This is explained in Appendix G, which shows that the radial component of drift amplitude becomes:

$$\bar{A}_r \approx \bar{R}_r(\sigma_D^2 + \bar{D}^2)^{\frac{1}{2}} - 2\mathrm{cov}(R,D) \tag{27}$$

if we assume negligible drift bias $(\bar{R}_x, \bar{R}_y)$ and an Exponential distribution for duration with negligible A-period.[16] Although Equation 27 is approximate, it shows that mean drift magnitude (radial component) is proportional to the product of mean drift rate magnitude and mean duration *if* drift rate and duration are independent in Cartesian coordinates. This allows us to test this independence using means to

---

[16] We have used covariance rather liberally here to include any dependance and not just linear correlation.

reduce noise by decreasing sampling error: Fixations were grouped into duration intervals and the mean magnitude of drift was found for each interval. This gives a reasonable approximation of drift magnitude for different durations provided the interval widths are narrow enough so that there is little covariance within a single interval. Fixations were grouped by linear intervals, 50 msec wide. Since few subjects provided an adequate number of fixations for each interval, weighted means were taken across subjects according to the scheme in Appendix D. By subtracting machine noise (see Appendix G), estimated actual magnitude of eye drift can be estimated. These estimates are shown for the various stimulus conditions for infants and adults in Figures 31, 32, 33, and 34. The positive shape condition for the infants is not shown because of insufficient data. Data from adults viewing the spot and bar stimuli are not shown because there is considerable contamination from the stimulus being moved by the operator.[17]

If average drift rate were independent of fixation duration, then amplitude of drift would increase linearly with duration (see Equation 27). From Figures 31, 32, 33, and 34 it can be seen that this does not occur for durations longer than about 100 - 150 msecs, and amplitude either remains approximately constant or decreases with longer durations. This can only mean that average drift rate is not inde-

---

[17] As mentioned in Section 4, adults' fixations usually lasted until the stimulus was moved by the operator. Thus, durations were "prematurely" terminated which gives rise to spurious drift amplitudes. Nevertheless, the small proportion of fixations that were brief showed similar drift magnitudes as the infants' fixations for the spot and bar stimuli.

Figure 31

Mean drift magnitude for fixational segments grouped by duration for infants viewing the texture stimuli (upper panel) and negative shape stimuli (lower panel). Means were calculated from individual subject means and standard errors using the scheme in Appendix D. Machine noise has been subtracted from mean drift magnitude (see Equation G.11 in Appendix G). Note how mean drift magnitude does not increase appreciably with durations longer than about 150 msecs indicating the lack of independence between these two variables.

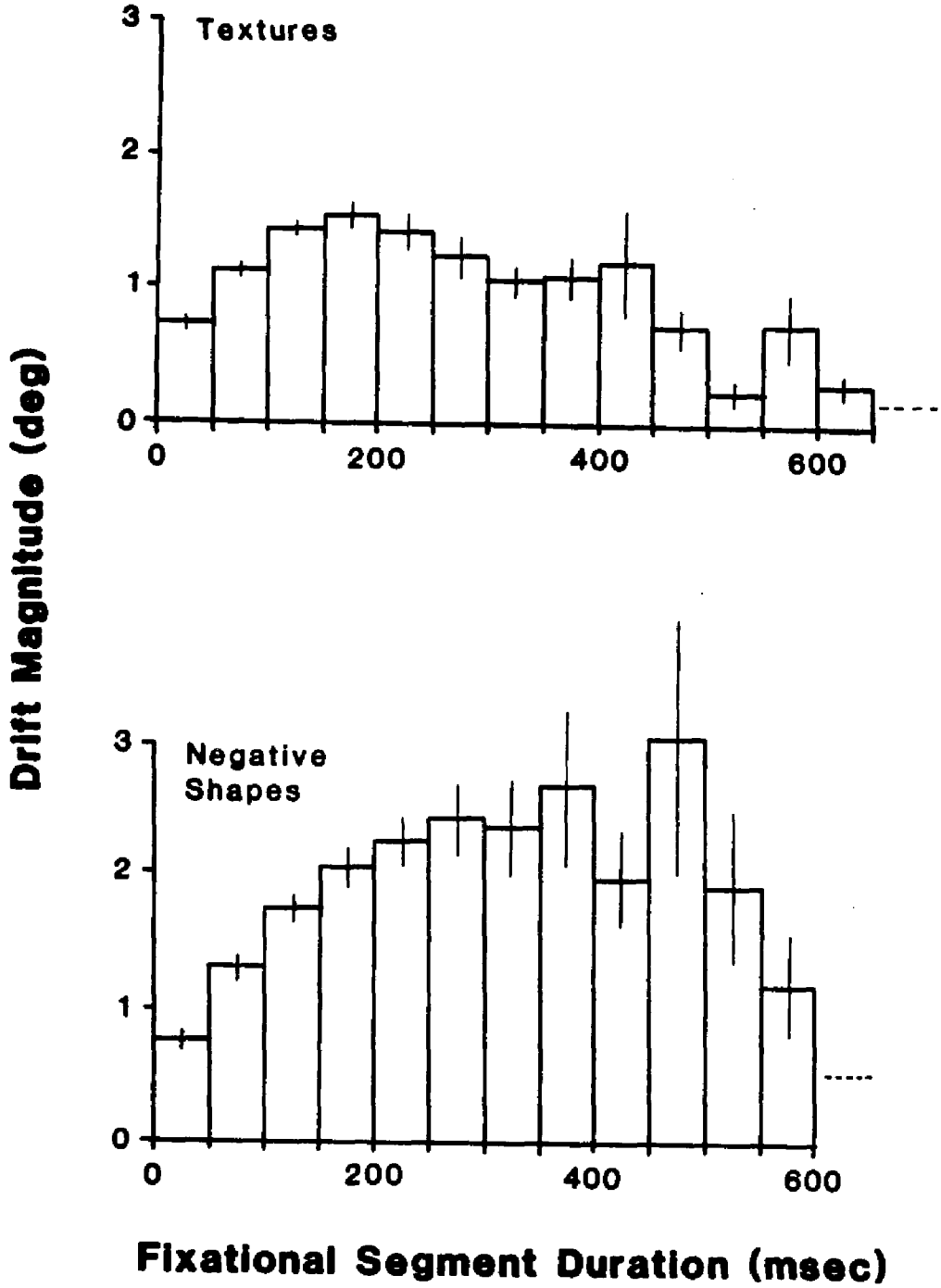
Textures
Negative Shapes
Drift Magnitude (deg)
Fixational Segment Duration (msec)
0
1
2
3
0
200
400
600

Figure 32

Mean drift magnitude for fixational segments grouped by duration for infants viewing the complex scenes stimuli (upper panel) and the single target with sounds (lower panel). Means were calculated from individual subject means and standard errors using the scheme in Appendix D. Machine noise has been subtracted from mean drift magnitude (see Equation G.11 in Appendix G). Note how mean drift magnitude does not increase appreciably with durations longer than about 150 msecs indicating the lack of independence between these two variables.

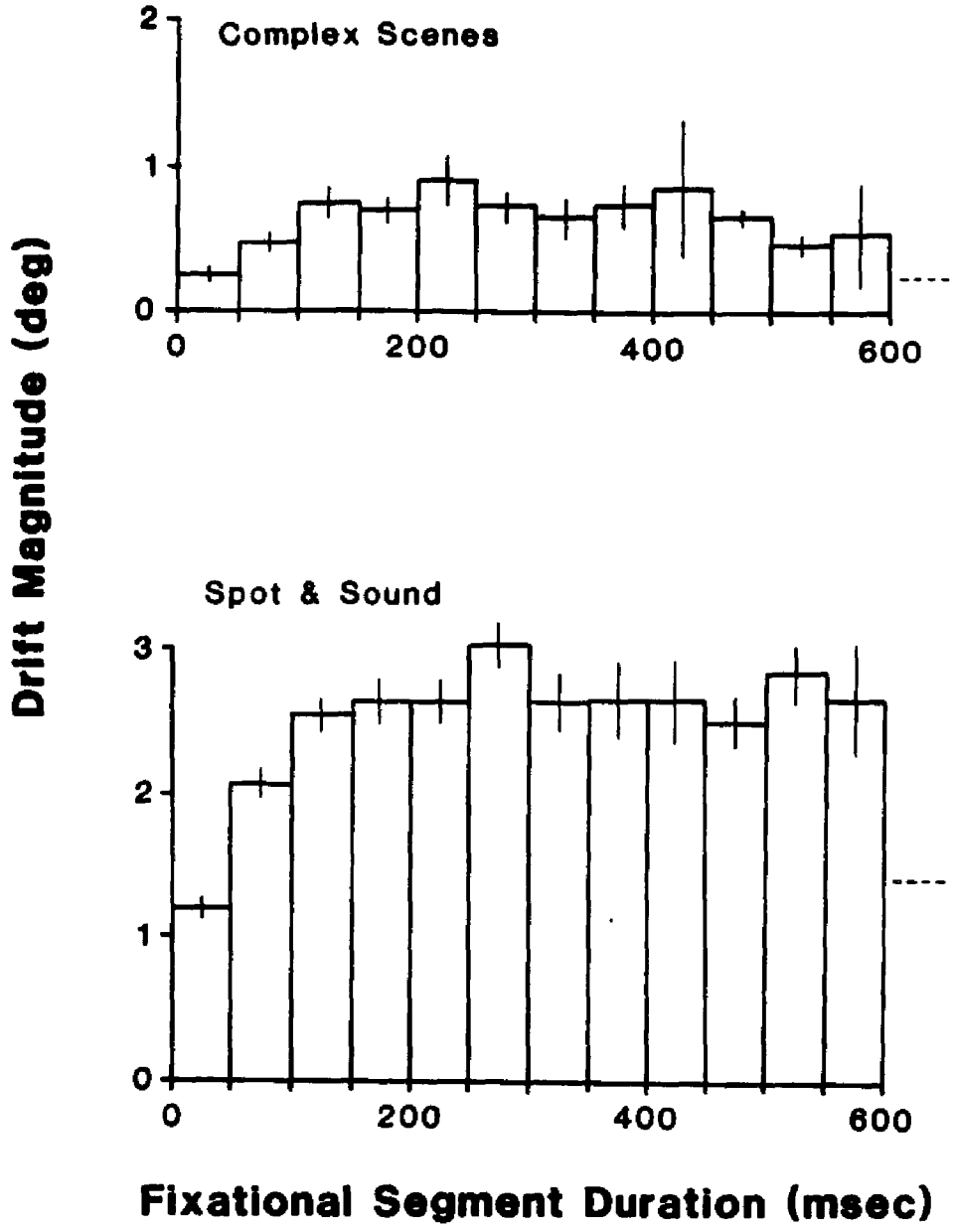
Complex Scenes
Spot & Sound
Drift Magnitude (deg)
Fixational Segment Duration (msec)
0
1
2
3
0
200
400
600

Figure 33

Mean drift magnitude for fixational segments grouped by duration for infants viewing the horizontal bar with sounds (upper panel) and the vertical bar with sounds (lower panel). Means were calculated from individual subject means and standard errors using the scheme in Appendix D. Machine noise has been subtracted from mean drift magnitude (see Equation G.11 in Appendix G). Note how mean drift magnitude does not increase appreciably with durations longer than about 150 msecs indicating the lack of independence between these two variables.

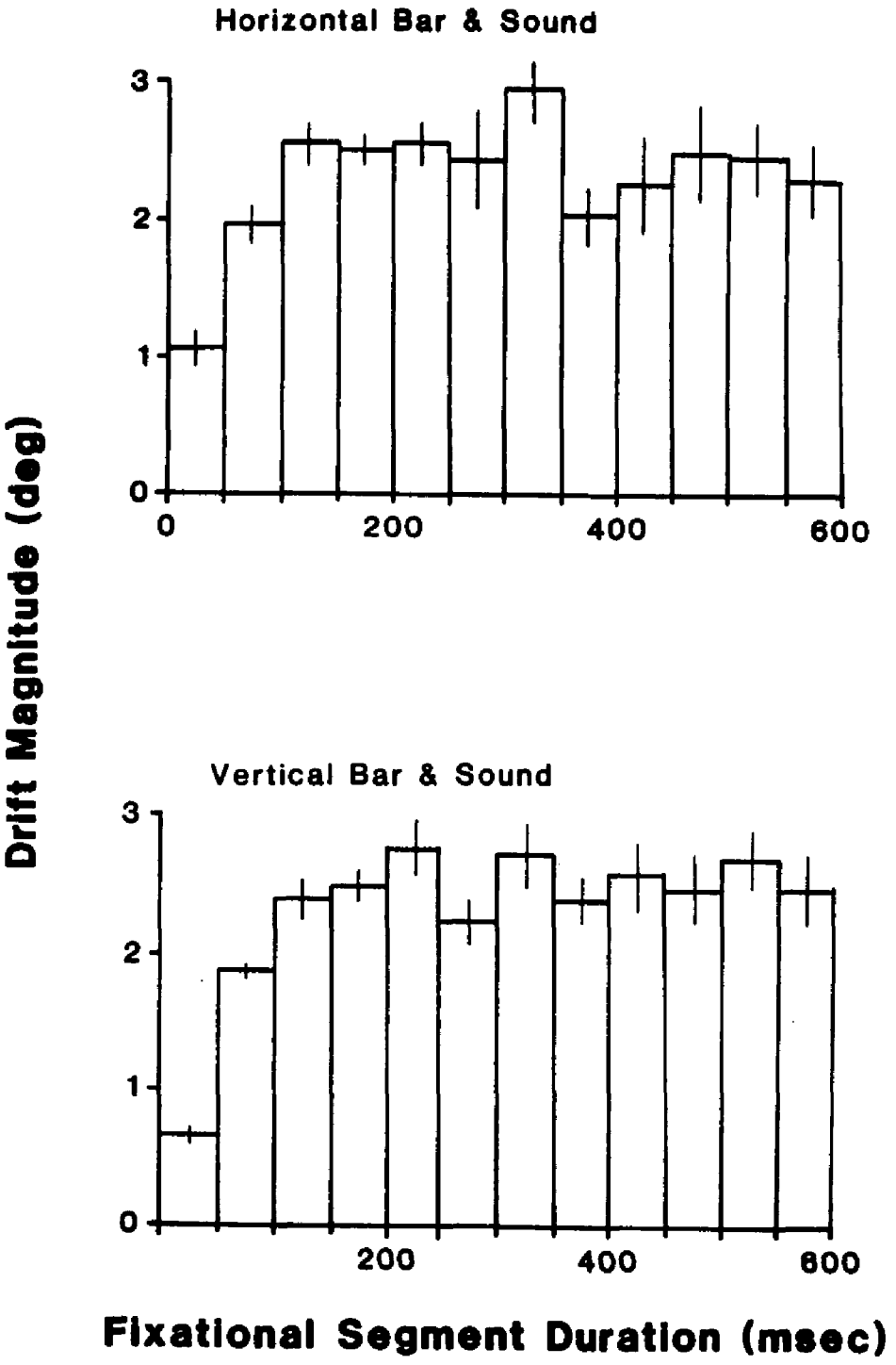
Horizontal Bar & Sound
3
2
1
0
0
200
400
600
Vertical Bar & Sound
3
2
1
0
200
400
600
Drift Magnitude (deg)
Fixational Segment Duration (msec)

Figure 34

Mean drift magnitude for fixational segments grouped by duration for free-viewing adults. Means were calculated from individual subject means and standard errors using the scheme in Appendix D. Machine noise has been subtracted from mean drift magnitude (see Equation G.11 in Appendix G). Note how mean drift magnitude does not increase appreciably with duration indicating the lack of independence between these two variables.

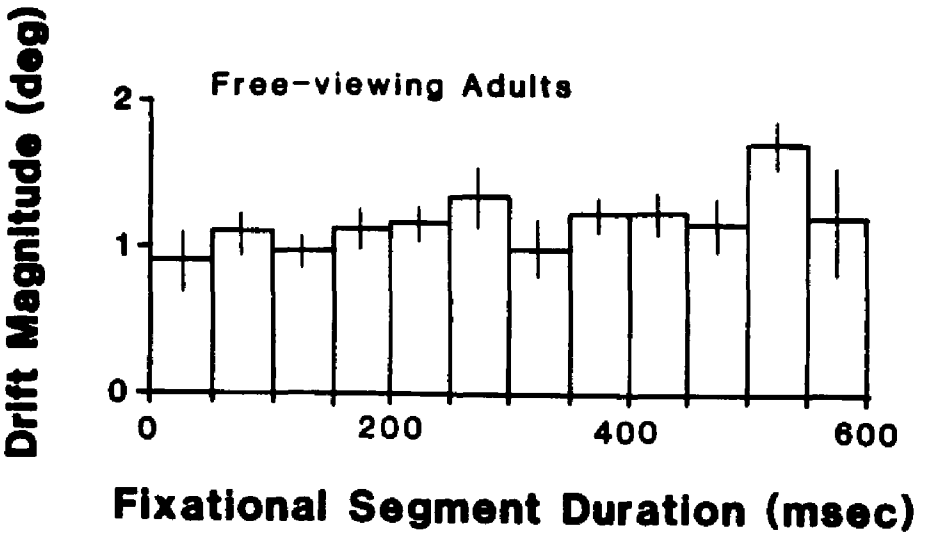
Drift Magnitude (deg)
Free-viewing Adults
2
1
0
0
200
400
600
Fixational Segment Duration (msec)

pendent of duration - the longer the fixation the lower the average drift rate. This is important and warrants discussion since it implies that average drift rate and duration must be causally linked. There are three *a priori* possibilities: Either drift rate is determined by duration, or duration is determined by drift rate, or both drift rate and duration are determined by some other variable(s). These will now be discussed in turn.

(i) Drift Rate Affected By Duration?

Drift rate cannot be affected by duration since this would violate causality - the event which terminates a fixation cannot, *itself*, affect the drift rate during the fixation. However, the validity of this statement depends crucially on the finding that drift rate is a true parameter of fixations. Otherwise, it could be argued that the roughly constant amplitude in Figures 31 - 34 reflect some unknown noise process and that drift rate is only an artifact depending on the duration of the fixation. This is why it has been important to show that drift rate is a physiologic parameter of fixations in Section 6.1.

(ii) Duration Affected By Drift Rate?

The simplest and most parsimonious explanation is that duration is affected by drift rate, even though duration is a random variable. It is well known that the sensitivity of the retina to contrast depends on the temporal component of the stimulus (see Kelly, 1985, for a review). Kelly (1979) has shown that contrast sensitivity is drastically reduced if the image of a grating is stabilised on the retina. Sensitivity increases as stimulus velocity increases up to about

0.5 degrees/sec. Further increases in velocity increase sensitivity at low spatial frequencies but decrease sensitivity at high spatial frequencies. For a thin line moving across the fovea, sensitivity increases with velocity up to about 1 degree/sec and thereafter decreases (Kelly, 1985). The spatiotemporal response of the retina to moving stimuli is dependent on luminance, retinal eccentricity, and the spatial frequency content of the stimulus. It seems likely, therefore, that potential targets would become more salient, that is more likely to trigger a saccade, the faster their images move across the retina - at least up to some critical speed. For a particular fixation, the terminating event would still be random (Exponentially distributed) but the average duration would depend on the rate of drift for that particular fixation. In general, each fixation will have a different drift rate and therefore a different mean duration. The distribution of a single fixation is, of course, not observable; we can only estimate a distribution from many fixations - each Exponentially distributed but with a different mean. Such an observed distribution is a Compound Exponential and it depends on the distribution of the means, and hence the distribution of drift rates across the observed fixations. Nevertheless, regardless of the compounding distribution, the observed distribution will *always* be hyperexponential as found in Section 4 - the pure Exponential distribution would be the limiting case where there is no variance among the duration means and the drift rates would have to be identical for each fixation.[18]

---

[18] In fact the compounding distribution can have considerable variance before the Compound Exponential is easily distinguishable from the

This is a simple explanation of the observed relationships among amplitude, drift, and duration and only requires the postulate that the saliency of a target increases, on average across subjects, with the speed of the target's image on the retina.

As discussed in Section 5, retinal information must require a transmission time to reach the oculomotor centres and so there should be a period during a fixation when a saccade cannot be triggered via the retina (part of the A-period). In this period, then, drift rate should be independent of duration. This may be the explanation for the increase in amplitude with duration for fixations less than about 100 - 150 msecs (see Figures 31 - 34). An alternative explanation for this trend is that there is a limit to how fast the eye drifts, so that for very brief fixations there is also an upper limit to how far the eye can drift.

It can be seen from Figures 31 - 34 that the magnitude of drift also depends on the stimulus conditions. The magnitude (which is proportional to drift rate for a given duration, see Equation 27) is noticeably higher for the subjects viewing the spot and bar stimuli than the other stimuli (except the geometric forms). Yet these stimuli yield the longest durations - seemingly contradicting the inverse relationship between drift rate and duration, so apparent within each stimulus condition. This can be resolved by referring again to the multiple target model outlined in Section 5: The duration of a fixation is determined by the total saliency of the potential targets. The prob-

---

pure Exponential. This is because the Exponential is already an extremely dispersive distribution.

ability of a saccade occurring will not only depend on the number of potential targets but also, as we now suggest, the speed of each target across the retina. For self-induced retinal slip (drift) all potential targets will have the same velocity.[19] Assuming no interaction between targets, the probability of saccade occurrence will depend approximately on the *product* of the number of targets and their speed. Therefore, fixations of a *given* mean duration can be elicited either by a stimulus with many potential targets and slow fixational drift rate, or, by a stimulus with few targets and high drift rate. By necessity, the latter will produce greater drift amplitudes for the given duration. There is no doubt that the spot and bar stimuli are more sparse in potential targets than the other stimuli. The geometric form stimuli seem to be an exception, however.

(iii) Drift Rate and Duration are Determined By Other Variable(s)?

The third possibility for the inverse relationship between drift rate and duration is that another variable is the causative factor.

---

[19] In adults, the temporal response of the retina appears to be roughly the same at eccentricities up to about 30 degreees, but the spatiotemporal interactions are very sensitive to eccentricity. Larger receptive fields are maximally tuned to higher stimulus velocities than smaller receptive fields (Kelly, 1985). However, larger receptive fields are also maximally tuned at lower spatial frequencies. Thus, the pattern of response of the retina to a drifting stimulus is complex and it is not clear whether there will be any inhomogeneity in the change in saliency as drift changes. This situation is further complicated by the differential effect of luminance at various eccentricities (Brown, 1966). However, this does not alter our basic argument for velocities up to a few degrees/sec. For higher velocities, the loss of sensitivity to high spatial frequencies will change the pattern of saliency across the retina appreciably depending on the stimulus. However, for infants who already have poor high spatial frequency response, it is possible that the retina can withstand higher stimulus velocities before there is any appreciable decrease in sensitivity.

There may exist an endogenous variable which simultaneously affects drift rate and the duration of fixations. One could argue (teleologically) that for an interesting or salient stimulus feature, it behoves the subject to maintain a "long and steady gaze" at the feature. For less salient features a "quick glance" may be all that is required. Thus, maybe some attentional/arousal state variable affects both drift rate and duration. Attention could mask out and/or enhance areas of the visual field, thereby affecting the number and saliency of potential targets which would affect mean duration. Attention or arousal could also change average drift rate by altering the gain of a control system governed by retinal slip (smooth pursuit at zero stimulus velocity). Again, though, the inverse relationship between drift rate and duration seems rather coincidental.

While we cannot discount the effect of other variables, it seems non-parsimonious to consider drift rate and duration to be linked causally only by a common dependence on another variable, especially in view of the simple and plausible hypothesis that duration could be determined directly by the visual affect of drift as outlined above.

Summary

Instrument noise has made it impossible to measure drift rate of the eye during fixations directly. To circumvent this problem, we have established that drift does exist by examining moments of drift amplitude in Cartesian coordinates. It was then shown that fixation duration is inversely related to the radial component of drift rate (drift rate magnitude), which supports the notion that target saliency increases with retinal image speed. It has been difficult to estimate

the actual magnitude of drift rate because of the complex statistical relationships between polar and Cartesian coordinates, but, for the infant it appears from Figures 31 - 34, that drift rate magnitude varies from about 5 degrees/sec for brief fixations (<200 msecs) to under 1 degree/sec for long fixations. Even adults show considerable drift (<4 degrees/sec), depending on fixation duration.

It remains equivocal, therefore, whether infant fixations are so brief because of excessive drift. Infants do not show drift rates that are outstandingly more than adults. Nevertheless, as will be discussed in the next Section, maybe fixation duration (or saliency) is very sensitive to small changes in drift speed.

The question that remains is why are the drift rates of our subjects so high. It is customary to consider fixations as being very stable and exhibiting only very slow drifts, usually less than 15 minarc/sec - an order of magnitude below our drift rates. However, most studies have measured fixation stability under quite extraordinary conditions: Subjects are usually well practised and highly motivated (frequently the experimenters themselves). Subjects use bite bars to keep the head immobile and the targets are very small and have high contrast in order to encourage precise fixations. Data records and subjects are often selected for stability of eye position. These experimental conditions test what the fixational system is capable of, but are in marked contrast to normal everyday viewing conditions. Indeed, when the head restraint is relaxed, eye stability decreases, and drift rate increases to 0.5 deg/sec or more (Skavenski, Hansen, Steinman, and Winterson, 1979). There has been no systematic study

of how the fixation system performs under more normal viewing conditions where target contrast is low with many adjacent and peripheral patterns of luminance, and subjects are not motivated to maintain their best possible performance.

To maintain stable fixation, feedback of eye position is needed, and it has been argued that drifts and microsaccades tend, on average, to correct eye position during fixation (St. Cyr and Fender, 1969; de Bie and van den Brink, 1984). Although the feedback error signal is usually provided by the retina, under special circumstances this feedback can be provided extraretinally when the subject is in the dark (Skavenski and Steinman, 1970), or even provided by the experimenter in the form of auditory feedback for amblyopic subjects (Flom, Kirschen and Bedell, 1980). When using visual feedback, fixation stability will depend on the integrity of the retinal error signal and the gain in the closed loop. If, for any reason, the quality of the error signal is poor or the loop gain is low, then fixation instability will increase. Presumably, this is why fixation stability is poor in the dark and for amblyopic eyes. For this reason, it could be argued that the immature fovea renders the young infant effectively "amblyopic" and so causes poor fixation stability. Indeed, the eye position records of our infants are reminiscent of the examples shown for an amblyopic subject by Ciuffreda, Kenyon, and Stark (1979) which have high drift rates and saccadic intrusions. Nonetheless, this does not explain why older infants and our (normal) adults also exhibited large drifts.

Another possibility is that subjects fixate as well as they need to

in order to maintain visibility of that aspect of the stimulus that they *attend*. Thus, if a subject attends only coarse stimulus features (low spatial frequencies as in recognition tasks) then higher drift rates are not only permissible, but may even be preferable to maintain high visibility of these features (Kelly, 1979). If, on the other hand, the subject is instructed to attend fine detail (high spatial frequencies), he can tolerate only small drift rates before visibility is degraded. For the highly motivated experimenter/subject any sharp edge could provide a sufficiently accurate retinal error signal to maintain very stable fixations (for example, Steinman, 1965). The obvious experiment is to record fixations using a high resolution eye-tracker when subjects are viewing high quality sinusoidal gratings.

[7]

AROUSAL AND FIXATION DURATION IN INFANTS

It is still not clear why infants make such brief fixations. According to the multiple target model, potential targets would have to have extremely high saliencies or there would have to be many more targets for the infant than for the adult. The last Section showed that drift rate affected saliency but that there may not be a difference between infants and adults to account for the difference in fixation duration. In this Section we will examine the effects of arousal and show that the brief fixations could be accounted for by low arousal.

For the infant, state is a much more important variable of behaviour than for the adult, and it is probably part of the reason for the notorious vicissitudes of the infant and the large variablity in behavioural measures obtained from infants. An aspect of using a corneal eye-tracker with the infants held upright is that eye movements can only be recorded with some cooperation from the infant: The infant must be still or else the head will move out of the field of view of the infrared camera. The infant's eyes must be open in order to form the optical images needed to compute eye position. In order to obtain a useable pupil image, the pupil must be quite wide and stable, and the subject must roughly accommodate the plane of the

stimulus in order for enough diffuse retinal IR reflection to reach the camera. Using the state classification after Wolff (1966), the infant must be in a continuous state of "alert inactivity" during a recording session. A session had to be halted if the subject fell into a state of "drowsiness" or became "waking active." However, this classification is only a coarse ordinal scheme and there may be considerable variation in arousal within the class of "alert inactivity." We shall use the ratio of a saccade's peak velocity to its magnitude as a finer measure of arousal. This measure has not been used before as an independent measure of arousal in the infant or adult, although this ratio is sometimes used as a dependent measure or a screening device in adult saccade studies. We will first justify this measure before reporting its relationship with fixation duration.

7.1 The Main Sequence as a Measure of Arousal

During a saccade, the eye accelerates first to a peak velocity and then decelerates until it reaches its new resting position. For normal saccades it has been found that the magnitude of the peak velocity attained by the eye is strongly related to the magnitude of the saccade (Westheimer, 1954). The peak velocity increases linearly with magnitude for small saccades but begins to saturate as magnitude exceeds about 10 degrees. By about 30 degrees, saccades have reached their maximum peak velocity. This relationship between peak velocity and magnitude has been termed the "Main Sequence" by

Bahill, Clark and Stark (1975)[20] and has been used as a reliable phenomenon to identify saccades (Ron, Robinson and Skavenski, 1972). Subjects produce saccades that have similar Main Sequences, so that for a given saccadic magnitude, there is a limited range of peak velocities (Boghen, Troost, Daroff, Dell'Osso, and Birkett, 1974). Other species also have Main Sequences; the monkey produces faster saccades (Fuchs, 1967) while the cat produces slower saccades (Crommelinck and Roucoux, 1976) than the adult human.

Although the peak velocity of a saccade is not under voluntary control, it is affected by the alertness of the subject. Saccades have peak velocities below normal when the subject is fatigued (Bahill and Stark, 1975; Abel, Traccis, Troost and Dell'Osso, 1983), or under the influence of depressants such as alcohol (Dodge and Benedict, 1915; Miles, 1924) and diazapam (Aschoff, 1968), or in the dark (Becker and Fuchs, 1969). Similar changes in peak velocity are found in the cat (Crommelinck and Roucoux, 1976), and in the monkey (Ron, Robinson and Skavenski, 1972).

Physiology of Peak Velocity

Neurophysiological studies permit a better understanding of the Main Sequence of saccades. During a saccade, the motoneurons which innervate the extra-ocular muscles exhibit tonic and phasic components (Fuchs and Luschei, 1970). The phasic component provides a burst of firing that boosts the eye velocity to its peak. The burst

---

[20] Bahill et al. (1975) used the term, "Main Sequence", to include also the relationship between saccade duration and saccade magnitude. However, we shall be only concerned with peak velocity.

then decays to a more or less constant tonic firing rate which maintains sufficient tension in the muscles to keep the eye in its new position. Pre-motor neurons have been identified in the paramedian pontine reticular formation which are silent except for this burst during saccades (Luschei and Fuchs, 1972). It appears that the peak velocity depends on the magnitude and duration of the burst in these pre-motor neurons. As the saccadic demand (distance to the saccadic goal) increases, the rate of firing in the burst also increases, which in turn, drives the eye to a greater velocity. However, eventually, the burst rate saturates and the eye cannot be driven any faster. Thus, the peak velocity of the eye saturates with increasing saccadic magnitude. The actual change in eye position during a saccade depends on the profile of the burst and the dynamic mechanical properties of the eye including the muscles etc. (sometimes called the "ocular plant"). The accuracy of saccades is thought to come about because of a closed loop based on "motor copy." In this generally accepted model (Robinson, 1981), a copy of eye position error (the difference between the desired eye position and current eye position) is used as negative feedback to drive the pre-motor burst units. At the beginning of a saccade, there is a large error which drives the burst units very hard. As the eye approaches its goal, the error diminishes which causes the burst to decrease. High loop gain is thought to be responsible for the very fast rise time and slower (but still rapid) fall time of the burst. The effect of this motor copy closed loop is to ensure that the eye reaches its desired target regardless of the precise shape of the burst component. Thus, if the

peak firing rate or loop gain are below normal, the loop will drive the burst for longer until the eye position error (actually its copied version) reaches zero. This will manifest as a saccade with low peak velocity and long duration. Conversely, if the burst rate were high for any reason, the saccade would have a high peak velocity and short duration but would still be on target.

A reduction in peak velocity for a given saccadic magnitude could be caused by a variety of factors. One possibility is extraocular muscle fatigue. In this event, one would expect a discrepancy between the motor copy and the actual motor performance, which would give rise to slow saccades that fall short of their target. One would expect these hypometric saccades to be compensated by corrective (or multiple) saccades. Bahill and Stark (1975) have reported this kind of deficit in fatigued subjects, but they note that by prompting, the subject can produce normal saccades again.

Reduced peak velocity could also be caused by low brainstem arousal which would result in poor neural performance in the saccadic generator. If the phasic component were low in intensity because of inadequate recruitment, low loop gain, or low burst saturation level, saccades would still be accurate because of the closed loop but the eye would now be driven to a low peak velocity and would take longer to reach its target. If the phasic component were very depressed in magnitude then one would expect, not only low peak velocities, but also the eye would spend more time at the end of saccade at very low velocity, and the eye would appear to drift towards its target. Such eye movements (glissades) have also been reported in fatigued sub-

jects by Bahill and Stark. However, even with prompting, saccades in their fatigued subjects did not reach their normal level.

Fuchs and Binder (1983) failed to find any fatigue effects in the extraocular muscles. They did find a modest reduction in peak velocity which they attributed to low arousal or inattention because their subjects could raise peak velocities back to control levels with prompting. Schmidt, Abel, Dell'Osso and Daroff (1979) also found little evidence for short-term muscle fatigue and they attributed changes in peak velocity to "mental fatigue" (tiredness).

Notwithstanding some discrepancies among the results of Bahill and Stark (1975), Fuchs and Binder (1983), and Schmidt et al. (1979), it seems that the peak velocity of saccades is quite sensitive to changes in arousal caused by inattention, mental fatigue, or induced by drugs.

The Main Sequence in Infants

The problem of using peak velocity as a measure of state with infants is mostly methodological. As discussed in Methods, the measurement of eye velocity (especially peak velocity) is very sensitive to instrument bandwidth. This TV-based eye-tracker has low bandwidth because of the inherent 60 Hz sampling rate and also because of the persistence of the TV camera's vidicon. This yields apparent peak velocities below their true values for any subject. To overcome this problem it was necessary to calibrate the eye-tracker dynamically with an artificial eye (see Appendices B and C). After calibration the peak velocities from adult saccades were in good agreement with those recorded from faster eye-trackers (e.g., Boghen et al., 1974).

Appendix H describes a study of saccades from infants viewing the geometric forms and texture stimuli. With respect to the main sequence Appendix H can be considered as preliminary. As expected, the peak velocity of fast eye movements from infants is related to the magnitude of the movements. There was no reliable indication that peak velocity saturated for high magnitude. However, this may be because of noise (both subject and instrument) and because infants did not make many large saccades under the free-viewing condition. Linear regression of peak velocity against magnitude was performed for each subject. It was found that the slopes averaged across infants for the geometric forms and texture stimulus conditions were different. Infants' saccades for the texture stimulus had slopes similar to adults. This demonstrates that infants *can* produce saccades of the same speed as adults and that the infant saccadic generator is not intrinsically immature. Since the saccadic generator is located in the brainstem, it is perhaps not surprising that it can function in the young infant given the cervicofugal development of the brain (Peiper, 1963). For the geometric form stimuli, the average Main Sequence slope was much lower. This suggests that the infants were at a lower level of arousal when they viewed this stimulus. We will now extend this result to the other stimulus conditions and investigate its relationship with fixation duration.

7.2 Dependence Between Fixation Duration and Main Sequence

Figure 35 shows the mean duration of all fixation segments against the mean Main Sequence slope for all subjects for each stimu-

Figure 35

Plot of mean FS duration against mean Main Sequence slope for infants viewing the different stimulus conditions. Only subjects who produced ten or more AISI's and had significant correlation between saccade peak velocity and saccade magnitude ($p<0.005$, 1 tail, Fisher r-z transform) are included. For each stimulus condition, subject means were combined using the scheme in Appendix D. Note how different stimulus conditions invoke different Main Sequence slopes as well as different mean FS durations.

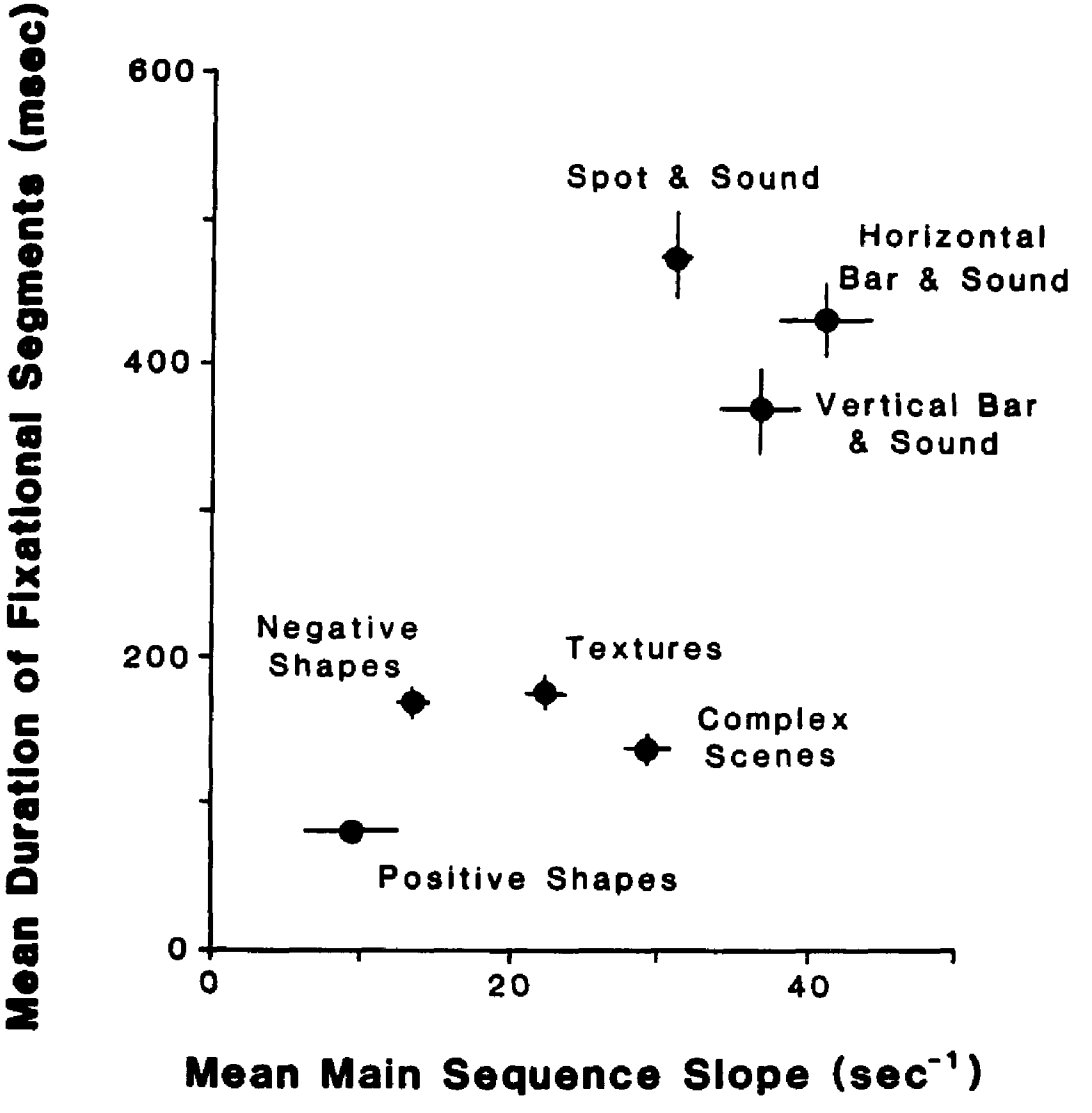
Mean Duration of Fixational Segments (msec)
600
400
200
0
0
20
40
Mean Main Sequence Slope (sec^{-1})
Spot & Sound
Horizontal Bar & Sound
Vertical Bar & Sound
Negative Shapes
Textures
Complex Scenes
Positive Shapes

lus condition. Only those subject sessions were included which had more than ten AISI's and whose Main sequence correlation coefficients were signicant ($p<0.005$, 1-tail, Fisher r-z transform). Not only do the different stimuli elicit different Main Sequence slopes, but there is a significant correlation between mean Main Sequence slope and mean FS duration ($r=0.80$, $p<0.05$). The possible link between arousal level and fixation duration is important and warrants further discussion.

First, we will eliminate two possible artifactual explanations. It could be argued that eye position stability is poor with low arousal levels: The eye movement records would be more noisy and there would be a greater likelihood that an inter-saccadic interval would be parsed as a sequence of FS's instead of one ISI. This can be ruled out, however, since AISI's also show the same relationship with Main Sequence slope (Figure 36) for different infant stimulus conditions. As discussed earlier (see Section 3), AISI's can only be an overestimate of inter-saccadic interval - not an underestimate.

Another possible artifact could arise from the regression of saccadic peak velocity against saccadic magnitude that was performed on each subject session in order to find the main sequence slope: If there were a strong saturating relationship between peak velocity and magnitude, subjects who only produced small saccades would yield higher regression slopes than those subjects who produced a greater range of saccadic magnitudes. Although no saturation could be discerned from any single subject, an average effect might not be detected, and if it were stimulus dependent, this change in

Figure 36

Plot of mean AISI duration against mean Main Sequence slope for infants viewing the different stimulus conditions. Only subjects who produced ten or more AISI's and had significant correlation between saccade peak velocity and saccade magnitude ($p<0.005$, 1 tail, Fisher r-z transform) are included. For each stimulus condition, subject means were combined using the scheme in Appendix D. Note how different stimulus conditions invoke different Main Sequence slopes as well as different mean AISI durations.

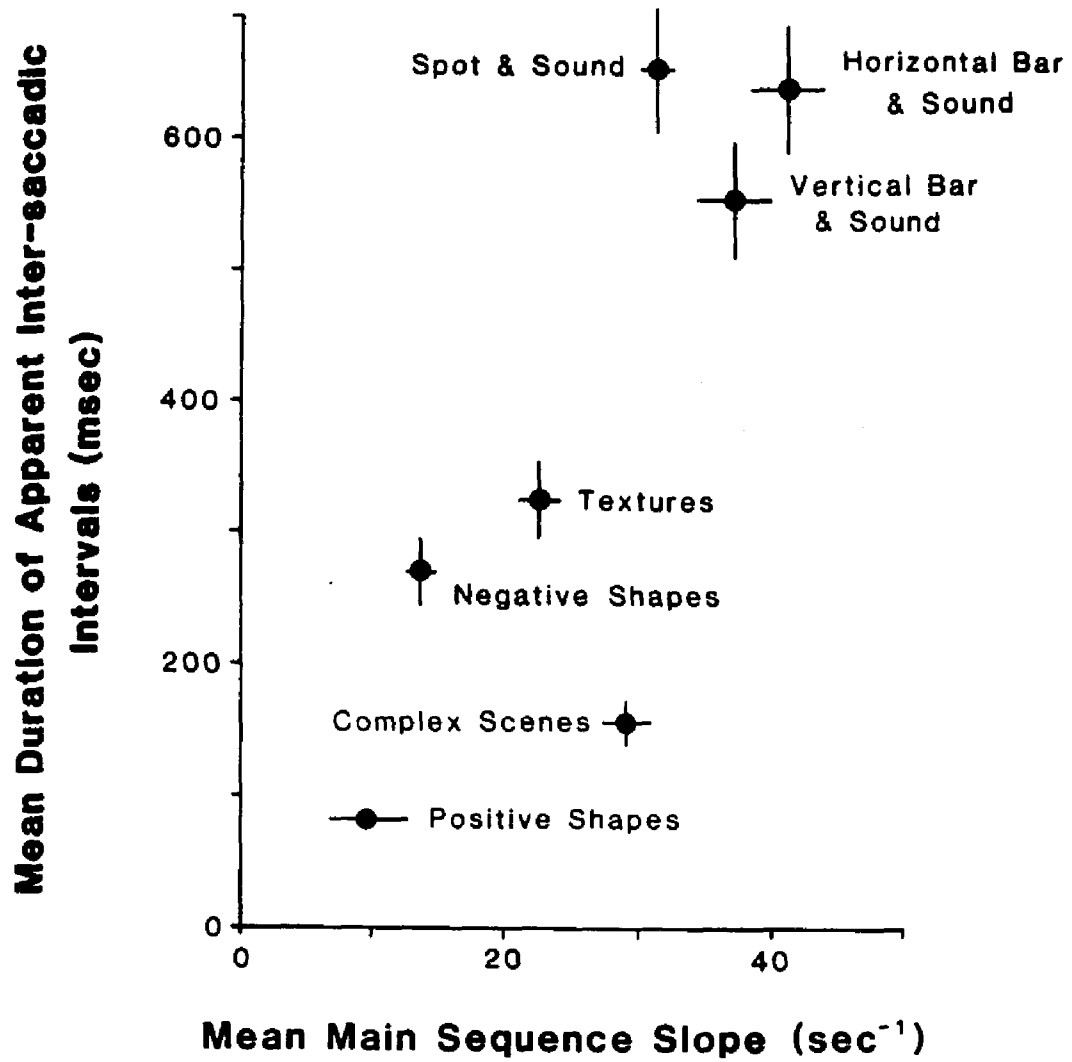
Spot & Sound
Horizontal Bar & Sound
Vertical Bar & Sound
Textures
Negative Shapes
Complex Scenes
Positive Shapes
600
400
200
0
0
20
40
Mean Duration of Apparent Inter-saccadic Intervals (msec)
Mean Main Sequence Slope (sec⁻¹)

regression slope could cause the correlation in Figures 35 and 36. This was easily tested by plotting average saccade magnitude against Main Sequence slope for the different stimulus conditions (Figure 37) for different infant stimulus conditions. As can be seen, there is little relationship between mean saccade magnitude and mean Main Sequence slope, except that the complex scene stimulus condition elicited much shorter saccades than the other conditions, but it also deviates the most from the correlation between fixation duration and Main Sequence slope in Figures 35 and 36. We conclude that the correlation between fixation duration and Main Sequence slope is not artifactual.

This leaves three possibilities; changes in saccadic peak velocity are caused by fixation duration, changes in fixation durations are caused by changes in saccadic peak velocity, or both fixation duration and saccadic peak velocity are affected by some stimulus-borne variable(s). Although fatigue may not have affect on peak velocity in the adult (as discussed above), we cannot assume that the same resistance to fatigue occurs in the infant. Therefore, we will first examine the possible affects of fixation duration (saccade rate) on saccade peak velocity.

Fatigue

Short fixation durations entail the production of many saccades, which in turn, could lead to fatigue and lower Main Sequence slopes. However, if fatigue occurred because of the sheer number of saccades, one would expect a correlation of the opposite sign than shown in Figures 35 and 36. This is because subjects produced many more

Figure 37

Plot of mean saccade magnitude against mean Main Sequence slope for infants viewing the different stimulus conditions. Only subjects who produced ten or more AISI's and had significant correlation between saccade peak velocity and saccade magnitude ($p<0.005$, 1 tail, Fisher r-z transform) are included. For each stimulus condition, subject means were combined using the scheme in Appendix D. Note how mean saccade magnitude does not change appreciably with stimulus conditions (except for comple scenes).

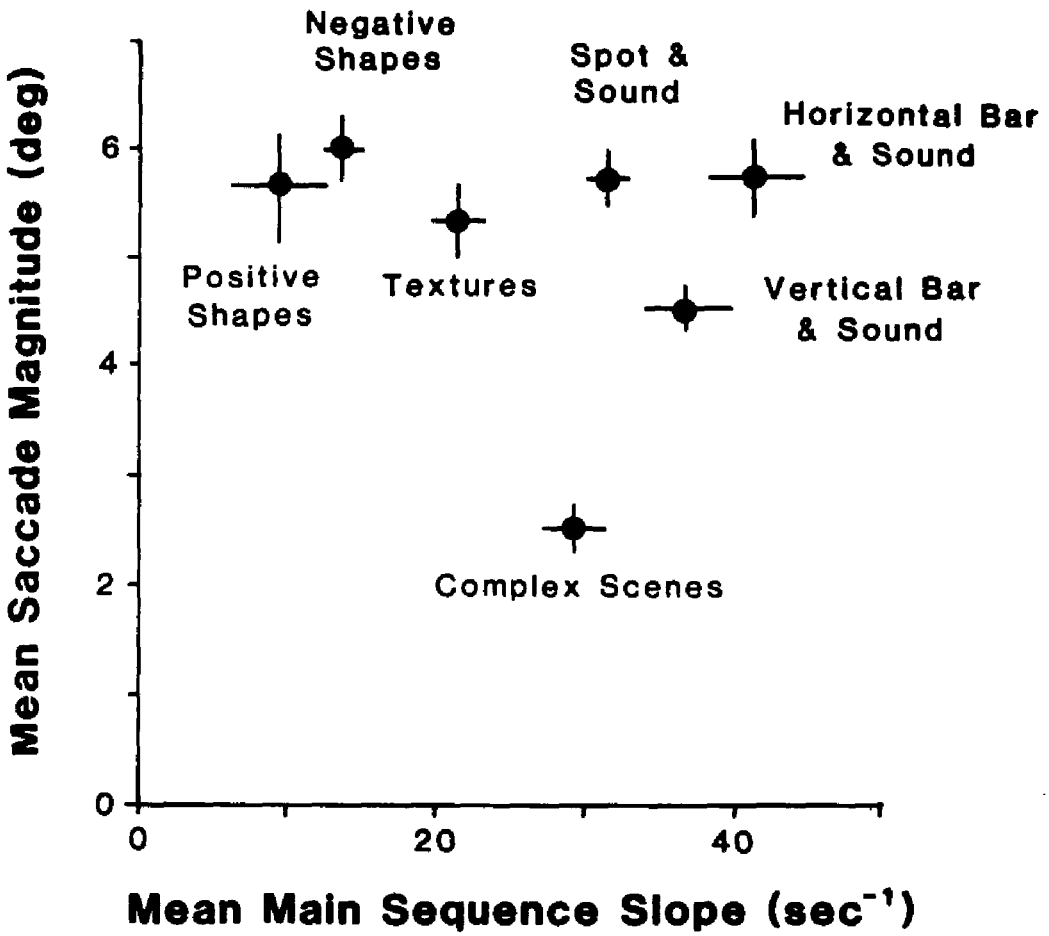
Negative Shapes
Spot & Sound
Horizontal Bar & Sound
Positive Shapes
Textures
Vertical Bar & Sound
Complex Scenes
Mean Saccade Magnitude (deg)
0
2
4
6
0
20
40
Mean Main Sequence Slope (sec⁻¹)

saccades (on average, 107 per subject session) for the spot and bar stimuli than the static stimuli (on average, 47 per subject session) which were presented for only ten seconds. One would have expected, therefore, that the spot and bar stimuli were more likely to induce fatigue.

Large saccades have a greater fatiguing effect than small saccades (Bahill and Stark, 1975). However, with the exception of the complex scene stimulus, there is little difference in the average saccade magnitude (Figure 37).

It seems that the differences in mean Main Sequence slope across stimulus conditions are not due to differential fatiguing induced by the different degrees of oculomotor activity. It is more likely that the difference in Main Sequence slopes are due to different levels of brainstem arousal which are induced, somehow, by the different stimulus conditions.

Stimulus Effects on Arousal

For the static stimuli, the geometric forms are associated with lowest level of arousal followed by the texture stimuli and then the complex scenes. With respect to these static stimuli, their "complexity" (as judged by an adult) have the same ordinal relationship. The geometric forms have the least amount of contour and the least range of spatial frequencies per unit area of the stimulus (except possibly at the boundary of the form). On the other hand, the complex scenes have the most contour and spatial frequency range per unit area. The textures lie somewhere between these two extremes. The correspondence between arousal and complexity is significant since the chance

of four single measurements having a given sequence is 0.042 - and because each point in Figure 35 represents a mean, this probability will be much lower. The highest Main Sequence slopes were elicited by the spot and bar stimuli. Although these were the "simplest" stimuli, they were accompanied by sounds to attract the infants' attention (Methods). Thus, the high arousal could have been induced by the auditory and not the visual content of the stimuli. Indeed, without any sound, it was very difficult to record any data because subjects tended not to look at the stimulus. We, therefore, postulate that different stimuli induce different levels of arousal. The visually evoked component of this arousal seems to increase with the apparent "complexity" of the visual pattern of the stimulus.

The stimuli can also be ordered by their average spatial frequency content per unit area (although an actual Fourier analysis was not performed). Thus, the complex scenes represent a broadband stimulus with contrast at all spatial frequencies (visible to the infant) over their entire areas. The texture stimuli, which consisted of periodic lines and checkerboards, have contrast mostly at discrete spatial frequencies (harmonics of their periodicities), also over their entire areas. The geometric forms (and spot and bars) have contrast at many spatial frequencies because of the contrast edges, but these are restricted to small regions of the stimulus areas. On average, these stimuli have low contrast per unit area. The spatial frequency content of the stimuli are filtered by the visual system (at least at the retinal level) which would depend on the infant contrast sensitivity function, spatial frequency channels, mean luminance, and age. It

seems therefore, that a case could be made to suggest that arousal, as measured by Main Sequence slope, is affected by the level of excitation reaching the brainstem via the optic nerve.[21] A similar kind of argument has been made by Gayl, Roberts and Werner, (1983) about infants' visual preference. They showed that the total integrated contrast over a band of spatial frequencies centred on the spatial frequency with the most visible contrast was a good predictor of infants' preference for regular and random checkerboards.

7.3 Effects of Arousal on Fixation Duration

We now return to the correlation between Main Sequence slope and mean fixation duration shown in Figures 35 and 36, assuming the change in Main Sequence slope is due to different levels of arousal elicited by the stimulus conditions. The question is whether fixation duration is directly dependent on arousal or whether the correlation appears because of a common dependence on stimulus conditions.

It is possible that arousal and fixation duration are independent of each other functionally. According to the multiple target model, those stimuli with the greatest total saliency will elicit the shortest fixations. Stimuli with the greatest total saliency will also have the broadest band of spatial frequencies (that is, they will appear most "complex"), and so will evoke the highest level of arousal. Thus, in this manner, the visual pattern would determine separately arousal

---

[21] If this is the case, it suggests that the infant CSF might be derived from the Main Sequence slope recorded from saccades made by infants viewing sinusoidal spatial frequency gratings.

and fixation duration. According to the multiple target model, the small spot and narrow bar are sparse in potential saccade targets and so fixations would be long. These stimuli will also elicit low levels of arousal which explains why the subjects tended not to look at them. However, the addition of attractive sounds to this stimulus condition raises arousal via another modality but does not affect the saliency of visual pattern, and so fixations remain long. Although this is a simple model to explain the correlation in Figures 35 and 36, it still does not explain why the fixations are so brief in the infant.

At the other extreme, it could be postulated that fixation duration is causally determined by arousal level. Thus, mean fixation duration changes with stimulus only by virtue of the different levels of arousal that the stimuli elicit, and not by any direct visual evocation. This is not to say that the infant is blind, but that the saccadic trigger is somewhow determined by arousal, so that raising the arousal level decreases the probability of a saccade occurring. This model of total dependence allows for very brief fixations if the level of arousal is sufficiently low, but it does not account for the effects of drift rate on fixation duration that was found in Section 6. Furthermore, there is no simple mechanism that would account for this dependency *and* also explain the multiple target model in adults.[22]

By rejecting both the independent and total dependent models,

---

[22] If the multiple target model were rejected in favour of an arousal mechanism in adults (the Spontaneous Saccade model, see Section 4), then it would have to explain why increasing stimulus size decreases fixation duration (Figure 15) rather than increasing duration as in the infant (Figures 35 and 36).

we are left with a mixed model: Fixation durations are affected by both the visual component of the stimulus and also by the subject's level of arousal (which may also, itself, be affected by the visual content of the stimulus).

7.4 A Model of Infant Fixation Duration

We will extend the multiple target model to allow for an influence from the infant's arousal level. This discussion is restricted to infants who are in the alert-inactive state, since this is the only state which permitted us to record eye movements. Here, we are not concerned with how arousal level is changed but rather how it can affect fixation duration. The key to this lies in the mechanism which determines a potential target's saliency. To discuss this, it is necessary to be more specific about the saccadic triggering mechanism. However, it should be noted at the outset that we are not building a physiological model, and we leave the possible neural mechanisms and pathways to conjecture.

We have a reasonable idea of how the visual system works at least at the retinal level. We have a similar level of understanding of the physiology of the saccadic generator and the extraocular musculature. Unfortunately, we have much less knowledge about the intervening pathways, even to the extent of cortical and subcortical involvment in visually evoked saccades. However, because of the all-or-none nature of saccades, it is reasonable to assume that there is a saccadic trigger. That is, there is a threshold level which must be exceeded by some signal in order for the saccadic generator to be

switched on. Since the eye executes only one saccade at a time, there can be only one trigger, at least conceptually; there may be many triggers but a decision has to be made eventually (e.g., first-come-first-served). According to the multiple target model, saccades are triggered visually by many retinal channels (the retinal ganglion cells). One possibility, therefore, is that saccades are triggered whenever a signal *derived* from a retinal ganglion cell's output exceeds the trigger's threshold. Of course, a retinal ganglion cell's output undergoes many transformations in the visual system before being compared to the saccade trigger level. However, for the sake of simplicity, we will refer the signal back to the retinal ganglion cell.

The output of a retinal ganglion cell is actually a stochastic signal and there will be random fluctuations in the ganglion cell's output signal around a mean level. Thus, we argue that whenever a fluctuation (or a manifestation of a fluctuation later in the visual system) crosses the trigger threshold, a saccade will be triggered. Provided the ganglion cell's signal is statistically stationary, the probability of such a fluctuation is constant in time regardless of the actual probability distribution in the fluctuations. Therefore, the time before a triggering fluctuation occurs will be an Exponential probability distribution.

Now, the probability of a triggering fluctuation will depend on the mean signal level, the probability distribution of the fluctuations, and the triggering threshold level. However, regardless of the exact form of the probability distribution of the fluctuations, the probability of a triggering fluctuation will increase very rapidly as the difference

between the threshold and mean level decreases. This is illustrated in Figure 38. For example, consider the ganglion's mean level to be 100 spikes/sec with additive white Gaussian noise having a standard deviation of 10 units. If the saccadic trigger threshold were at 130 units, the probability per unit time (saliency) of a noise fluctuation exceeding the threshold is 0.0013, and we would have to wait, on average, for 769 seconds for such an event. If the threshold level were reduced to 120 spikes/sec, the probability of a triggering fluctuation would increase to 0.023, and now we would wait only 43 seconds. A further decrease in the threshold to 110 spikes/sec would decrease the waiting time to six seconds. Thus, the probability that a saccade will occur is very sensitive to the difference between the mean signal level of a ganglion's output and the saccadic trigger level. It can now be appreciated that the saliency of a potential visual target depends not only on the level of excitation it causes in a ganglion cell (via the receptive field) but also on the level of the saccadic trigger threshold.

a) Saccadic Trigger Level Modulated By Arousal

We propose that the trigger level is affected by the subject's arousal level (at least in the infant), so that high arousal elevates the trigger threshold. Clearly then, if the threshold is very high because of high arousal, only highly salient targets will trigger saccades, on average. This will yield very long fixations, and it would appear to the experimenter as if the subject were "captured" by the current target or that the subject were being very attentive to the stimulus. (Indeed, arousal seems to be a pre-requisite of attention.)

Figure 38

Hypothetical relationship among saliency, fixation duration, and the saccade trigger level. Upper panel illustrates a noisy signal showing mean signal level and the saccade trigger threshold. Whenever the signal exceeds the threshold the saccade generator is triggered. The lower panel shows the probability per unit time (saliency) of such an event (assuming Gaussian signal noise) for different threshold levels (in standard deviation units of the signal noise). The mean waiting-time (or fixation duration) is the reciprocal of saliency.

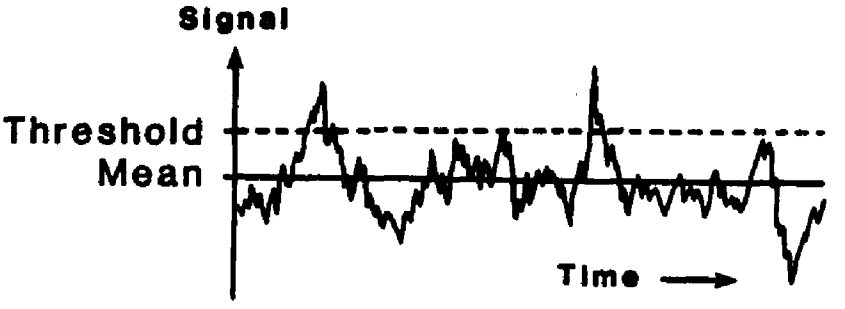
Signal
Threshold
Mean
Time

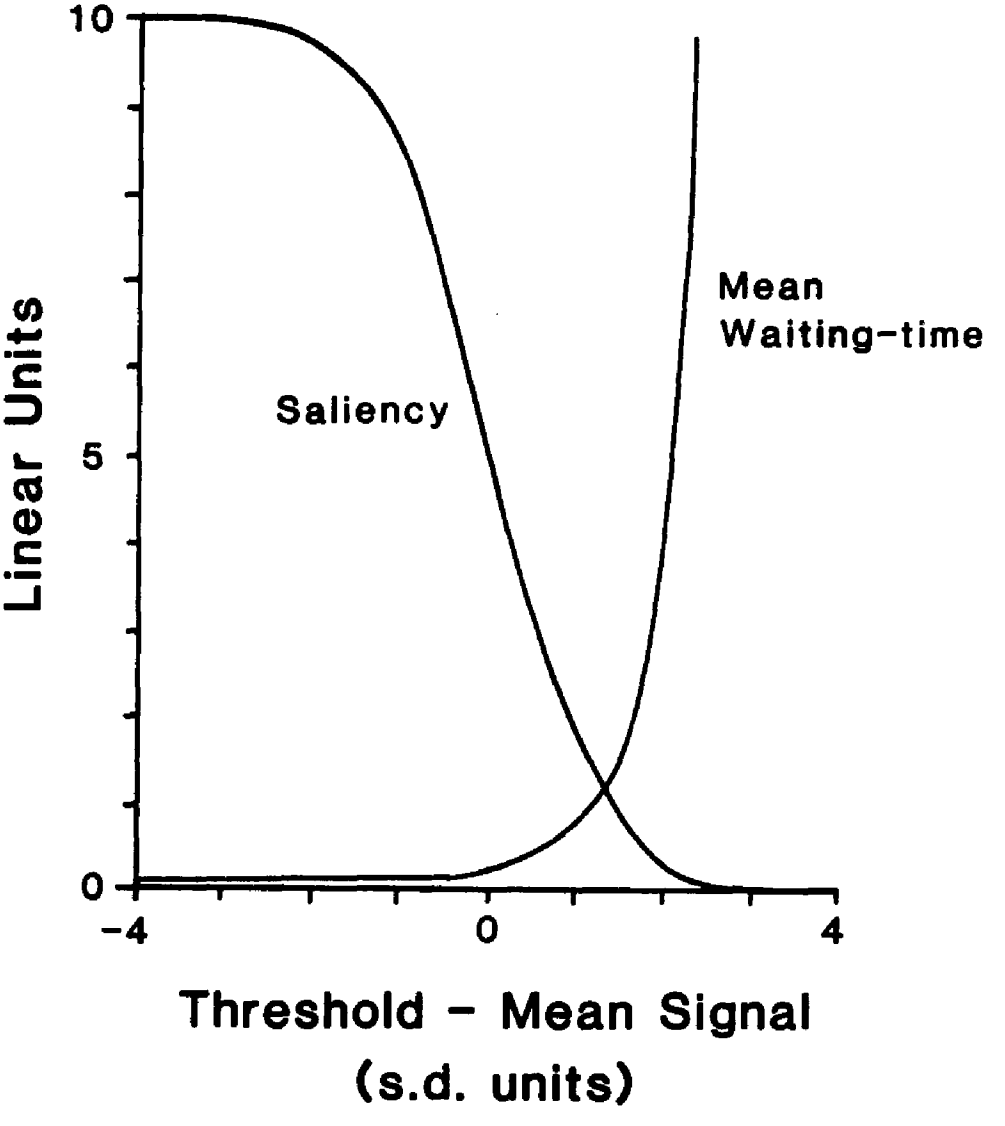
10
5
0
Linear Units
Saliency
Mean
Waiting-time
-4
0
4
Threshold - Mean Signal
(s.d. units)

If the saccadic trigger threshold were of a moderate level, the saliency of potential targets would increase and significant "competition" between the targets would appear. This is the threshold regime in which adults freely view stimuli, and all the properties of the multiple target model (see Section 5) would be observable. If the threshold is very low because of low arousal, the saliency of targets will increase and fixations will become brief, as observed in many infants. Even the fluctuations from ganglion cells which are firing at their spontaneous rate will sometimes exceed the trigger threshold and initiate saccades. There may be so many spontaneous saccades that potential targets could be pre-empted (see Section 5). The experimenter would observe many saccades, many of which will place the fovea (or central retina) where there is no apparent stimulus target. It might be construed that the subject does not see the target or does not pay the stimulus much attention.

b) Overall Stimulus Saliency Modulated By Arousal

An equivalent model is that the saliency of all targets, rather than the trigger level, is modulated by the subject's level of arousal. In this case, overall saliency would have to be decreased by higher arousal. An intriguing possibility is that arousal raises or lowers drift rate which then affects overall saliency of targets by virtue of their retinal motion. For example, if the subject has a high level of arousal, the average drift rate is decreased, by say, an increase in a controller's loop gain. This lowered drift rate would then effectively lower the saliency of all targets and thereby increase the average fixation duration. As shown in Figure 38, fixation duration could be

very sensitive to small changes in average drift rate which might be undetected by our apparatus (see Section 6).

We postulate that the difference between the trigger threshold and the mean signal level is determined, in part, by arousal level. However, there is an interesting consequence of this model as follows: As discussed above, the arousal level is affected by the visual content of the stimulus (Figure 37) and it was suggested that the arousal level was determined by the total excitation transmitted along the optic nerve. This level of excitation will depend on where the eye is pointing in the visual scene. Thus, if a fixation places the fovea over an area of the stimulus which has little contrast at a only a few spatial frequencies (on average per unit area of the stimulus) then arousal will be low. This will lower the saccadic trigger threshold and the saccade rate will increase, thereby moving the eye quickly away from this location. If, on the other hand, the eye fixates a high contrast broadband stimulus area, arousal will be high and the trigger level will be raised, which will decrease saccade rate. The eye will therefore spend more time over high contrast areas with many spatial frequencies such as edges and details. This may be a rudimentary form of attention. If the level of the trigger threshold came under cortical control, then the subject could indirectly control fixation duration by modulating the B-period and pay more or less "attention" to the current target by reducing or increasing the saccade rate.

[8]
SUMMARY AND DISCUSSION

In this final Section we shall first summarise the most important findings. We shall then discuss how this model fits with other studies of infant scanning and its implications for infant psychophysics and approaches to studying infants in general.

8.1 Summary

(1) It was shown that mean fixation durations from infant subjects were highly variable and there were strong stimulus effects. On average, infants' fixations were much briefer than fixations from adults viewing comparable stimuli.

(2) The frequency distributions of fixation duration had the same form for all infant subjects and free-viewing adult subjects. The distribution was identified using the method of moments as being basically the Exponential with a small degree of hyperexponentiality.

(3) The Exponential distribution is indicative of a waiting-time problem. It was shown that a fixation could be divided into two temporal regimes, the A- and B-periods: The A-period is roughly a constant refractory period having a duration of about 50 msecs in infant fixations and 100 msecs in fixations from adults under our free-viewing conditions. The B-period is a waiting-time for a fixation ter-

mination event. The Exponential shape of the duration distributions indicates that the terminating event occurs randomly in time. The hyperexponentiality could be explained if the mean B-period varied from fixation to fixation, which would yield a Compound Exponential distribution.

(4) Three models were entertained - a spontaneous saccade model, a reflexive saccade model (the "multiple target model"), and a high-level processing model (the "CPU model"). It was argued that the multiple target model was the most likely explanation for the observed Exponential distribution for fixation durations.

(5) The mean fixation duration was shown to be very sensitive to the size of the stimulus for the free-viewing adult. This is in agreement with an early study by Enoch (1959). Fixations decrease in duration as stimulus size increases, even up to at least 40 degree diameters. This supports the multiple target model.

(6) The multiple target model was formalised with respect to the B-period of fixations. Saliency, Eminency, and Pre-emption were defined. It was shown that the multiple target model was equivalent to a Markov process where the transition probabilities represented the probabilities of saccadic eye movements from one position to another. These probabilities were considered to be constant in time and set by the stimulus and the receptive field organization of the retina. For the case of the homogenous stimulus, it was shown that the model predicted saccade magnitude distributions and the relationship between mean saccade magnitude and stimulus size with some precision. This makes for a persuasive case for the multiple target model

of visual scanning in the free-viewing adult.

(7) It was concluded that the A-period of fixations depended on the subject's task. In addition to conduction time, it was argued that the A-period reflected some kind of visual information processing or acquisition time. A two-level system was proposed: A low-level reflexive system, which is responsible for the B-period, can be inhibited by a high-level process, which is responsible for part of the A-period. It follows, therefore, that the brief infant A-periods reflected very little (if any) of this kind of high-level processing.

(8) The effects of stimulus size were much less pronounced in the infant. It was suggested that this may be a saturation effect because infant fixations were already very brief.

(9) Effects of eye drift during fixations were examined. It was shown that drift rate could not be reliably measured directly because of instrument noise. By using the method of moments, it was inferred that non-zero drift rate existed by showing that drift amplitude was the product of two random variables, one of which was duration. It was shown that for fixations longer than about 150 msecs, mean drift magnitude remained approximately constant with fixation duration. It was argued, therefore, that fixation duration and drift rate were reciprocally related in such a way that increasing drift rate augmented target saliency, and thereby reduced mean duration. The change in mean duration from fixation to fixation accounted for the hyperexponentiality of the duration distributions. We were unable to show that infant fixations were so brief because of high drift rate, but this remains an intriguing possibility.

(10) It was shown that each stimulus elicited, on average, different saccadic Main Sequence slopes from infants. This was interpreted as a correlation between fixation duration and arousal level. It was proposed that overall saliency could be changed if a saccadic trigger threshold were sensitive to arousal level.

8.2 Visual Scanning in Infants

Although most of the studies on visual scanning in infants suffer from calibration problems, there have been some consistent results. We will show that the multiple target model is consistent with these findings.

One of the most consistent findings is that infant fixations tend to cluster around the edges or vertices of stimulus figures (Salapatek and Kessen, 1966; Salapatek, 1968; Haith, 1980). This phenomenon is readily explained by the model: Because edges have more spatial frequency content than blank areas of a stimulus, edges will be more salient and therefore more likely to win the competition for foveation. Thus, on average, one would expect most fixations (but not all) to occur on or near edges or vertices. It is also quite possible that the subject would only fixate a small part of the stimulus because edges and vertices far from the current fixation would have relatively low saliency because of their peripheral retinal location. These other edges would also have low eminency because of pre-emption by the current region of fixation. Therefore, depending on the size of the stimulus figure, the subject would be expected, on average, to fixate only a local stimulus area. This would be particularly noticeable in

infants who have small visual fields (discussed below).

It should be remembered that this is a probabilistic model. A peripheral target could win foveation and then fixations would cluster around another part of the stimulus. Thus, the overall breadth of scan (dispersion of fixations) will be dependent on the dispersion of the potential targets. Large stimuli will have a tendency to increase the breadth of scan, at least for those subjects who do scan more than one local feature of the stimulus. This has been reported by Salapatek (1968) and Hainline and Lemerise (1982) (see also Section 5). The same argument can be used to explain why breadth of scan is less for small stimuli than for a blank field (Salapatek and Kessen, 1966; Salapatek, 1968;, Lewis and Maurer, 1980). Although the blank field is not an homogenous stimulus, peripheral targets will have more eminency when there are no highly salient central targets and so breadth of scan should be more for the blank field.

More quantitative tests will have to wait until more quantitative research has been carried out with the infant, not only in terms of instrument accuracy (spatial and temporal), but also in terms of careful stimulus definition and constant arousal level. The important aspect of this model is that scanning in the infant as well as the free-viewing adult is reflexive and does not *need* any complex cortical involvement. This whole mechanism could be maintained by a retinal - subcortical - oculomotor pathway. The model also separates visual processing ("seeing") from visual orientation ("looking"). This is of considerable importance and will be discussed further.

8.3 Preferential Looking and Visual Perimetry

A common tool for assessing visual functions of the infant is to present stimuli and detect where the infant looks. The rationale behind this approach is that looking behaviour reflects visual function. Two notable techniques are preferential looking and visual field estimation. We shall briefly examine the basic principles of these techniques for two reasons. First, we shall present an alternative approach to understand the mechanisnms of these techniques based on reflexive looking rather than visual processing. Second, we can also illustrate how the model can be applied without detailed knowledge of the stimuli; that is, the principles of the model alone permit a moderately sophisticated analysis.

Preferential Looking in the Infant

Preferential looking is probably the most commonly used technique for assessing an infant's visual abilities. There are many variations on the basic theme but we will only consider a simple version. Here, the infant is held stationary and is presented with two stimuli. A suitably chosen measure of the infant's looking behaviour indicates which stimulus the subject "prefers." The assumption (usually implicit) is that the infant centrally compares the two stimuli and thereby creates his/her preference. However, the subject is not under any instruction and so he will freely scan the stimuli (and any other parts of the visual field) and our model should therefore apply to this situation.

A variety of measures have been used; we shall only consider

two. To begin, we shall consider the first-look measure because it is simple to analyse. Consider two target stimuli, L and R, whose centres are separated by a visual angle, d. These two stimuli are surrounded by a dark background, S. At the beginning of a trial, the subject is assumed to be looking straight ahead bisecting the two stimuli. The subject will then either first look at stimulus L (a "hit") or look first at stimulus R (a "miss"). The trial continues until one of these outcomes occurs. To simplify, we shall assume that the subject's behaviour is stationary across trials, so that arousal level remains constant and/or no habituation occurs to the stimuli. Then the proportion of hits over many trials will asymptote to the probability that the subject will first orient towards stimulus L. According to the multiple target model, this probability is given by the eminency of stimulus L given that the subject is looking between the stimuli.

To show this, we consider saliencies to be additive (as we have throughout; see Section 5). The total saliency of the visual field can be broken down into three components, namely, the saliencies of the two stimuli, $L_{d/2}$, $R_{d/2}$ (the subscripts refer to the eccentricities of the stimuli centres relative to the point of subject's regard), and the saliency of the surround, S. The total saliency will then be: $L_{d/2}$ + $R_{d/2}$ + S, and the reciprocal of this quantity will be proportional to the B-period of fixation duration. To simplify further, we shall assume the background saliency to be negligible compared to any stimulus saliency. The probability of a hit is then given by:

$$P(\text{Hit}) = \frac{L_{d/2}}{L_{d/2} + R_{d/2}} = \frac{1}{1 + R_{d/2}/L_{d/2}}. \qquad (28)$$

Similarly, the probability of a miss is given by:

$$P(\text{Miss}) = \frac{R_{d/2}}{L_{d/2} + R_{d/2}} = \frac{1}{1 + L_{d/2}/R_{d/2}}. \qquad (29)$$

As expected, the 50% hit rate occurs when the two stimuli have the same saliency. Note that it is only the ratio of the saliencies of two stimuli that determines the hit and miss rates. The important point, here, is that the saliencies are at the peripheral retinal location, d/2.

Another important variable is the amount of time spent looking at each stimulus. We will find the mean time spent looking at a stimulus before looking at the other stimulus. The multiple target model permits an approximate prediction of this time. After the first look, the subject looking at one of the stimuli, say stimulus R, which we shall call the "central" stimulus. Now the subject can either scan this stimulus by making saccades within (or nearby) this stimulus, or the subject can make a saccade to the other stimulus, the "peripheral" stimulus, A. Assuming again that all the potential targets within and between the stimuli are independent (additive saliencies), the total amount of B-period spent looking at stimulus R before a saccade is triggered by the stimulus L is simply proportional to the reciprocal of the saliency of stimulus L, and (because of our assumption) is inde-

pendent of the currently viewed stimulus R.[23] However, there is a complication since we have not yet considered the other components of looking time, namely, fixation A-periods and saccade duration. To find actual average looking-time at stimulus R before orienting towards stimulus L, we must add the A-period to each fixation and the saccade duration to the end of each fixation (except the last) that occurs while the subject is looking at the central stimulus R. The A-period seems to be task-dependent (Section 5) and saccade duration depends on saccade magnitude which, in turn, depends on stimulus size (Section 5). Saccade duration probably also depends on arousal level in the infant (as peak velocity does). However, we have not found any evidence to suggest that these are appreciably affected by target saliencies and so we can just add a constant to each fixation. We now need to find the average number of fixations (and saccades) made during the looking-time at the central stimulus before the subject views the peripheral stimulus. The precise distribution of this quantity, as predicted by this model, is somewhat complicated and will not be shown here, but the mean number of fixations is simply the average total B-period divided by the average B-period of a single fixation and is given by:

---

[23] It may seem paradoxical that the average amount of B-period fixation time spent on the currently viewed stimulus is independent of the contents or saliency of that stimulus, but is dependent only on the peripheral stimulus. This is a key feature of the multiple target model; the peripheral stimulus "pulls" the eye away from the central stimulus rather than the central stimulus "holding" the eye. It is in this important respect that we differ from the more conventional view that the infant evaluates the central stimulus and makes some decision to maintain the current gaze.

$$\bar{N}_R = R_0/L_d. \tag{30}$$

From this we can then find the average looking time by adding the B-period, A-period, T_A, and saccade duration, T_S, components:

$$(T_A + T_S)R_0/L_d + \lambda/L_d \tag{31}$$

where λ is the constant of proportionality of saliency. The mean looking-time at the other stimulus is similarly given by:

$$(T_A + T_S)L_0/R_d + \lambda/R_d. \tag{32}$$

These expressions are more complicated than those for the first-look measure (Equations 28 and 29). Nevertheless, mean looking time depends mainly on the saliency of the peripheral stimulus at an eccentricity of d (rather than d/2 with the first-look measure). There is also a dependency on the central stimulus (at no eccentricity) which will depend on the average relative duration of A-period and saccades to the duration of the B-period. The major determinants of this will be the saliency of the currently viewed stimulus and the arousal level of the subject (Section 7). If the subject's fixations have long B-periods, so that the A-periods and saccade durations are relatively brief, then the average looking time will depend mostly on the saliency of the peripheral stimulus. This will happen if, for example, the stimuli are low in total saliency or the subject is at a high

level of arousal. If arousal is low then the centrally viewed stimulus will begin to have a greater contribution to looking time.

Any measure that is based on the looking behaviour of the infant[24] will be determined either exclusively or largely by the stimulus not being currently viewed. In certain applications of the preferential looking technique, this has important implications, especially those applications which attempt to measure a visual capacity that is known to be sensitive to retinal location. For example, in using preferential looking to measure infant contrast sensitivity functions (CSF's), one stimulus contains a sinusoidal grating and the other stimulus contains a blank field at mean luminance (Atkinson, Braddick and Moar, 1977; Banks and Salapatek, 1981). Contrast of the grating is decreased until the subject shows no preference for it over the blank stimulus. The CSF obtained will, according to our model, be a composite CSF, with the greatest contribution being from that part of the retina excited by the sinusoidal grating when the subject is viewing the blank stimulus. There will be a smaller contribution to the composite CSF from the central retina. The obtained CSF will depend on the stimulus areas, their separation and the actual response measure to some degree. Nevertheless, if our interpretation is correct, the CSF will not be a true measure of central retinal spatial frequency sensitivity. It may give the wrong impression of infant vision (CSF's or acuity limit), if the central retina of the infant has

---

[24] We have not considered other effects the stimuli may have on the subject such as startle and/or pupillary reflexes. These non-looking behavioural variables may contribute to an observer's opinion of which stimulus is preferred by an infant.

higher resolution than the peripheral retina. This may explain why CSF's obtained by the preferential looking technique (Atkinson et al., 1977a,b; Banks and Salapatek, 1981) have lower sensitivity and acuity than CSF's obtained by cortically evoked potentials (Norcia, Tyler, and Allen, 1986; see also Dobson and Teller, 1978) which present a single stimulus centrally. The preferential looking technique essentially measures the sensitivity of the peripheral retina. This is also consistent with the increased sensitivity obtained if the stimulus in preferential looking is drifted (Atkinson, Braddick, and Moar, 1977b). Here, the saliency of the stimulus is increased because of its temporal component (see Section 6).[25]

Preferential looking has also been used to estimate the colour vision of the human infant (Ankrum, Clavadetscher and Teller, 1986; Ladenheim and Gordon, 1986). Both of these studies have shown an increased sensitivity for short wavelengths relative to long wavelengths in the infant when compared to the adult. However, the adult control groups were allowed to use their central retina while the infants, of course, were under the preferential looking paradigm. This short wavelength sensitivity is consistent with the spectral sensitivity of the adult peripheral retina (Abramov and Gordon, 1977) and does not necessarily reflect a difference between adult and infant spectral sensitivities.

---

[25] It should be noted that this model does not predict "negative preference" which sometimes occurs when the infant prefers the blank field over a grating near threshold (Held, Gwiazda, Mohindra and Wolfe, 1979). However, "negative preference" is not found by other researchers (Banks, Stephens and Dannemiller, 1982; Teller, Mayer, Makous and Allen, 1982).

The Visual Field in Infants

It is well known that the infant has a small visual field compared to adults (P.Harris and MacFarlane, 1974; MacFarlane, P.Harris, and Barnes, 1976; Cummings, Mayer, Hansen, and Fulton, 1986; Dobson, Schwartz, and Sandstron, 1986; van Hof-van Duin and Mohn, 1986). This has been measured by presenting stimuli at different eccentricities (usually in the presence of a central fixation target) and noting the saccadic or head orienting response. The multiple target model shows that the probability of a response is determined by the eminency of the target. However, eminency depends not only on the saliency of the target at its retinal locus, but also on the total saliency of all other targets. Thus, if the test target has to compete with other targets (even spontaneous targets), there will be less chance of observing an orienting response *but* this does not mean that subject does not *see* the test target with the peripheral retina. The dependency of the probability of an orienting response on the contents of the visual scene has been observed by P.Harris and MacFarlane (1974) and MacFarlane, P.Harris, and Barnes (1976). They found that the size of the visual field decreased when a central dot was also present. MacFarlane et al. also found that non-nutritive sucking (used to calm their subjects) also reduces the visual field. MacFarlane et al. suggested that this was due to a decrease in head mobility induced by sucking. An alternative explanation is that sucking lowers the infant's level of arousal which lowers the saccadic trigger level (or increases saliency of all targets, see Section 7). This would increase the eminency of the central target at the expense of the

peripheral test target, and so reduce the probability of orienting to the peripheral target.

8.4 Conclusions

It has been shown that free-viewing by the adult or infant can be explained by the multiple target model. The model is based on reflexive saccadic triggering by visual targets and does not require the existence of high-level perceptual processes. The simplest manifestation of this basic behaviour is the saccadic reflex to an extremely salient target, but this reflex is occurring continuously to targets in the visual field in a probabilistic manner depending on the contents of the visual field and their retinal locations. Although we do not deny the influences of high-level processes, we believe that there is a substrate of primitive scanning behaviour that exists from birth. We propose that this substrate remains essentially the same throughout life, but it can be modulated by perceptual and/or attentional processes.

An important feature of this model is that it makes quantitative predictions and, therefore, it is testable. Some predictions have been corroborated with adults free-viewing homogenous stimuli. For non-homogenous stimuli, computer simulations would be the best way of testing the model against actual scanning patterns. Perhaps, the most incisive experiment to test the model would manipulate the visual targets in numerosity, retinal location, luminance, and in their temporal component. This could be accomplished simply by presenting various arrays of luminous dots, and giving the adult subject a variety

of instructions. This experiment would go a long way to directly testing the basic tenet of the model, namely, that scanning saccades are visually triggered and that the B-period of fixations depends on total target saliency of the stimulus. The different instructions might also indicate which high-level processes need to be invoked to cause the model to break down. Different instructions may also give some insight into the control and function of the A-period of fixations.

If we accept this model as the underlying mechanism by which visual scanning operates, then we must also accept that "looking" and "seeing" are not *necessarily* the same function. The process of orienting the eye and the process of gathering visual information are inherently closely linked. This is obvious for foveal vision where the visual information depends crucially on where the eye is pointing. However, it is unclear how much foveal vision is actually used in normal free-viewing by adults, and it is also unclear how much foveal vision is even possible in the newborn with its attendant immature macular region.

The difference between looking and seeing is more than just an issue of which part of the retina is used for gathering visual information. Looking and seeing are really distinct and have different psychophysical response functions. Thus, the probability that a peripheral object can be resolved (peripherally) decreases approximately linearly with foveal eccentricity, but, the probability that a saccade will occur to the object decreases much more rapidly with foveal eccentricity - at least with the square of eccentricity and possibly as high as the sixth power of eccentricity (Findlay, 1980). This dis-

tinction becomes critical when visual function of the infant is to be assessed. Because the infant cannot report to the experimenter whether he can see an object or stimulus, the experimenter must resort to measuring behavioural or physiological responses. There is a danger that a heavy reliance on looking behaviour as a measure of visual sensitivity will give a false impression of the infant's visual capacity. Asking whether an infant looks at a stimulus is not equivalent to asking whether an adult can see the stimulus.

Finally, considerable effort has been taken here to examine fixations and visual scanning with as few explicit or implicit *a priori* assumptions as possible. Such an approach is particularly advantageous when studying infants, because it is very easy to slide into adultomorphisms and attribute to the infant similar processes that appear in the adult. Arriving at theories with either data-driven or "top-down" approaches may both come under the rubric of "empiricism"; however, the elementary approach is always to be preferred, as articulated by a lesser-known British empiricist:

> It is a capital mistake to theorize before one has data. Insensibly one begins to twist facts to suit theories, instead of theories to suit facts.
>
> "A Scandal in Bohemia"
> Sir A.C.Doyle

Appendix A

DIOPTRICS OF THE EYE TRACKER

This appendix calculates the movement of the first Purkinje image h_1, and the centre of the image of the pupil, h_2, for a rotating eye with an aspheric cornea. The difference between these two images is used by the eye-tracker to estimate eye rotation independent of head position. Young and Sheena (1975) have shown that this difference is related to the angle of eye rotation by:

$$h_1 - h_2 = k\sin\theta \qquad (A.1)$$

where k is the axial distance between the entrance pupil (the image of the pupil as seen through the cornea) and the centre of curvature of the cornea; and where θ is the angle (in radians) between the optical axis of the camera lens and the eye's optic axis. For this system, the eye-tracker's optic axis is roughly colinear with the eye's optic axis when the subject is looking straight ahead; thus the primary gaze position of the subject corresponds approximately to $\theta = 0$. The advantage of a colinear eye-tracker is that for small angles of eye rotation, $\mathrm{SIN}\theta \approx \theta$, and the system becomes virtually linear. However, the problem with equation A.1 is that it assumes the cornea

is spherical. It is well known that the normal human adult and infant corneas are aspherical and have prolate meridional cross-sections (e.g., Mandell, 1967). The radius of curvature of the cornea from a typical infant (4 - 15 days) changes from about 6.8 mm at the pole to about 7.5 mm at 3 mm from the pole. For an adult the change is less - 7.8 mm to 8.3 mm (Mandell, 1967). As can be seen, there is a 5% to 10% increase in the radius of curvature by 3mm from the corneal pole. The problem to be analysed here is whether this change in curvature will give rise to a significant departure from linearity at the output of the eye-tracker.

The incident infrared beam of the eye-tracker is assumed to be collimated about the eye-tracker's optic axis - the reference axis. The light reflected back out of the eye is collected by the objective lens of the camera. The aperture of this lens and its distance from the subject's eye defines the maximum angle of incidence at the cornea. For this system, the 270 mm f/4 objective has an aperture of about 7.5 cm and is 60 cm from the eye. This creates a maximum angle of incidence of 1.8 degrees at the cornea, which is sufficiently small to permit paraxial analysis of the first Purkinje and pupil images.

A.1 First Purkinje Image

The cornea acts as a convex mirror in forming the first Purkinje image, P1. The image is virtual and behind the cornea. The paraxial focus is midway between the centre of curvature and that part of the cornea which intersects the reference axis (incidence point). As the eye rotates, therefore, P1 will move away from the reference axis in

the direction of rotation by an amount:

$$h_1 = \frac{r}{2}\sin\theta. \qquad (A.2)$$

For an aspheric cornea, however, both the radius of curvature and the centre of curvature (the evolute) vary according to the shape of the surface. Before specifying a particular corneal profile, the general equation for the position of the P1 formed by a collimated incident beam will be derived.

A sagittal cross-section is taken and assumed to be radially symmetric. The surface is denoted by the function s=u(t), where a point on the corneal surface (s,t) has an axial distance, s, relative to the corneal pole, and a distance, t, perpendicular from the eye's axis. The surface, u(t), has a radius of curvature, r(s,t), and a centre of curvature, $(C_s(t), C_t(t))$ at a point (s,t) on the surface. Thus, for example, a spherical cornea with a radius of curvature, R, would be represented by $s=R^2-u^2$, r(s,t)=R, and $C_s(t)=R$, $C_t(t)=0$.

Figure 39 illustrates the formation of P1 by an aspheric cornea when the eye is rotated through angle θ. P1 will be displaced laterally by the same amount as the centre of curvature is displaced laterally (due to eye rotation). This can be expressed in terms of the corneal evolute:

$$h_1 = [C - C_s(t_i)]\sin\theta - C_t(t_i)\cos\theta \qquad (A.3)$$

where C is the distance from the centre of rotation of the eyeball to

Figure 39

Schematic showing the formation of the first Purkinje image (P1) by an aspheric cornea. Eye is shown rotated (down) through an angle, θ. Small area of incidence of the collimated IR beam is at (s_i, t_i), which has a centre of curvature (evolute), $C_s(t_i), C_t(t_i)$, which is not on the axis for an aspheric surface. Note: coordinate system is s,t where s is the distance along the eye axis and t is the distance perpendicular to the eye axis. The origin is at the corneal pole.

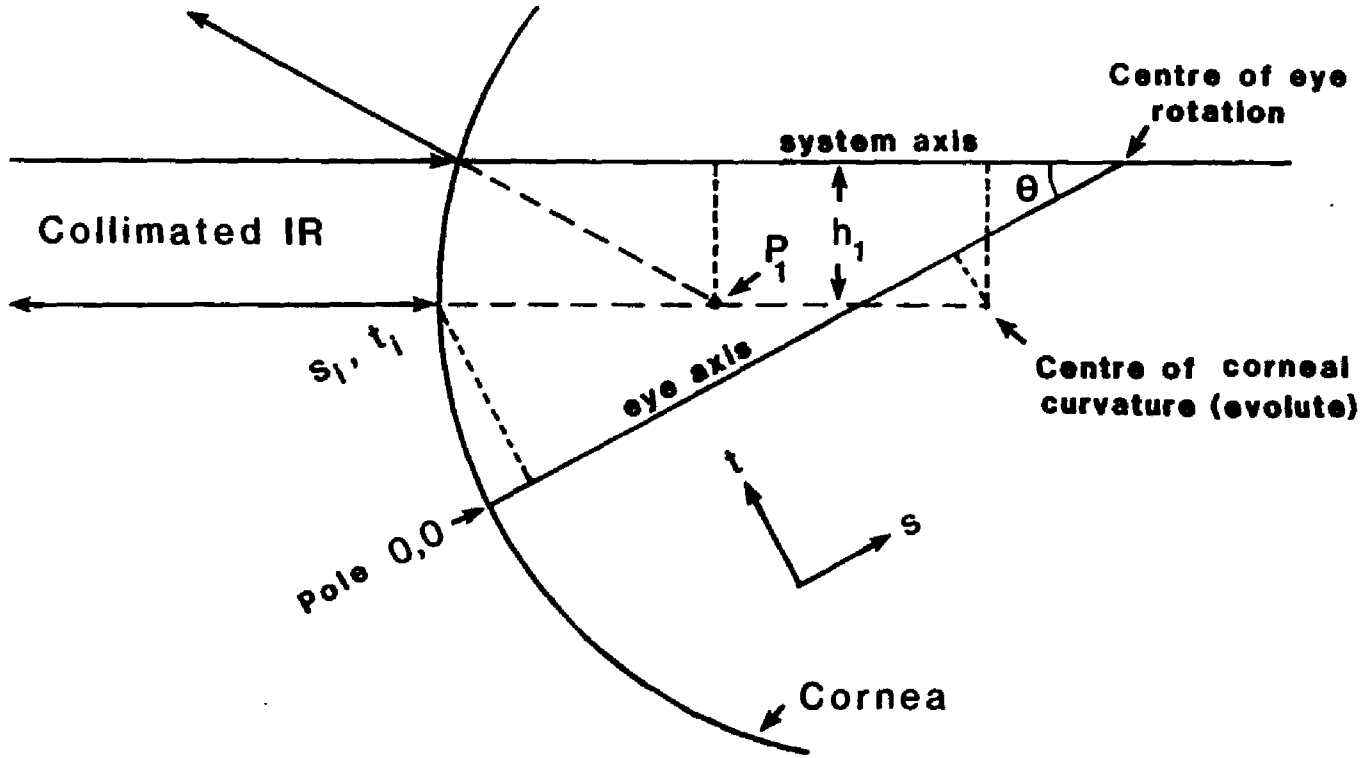
Centre of eye rotation
system axis
θ
Collimated IR
h_1
P_1
s_1, t_1
eye axis
Centre of corneal curvature (evolute)
t
s
pole 0,0
Cornea

the corneal pole. For a spherical cornea, the evolute is a single point and the lateral displacement of P1 will be given by (C-R)SINθ. For an aspherical cornea, it is necessary to find the coordinates of the point of incidence on the cornea (s_i,t_i) for a given angle of eye rotation. From Figure 39 these coordinates can be found by solving the simultaneous equations:

$$\begin{aligned} t_i &= (C - s_i)\tan\theta \\ s_i &= u(t_i). \end{aligned} \qquad (A.4)$$

However, it is more convenient to solve for θ and use s_i as the independent variable:

$$\tan\theta = t_i/(C - s_i). \qquad (A.5)$$

Thus, for any given s_i, the required eye rotation can be found from Equation A.5 and related to the lateral displacement of P1 by Equation A.3. A specific corneal surface must be assumed to evaluate these equations.

Mandell and York (1969) have shown that the adult cornea can be modelled by an ellipsoid with an eccentricity, e=0.48, and a radius of curvature at the corneal pole of r(0,0)=7.7 mm. This is a reasonable approximation if the peripheral cornea is ignored. Using this approximation, the corneal surface, u(t), can be modelled by:

$$s = \frac{b}{a}(a^2 - t^2)^{\frac{1}{2}} \qquad (A.6)$$

where a and b are the semi-major and -minor axes. The evolute of this ellipse is given by:

$$C_t(t) = (b^2 - a^2)t^3/b^4, \qquad C_s(t) = (a^2 - b^2)s^3/a^4. \qquad (A.7)$$

By choosing various numerical values for s_i, these equations permit t_i, C_s, and C_t to be found. Then, from Equations A.5 and A.3, the angle of rotation and the lateral position of P1 can be found. Table A1 shows these computations for both an ellipsoidal and a spherical cornea. As can be seen there is only a small difference (<1%) between these two profiles. Therefore, the asphericity of the cornea has only a small effect on the position of the first Purkinje image.

TABLE A1

t_i	s_i	$r(s_i,t_i)$	θ	h_1 Ellipsoid	h_1 Sphere
mm	mm	mm	deg	mm	mm
0	0	7.7	0	0	0
1.0	0.07	7.8	4.8	0.360	0.359
2.0	0.26	8.1	9.7	0.726	0.722
3.0	0.60	8.5	14.7	1.088	1.090
4.0	1.08	9.1	20.1	1.470	1.479

A.2 Position of the Centre of Pupil

In order to calculate the position of the centre of pupil image as seen by the eye-tracker's camera, we will assume the cornea and the anterior chamber to be equivalent to a simple single surface optical system; this is the approximation used in the Gullstrand eye (e.g., see Wyszecki and Stiles, 1967). The infrared beam will be diffusely reflected from the retina and it will back-illuminate the pupil. The bright pupil will then be magnified by the dioptric power of the cornea and imaged by the eye-tracker's objective lens. The resulting image will be an ellipse with an eccentricity depending on the angle of eye rotation.

From Figure 40 it can be seen that the pupil centre will be displaced laterally in the direction of eye rotation, and it will follow a circular locus centred at the point of eyeball rotation:

$$h_2' = r_p \sin\theta. \qquad (A.8)$$

The effect of the cornea is to magnify this displacement giving rise to an erect and virtual entrance pupil. The magnification will depend on the power and hence the radius of curvature of that part of the cornea that is forming an image of the pupil. Thus, in general the lateral displacement of the centre of the entrance pupil will be given by:

Figure 40

Schematic of the formation of the image of the centre of pupil by an aspheric cornea. The image is formed by the small area of cornea around the point of incidence, (s_i, t_i).

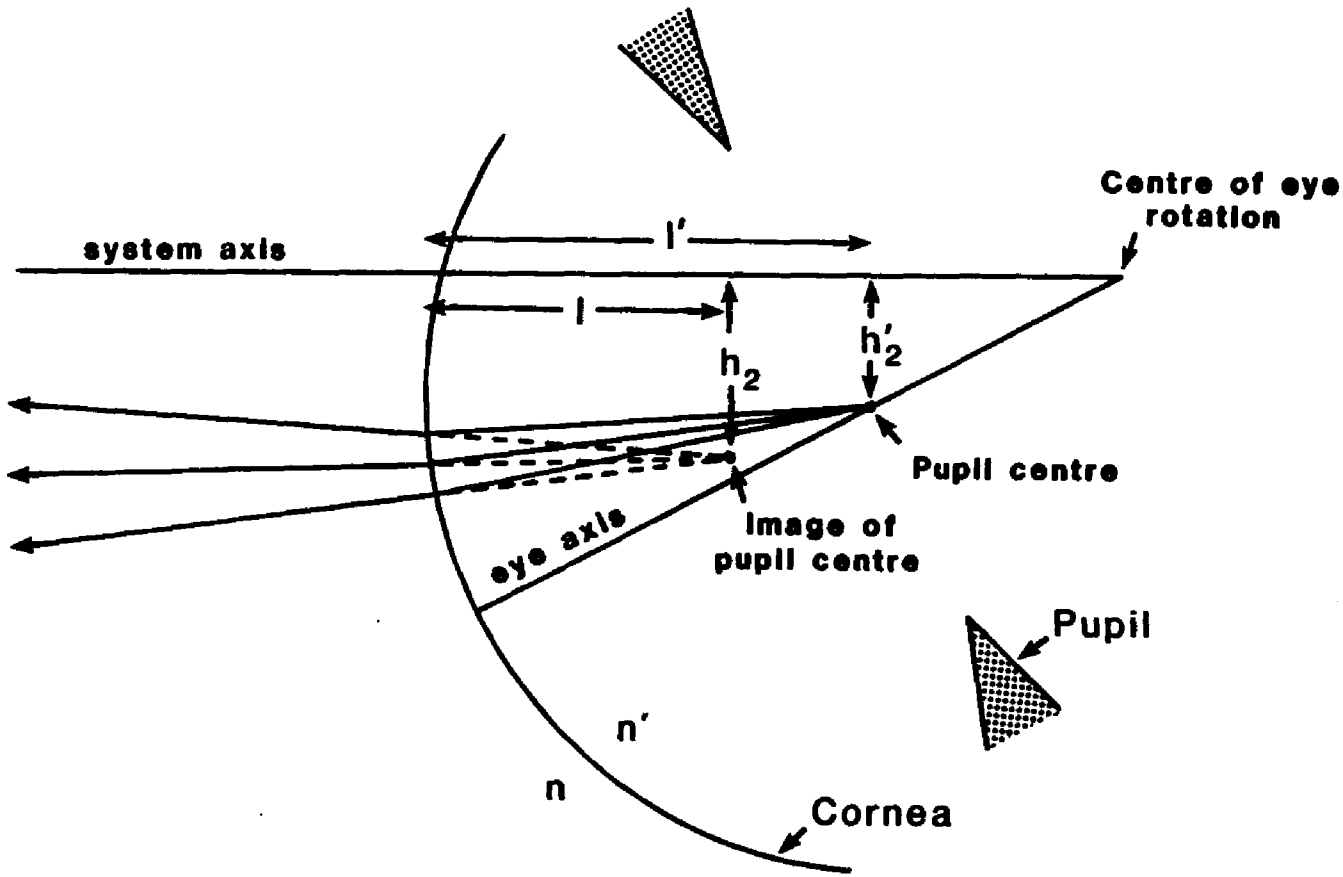
Centre of eye rotation
system axis
l'
l
h_2
h'_2
Pupil centre
Image of pupil centre
eye axis
Pupil
n'
n
Cornea

$$h_2 = m(\theta) r_p \sin\theta \qquad (A.9)$$

where $m(\theta)$ is the magnification of the pupil by the cornea for a given eye rotation, θ. As with P1, paraxial imaging can be considered to take place, not about the corneal pole, but about that part of the cornea between the entrance pupil centre and the camera's objective. For refraction at a single surface:

$$n'/l' - n/l = (n' - n)/r(s_i, t_i) \qquad (A.10)$$

where l and l' are object and image distances, and n and n' are the refractive indices specified at infrared wavelengths. Using Snell's law for paraxial imaging:

$$nh/l = n'h'/l' \qquad (A.11)$$

and the magnification of the pupil by the cornea is given by:

$$m(\theta) = h/h' = [1 - (n'-n)l'/nr(s_i, t_i)]^{-1}. \qquad (A.12)$$

Setting the depth of the anterior chamber, l', to 3.6 mm (Bennett and Francis, 1962) and using values from Table A.1, the magnification of the centre of pupil will vary from 1.18 to 1.16 as the eye rotates through 15 degrees, which is a change of less than 2%.

A.3 Summary

Even though the corneal radius of curvature can increase by as much as 10% from the pole to the periphery, there is less than 2% change in the displacement of either the first Purkinje or pupil centre images as compared to a spherical cornea. This conclusion is based on the ellipsoidal approximation of Mandell and York (1969) of the corneal profile. Any small errors in their approximation can have no significant effect on this conclusion. Therefore, to a good approximation, the response of the eye-tracker to eye rotation is still given by Equation A.1, or for small angles of rotation (<20degrees):

$$h_1 - h_2 \approx k\theta . \qquad (A.13)$$

A.4 References

Bennett, A.G., & Francis, J.L. (1962). The eye as an optical system. In H.Davson (Ed.), *The eye* (Vol. 4). London: Academic Press, 101-131.

Mandell, R.B. (1967). Corneal curvature of the human infant. *Archives in Ophthalmology, 77,* 345-348.

Mandell, R.B., & York, M.A. (1969). A new calibration system for photokeratoscopy. *American Journal of Optometry, 46,* 410-417.

Wyszecki, G., & Stiles, W.S. (1967). *Color science.* New York: Wiley.

Young, L.R., & Sheena, D. (1975). Survey of eye movement recording methods. *Behavior Research Methods & Instrumentation, 1,* 397-421.

Appendix B

Instrument considerations in measuring fast eye movements

(Reprinted by permission of the Psychonomic Society, Inc.)

CHRISTOPHER M. HARRIS, ISRAEL ABRAMOV, and LOUISE HAINLINE
Brooklyn College, City University of New York, Brooklyn, New York

The dynamic limitations of eye movement recorders can distort the measurement of fast eye movements such as saccades and nystagmic quick phases. In this paper, the effects of the bandwidth and noise of recording methods and the problems incurred by digital sampling are discussed theoretically with respect to the measurement of peak velocity and duration of fast eye movements. As a practical example, a TV-based infrared corneal reflex system is examined and a method for calibrating it for peak velocity measurement is described.

The measurement of eye movements (EMs) is becoming increasingly relevant in fields other than those concerned with the analysis of the oculomotor system itself. For example, correlations between unusual EMs and neurological pathologies have been made by Hamann (1979) and Zee, Optican, Cook, Robinson, and Engel (1976). There is also a large body of literature on the relationship between reading and EMs (e.g., Levy-Schoen & O'Regan, 1979). Furthermore, EM measurement is beginning to be used in the developmental study of the human infant (Aslin & Salapatek, 1975; Hainline, 1981). Each application of EM measurements has its own technological priorities. Some research questions require that the measuring system have great speed and resolution, whereas others require that intrusiveness upon the subject be minimized. In most current systems, there is a tradeoff among resolution, intrusiveness, and, of course, cost.

The various instruments and their merits have been discussed elsewhere (e.g., see Young & Sheena, 1975, for a comprehensive review). However, for efficient progress, it is essential to be able to compare data from different instruments in different settings. To this end, McConkie (1981) stressed the need for investigators to report the quality of their data, such as sampling rate, drift, noise, accuracy, and short- and long-term repeatability. But such reporting necessitates an intimate understanding of one's EM recording instrument.

The need for calibrating an instrument so that the direction of the subject's eye is precisely mapped onto stimulus space is self-evident, and there are various schemes for doing this (Bullinger & Kaufmann, 1977); Carmody, Kundel, & Nodine, 1980; Harris, Hainline, & Abramov, 1981; Kliegl & Olson, 1981; Mendelson, Haith, & Goldman-Rakic, 1981). It is less appreciated, though, that even an accurate mapping procedure does not calibrate the instrument for all purposes. For example, during measurement of fast EMs such as saccades or nystagmic quick phases, the bandwidth and noise of the recording system can degrade the recording of dynamic responses. The most commonly used parameters for describing fast EMs are peak velocity (PV) and duration. In this paper, we discuss the general effects of a system's bandwidth and noise on the measurement of these two parameters of fast EMs. As an example, we present the results of a dynamic calibration of a TV-based, infrared, corneal-reflex system (Hainline, 1981) for the measurement of PV. Although this kind of instrument is certainly less than ideal for recording fast EMs, it has the advantage of being nonintrusive to the subject, which makes it useful for recording from infants and young children. We show that PVs of fast EMs can be recovered from such slow eye trackers, thereby increasing the information that can be derived from their recordings. Even though a slow system is used as an example, the arguments we present are generally applicable to all eye trackers.

This work was supported in part by Grants 13484 and 662199 from the PSC-CUNY Research Award Program and NIH Grant EY-03957.
The authors' mailing address is: Department of Psychology, Brooklyn College of CUNY, Brooklyn, NY 11210.

Behavior Research Methods, Instruments, & Computers
1984, 16 (4), 341-350

THEORETICAL CONSIDERATIONS

Bandwidth

The first consideration is the effect of the recording instrument's bandwidth on the integrity of fast EM data. Here, the recording instrument is taken to include all aspects of the system (except the subject) and also any digitization process for on- or off-line computation. The final recording of the EM will be called the output of the instrument, o(t). During a fast EM such as a saccade, the eye position, e(t), changes rapidly in time with some profile. This profile can be broken down into its spectrum of frequencies, E(f), by Fourier analysis, with the result that, the faster the EM, for a given amplitude, the more pronounced are its higher frequency components. If the

instrument acts as a low-pass filter, these higher frequency components will be attenuated and an apparently slower movement will be recorded. Consequently, the duration of the EM would be overestimated. Equivalently, bandwidth distortion results from an instrument with a time constant comparable to, or longer than, the EM itself.

The relationship between the output and the EM is illustrated in stylized form in Figure 1, and can be summarized by:

$$O(f) = H(f)E(f). \quad (1)$$

We will follow the convention that functions denoted by uppercase refer to the Fourier transform of the corresponding temporal functions in lowercase.[1] Here, E(f) is the Fourier transform of the EM, e(t); H(f) is the transfer function of the instrument or the profile of its filtering action; and O(f) is the transform of the output, o(t). The actual time course of the output can be recovered from Equation 1 by taking inverse Fourier transforms (e.g., Champeney, 1973):

$$o(t) = \int_{-\infty}^{\infty} h(\tau)e(t-\tau)d\tau. \quad (2)$$

The output will be a faithful representation of the EM only if the instrument's filtering profile is flat to at least the highest frequency component in the EM. Although EMs do not have a cutoff frequency, but approach zero asymptotically, from a practical point of view they have effective components up to about 50 Hz (see Zuber, Semmlow, & Stark, 1968).

It is frequently more relevant to consider eye velocity rather than eye position, and to find the relationship between the instrument's output velocity, v(t), and the actual eye velocity, $\dot{e}(t)$ (the time derivative of a function will be denoted by a dot over it). This can be found by taking the time derivative of Equation 2 (see also Figure 1):

$$v(t) = \int_{-\infty}^{\infty} h(\tau)\dot{e}(t-\tau)d\tau. \quad (3)$$

Equations 2 and 3 are similar because the instrument has been considered to be linear and time-independent. Although the filtering action of the instrument on its input has not changed, it now acts on eye velocity rather than position. By taking the Fourier transform of Equation 3, the spectrum of the output velocity, V(f), is given by:

$$V(f) = H(f)\dot{E}(f) = 2\pi jfH(f)E(f). \quad (4)$$

The spectrum of the actual eye velocity, $\dot{E}(f)$, differs from the eye position spectrum by the factor $2\pi jf$. Apart from a phase lead of 90°, this factor indicates that the magnitude of any frequency component in the position spectrum must be multiplied by the frequency of that component to give the corresponding magnitude of the component in the velocity spectrum. In other words, the higher frequency components of the velocity profile are more prominent than those of the position profile, so that any filtering distortion will be worse for velocity measurements than for position measurements. Therefore, it is important to bear in mind that velocity recording requires a higher bandwidth for a given accuracy.

In order to quantify the effect of suboptimal bandwidth, it is necessary to specify shapes for the EM profile, e(t) or E(f), and the filtering action of the instrument, H(f). For clarity, we will represent a fast EM by a unit step function. Although this is an extreme case, its mathematical treatment is simple; later we will introduce a more realistic representation. A step input has infinite velocity and infinitessimal duration and thus represents a physically limiting case. The velocity profile of this idealized input is given by the impulse function, which has a spectrum of unity. Thus, from the inverse transform of Equation 4, the velocity profile of the output will be:

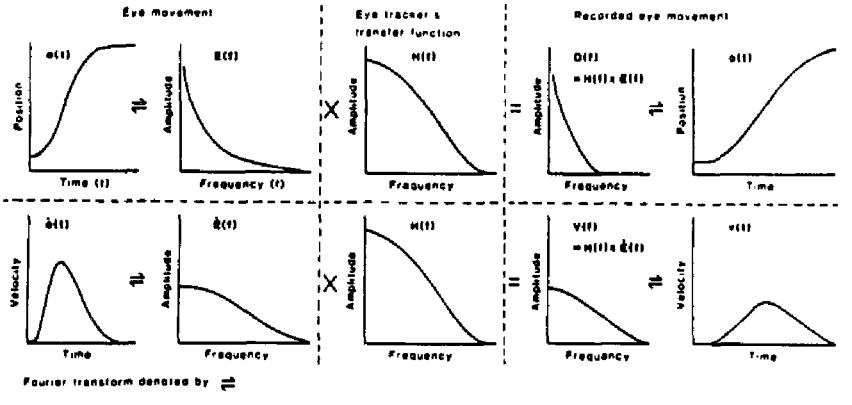

Figure 1. Stylization of the possible effect of an eye movement recorder on a saccade. Top row shows the transfer of the positional signal of the eye movement. Bottom row shows the transfer of the velocity signal. Note the reduction in peak velocity and the increase in duration caused by using an instrument with too-limited bandwidth.

$$v(t) = \int_{-\infty}^{\infty} H(f)e^{2\pi ft}df. \quad (5)$$

This result is quite general for any physically realizable system. In any system, there will be a delay between input and output; however, provided this delay is the same for all input frequency components, the system acts as a pure-delay passive filter. As a consequence, the pure delay can be ignored, but not forgotten, and the output velocity of such a filtering system is given simply by the real part of Equation 5:

$$v(t) = 2\int_0^{\infty} H(f)\cos(2\pi ft)df. \quad (6)$$

This output has two important features. First, the peak velocity (PV) will always occur at $t = 0$ (since pure delay is being ignored and the input is a step function), and will be given by:

$$PV = 2\int_0^{\infty} H(f)df. \quad (7)$$

In other words, the maximum velocity that such an instrument can yield for a unit step input is equal to twice the area under the instrument's filtering profile (including positive frequencies only). For example, consider the instrument's filtering profile to be that of a low-pass rectangular filter with a cutoff frequency of 20 Hz. For a 1° step input, the peak output velocity will be reduced to 40°/sec by the bandwidth of the instrument. Similarly, for a 10° step input, the peak output velocity will be 400°/sec.

The second feature of Equation 6 is that it permits the calculation of duration of the output provided H(f) is known. If the start and end of the output are defined as occurring when velocity just reaches zero, from a rectangular filter with a cutoff frequency f_0, the duration of the output will be given by $1/f_0$ for a step input of *any* amplitude. Thus, any step input to a 20-Hz low-pass rectangular filter will yield an output with a duration of 50 msec. Of course, the durations of real EMs will vary with amplitude, but it will not be possible to record accurately durations less than the minimum duration imposed by the instrument's bandwidth.

These examples illustrate the effect of bandwidth in the limiting case. Actual fast EMs are not step functions, but have finite PVs and nonzero durations. In order to be more realistic, it is useful to model the human saccadic system so that computations can easily be made. It is well established from physiological work that the saccade is generated by the action of a combination of a phasic pulse and a tonic step input to the extraocular muscles (e.g., Robinson, 1981). We therefore idealize the saccadic generator as a second-order system with both accelerative and velocity terms. Actual values for the time constants of these terms are taken from Zee and Robinson (1979). The driving input for this system is idealized as a rectangular pulse superimposed on a step. No assumption is made concerning the mechanism involved in determining the pulse width and pulse height relative to the step height. Values for these parameters are taken from Collins (1974) and are slightly modified, when necessary, to generate saccades with typical PVs and durations. These approximations provide a means of generating a reasonable facsimile of a human adult saccade in the computer, from which spectra and the effects of bandwidth can be computed. We have chosen to simulate fast EMs according to the above model for the sake of computational simplicity. The general conclusions are affected only in detail by variations in the EM profile. Figure 2 shows the effect of a recording system with a rectangular filtering profile on these simulated saccades. The solid lines represent responses to simulated saccades, and the dashed lines depict responses to ideal step inputs; amplitudes range from 5 to 30°. In Figure 2a, each curve plots the PVs and durations that would be measured for any one EM by a system with a low-pass rectangular filtering profile with a cutoff frequency, f_0, shown along the abcissa. For ex-

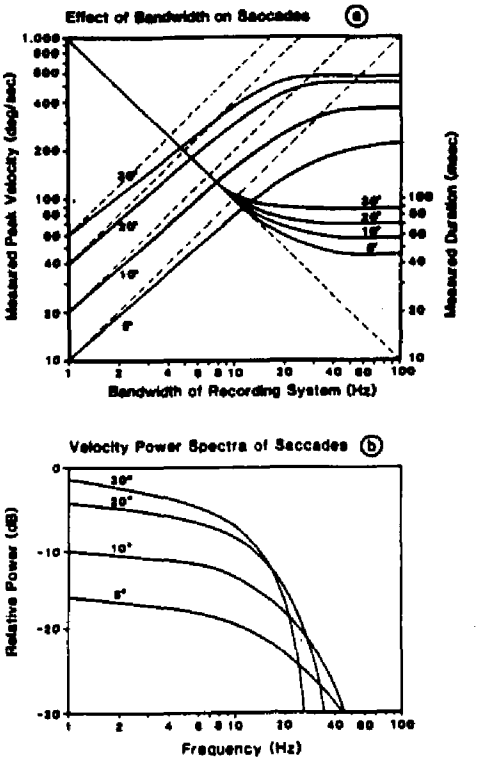

Figure 2. Effect of eye movement recording instrument's bandwidth on computer-simulated saccades (solid lines) and step inputs (dashed lines). (a) The left-hand ordinate shows the peak velocity that would be measured for 5-, 10-, 20-, and 30° simulated saccades and step inputs by an instrument with a rectangular low-pass filtering profile with a cutoff frequency shown along the abscissa. The right-hand ordinate shows the measured duration of the instrument's output for the same inputs. (b) Power spectra of the velocity of the simulated saccades in decibels, normalized to a 30° saccade.

ample, consider a simulated 10° saccade. If the cutoff frequency of the instrument is 10 Hz, the measured PV will be only about 150°/sec, as opposed to an actual PV of about 350°/sec (see asymptote of 10° curve); to measure this true PV, an instrument cutoff frequency of at least 50 Hz is needed. For the same 10° simulated saccade with an instrument cutoff frequency of 10 Hz, measured duration will be 100 msec, instead of about 55 msec. Figure 2b shows the power spectra, measured in decibels, for the velocity of the simulated saccades and step inputs; the spectra have been normalized with respect to a 30° saccade.

As expected from the above discussion, once the bandwidth of the instrument's filtering profile exceeds that of the saccade, the measured PV and duration will be accurate. For instrument bandwidth below about 50 Hz, however, distortion becomes pronounced, giving rise to an underestimation of PV and an overestimation of duration. These effects are particularly important for shorter saccades, whose power spectra contain higher frequency components. The change in spectra with amplitude is a direct consequence of the step-pulse mechanism that generates saccades; the pulse is more prominent for shorter saccades, but the step is dominant in larger saccades. For very low instrument bandwidths, the output is determined almost entirely by the instrument's bandwidth, and no information about the input profile (except amplitude) can be recorded. Another consequence of low bandwidth (not shown here) is "ringing." This easily can be mistaken for, or can obscure, actual overshoots in EMs.

Noise

Our second major consideration is the effect of noise on the measurement of fast EMs. Only noise with sufficient bandwidth to distort the profile of a fast EM will be considered here; slow "dc" drifts, commonly found in electrooculograms (EOGs), will be ignored because they belong more to the realm of static calibration. Four independent noise sources are identified.

(1) Holder. Noise may originate in the device, or the person, holding the subject's head stationary. Vibrations transmitted to the subject via a chinrest or bitebar are small in the laboratory environment. Detectable head movements are more likely to occur if the subject's head is minimally restrained (e.g., Bronson, 1982; Haith, 1980) or is held by an assistant (Hainline, 1981), which is the case with infant subjects.

(2) Head movements. This source of noise is distinguished from the above in that it originates in the subject rather than in the environment. At one extreme, the dental bitebar represents the most effective (and intrusive) means of eliminating head movements for human subjects. At the other extreme, the head is allowed to move freely within a restricted region, and head movements are corrected electronically or optically. This compensation must require the detection of head movements, and it will not only leave a residual noise, but also have a finite bandwidth, thereby increasing the possibility of error caused by fast head movements. Since, in free viewing, saccades often precede head movements, a strong possibility of signal-dependent noise arises.

(3) Oculomotor noise. Oculomotor noise may be considered as time variations in extraocular muscle tension, neuronal shot noise, any noise in the target localization process of the subject, and so forth. Unlike the other noise sources, this noise cannot be considered to be an artifact, since it is inherent in the system under scrutiny.

(4) Recording system noise. As with any other measuring device, the instrument will introduce its own noise. The most sensitive part of most instruments in this respect is the detector, namely, the receiving coil, electrodes, photomultiplier, photodiode(s), or TV camera. Although most system noise will originate at this level, significant sources, such as amplifier noise and analog-to-digital conversion noise, may be injected later in the system.

Usually, noise from these sources will combine independently and will be filtered by the instrument along with the actual eye position signal. The noise at the output will therefore also be band limited. If the combined noise referred to the instrument's input has a power spectrum given by N(f), then, for measures of eye position, the root-mean-square (RMS) noise appearing at the output will be given by (see, e.g., Pierce & Posner, 1980):

$$\sigma_{pos} = \left[\int_{-\infty}^{\infty} N(f)|H(f)|^2 df\right]^{1/2}. \quad (8)$$

This describes the well-known phenomenon that, the greater the bandwidth of a recording system, the greater the RMS noise will be at the output. For the sake of illustration, consider the instrument filtering profile to be a low-pass rectangle with cutoff f_0, and also assume the noise to be white and gaussian with a spectral power density of $N_0/2$. For this case, the RMS positional noise will be given by $(N_0 f_0)^{1/2}$. In other words, the standard deviation of the noise appearing on the position data will be proportional to the square root of the bandwidth of the instrument.

Since velocity measures contain augmented high-frequency components (see Equation 4), velocity noise will be greater than position noise. The RMS noise on the velocity signal at the instrument's output will be given by:

$$\sigma_{vel} = 2\pi\left[\int_{-\infty}^{\infty} f^2 N(f)|H(f)|^2 df\right]^{1/2}. \quad (9)$$

If, as before, we assume a low-pass rectangular filter for H(f) and white noise, the standard deviation of the noise on the velocity signal will now be $2\pi(N_0 f_0^3/3)^{1/2}$; velocity noise now depends on bandwidth raised to 3/2, rather than 1/2. In short, extending the bandwidth of the instrument beyond that of the EM increases the noise unnecessarily.

The presence of velocity noise precludes the use of zero velocity as the criterion for deciding when a fast EM starts and stops, that is, its duration. It is therefore common to require that velocity fall below some small criterion.

However, this would underestimate the duration. Furthermore, if the criterion is held constant, this underestimation will be more severe for small saccades than for large saccades. Although this effect is small, it may confound the duration/amplitude relationship found for low-amplitude saccades ($< 10°$) in human adults (e.g., Howard, 1982, p. 262). An alternative scheme is to allow the criterion to vary proportionately with the amplitude. This is particularly useful for noisy data, but becomes inoperative for small-amplitude movements, since the criterion will eventually become embedded in noise.

Sampling

Digitization of analog data for computer analysis must involve sampling. Analog-to-digital conversion may take place at such a fast rate that there is virtually no distortion in the measurement of PV or duration from digital records. However, systems that operate with TV video cameras have an intrinsic sampling problem, since eye position can be estimated no faster than TV field rate. In order to discuss sampling distortion, it is necessary to describe the sampling function utilized by the system. A signal can be sampled instantaneously every sampling period, or a sample can be obtained by averaging the signal throughout each sampling period. These sampling functions represent two extreme forms of sampling, and each has its own drawback. The instantaneous sampling function can give rise to serious aliasing problems. Aliasing occurs whenever there exist components in the input signal above half the sampling rate—the Nyquist, or "folding," frequency. The frequency of these components will be translated, or "folded back," to new frequencies below half the sampling rate, and will confound signal components already at these lower frequencies. For example, when sampling occurs at 60 Hz (TV rate), the Nyquist frequency is 30 Hz. If the input signal has a component at 50 Hz, it will appear in the sampled signal, not at 50 Hz, but at 10 Hz and will be superimposed on any original 10-Hz signal component. The usual remedy for aliasing is to filter out the signal components above the Nyquist frequency with a low-pass antialiasing filter before sampling takes place; however, this is free of distortion only if the sampling rate is at least twice the highest frequency component in the signal that is to be sampled. For fast EMs with a bandwidth of about 50 Hz (see Figure 2b), a minimum sampling rate of 100 Hz is needed. At the other extreme, a sampling function that lasts the whole sampling period reduces aliasing to a minimum, but at the expense of bandwidth. For this type of sampling function, any movement of the eye occurring within the sampling period will be lost or "smeared out," thus effectively reducing bandwidth. Formally, the filtering effect of sampling is given by the Fourier transform of the sampling function, so that the rectangular sampling function, lasting the whole sampling period, represents the worst case in lowering bandwidth. The filtering effects of sampling at 60 Hz for these two extremes are shown in Figure 3 (Curves a and b). Depending on the precise method of estimating eye position, TV systems will fall somewhere between these two extremes.

Another sampling problem, besides general bandwidth reduction and aliasing, is that of sampling error. It is common practice to estimate eye velocity by taking the difference between two samples of eye position and dividing

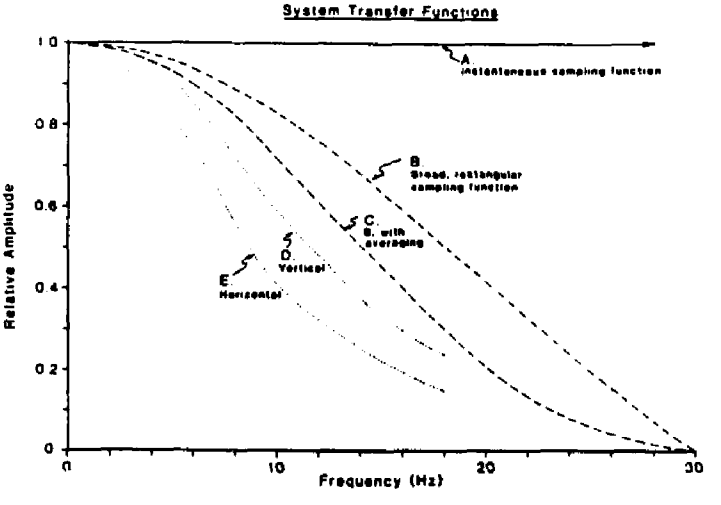

Figure 3. System transfer functions. (a) Due to an instantaneous sample taken at the sampling rate, r = 60 Hz. (b) Due to a rectangular sampling function lasting a complete sampling period: $\sin(2\pi f/r)/(2\pi f/r)$, r = 60 Hz. (c) Averaging consecutive samples obtained via (b). (d) Transfer function of the authors' instrument based on sinusoidally oscillating a mechanical "artificial eye" (see text) in the vertical plane. (e) Same as (d), but in the horizontal plane.

this by the interval. An estimate of eye velocity that is based on only two eye position samples is intrinsically inaccurate. This is true even if the sampling rate (r) is more than twice the signal bandwidth because, although the samples may contain all the information in the original eye position signal, the latter should first be reconstructed from the samples by filtering at the Nyquist frequency before differentiating to find velocity. If this is not done, the best estimate of eye velocity, $\hat{v}(t)$, based on two consecutive samples is given by:

$$\hat{v}(t) = \int_{-\infty}^{\infty} \hat{E}(f)H(f)\sin(\pi f/r)/(\pi f/r)e^{2\pi jft}df. \quad (10)$$

The sampling error term, $\sin(\pi f/r)/(\pi f/r)$, acts on the true velocity spectrum, $\hat{E}(f)$, in addition to the filtering profile of the instrument, $H(f)$, which is in itself partly determined by the sampling function as described earlier. Thus, even if the sampling rate is more than the highest frequency component in the instrument's output, eye velocity will still always be underestimated when it is based on only two samples of eye position. An important case arises when PV is to be measured. If the true PV happens to occur in the middle of a sampling interval, then the underestimation will be at a minimum and is given by the above equation. If, however, the PV occurs elsewhere in the sample period, there will be further underestimation, the worst case arising when PV occurs at either end of a sampling period. To illustrate the degree of underestimation, consider the example shown in Figure 4a. For computational simplicity, a saccade is approximated by a step function passed through a low-pass rectangular filter with cutoff f_0 (the results of the computation would not be seriously changed if a more realistic EM were used). The bandwidth of the recording instrument can represent this filter. Without sampling, the measured PV would be equal to $2f_0$. However, when the output of the instrument's profile is sampled at k times f_0 (abcissa in Figure 4a), the percentage reduction in measured PV, for both best and worst cases, is shown along the ordinate. For example, in order to keep sampling error below 5%, a sampling rate of at least six times the instrument's bandwidth must be employed. Moreover, the absolute error will be proportional to PV, so that larger fast EMs with higher PVs will be prone to larger errors.

Another consequence of estimating eye velocity from only two samples is quantization error. Recording systems with high sampling rates are particularly prone to this error, which arises from the digitization process. It is best illustrated by example. Consider a system with 12-bit accuracy covering a full scale of 100° of eye movement. Each level of the output will correspond to 0.024°. If the sampling rate is 1 kHz, the minimum detectable velocity based on two consecutive samples would be 0.024° in 1 msec, or about 24°/sec. Thus, eye velocity could only be measured in steps of 24°/sec. On the other hand, a slower system with a 100-Hz sampling rate would measure eye velocity in steps of 2.4°/sec.

Sampling error, but not quantization error, can be made

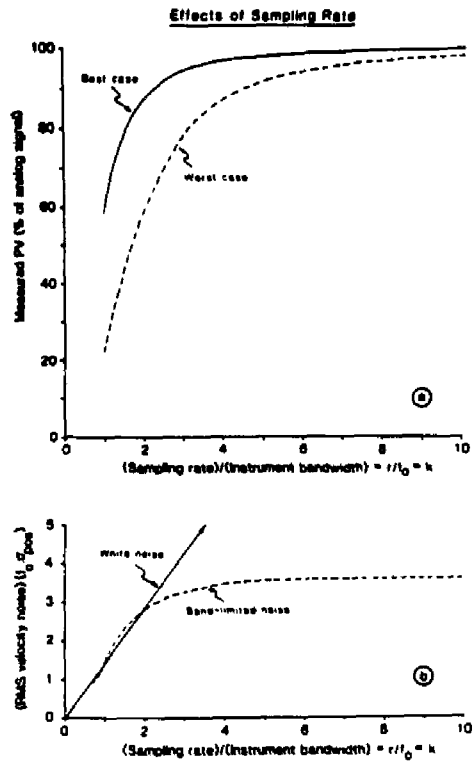

Figure 4. Effect of sampling rate on the measurement of peak velocity (PV) and on RMS velocity noise, when the eye velocity is estimated from two consecutive samples of eye position. Instrument has bandwidth of f_0. (a) Shows best and worst cases for PV as a percentage of $2f_0$—the true analog PV at the output for a unit step input. Best case occurs when true PV is midway between samples, and worst case occurs when true PV is at a sampling point. (b) Shows RMS velocity noise for uncorrelated noise samples (solid line) and band-limited noise (dashed line). RMS velocity is shown in units of $f_0\sigma_{pos}$, where σ_{pos} is the RMS position noise.

arbitrarily small by sampling at a sufficiently high rate, but this may not always be practical and is impossible for TV-based systems. Alternatively, sampling error and quantization error in eye velocity measurements can be reduced by reconstructing the original EM: eye velocity can then be estimated from the "smooth" response, rather than from two samples of eye position. Obtaining velocity via a reconstructed position signal can be accomplished in one step by applying an appropriate digital filter (a weighted "window") directly to the position samples (Engelken, Stevens, & Wolfe, 1982). The optimal digital filter will depend on the sampling rate, the noise in the instrument's output, and the number of data points considered in the window. The reader is referred to any standard text for further details (e.g., Blackman, 1965; Hamming, 1983).

If digital filter techniques are not employed, other events, such as the beginning and end of a fast EM, cannot be determined within a sampling period. Since the start of a fast EM can occur at any time during a sample period,

its detection will have a flat probability distribution with a standard deviation of $1/\sqrt{12}r$. The detection of the end of a fast EM will suffer a similar error. The error in duration measurements could therefore have a standard deviation of $1/\sqrt{6}r$, although, since fast EMs tend to have fixed durations for a given amplitude, the errors in detecting beginning and end will probably be correlated.

Besides the possibility of inaccuracy due to coarse sampling, velocity noise will also be affected by the sampling rate. If the noise characteristics do not change in time (i.e., the noise is stationary) and the noise is additive with a mean amplitude of zero, the velocity RMS noise will be given by the standard deviation of the difference between two correlated consecutive position samples divided by the sampling interval:

$$\sigma_{\dot{v}} = \left\{2r^2[\sigma^2_{pos} - C(1/r)]\right\}^{1/2}, \quad (11)$$

where C(1/r) is the covariance of two consecutive noise samples. If the noise bandwidth is much greater than the sampling rate, then consecutive noise samples will be virtually independent with no covariance. This is illustrated by the solid line in Figure 4b. As the sampling rate increases, the RMS velocity noise will increase linearly with a slope of $\sqrt{2}$. However, if the noise source is early in the system and is subjected to the instrument's filtering profile, then the noise bandwidth will be lower than the sampling rate, in which case there will be covariance between consecutive samples and the RMS velocity noise will be less. For example, consider white noise with a spectral density given by $N_0/2$, subject to a low-pass rectangular filtering profile with cutoff frequency f_0. By deriving the covariance of two consecutive samples from the inverse Fourier transform of this noise spectrum, the RMS velocity noise can be shown to be:

$$\sigma_{\dot{v}} = \left\{2r^2\sigma^2_{pos}[1 - \sin(2\pi f_0/r)/(2\pi f_0/r)]\right\}^{1/2}. \quad (12)$$

The RMS velocity noise with sampling at k times the cutoff frequency is shown by the dotted line in Figure 4b. As the sampling rate increases, the RMS noise increases, until a maximum is reached. This maximum corresponds to the analog band-limited RMS velocity noise in Equation 9, and is equal to $\sqrt{4/3}\pi f_0\sigma_{pos}$.

In short, Figure 4 shows a tradeoff: Noise can be reduced only at the expense of accuracy. If velocities are estimated from consecutive samples, a surprisingly high sampling rate is required for a reasonable accuracy; this sampling rate is considerably more than twice the Nyquist frequency. Therefore, when feasible, digital filtering techniques should be used; but this is only successful when instrument bandwidth exceeds the highest frequency component in the velocity signal. Of course, digital filtering will not reduce band-limited noise.

When digital filtering techniques are not used (as with systems whose bandwidths are inherently too low) and velocities are estimated from consecutive samples, additional problems arise. For example, estimates of PV will be especially distorted by noise. Noise can subtract or add to the true velocity in any interval; however, in most cases only the interval to which noise has added will be picked as the peak. This is a nonlinear effect, since for slow EMs a spuriously large PV will usually be found. On the other hand, sampling will produce an underestimation of PV because, on the average, the true peak will occur within an interval and be missed; this underestimation is more pronounced for faster EMs.

Conclusions

Bandwidth. There are two conflicting bandwidth requirements for the recording of fast EMs: (1) The recording instrument should have a flat frequency response up to the maximum frequency component in the fast EM. For correctly measuring eye velocity, this component is about 50 Hz for human adults, although nonhuman fast EMs may have significantly different power spectra. (2) Bandwidth should be kept as low as possible, since noise, especially on the velocity signal, increases with bandwidth.

Sampling. Sampling can have two distinct effects: (1) The sampling rate and sampling function can reduce the effective bandwidth; this is unavoidable with systems using standard TV video rates. (2) Sampling also causes error in the temporal localization of events, such as the beginning and end of a saccade or the occurrence of PV. Sampling problems can generally be avoided by sampling at as high a rate as feasible and employing digital filtering techniques to evaluate the EM parameters of interest.

EVALUATING A SPECIFIC VIDEO-BASED SYSTEM

To understand the dynamic properties of a specific recording system, it is necessary to know the system's filtering profile (or transfer function), H(f). The only certain method for finding H(f) is to present the instrument with several known inputs and to measure the corresponding outputs. Our instrument was an infrared corneal-reflection eye tracker based on a TV camera (Applied Science Laboratories Model 1994 Eye View Monitor; Hainline, 1981). This is a common type of TV system for EM recording. As the eye rotates, there is a differential motion of two images; the corneal reflection of the tracker's illuminator (first Purkinje image) and the pupil. The instrument analyzes this differential motion to estimate the direction of the optic axis of the subject's eye.

This instrument produces an estimate of eye position at the end of each interlaced TV field (60 Hz), and can average consecutive estimates. Averaging has the desired effect of reducing noise and increasing resolution, but has the drawback of reducing bandwidth (averaging is a simple low-pass digital filter). This additional reduction in bandwidth is illustrated by Curve c in Figure 3.

An "artificial eye" that emulated optically the first Purkinje and pupil images was used to provide known inputs to the eye tracker. It was rotated about a point equivalent to the center of rotation of an eye. By oscillating the ar-

tificial eye sinusoidally with a known amplitude at different angular frequencies, the transfer function H(f) was measured. This is shown in Figure 3 for both horizontal (Curve e) and vertical (Curve d) axes. As can be seen, the bandwidth is lower than would be predicted by sampling at TV rates even with a broad sampling function and averaging consecutive fields (Curve c). Investigation of this deficit indicated that the persistence of the response of the TV camera's vidicon tube extended beyond one sampling period. This persistence lengthens the instrument's time constant and reduces the bandwidth still further.

As shown earlier, twice the area under a transfer function is equal to the PV of the response of the instrument to a step input (Equation 7). The areas under the transfer functions in Figure 3 (Curves d and e) were about 15 and 20 Hz. Thus, for horizontal EMs, the greatest PV that can be registered for a 10° input is about 300°/sec. However, with this instrument we have recorded adult saccades with PVs in excess of this theoretical limit. This discrepancy suggests that the sinusoidal method of obtaining the transfer function did not truly describe the instrument. The difference in horizontal and vertical transfer functions suggests that this instrument is anisotropic in its response.

Anisotropy

An alternative procedure for describing a system is to present it with step inputs in various directions. The artificial eye could not provide a perfect step but was capable of a PV of about 1,000°/sec for a 10° excursion—much faster than a human EM of the same amplitude. It was found that rightward (in the direction of the TV raster) inputs produced outputs with PVs different from those produced by leftward inputs. The amount of this anisotropy was found to depend on the precise settings of the electronics in the TV image analyzer. This is because our particular model of instrument estimates eye position based on only the left half of the pupil and the first Purkinje images. Any persistence in the system has a differential effect depending on whether the brighter first Purkinje image is moving away from or toward the left half of the pupil image, giving rise to erroneous PVs. The vertical/horizontal anisotropy was also found to be caused by TV persistence.

Peak Velocity Calibration

Once the transfer function(s) is found, it becomes possible to "work backward" from an output to find the true input. This deconvolution process is probably worthwhile for only "clean" systems with bandwidth sufficient to embrace the input spectrum. A more tedious, but simpler, approach, more suited for noisy data and instruments with low bandwidths, is to simulate mechanically a range of inputs and record output values for specific parameters, and thus provide a set of lookup calibration curves for these parameters. Since we were interested primarily in PV, single ramps of various slopes and magnitudes were presented to the system. Although actual fast EMs do not have ramp profiles, these inputs were considered to be close enough with respect to PV and were easy to generate. The results

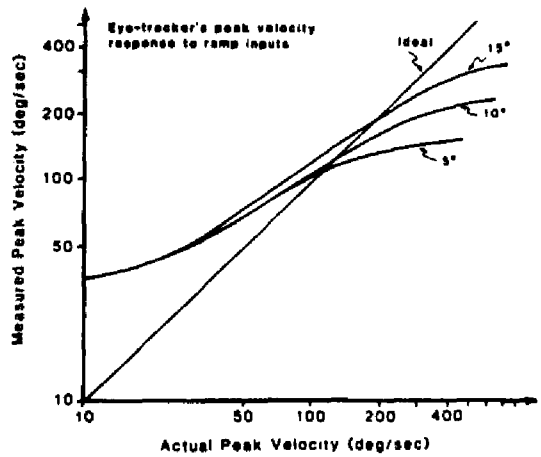

Figure 5. Peak velocity measured on the authors' instrument for ramp inputs of various slopes (abscissa) made by a mechanical "artificial eye" (see text); parametric in amplitude.

for leftward ramps are shown in Figure 5. Similar sets of curves exist for other directions. Here, the PV, as measured on the output (ordinate), is plotted against the actual ramp velocity of the input (abcissa) for three amplitudes. For example, most of our adult subjects produced 10° saccades with an apparent PV of about 200°/sec. Figure 5 indicates that the true PV was closer to 350°/sec.

Noise Measurement

By maintaining the artificial eye in a stationary position, the static RMS noise of the system was estimated. The instrument output was monitored with the artificial eye pointing in various horizontal and vertical directions. The RMS noise was found to be about 3/8° and to be independent of direction. This is in good agreement with the manufacturer's claim of 1/2° accuracy. No correlation was found between vertical and horizontal noise components. From Equation 11, a system with a 15-Hz bandwidth and a sampling rate of 60 Hz should give a RMS velocity noise of about 20°/sec. If the noise, however, originates later in the system, so that there is little covariance between noise samples, then a RMS velocity of about 30°/sec would be expected. The actual RMS velocity noise was measured to be about 22°/sec. This indicates that most of the noise originates in or before the detector and only a little noise is introduced later. This deduction was confirmed by finding the square root of the noise power spectrum and comparing its envelope to the transfer functions in Figure 3 (Curves d and e).

Discussion

As a practical demonstration of compensating for the dynamic response of our instrument, consider Figure 6 (left-hand ordinate). Here, PV is plotted against amplitude for a series of saccades from an adult human subject (a static calibration had been performed for this subject; see

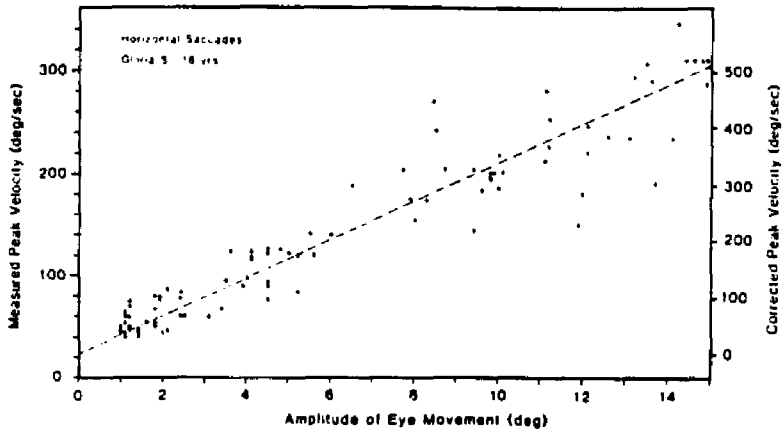

Figure 6. Left-hand ordinate—relationship between peak velocity of typical adult saccades and amplitude of saccades, as measured on the authors' instrument. Note the low slope and the nonzero intercept. Right-hand ordinate—relationship after calibration.

Harris et al., 1981). There are three main artifactual features. First, the variability in measured PV increases as PV increases. At least in part, this must be due to sampling error and cannot be reduced without incorporating signal reconstruction techniques (see "Sampling," above). Second, the slope of the PV versus amplitude relationship is much lower than that normally reported (see "Bandwidth," above). This is due to the low bandwidth of the system, as shown by Curve e in Figure 3, and can be corrected by the calibration curve in Figure 5. Third, the nonzero intercept in Figure 6 is due to velocity noise (see "Noise," above) and is also corrected by the calibration curve in Figure 5. The right-hand ordinate of Figure 6 shows the corrected PV for this subject. Thus, although this TV-based instrument falls short of the ideal in terms of dynamic response, it can, nevertheless, be used to measure fast EMs.

As stated earlier, each system must be evaluated with respect to its application. The authors' experience has been that design specifications and manufacturers' claims are no substitute for an empirical evaluation of the overall system—from the eye via the computer to the final measured EM parameter.

REFERENCES

Aslin, R. N., & Salapatek, P. (1975). Saccadic localization of visual targets by the very young infant. *Perception & Psychophysics*, 17, 293-302.

Blackman, R. B. (1965). *Data smoothing and processing*. Reading, MA: Addison-Wesley.

Bronson, G. (1982). *The scanning patterns of human infants: Implications for visual learning*. Norwood, NJ: Ablex.

Bullinger, A., & Kaufmann, J. L. (1977). Technique d'enregistrement et d'analyse des mouvements oculaires. *Perception*, 6, 345-353.

Carmody, D. P., Kundel, H. L., & Nodine, C. F. (1980). Performance of a computer system for recording eye fixations using limbus reflection. *Behavior Research Methods & Instrumentation*, 12, 63-66.

Champeney, D. C. (1973). *Fourier transforms and their physical applications*. London: Academic Press.

Collins, C. C. (1974). The human oculomotor control system. In G. Lennerstrand & P. Bach-y-Rita (Eds.), *Basic mechanisms of ocular motility and their clinical implications* (pp. 145-182). Oxford: Pergamon Press.

Engelken, E. J., Stevens, K. W., & Wolfe, J. W. (1982). Application of digital filters in the processing of eye movement data. *Behavior Research Methods & Instrumentation*, 14, 314-319.

Hainline, L. (1981). An automated eye movement recording system for use with human infants. *Behavior Research Methods & Instrumentation*, 13, 20-24.

Haith, M. M. (1980). *Rules that babies look by: The organization of newborn visual activity*. Hillsdale, NJ: Erlbaum.

Hamann, K. (1979). Verlangsamte Sakkaden bei verschiedenen neurologischen Erkrankungen. *Ophthalmologica, Basel*, 178, 357-364.

Hamming, R. W. (1983). *Digital filters* (2nd ed.). Englewood Cliffs, NJ: Prentice Hall.

Harris, C. M., Hainline, L., & Abramov, I. (1981). A method for calibrating an eye-monitoring system for use with infants. *Behavior Research Methods & Instrumentation*, 13, 11-17.

Howard, I. P. (1982). *Human visual orientation*. New York: Wiley.

Kliegl, R., & Olson, R. K. (1981). Reduction and calibration of eye monitor data. *Behavior Research Methods & Instrumentation*, 13, 107-111.

Levy-Schoen, A., & O'Regan, K. (1979). The control of eye movements in reading. In P. A. Kolers, M. E. Wrolstad, & H. Bouma (Eds.), *Processing of visible language 1* (pp. 7-36). New York: Plenum.

McConkie, G. W. (1981). Evaluating and reporting data quality in eye movement research. *Behavior Research Methods & Instrumentation*, 13, 97-106.

Mendelson, M. J., Haith, M. M., & Goldman-Rakic, P. S. (1981). Monitoring visual activity in infant rhesus monkeys: Method and calibration. *Behavior Research Methods & Instrumentation*, 13, 709-712.

Pierce, J. R., & Posner, E. C. (1980). *Introduction to communication science and systems*. New York: Plenum.

Robinson, D. A. (1981). The use of control systems analysis in the neurophysiology of eye movements. *Annual Review of Neuroscience*, 4, 463-503.

Young, L. R., & Sheena, D. (1975). Survey of eye movement recording methods. *Behavior Research Methods & Instrumentation*, 1, 397-429.

Zee, D. S., Optican, L. M., Cook, J. D., Robinson, D. A., & Engel,

W. K. (1976). Slow saccades in spinocerebellar degeneration. *Archives of Neurology*, 33, 243-251.

ZEE, D. S., & ROBINSON, D. A. (1979). A hypothetical explanation of saccadic oscillations. *Annals of Neurology*, 5, 405-414.

ZUBER, B. L., SEMMLOW, J. L., & STARK, L. (1968). Frequency characteristics of the saccadic eye movement. *Biophysical Journal*, 8, 1288-1298.

NOTE

1. A more comprehensive derivation of the formulae presented here can be supplied upon request.

(Manuscript received February 7, 1984;
revision accepted for publication July 11, 1984.)

Appendix C

Artificial eye for assessing corneal-reflection eye trackers

(Reprinted by permission of the Psychonomic Society, Inc.)

ISRAEL ABRAMOV and CHRISTOPHER M. HARRIS
Brooklyn College of CUNY, Brooklyn, New York

An artificial eye for assessing corneal-reflection eye trackers is described. The "eye" simulates an adult human eye and consists of a contact lens of the same curvature as the cornea.

To assess the performance of an eye tracker, it is necessary to present it with a precisely known input. For a corneal-reflection eye tracker with a bright-pupil (e.g., Hainline, 1981; Young & Sheena, 1975), this can be provided only by a device that simulates the optics of the human cornea and pupil. Such a device is shown in Figure 1. This "artificial eye" consists of a contact lens of the same curvature as the human cornea; the image of the illuminator that is reflected by this surface provides one of the two required images for the eye tracker. The second image, the bright-pupil, is provided by an aperture situated at the correct optical distance behind the "corneal" pole; this aperture is backed by white paper that serves as a diffuse reflector to simulate the fundus. The arrangement is rotated about a point, equivalent to the center of rotation of the human eye, by a fast high-torque galvanometer motor. The motor is specified in Figure 1; however, a pen motor from a good chart recorder would suffice. The shaft of the motor is also connected with a zero-backlash coupling to a linear potentiometer, which provides a precise and continuous readout of the angular position of the device. This is a simple and inexpensive arrangement and can be driven by a signal generator or a computer-generated signal. An outline of the artificial eye is shown in Figure 1a. All surfaces in the field of view of the eye tracker are painted flat black.

The optical geometry shown in Figure 1b is based on a simplified schematic eye of the adult human (see Bennett & Francis, 1962). The meniscus contact lens has zero power and the same curvature as the real cornea. (Unfortunately, a plano-convex lens, although cheaper, also produces a very bright reflected image from its second surface, and this image confuses the image-processing electronics of the eye tracker.) Since this lens has no dioptric power, it is necessary to position the sharp-edged "pupil" 3.05 mm behind the pole, rather than 3.6 mm,

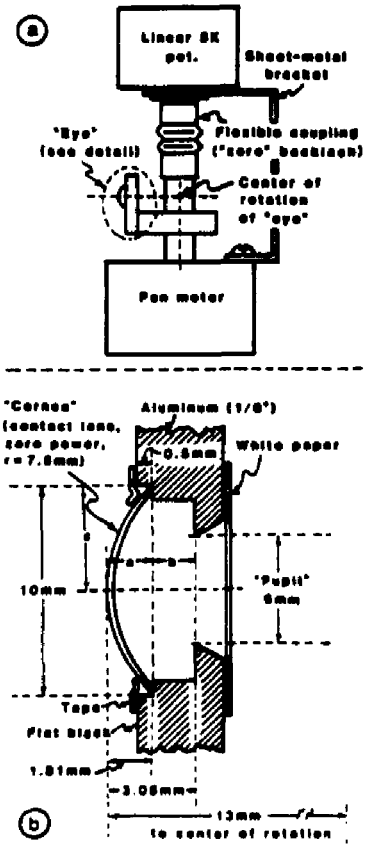

Figure 1. Outline of artificial eye for bright-pupil corneal-reflection eye tracker. Not to scale. Specific components used were: (1) corneal contact lens—zero power, 7.8-mm base curve, 0.2 mm thick, 10 mm in diameter, from Dow Corning Ophthalmics, Norfolk, VA; (2) pen motor—optical scanner G-330, from General Scanning, Watertown, MA; (3) flexible coupling—"nickel bellows" type, from Servometer, Cedar Grove, NJ.

This work was supported in part by Grants 661078 and 662199 from PSC-CUNY Research Award Program and NIH Grant EY-03957. The author's mailing address is: Department of Psychology, Brooklyn College of CUNY, Brooklyn, NY 11210.

Behavior Research Methods, Instruments, & Computers
1984, 16 (5), 437-438

as in the natural eye. Figure 1b also shows the details of the lens mounting. Care must be taken in placing the lens the correct distance [(a+b) in Figure 1b] in front of the aperture, since this determines the eye tracker's gain. Assuming the lens is spherical, the depth of the contact lens (dimension labeled "a" in Figure 1b) is $r+\sqrt{(r^2-c^2)}$, where r is the radius of curvature and c is the radial width of the lens. Calculation of the depth allows the correct indentation of the recesses to be made.

Although the artificial eye can rotate in only one dimension, it is small enough to be mounted on a camera tripod so that the tripod's panhead can be used to set the artificial eye's axis of rotation at any angle. Thus, the performance of the eye tracker in any direction can be assessed. The potentiometer not only provides the necessary readout for precisely adjusting the excursion of the "eye," but also mechanically damps overshoots from step inputs to the motor. By trial and error, we found a potentiometer that damped overshoot to less than 5% for a 10° movement while still maintaining a speed of 1,000°/sec for a step input; this is adequate to simulate even fast human saccades.

This artificial eye simulates an adult human eye, but it can also be used to approximate an infant eye. The gain of the eye tracker is proportional to the distance between the center of curvature of the cornea and the plane of the entrance pupil (e.g., see Young & Sheena, 1975); corneal asphericity has negligible effect. In the infant, the depth of the anterior chamber is about 70% of the typical adult's (Larsen, 1971). On the other hand, the radius of corneal curvature is only about 85% of the adult's (Mandell, 1967). These conditions cause the distance between the entrance pupil and the center of curvature to remain approximately constant from birth (see Bronson, 1982).

REFERENCES

Bronson, G. (1982). *The scanning patterns of human infants: Implications for visual learning*. Norwood, NJ: Ablex.

Bennett, A. G., & Francis, J. L. (1962). The eye as an optical system. In H. Davson (Ed.), *The eye* (Vol. 4). London: Academic Press.

Hainline, L. (1981). An automated eye movement recording system for use with human infants. *Behavior Research Methods & Instrumentation*, 13, 20-24.

Larsen, J. S. (1971). The sagittal growth of the eye. I. Ultrasonic measurements of the depth of the anterior chamber from birth to puberty. *Acta Ophthalmologica*, 49, 239-262.

Mandell, R. B. (1967). Corneal contour of the human infant. *Archives of Ophthalmology*, 77, 345-348.

Young, L. R., & Sheena, D. (1975). Survey of eye movement recording methods. *Behavior Research Methods & Instrumentation*, 1, 397-429.

(Manuscript received July 11, 1984;
revision accepted for publication September 12, 1984.)

Appendix D

COMBINING SUBJECT MEANS

For descriptive and inferential purposes it is often useful to find an average statistic based on measurements from a group of subjects (or treatments) when the subject means are themselves prone to error. Even though this situation arises frequently, it is poorly treated (if at all) by standard texts.

We wish to combine M subject means to find a "grand mean", $\bar{\bar{X}}$, when each subject mean is itself an estimate with an associated standard error. We also wish to find the variance of this grand mean so that confidence intervals can be constructed. We will restrict ourselves to a linear combination of the subject means as follows:

$$\bar{\bar{X}} = w_1\bar{X}_1 + w_2\bar{X}_2 + \cdots w_M\bar{X}_M \qquad (D.1)$$

where

$$\sum_{i=1}^{M} w_i = 1. \qquad (D.2)$$

Here each subject's mean is weighted by some number, w_i, which will reflect the relative importance of each subject's contribution to the

grand mean. Assuming subjects are independent from one another, then the variance of the grand mean is given by:

$$\mathrm{var}(\bar{\bar{X}}) = \sum_i w_i^2 \mathrm{var}(\bar{X}_i). \qquad (D.3)$$

In order to find these variances, it is necessary to model the sources of error. For our purposes the simple variance-component model as used in ANOVA is adequate (see Winer, 1971). Here, the jth measurement from the ith subject, x_{ij}, is perturbed by a random variable, β_i, (between) with zero mean and variance, σ_b^2, and a measurement random variable, ω_{ij}, (within) with zero mean and variance, σ_i^2, depending on the subject:

$$x_{ij} = \mu + \beta_i + \omega_{ij}. \qquad (D.4)$$

The expected value for the ith subject is then:

$$\bar{X}_i = \mu + \beta_i + E[\omega_{ij}] = \mu + \beta_i \qquad (D.5)$$

and the variance of this expectation is:

$$\mathrm{var}(\bar{X}_i) = \sigma_b^2 + \sigma_i^2/N_i. \qquad (D.6)$$

Substituting Equation D.6 into Equation D.3, the overall variance of the grand mean is then:

$$\text{var}(\bar{\bar{X}}) = \sum_i w_i^2 (\sigma_b^2 + \sigma_i^2/N_i). \qquad (D.7)$$

Thus, the overall variance is the weighted sum of the between variance and the variance of each subject's mean. Clearly, ignoring either of these components, σ_b^2 or σ_i^2/N_i, will underestimate the total variance and thereby inflate any obtained statistic, and increase the probability of a type I error.

The results in Equations D.1 and D.7 are accurate regardless of the scheme for choosing the weights. Choosing a set of weights is a separate problem and depends on the *a priori* assumptions one is willing to make.

The simplest scheme is to weight each mean equally, so that $w_i=1/M$. In this case, the grand mean is merely the mean of means and the variance is:

$$\text{var}(\bar{\bar{X}}) = \sigma_b^2/M + \sum_i \sigma_i^2/(MN_i) \qquad (D.8)$$

Of course there are still the two components to this variance - between and within. However, equal weights attach equal importance to each subject's mean. This may not always be appropriate (as in these experiments) because each subject's mean may not be obtained from equal sample sizes, and/or the measurement random variable, ω, may be different for each subject. It would therefore seem more

appropriate to weight more heavily those subjects' means which are known with more confidence; that is the weights should depend on the sampling variance of each subject's mean. This is embodied in the "minimum variance" approach. By this scheme, the weight are chosen to minimise the total variance in Equation D.7. This produces the optimal set of weights in the least squares sense. These weights can be found from Equation D.7 by employing Lagrange multipliers using the constraint that the weights sum to unity (Equation D.2). The optimal weights are then given by:

$$w_i = [(\sigma_b^2 + \sigma_i^2/N_i) \sum_j (\sigma_b^2 + \sigma_j^2/N_j)^{-1}]^{-1}. \qquad (D.9)$$

The computation of these weights is somewhat involved but easily accomplished by computer. No assumption of Normality is necessary for these statistics although some parametric assumption would be necessary for constructing a confidence interval around the grand mean.

One possible drawback with the minimum variance scheme is that it fails to distinguish between different sources of within variance. The mean and variance of most random variables are not independent and there is the possibility that those subjects with, say, low means may also have low variances and so will have higher weights by virtue of their means, not necessarily because of their measurement error. A better approach may then be to pool the within variances so that they do not differentially affect the weights. The weights would then only vary according to each mean's sample size. This

possibility is noted here but not expanded upon because, in practice, this problem can only occur if there is considerable variability between subject means. This between variability would automatically cause the within variability to become negligible.

In summary, when combining means both the variance between the means and each mean's own sampling variance should be taken into account. If each mean is known with a high degree of confidence relative to the dispersion between means, then the within terms become negligible and the optimal weights approach equality. If, on the other hand, the variability between the means is small compared to variance associated with each subject's mean, then the between term can be ignored and the optimal weights become:

$$w_i = [\sigma_i^2/N_i \sum (N_j/\sigma_j^2)]^{-1}, \qquad (D.10)$$

which is the standard method for combining independent experimental results (Barford, 1967). However, for many situations neither of these extremes is valid and the complete equations must be used.

Finally, all the above are population variances which are, of course, unknown. Since only linear combinations of variances have been considered, these population variances can be replaced by their unbiased estimators, term for term. The variance of the grand mean can then be estimated by:

$$\tilde{var}(\bar{\bar{X}}) = \sum_i w_i^2 (\tilde{s}_b^2 + \tilde{s}_i^2/N_i) \qquad (D.11)$$

where $\tilde{s}_b^2$ and $\tilde{s}_i^2$ are unbiased estimators of σ_b^2 and σ_i^2. Similarly, the weights will be given by:

$$w_i = [(\tilde{s}_b^2 + \tilde{s}_i^2/N_i) \sum_j (\tilde{s}_b^2 + \tilde{s}_j^2/N_j)^{-1}]^{-1}. \qquad (D.12)$$

This scheme (Equations D.11 and D.12) is used throughout this study.

D.1 References

Barford, N.C. (1967). *Experimental measurements: Precision, error and truth.* London: Addison-Wesley.

Winer, B.J. (1971). *Statistical principles in experimental design* (2nd ed.) New York: McGraw-Hill.

Appendix E

MOMENTS

This appendix discusses moments and their estimation. Equations will not be derived with rigour. For an exhaustive discussion of moments see Kendall and Stuart, 1977.

E.1 Definitions

Consider a continuous probability distribution, f(x), of the random variable, x, defined over the region, R. The *nth moment about the origin* is defined as:

$$ {}_{n}'\mu_x = \int_R f(x)x^n.dx \qquad (E.1) $$

where ${}_{0}'\mu_x = 1$, and the first moment about the origin, ${}_{1}'\mu_x$, is the mean, which will be abbreviated to μ. The prime superscript indicates that the moment is about the origin. The presubscript indicates the order of the moment.

The *nth moment about the mean* or *nth central moment* is defined as:

$$ {}_n\mu_x = \int_R (x - \mu)^n f(x).dx \ . \qquad \text{(E.2)} $$

The first central moment, ${}_1\mu_x$, is zero and the second central moment, ${}_2\mu_x$, is known as the variance and will be written as σ_x^2.

Moments about the origin and moments about the mean are related by the two sets of equations:

$$ \sigma_x^2 = {}_2'\mu_x - \mu_x^2 \qquad \text{(E.3)} $$

$$ {}_3\mu_x = {}_3'\mu_x - 3{}_2'\mu_x\mu_x + 2\mu_x^3 $$

$$ {}_4\mu_x = {}_4'\mu_x - 4{}_3'\mu_x\mu_x + 6{}_2'\mu_x\mu_x^2 - 3\mu_x^4 $$

$$ {}_2'\mu_x = \sigma_x^2 + \mu_x^2 \qquad \text{(E.4)} $$

$$ {}_3'\mu_x = {}_3\mu_x + 3\sigma_x^2\mu_x + \mu_x^3 $$

$$ {}_4'\mu_x = {}_4\mu_x + 4{}_3\mu_x\mu_x + 6\sigma_x^2\mu_x^2 + \mu_x^4 \ . $$

The *nth standardised moment* is defined as:

$$ {}_n\gamma_v = {}_n\mu_x/\sigma_x^n \qquad n = 3,4,5 \ldots . \tag{E.5} $$

Standardised moments are dimensionless quantities. The third standardised moment is sometimes known as "skewness", and the fourth as "kurtosis" or "excess" (however, other definitions and nomenclature exist; Abramowitz and Stegun, 1972).

We shall often refer to the *nth root moment* as the nth root of the nth central moment.

E.2 Identifying a Distribution by its Moments

A distribution can be identified by its moments provided the moments are defined. To see this, we find the characteristic function of the distribution, $\Phi(\omega)$, by taking its Fourier transform over the region R:

$$ \Phi(\omega) = \int_R f(x)e^{i\omega x}dx . \tag{E.6} $$

We can also find the probability distribution from the characteristic function by taking the inverse Fourier transform:

$$ f(x) = (2\pi)^{-1} \int_{-\infty}^{\infty} \Phi(\omega)e^{-i\omega x}d\omega . \tag{E.7} $$

Differentiating Equation E.6 n times with respect to ω:

$$\frac{d^n}{d\omega^n}\{\Phi(\omega)\} \equiv \Phi^{(n)}(\omega) = i^n \int_R x^n f(x) e^{i\omega x} dx . \qquad (E.8)$$

From these relationships it can easily be seen that:

$$\Phi^{(n)}(0) = i^n {}_n'\mu_x . \qquad (E.9)$$

Thus, moments about the origin (and hence central moments) can be generated from the characteristic function.

Expanding the characteristic function in a Taylor series about $\omega = 0$, we obtain:

$$\Phi(\omega) = \Phi(0) + \Phi'(0) + \Phi''(0)\omega^2/2 + \ldots \qquad (E.10)$$

which, from Equations E.9, becomes

$$\Phi(\omega) = 1 + {}_1'\mu_x \omega + {}_2'\mu_x \omega^2/2 + \ldots \qquad (E.11)$$

or

$$\Phi(\omega) = 1 + \sum_{k=1}^{\infty} i^n {}_k'\mu_x \omega^k/k . \qquad (E.12)$$

Therefore by knowing all the moments of a distribution (about the origin or mean), we know the characteristic function of the distribution. The actual distribution can then be recovered from the characteristic function by Equation E.6. In other words, a probabil-

ity distribution can be identified by its moments, assuming that they are defined.

To know precisely a probability distribution, all moments most be known. In practice, however, the most common distributions can be identified by only their first few moments. In particular, Pearson has shown that distributions which are unimodal and have high order contact are completely specified by, at most, the first four moments (the so-called Pearson type III distributions; see Kendall and Stuart, 1977). This class of distributions includes the Gamma-type distributions, such as the Exponential. It is not usually worth examining fifth order or higher moments because of sampling error unless huge samples are available.

We are interested in identifying the parent distributions from samples from different subjects and to see if there is any similarity in each subject's parent distribution. This is easily accomplished if we plot one moment against another for each subject. A common distribution among subjects will appear as a trend, either linear or curvilinear, depending on the form of the actual distribution. This can be a powerful technique if there are many subjects with a wide range of scale factors. In Table 2., the relationships between the first four moments is summarised for some common probability distributions. Of course, there is an infinite number of distributions, each having different moments. However, the method of moments does allow classes of distributions to be distinguished. A particular class of distributions may sometimes suggest a particular mechanism.

Table E1

Relationships Among Root Moments For Some Common Probability Distributions

NAME	FORM	MEAN μ	STD. DEV. σ	$_3\mu^{1/3}/\sigma$	$_4\mu^{1/4}/\sigma$
Exponential	$\exp(-(x-\alpha)/\beta)/\beta$	$\alpha+\beta$	$\mu-\alpha$	1.26	1.73
Gamma	$x^{p-1}\exp(-x)/\Gamma(p)$	p	$\sqrt{\mu}$	$1.26/\mu^{1/6}$	$(3+6/p)^{1/4}$
Normal	$\exp(-(x-\mu)^2/2\sigma^2)/\ 2\pi\sigma^2$	μ	σ	0	1.32
Rectangular	$1/h,\ 0<x<h$	$h/2$	0.58μ	0	1.16
Poisson	$\exp(-\mu)\mu^r/r!$	μ	$\sqrt{\mu}$	$1/\mu^{1/6}$	$(3+1/\mu)^{1/4}$
Laplace	$\exp(-\lvert x-\alpha\rvert/\beta)/2\beta$	α	1.41β	0	1.57
Rayleigh	$x\exp(-x^2/2\alpha^2)/\alpha^2$	1.25α	0.52μ	1.08	1.69

E.3 Estimating Moments

We shall be concerned with the estimation of a distribution's moments based on a finite random sample of size, N. We shall only be concerned with the estimation of central moments.[26] We define the sampling (central) moments by:

$$ {}_n m_x = \frac{1}{N} \sum_{i=1}^{N} (x_i - \bar{X})^n . \qquad (E.13) $$

The sampling moments are biased estimators of the parent distribution's moments. Therefore, sampling moments must be corrected especially for small sample sizes. This correction is most familiar for variance where sample size is replaced by degrees of freedom:

$$ \tilde{{}_2 m_x} = \frac{1}{N-1} \sum_{i=1}^{N} (x_i - \bar{X})^2 = \frac{N}{N-1} {}_2 m_x . \qquad (E.14) $$

By using tables after Wishart shown in Kendall and Stuart (1977), an unbiased estimator of the third central moment is:

$$ \tilde{{}_3 m_x} = \frac{N^2}{(N-1)(N-2)} {}_3 m_x \qquad (E.15) $$

and an unbiased estimator of the fourth central moment is:

---

[26] The original study used central moments. With hindsight, moments about the origin would have been computationally simpler.

$$\tilde{{}_4m_x} = \frac{N^2(N+1)+3N(N-1)}{(N-3)(N-2)(N-1)}\ {}_4m_x \qquad \text{(E.16)}$$

$$- \frac{3N(3-2N)}{(N-3)(N-2)(N-1)}\ {}_2m_x^2 \ .$$

Throughout our analyses we have used these unbiased estimators. Since we have been taking root moments, there is still some residual bias. However, this is small and also there does not seem to be a scheme for finding unbiased estimators of root moments.

E.4 Moments of the Sum of Two Random Variables

It is sometimes useful to be able to express the moments of a random variable in terms of the moments of other random variables. This is particularly useful if a random variable is the sum of two independent random variables. This situation occurs frequently when a random variable is perturbed by additive noise.

We consider a random variable, z, which is the sum of two independent random variables, x and y. We can then express the nth moment about the origin by taking the expectation of the random variable raised to the nth power:

$$E[z^n] = E[(x+y)^n]. \tag{E.17}$$

Expanding Equation E.17 and transforming all moments about the origin to central moments, we obtain the relationships:

$$\mu_z = \mu_x + \mu_y \tag{E.18}$$

$$\sigma_z^2 = \sigma_x^2 + \sigma_y^2$$

$${}_3\mu_z = {}_3\mu_x + {}_3\mu_y$$

$${}_4\mu_z = {}_4\mu_x + {}_4\mu_y + 6\sigma_x^2\sigma_y^2.$$

Note that only the first three central moments are purely additive.

E.5 Moments of the Product of Two Random Variables

We now consider the case where the random variable, z, is the product of two random variables, x and y. Providing x and y are independent, we can find moments about the origin again by taking expectations:

$$E[z^n] = E[x^n y^n] = E[x^n]E[y^n]. \tag{E.19}$$

Converting to central moments, we find:

$$\mu_z = \mu_x \mu_y \tag{E.20}$$

$$\sigma_z^2 = \sigma_x^2 \sigma_y^2 + \mu_x^2 \sigma_y^2 + \mu_y^2 \sigma 2$$

$${}_3\mu_z = {}_3\mu_x {}_3\mu_y + {}_3\mu_x Y[3\sigma_y^2 + Y^2] + {}_3\mu_y X[3\sigma_x^2 + X^2] + 6XY\sigma_x^2\sigma_y^2$$

$${}_4\mu_z = {}_4\mu_x {}_4\mu_y + [4_3\mu_y Y + 6Y^2\sigma_y^2 + Y^4] + 12XY {}_3\mu_x {}_3\mu_y$$
$$+ 6X^2Y^2\sigma_x^2\sigma_y^2 + 12XY^2 {}_3\mu_x\sigma_y^2 + 12YX^2 {}_3\mu_y\sigma_x^2.$$

E.6 References

Abramowitz, M., & Stegun, I.A. (1972). *Handbook of mathematical functions* (9th ed.). New York: Dover.

Kendall, Sir M., & Stuart, A. (1977). *The advanced theory of statistics* (Vol. 1, 4th ed.). New York: Macmillan.

Kendall, Sir M., & Stuart, A. (1979). *The advanced theory of statistics* (Vol. 2, 4th ed.). New York: Macmillan.

Appendix F

THE EXPONENTIAL WAITING-TIME DISTRIBUTION

F.1 Waiting-Time Distributions

We shall derive the Exponential distribution as a special case of the class of waiting-time distributions. To do this we consider a system to be initially in a particular unambiguous state (the oculomotor system in the state of "fixation"). We define the "termination rate", $\beta(t)$, such that, $\beta(t)\delta t$ is the probability that the state will terminate in the time interval $(t, t+\delta t)$ given that the state has not already terminated. Obviously, we assume that termination is also unambiguous ("saccade"). It follows from the definition of conditional probability that:

$$\beta(t) = f(t|x \geq t) = f(t)/[1-F(t)] \qquad (F.1)$$

where $F(t)$ is the probability function that the system will be in the state after time, t; and $f(t)$ is the corresponding probability density. Integrating Equation F.1:

$$\int_0^t \beta(x).dx = -\log[1 - F(t)] \qquad (F.2)$$

and putting F(0)=0:

$$F(t) = 1 - e^{-\int_0^t \beta(x).dx} \qquad (F.3)$$

and so

$$f(t) = \beta(t)e^{-\int_0^t \beta(x).dx} \qquad (F.4)$$

which defines the probability density of the class of so-called "waiting-time" distributions (see Papoulis, 1965). Waiting-time distributions are uniquely determined by the termination rate, $\beta(t)$. There are, therefore, an infinite number of waiting-time distributions depending on the functional form of the termination rate. The only restrictions on this function is that it be positive and tend to zero as time tends to infinity, because we assume that termination must occur with certainty at some finite time. The essential importance of waiting-time distributions is that it is the termination rate which defines the distribution, that is, the waiting-time is not the underly-

ing random variable but rather the consequence of the termination random variable.

F.2 The Exponential Distribution

The simplest distribution is for a constant termination rate, $\beta(t) = \lambda$. From Equation F.4, the waiting-time distribution becomes the Exponential:

$$f(t) = \lambda e^{-\lambda t}. \qquad (F.5)$$

The constant termination rate means that the probability per unit time of a temination event remains the same throughout time. Since the termination rate is constant, the Exponential is the only waiting-time distribution that has no "memory." Conversely, any other termination rate requires that the system "knows" where it is in time, and must have memory. In this respect, the Exponential is an important and basic waiting-time distribution. The Exponential distribution is also used as a reference distribution. Waiting-time distributions whose termination rates increase in time are more dispersive than the Exponential and are called "hyperexponential", while those distributions whose termination rates decrease in time are called "hypoexponential" because they are less dispersive than the Exponential.

F.3 Moments of the Exponential Distribution

From Equation F.4, it can be seen that the modal waiting-time is zero. In many physical and biological processes there is a refractory

period during which a termination cannot occur. This creates a minimum waiting-time, and it may occur because of some initial preparation time or a period to instigate the termination event, etc.. Under these circumstances, the Exponential distribution is generalised to include a location parameter, A:

$$f(t) = \lambda e^{-\lambda(t-A)}. \qquad (F.6)$$

The first four moments about the origin can be found easily to be:

$$\begin{aligned} \mu_t &= A + 1/\lambda \\ {}'_2\mu_t &= A + 2/\lambda^2 \\ {}'_3\mu_t &= A + 6/\lambda^3 \\ {}'_4\mu_t &= A + 24/\lambda^4. \end{aligned} \qquad (F.7)$$

The central moments can then be found:

$$\begin{aligned} \sigma_t^2 &= 1/\lambda^2 \\ {}_3\mu_t &= 2/\lambda^3 \\ {}_4\mu_t &= 9/\lambda^4 \end{aligned} \qquad (F.8)$$

which, of course, are independent of the location parameter. We can

also find the root moments and relate them by:

$$\sigma_t = \mu_t - A \qquad \text{(F.9)}$$

$$\sqrt[3]{\mu_t} = 2^{\frac{1}{3}}\sigma \simeq 1.26\sigma$$

$$\sqrt[4]{\mu_t} = 9^{\frac{1}{4}}\sigma \simeq 1.73\sigma.$$

If we have a collection of Exponential processes with different termination rates but the same location parameter we can plot root moments to show the relationships in Equations F.9. Thus, if the standard deviation is plotted against the mean, we will find a linear trend with unity slope and intercept, -A. Plots of the third and fourth root moments against the standard deviation will also be linear with slopes of 1.26 and 1.73 and zero intercepts.

Other waiting-time distributions will have different slopes (or may not even be linear). Hyperexponential distributions will have higher slopes, and hypoexponential distributions will have lower slopes than the Exponential distribution.

F.4 Compound Exponential Distributions

In practice, if we wish to identify a distribution, we need a sample of observations from which to estimate the moments of the parent distribution. For waiting-time distributions this usually entails taking samples at different times. This raises the possibility that the termination rate may not remain precisely the same from one observa-

tion to the next; either because of random fluctuations, or because of systematic changes (non-stationarity). More specifically for the Exponential distribution, the termination rate may be at one constant value for one observation and at a different constant value for the next observation. Changes in the termination rate will always add more (never less) to the variance and to the higher moments of the Exponential, and so the resulting distribution will appear hyperexponential even though each observation is purely Exponential. The resulting distribution is a compound Exponential and it will depend on the distribution of the fluctuations (the compounding distribution) of the termination rate. Denoting this compounding distribution by $g(\lambda)$, the compound Exponential, $\tilde{f}(t)$, is given by the conditional distribution:

$$\tilde{f}(t) = \int_0^\infty \lambda e^{-\lambda(t-A)} g(\lambda).d\lambda. \qquad (F.10)$$

The moments about the origin of the compound Exponential are then generically given by:

$$\tilde{{}'_n\mu_t} = \int_0^\infty n\lambda^{-n} g(\lambda).d\lambda. \qquad (F.11)$$

By comparing Equation F.11 to Equation F.7, it can be seen that these moments are always greater than the moments for the exponential for any compounding distribution, $g(\lambda)$, which has non-zero variance.

A closed form for the compound Exponential only exists for a few

special cases of the compounding distribution. We will show this for the Gamma compounding distribution and the Rectangular compounding distribution.

The Gamma-Exponential Compound

We consider the compounding distribution to be the Gamma distribution:

$$g(\lambda) = [\gamma\Gamma(p)]^{-1}[\lambda/\gamma]^{p-1}e^{-\lambda/\gamma} \qquad (F.12)$$

where p is the index parameter of the Gamma distribution. The compound Exponential then becomes:

$$\tilde{f}(t) = \gamma p/(\gamma t+1)^{p+1} \qquad (F.13)$$

(This distribution is sometimes called the "Pareto", see Cox and Oakes, 1984). The moments about the origin can be found:

$$\tilde{\mu}_t = 1/[\gamma(p-1)] \qquad (F.14)$$

$$\tilde{\mu}_t' = 2/[\gamma^2(p-2)(p-1)]$$

$$\tilde{\mu}_t' = 6/[\gamma^3(p-3)(p-2)(p-1)]$$

$$\tilde{\mu}_t' = 24/[\gamma^4(p-4)(p-3)(p-2)(p-1)] .$$

The central moments can be found (somewhat tediously) but will not be shown here.

The Rectangular-Exponential Compound

We now consider the compounding distribution to be the Rectangular distribution:

$$g(\lambda) = \begin{cases} 1/(b-a), & a \le \lambda \le b \\ 0, & a > \lambda > b \end{cases}, \quad b > a. \tag{F.15}$$

In this case, the compound Exponential becomes:

$$f(t) = [(at+1)e^{-at} - (bt+1)e^{-bt}]/[(b-a)t^2] \tag{F.16}$$

and the moments about the origin can be found:

$$\tilde{\mu}_t = \log(b/a)/(b-a) \tag{F.17}$$

$$\tilde{{}_2\mu}_t = 2/(ab)$$

$$\tilde{{}_3\mu}_t = 4(a+b)/(a^2b^2)$$

$$\tilde{{}_4\mu}_t = b(a^{-3} - b^{-3})/(b-a).$$

From these moments the central moments can be calculated.

The central moments of both these compound distributions have been calulated and their relationships are briefly summarised in Table 1 in Section 4.

F.5 References

Cox, D.R. & Oakes, D. (1984). *Analysis of survival data.* New York: Chapman & Hall.

Papoulis, A. (1965). *Probability, random variables, and stochastic processes.* New York: McGraw-Hill.

Appendix G

STATISTICS OF VECTOR MAGNITUDE

The magnitude or radial component of a two-dimensional Cartesian vector is given by:

$$r = (x^2 + y^2)^{\frac{1}{2}}. \qquad (G.1)$$

The problem to be considered here is the statistical relationship between the radial component, r, and the Cartesian components, x and y, when these components are random variables. In the special case where x and y are independent Normal random variables with zero means and equal variances, the probability distribution of r can be found exactly and is the so-called Rayleigh distribution (e.g., Papoulis, 1965). However, for almost all other distributions for x and y, there is no closed form for the distribution of r. We will therefore find an approximation for the mean and variance of r in terms of the central moments of x and y by series expansion.

First we define two new random variables, U and V by:

$$U = x^2, \quad V = y^2. \tag{G.2}$$

Substituting into Equation G.1 and performing a two dimensional Taylor expansion of r about the means of U and V, (U,V) we obtain:

$$r = (U+V)^{\frac{1}{2}} - [\sigma_u^2 + \sigma_v^2 + \rho_{uv}\sigma_u\sigma_v]/[8(U+V)^{3/2}] + \ldots \tag{G.3}$$

and

$$\sigma_r^2 = [\sigma_u^2 + \sigma_v^2 + 2\rho_{uv}]/[4(U+V)] + \ldots \tag{G.4}$$

These radial moments are approximated by retaining only first and second order moments. If we then make the simplifying asumptions that x and y are independent with zero means:

$$U = \sigma_x^2, \quad V = \sigma_y^2 \tag{G.5}$$

and

$$\sigma_u^2 = {}_4\mu_x - \sigma_x^4, \quad \sigma_v^2 = {}_4\mu_y - \sigma_y^4, \quad \rho_{uv} = 0. \tag{G.6}$$

Expressing the mean and variance of the magnitude vector in standardised moments:

$$r \approx (\sigma_x^2 + \sigma_y^2)^{\frac{1}{2}} - [\sigma_x^4({}_4\gamma_x - 1) + \sigma_y^4({}_4\gamma_y - 1)]/[8(\sigma_x^2 + \sigma_y^2)^{3/2}] \qquad (G.7)$$

$$\sigma_r^2 \approx [\sigma_x^4({}_4\gamma_x - 1) + \sigma_y^4({}_4\gamma_y - 1)]/[4(\sigma_x^2 + \sigma_y^2)]. \qquad (G.8)$$

These relationships can be more easily seen if x and y have equal variance, σ^2, and kurtosis, ${}_4\gamma$:

$$r \approx \sqrt{2}\ (17 - {}_4\gamma)\sigma/16 \qquad (G.9)$$

and

$$\sigma_r^2 \approx ({}_4\gamma - 1)\sigma^2/4. \qquad (G.10)$$

Thus, the mean of the vector magnitude is roughly proportional to the standard deviation of the Cartesian components and is only weakly dependent on the kurtosis of the components. The variance of vector magnitude is much more sensitive to the kurtosis (or distribution form) of the Cartesian components. If each Cartesian component is perturbed by additive noise with zero mean and variance, σ_n^2, the apparent mean vector magnitude will be approximately:

$$r^2 \simeq \sigma_x^2 + \sigma_y^2 + 2\sigma_n^2. \qquad \text{(G.11)}$$

Here we have dropped higher order interactions between the noise and signal moments. Although this is only approximate, it does allow a reasonable estimate of a vector magnitude to be recovered.

G.1 References

Papoulis, A. (1965). *Probability, random variables, and stochastic processes*. New York: McGraw-Hill.

Appendix H

CHARACTERISTICS OF SACCADES IN HUMAN INFANTS

(Reprinted by permission of Pergamon Press, Ltd.)

LOUISE HAINLINE, JOSEPH TURKEL, ISRAEL ABRAMOV, ELIZABETH LEMERISE and CHRISTOPHER M. HARRIS
Department of Psychology, Brooklyn College of CUNY, Brooklyn, NY 11210, U.S.A.

(*Received* 30 *August* 1983; *in revised form* 6 *July* 1984)

Abstract—Infants (14–151 days) and adults were shown two-dimensional geometric forms or stimuli from a set of highly textured patterns. Their eye movements were recorded by an infrared corneal reflection eye movement recorder as they freely scanned the stimuli. For both infants and adults, linear relationships were found between the peak velocities of fast eye movements and their amplitudes (main sequences). Infants viewing texture stimuli had main sequences with slopes comparable to those of adults. Infants viewing simple geometric forms made slower saccades. They also showed more eye movement oscillations which analyses showed were probably back-to-back saccades. Both the slower saccades and saccadic oscillations were attributed to factors related to the attentional value of the stimuli.

INTRODUCTION

Although the properties of the adult saccadic system have been extensively studied (e.g. Yarbus, 1967; Carpenter, 1977; Robinson, 1981; Young, 1981), little research has been directed at how the oculomotor system develops the ability to execute saccades. Compared with the young of other species, the general level of neurological and motoric development of the human infant might preclude finely controlled rapid motor behaviors such as well-executed saccades. Studies of smooth pursuit (Aslin, 1981) and of optokinetic nystagmus (Atkinson and Braddick, 1981; Naegele and Held, 1982; Hainline *et al.*, 1984) support the general view that human infants have immature oculomotor systems. Furthermore, since saccades, particularly those accompanied by head movements, are generally seen as attempts to foveate some visual detail (Robinson, 1964), one might predict that the marked immaturity of the human fovea at birth (Abramov *et al.*, 1982; Hollyfield *et al.*, 1983) would also adversely affect saccades.

In a saccade, the eye is initially accelerated very rapidly to a peak velocity; the acceleration is due to the muscular effect of a burst of neural signals in the motorneurons of the pontine reticular formation; other brain stem motorneurons are responsible for the eye's more gradual deceleration (see, e.g. Robinson, 1981). The peak velocity of the eye during the saccade depends on the height and width of the neural pulse associated with the beginning of the saccade. Both pulse height and width increase with amplitude, up to a saturation amplitude of about 15 deg for human adults (Westheimer, 1954; Boghen *et al.*, 1974; Bahill *et al.*, 1975). The tight relationships which exist between saccadic peak velocity, saccade amplitude, and duration have been termed "main sequences" (Bahill *et al.*, 1975). Thus, evaluation of the nature of saccadic control in a target population (e.g. human infants), can be carried out by comparing their main sequences to those of normal adults (see, e.g. Hamann, 1979; Howard, 1982, p. 262).

Because of procedural limitations imposed by the use of uncalibrated EOG and low bandwidth corneal reflection techniques, previous studies of infants' fast eye movements (see Salapatek, 1975) have not analyzed the velocity parameters of the movements, or systematically compared the movements with those of adults. Dayton and Jones (1964) analyzed EOG recordings of movements which may have been saccades, from one 35-day-old subject, and failed to find an amplitude/velocity relationship, although average, rather than peak, velocity was considered. We present here a quantitative analysis of fast infant eye movements, in part to determine if their velocities are in fact saccadic in nature. For comparison, we also recorded saccades from adults in the same situation. Eye movements were measured while the subjects freely scanned visual stimuli presented for relatively long periods; this situation is less demanding for the infant than the paradigm more commonly used to study saccades in adults, in which saccades are elicited by small targets presented briefly at different positions in the visual field.

METHODS

Apparatus

Eye movements of infants and adults were recorded with a computer-controlled video system,

Vision Res. Vol. 24, No. 12, pp. 1771–1780, 1984

using infrared corneal reflection (Hainline, 1981). The system is shown schematically in Fig. 1.

Adults' heads were stabilized by a chin rest. Infants were held by an experimenter whose back was to the display. The infant looked over the experimenter's shoulder while the experimenter stabilized the infant's head by firmly pressing it against the experimenter's cheek and neck. Except for the most active infants, head motion could be restricted successfully. The small field of view of the camera effectively controlled for large head movements, since no data could be collected if the eye moved more than about a degree from the central position in the camera's field. Internal head movement circuitry in the eye tracker largely compensated for smaller head movements. T.V. monitors, showing the infant's face and eyes, provided the feedback the experimenter needed to keep the head upright, stable, and in the correct position. The system is based on an Applied Science Laboratories Model 1994 Eye View Monitor which we have modified for working with infants. The eye movement computer provided digital information on horizontal and vertical eye position at a 60 Hz rate. These data were fed into a larger, on-line computer (Digital Equipment Corp., PDP 8/e) which provided mass storage and stimulus control. The system estimates eye position from the relative locations of the subject's pupil and the corneal reflection of the infrared light source. As their eye movements were recorded, subjects viewed stimuli presented on a rear-projection screen; under these conditions, adult subjects could not see the infrared source and reported that the rest of the recording system was unobtrusive.

Calibration

The accuracy of the eye-monitoring system can be separated into two components: dynamic accuracy (correct reproduction of eye velocities) and positional accuracy (correct specification of where on the stimulus the eye is pointed). We have devised a spatial calibration procedure for use with infants which results in a correction polynomial that can be used to map eye position onto the stimulus plane correctly (Harris *et al.*, 1981). In most cases, the biggest correction is an additive offset term due to the fact that the eye is not necessarily on the optic axis of the eye monitor. Such a correction is not critical for this paper, since we are not relating the eye movements to specific features or regions of any stimulus. A second correction term is an over-all scale factor due to variations among subjects in the optical parameters of the eye; this correction can affect estimates of eye movement amplitude. In most cases, higher order correction terms are negligible.

For our type of system, the average positional calibrations are the same for groups of adults and groups of infants. The relevant optical parameters for corneal reflection systems are the radius of curvature of the corneal pole and the distance from the corneal pole to the plane of the entrance pupil (Young and Sheena, 1975). Changes in these factors during growth (Larsen, 1971; Mandell, 1976) are largely offset by each other (Bronson, 1982). With respect to measures of amplitude then, although there is individual variability in the most appropriate calibration settings for each subject, the measured amplitudes from infant and adult subjects are on the average close to actual amplitudes. More importantly, they

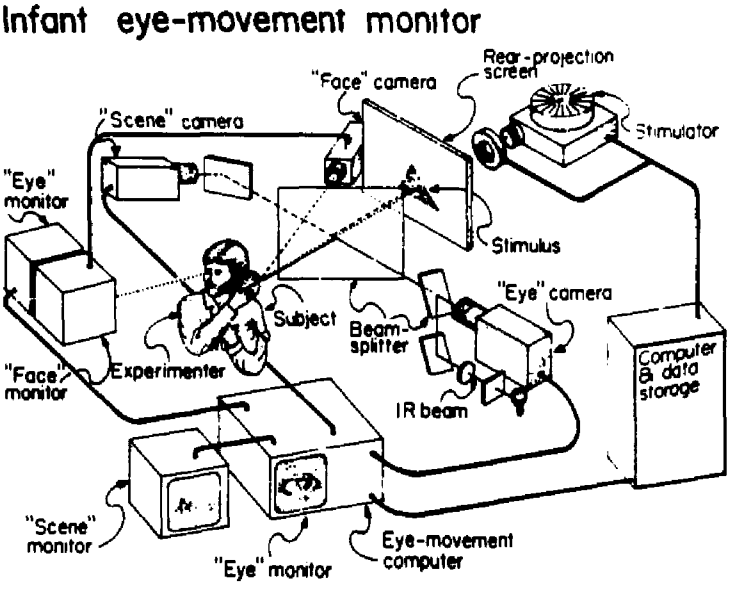

Fig. 1. A schematic representation of an eye movement recording system designed for use with infants.

can be directly compared across the age groups. Since the calibration procedure is lengthy and requires a very cooperative subject, it was not possible to use it on all of the subjects in this study. In order to keep the data from all subjects comparable, we analyzed data from both infants and adults using the same average calibration scale factor for all subjects. Given that individual calibrations have not been performed, our measures of velocity and amplitude should be viewed as relative, rather than absolute, measures. This does not present a major problem to the most important analyses at issue here. Many of our analyses are of the slopes of main sequences; since these functions relate peak velocity (the maximum amplitude moved per sample interval) and amplitude, any residual errors in estimates of amplitude will appear equally on both sides of the equation, and therefore will not contaminate the slope.

A television-based system for tracking eye movements has relatively low bandwidth, and thus is not ideal for velocity measurements. However, methods with higher bandwidths (see, e.g. Young and Sheena, 1975) are usually intrusive and difficult to use with infants. To obtain corrections for eye velocities as measured by our system, we used an artificial eye rotated at various velocities through a series of "saccades" of different amplitudes (Harris *et al.*, 1984). Each known input to the eye tracker was repeated many times and the corresponding outputs were averaged; these averages were used to create nomograms for correcting measured peak velocities. When we apply these corrections to peak velocities of the fast eye movements of our adult subjects, we obtain values close to those reported in the adult eye movement literature. However, because of the relatively low sampling rate of a T.V. system, there is an inherently large error in specifying the start and end of an eye movement; we have no straightforward method for correcting the data for this error. We are therefore not reporting measures of duration.

Stimuli

Stimuli were rear-projected on a screen viewed from a distance of 50 cm; the screen subtended approximately 45 deg horizontally and vertically. The stimuli projected were of two types: (i) simple black and white geometric forms (circles, squares and triangles) ranging in size from 5 to 30 deg (Hainline and Lemerise, 1982); (ii) textures consisting of black and white gradients of lines, and patterns created from juxtaposed checkerboards of different check sizes (e.g. see Gibson, 1950); the textures filled the whole viewing screen. The average luminance of the stimuli in each of the sets was approximately the same (about 10 cd/m^2). Stimulus presentation was under computer control. The set of form stimuli consisted of six different forms which were shown one at a time. The texture set contained five different patterns, also shown one at a time. Each stimulus was viewed for 10 sec, with a 5 sec interstimulus interval; eye movement data were stored only for the stimulus periods. Infants viewed either the form stimuli or the texture stimuli, but adult subjects were shown all of the stimuli in the two sets. Instructions to adults were simply to "look at the stimuli".

Subjects

Data were obtained from 64 infants (ages 14–151 days) and from 11 adult subjects (ages 18–36 years). Infant subjects were all healthy and full term; they were located through contacts with hospitals and physicians. Adult subjects were faculty, students, and research assistants.

Data analysis

The data for each stimulus period were initially screened for noise; bad data were usually caused by head movements or blinks, so that a clear image of the eye could not be maintained. The eye movement record was then scored with an interactive computer procedure which displayed the horizontal and vertical eye positions vs time on a CRT screen. An observer manipulated a set of cursors on the screen to select portions of the record judged to be eye movements. Essentially, these included all parts of a record not judged to be fixations or noise. All of the data from any given subject were scored by one person, to maintain consistent standards, but frequent checks on inter-rater reliability revealed very high agreement. After the observer determined the portion of the record to be analyzed, the computer calculated movement amplitude, instantaneous and peak velocities. All of the movements analyzed had discriminable peaks in their velocity profiles. In order to eliminate the influence of small-amplitude artifacts in the records, movements with amplitudes less than 2 deg or with extremely noisy velocity profiles were excluded from further analysis. Over 75% of the infant and 90% of the adult fast eye movements were retained for further analysis by standard statistical packages (BMDP; Dixon, 1981).

RESULTS

Description of infant eye movements

A total of 1248 infant and 1224 adult eye movements were analyzed. Examples of some of these eye movements are presented in Fig. 2, which shows eye position vs time for horizontal and vertical eye movement components. As illustrated in Fig. 2(a), (b), and (c), many infant eye movements look like adult saccades [Fig. 2(f)]. Horizontal and oblique movements [Fig. 2(a) and (c)] were the most frequent type observed in both infant and adult subjects, although vertical [Fig. 2(b)] movements were also observed at all ages.

Infants also made some eye movements which did not resemble those of normal adults. Under some conditions, infants' saccades did not attain "normal"

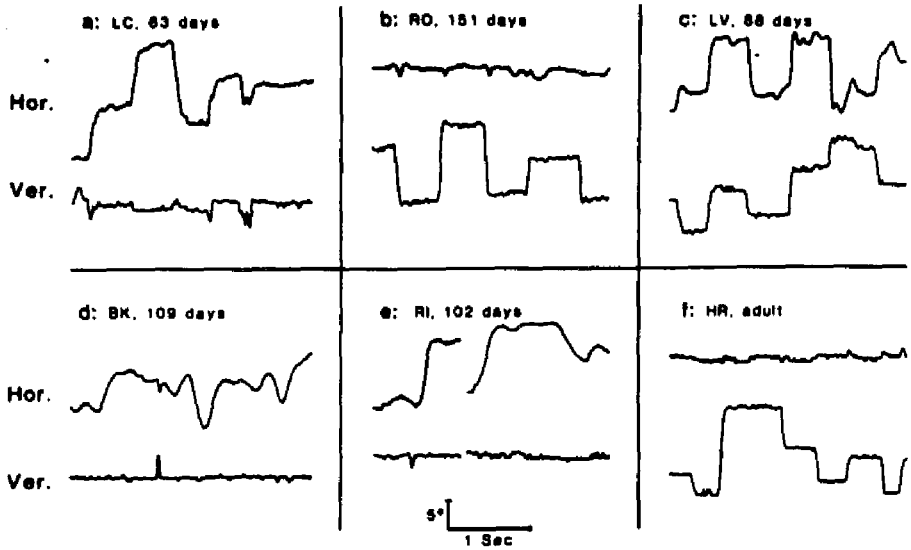

Fig. 2. Examples of fast eye movements of infants and adults. The top trace in each set is horizontal eye position and the bottom trace is vertical eye position, each plotted vs time. Examples show: (a) horizontal movements from a 63-day-old infant; (b) vertical movements from a 151-day-old infant; (c) oblique movements from an 88-day-old infant; (d) fast oscillations from a 109-day-old infant; (e) fast and slow "saccades" from a 102-day-old infant; (f) vertical saccades from an adult.

adult velocities, although they were otherwise regular in form. For example, Fig. 2(e) shows several saccades; except for the first, they are considerably slower than either adult saccades or other infant saccades of similar amplitudes [Fig. 2(f), and 2(a), (b), and (c)]. Figure 2(d) illustrates another example of an unusual infant eye movement characteristic, which was quite prominent in our data: several movements in opposite directions with very brief inter-movement intervals. Ordinarily for adults, successive saccades are separated by a minimum inter-saccadic interval of 200–250 msec (Carpenter, 1977; Vaughan, 1983), although for very large saccades or for corrective saccades (Becker and Jurgens, 1979), the next movement may be executed with reduced latency. However, in a high proportion of cases with our infants (about 38% of all fast eye movements), we see successive eye movements which occur much closer together than the canonical quarter second, with inter-saccadic intervals of 50 msec or less. These movements were often of equal amplitude, and were frequently large (5 or 10 deg). They usually occurred in groups of two or three, and were episodic rather than characteristic of an entire period's data or an entire infant's record. These oscillations were only seen in infant records. Not all infants showed oscillations, although most showed a few episodes at some time in the experiment. The oscillations did not reflect a total inability to maintain a steady fixation, and it is worth noting that infants were capable of holding their eyes steady in fixations of a half second or more [e.g. see Fig. 2(a), (b), and (c)].

For our infant subjects, the nonoscillating movements (which, for preliminary discussion, we will describe as "saccades") were 43% horizontal, 17% vertical, and 40% oblique. The oscillations were more likely to be horizontal and oblique; 66% of the oscillations were horizontal, 4% vertical and 30% oblique. Fewer than 5% of the infant eye movements showed a pattern of multiple saccades in the same direction. This pattern of "staircase" movements is superficially similar to the series of equal-sized hypometric "steps" described in previous research on infant saccades elicited by small flashing targets (Aslin and Salapatek, 1975; Salapatek *et al.*, 1980). However, the pause times between the steps that we measured (100 msec or less) were much briefer than the long inter-movement intervals of 500 msec or more reported by Salapatek, *et al.* (1980).

Quantitative analysis

If the main sequences of infants' movements have values like those of the adults, it would be strong evidence that infants' fast eye movements are saccades. In order to test whether any infant eye movements were saccadic, we initially treated their two types of fast movements ("saccades" and oscillations) separately. We plotted individual main sequences of peak velocity vs amplitude for each adult and infant subject, and tested whether a linear regression significantly fit the data ($P < 0.05$). In order to obtain a valid main sequence function for any given subject, we needed a reasonable number of eye movements across a range of amplitudes. Thus, we excluded from

this analysis subjects from whom we recorded no eye movements greater than 5 deg and from whom we did not have at least 10 eye movements within either of the oscillation or "saccade" categories; this criterion meant that in individual cases, there might have been fewer than 10 samples of a particular type of movement for a given subject. All the 11 adults met the criteria for range, number of eye movements and significance of the main sequence regressions. Of the infants, 19 (7 one-month olds, 4 two-month olds, 3 three-month olds and 1 five-month old) were excluded for having too few eye movements. Another 4 (1 one-month old and 3 two-month olds) were excluded for having eye movements with an insufficient range of amplitudes. Of subjects meeting our criteria, another 2 (1 each at two- and three-months) were excluded because their main sequence regressions for both "saccades" and oscillations were not significant. This selection process left us with data from a total of 39 infants ranging in age from 14 to 151 days. Because we were recording spontaneously occurring eye movements during fixed viewing periods, we did not collect equal numbers of eye movements from each infant, nor could we insure that a particular infant would show us the pattern we have described as oscillations.

Main sequences for a typical adult and four representative infants are shown in Fig. 3. The left ordinates show uncalibrated peak velocities as measured directly from the digital output of the eye tracker. The right ordinate in each panel shows peak velocity corrected from the peak velocity calibration nomograms (see above). To minimize the effects of noise, the corrections were applied to the main sequence regression lines, rather than to the individual saccades. Subsequent analyses are based on the corrected main sequence slopes. The non-zero intercept for the uncorrected data is due to the nonlinear effect of baseline noise on measures of peak velocity (Harris *et al.*, 1984). Figure 3(a) shows results from an adult, and Fig. 3(b) and (c) show infant main sequences for "saccades" and oscillations; all were viewing textures. For textures, the mean slope for all adults was 26.0 with a standard error (SE) of 5.4; the mean infant slope for "saccades" was 25.7 (SE = 8.1) and for oscillations, the mean infant slope was 29.6 (SE = 7.1). While the main sequences of adults viewing textures or forms were substantially the same, there was a marked effect of stimulus type on infants' main sequences; slopes of the main sequences were significantly lower when infants viewed forms. Examples of "saccades" and oscillations for infants viewing forms are shown in Fig. 3(d) and (e). The mean slope for adults viewing forms was 22.6 (SE = 1.9); the mean slope for infants' "saccades" to the form stimuli was 14.2 (SE = 1.5), and for oscillations to form stimuli, the mean slope was 12.1 (SE = 4.1). All the mean slopes are shown in Fig. 3(f). To test the "goodness" of the linear fit of the main sequences, we used Fisher's $Z(r)$ transform (Ferguson, 1971) on the correlation coefficient for each individual main sequence. Adults had significantly higher correlations (mean $r = 0.85$) than infants (mean $r = 0.76$), indicating that the infants' data were more variable. The correlation coefficients did not differ significantly between stimulus types for infants or adults, or between movement types for infants.

Comparisons between infants' oscillations and "saccades"

It can be seen from Fig. 3, that for a given stimulus type, infant oscillations and "saccades" are similar in their main sequence slopes. To support this observation, the data from a subset of 21 infants who had significant main sequence functions for both oscillations and "saccades" were subjected to a repeated-measures analysis of variance; movement type (oscillation or "saccade") was a within-subject variable and stimulus type (texture or form) was a between-subject variable. There were no significant differences between the two movement types in the slope of the main sequence function. Oscillations and "saccades" were also not significantly different in mean amplitude or in distribution of amplitudes. Thus, despite the fact that their inter-movement intervals were distinctly non-adult-like, we found no other quantitative data to indicate that oscillations were not "saccades", and so in most subsequent analyses, both types of fast movements (oscillations and "saccades") were combined into a single category.

Effects of stimulus on infant saccades

The stimulus being viewed had a strong effect on the slope of the infants' main sequences. Their main sequence slopes were significantly lower for the form stimuli than for the texture stimuli. This difference was found for both the combined saccade category, and for the sub-types of "saccades" and oscillations considered separately. The stimulus effect was found both in the repeated-measures analyses on the subset of 21 infants, and on the full data set. The magnitude of this stimulus effect is illustrated in Fig. 3(f). Although there was no significant difference in the frequency of eye movements (the number of eye movements per second of scoreable data) between the stimulus types, there was a higher percentage of usable data for textures than for forms. This suggests that infants may have paid more attention to the texture stimuli. For adults, there were no differences in saccade parameters depending on whether forms or textures were the stimuli.

In the analyses of variance, there was a single significant movement-type by stimulus interaction; infants made fewer oscillations than "saccades" to texture stimuli, and more oscillations than "saccades" to form stimuli. Either the highly patterned texture stimuli caused a suppression of oscillations, or alternatively, the geometric forms may have been particularly good elicitors of oscillations.

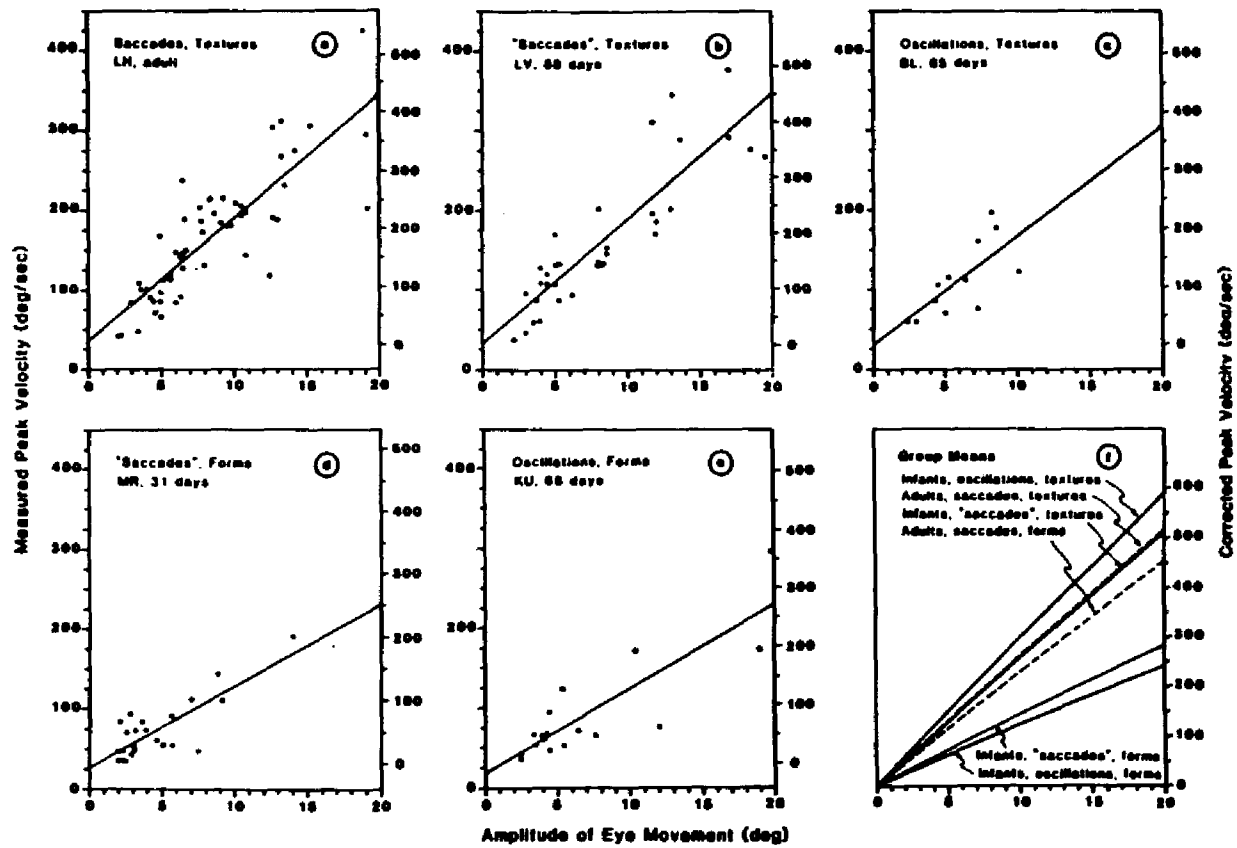

Fig. 3. Examples of typical main sequences for peak velocity vs amplitude of eye movement. The left ordinate shows measured, uncorrected values for peak velocity. The right ordinate shows corrected peak velocities for each individual's main sequence (see text). The solid lines are the result of a linear regression fit to the data. (a) Adult subject, texture stimuli; corrected slope is 21.6, $r = 0.85$. (b) 88-day-old infant, texture stimuli, "saccades" (nonoscillatory fast movements); corrected slope is 22.3 $r = 0.88$. (c) 65-day-old infant, texture stimuli, oscillations; corrected slope is 18.8, $r = 0.71$. (d) 31-day-old infant, form stimuli, "saccades"; corrected slope is 12.3, $r = 0.81$. (e) 68-day-old infant, form stimuli, oscillations; corrected slope is 12.8, $r = 0.85$. (f) Average main sequences for infant and adult subjects, plotted separately for form and textures. Infant curves are also shown separately for "saccades" and oscillations.

Comparisons of infant and adult saccades

For direct comparisons between infants and adults, one-way analyses of variance between the age groups for a particular stimulus type were performed; since adults were more cooperative subjects, for them stimulus type could be a within-subject factor, while it was a between-subject factor for infants. For the texture stimuli, there were no significant differences between infants and adults in the slope of the saccade main sequence function. However, when the stimuli were simple geometric forms, the main sequences of infants' saccades had significantly lower slopes than those of adults. The means and distributions of amplitudes were similar between infants and adults for both form and texture stimuli.

Developmental trends in infant saccades

To investigate developmental trends during infancy, regressions over age and analyses of variance with age as a factor were done. For neither stimulus set was there a change in infants' main sequence slopes with age. Infant eye movements did not become faster with age. There was, however, a significant decrease in the frequency of oscillations over age (25–151 days) for the texture stimuli. Oscillations were more frequent for the form stimuli, and their frequency did not show a significant decrease over the range of infant ages included here (14–123 days).

DISCUSSION

The major conclusion of the present work is that, under some conditions, infants make mature saccades. Using data from infants as young as several weeks who freely scanned visual patterns, we noted the absence of tremor or long episodes of apparently "out of control" movements reported in neonates (Haith, 1980). Fixations were often stable. Although we cannot specify precisely at what target the infants were "aiming" their eyes, we found that they could execute saccades whose mean amplitude was similar to that of adults. Their saccades showed regular main sequences. If we use adult main sequences as a standard, a significant proportion of infant saccades for some stimuli were mature in their execution.

We found two unusual properties of infant saccades, oscillations and slow saccades, whose incidence was strongly related to the type of stimulus infants were viewing. Because the oscillations were usually of approximately equal amplitude, they do not appear to be overshoots or small corrective saccades, in which the "return" is a fraction of the original movement's amplitude. They may be similar to the macro square wave jerks described in a clinical patient with a fixational disorder attributed to a cerebellar disfunction (Dell'Osso *et al.*, 1975). However, our infants showed many episodes of stable fixation in all regions of their visual field, and their oscillations, unlike those of the Dell'Osso *et al.*, patient, were not exclusively in the horizontal orientation. The infants' oscillations are too large and too fast to be vergence movements, which also do not typically show a reversal of direction. Because they did not have two distinct phases, but rather were fast movements in both directions, oscillations differed from classical bi-phasic nystagmus, though they may be similar to the spontaneous "nystagmus" which some adults can voluntarily trigger and in which the individual appears to be producing "back to back" saccades (Stark *et al.*, 1981). Bienfang (1974) and Hoyt and colleagues (Hoyt, 1977; Hoyt *et al.*, 1980) have observed a pattern of back and forth eye movements in young infants which was classified as opsoclonus, sometimes called ocular flutter, an eye movement disorder indicative of brain damage if observed in an adult (Zee and Robinson, 1979). Hoyt *et al.* (1980) comment on the intermittent nature of the opsoclonus they observed and mention that it seemed most noticeable just before feeding and sleeping; these observations imply a relationship to behavioral state. The so-called opsoclonus previously reported in infants may be the pattern we have called oscillation, which appears to be a normal occasional phenomenon in young infants and therefore unlikely to be related to brain damage.

Slow saccades have also been reported to appear in adults with cerebellar lesions (Zee *et al.*, 1976). Although the cerebellum develops markedly over the first year (Peiper, 1963), infants are not equivalent to adults with cerebellar disorders, since slow saccades tend to occur only in response to particular stimuli. Although there may be some development, the saccadic system appears to be one of the first finely controlled motor systems in humans.

We must deal with the possibility that the slow saccades are artifacts such as head movements or vergence movements. While head and vergence movements may be represented with some small frequency in the movements studied here, they cannot be the explanation for the slow saccades. Large head movements cannot be a part of the data base, because the head could not move more than one or two degrees without the eye leaving the camera's field of view. Smaller head movements that were not compensated for by the instrument would be likely to be excluded because of the amplitude cut-off of 2 deg that we imposed on the data. The slow saccades are probably not vergence movements either; although they were slow as saccades, they were faster than normal vergences. The average peak velocity for a ten degree "normal" saccade from infants or adults in our apparatus was on the order of 250–300 deg/sec, and that for a 10 deg "slow" saccade about 130 deg/sec. This is still significantly faster than a 10 deg vergence movement, which should have a peak velocity of considerably less than 100 deg/sec (Stark, 1983). Also, slow saccades were observed to the form stimuli only. Because the correlation coefficients of the linear

fits for the main sequences for forms (which elicited slow saccades) were comparable to those for textures (which did not), the main sequences in each case appear to have been derived largely from a single population of movements. If the slow saccades were actually vergences, we would need explanations both of why infants make faster vergence movements than adults, and why they never make saccades when viewing a particular type of stimulus. Our explanation that the movements in question are saccades slowed because of reduced arousal is more parsimonious, and consistent with the existing data on the effects of reduced arousal on saccades.

Rather than being permanent characteristics of the infant system, or some artifact of recording, we feel that the oscillations and slow saccades are the result of lapses in attention or changes in levels of arousal. It is well-documented that grosser measures of infant attention and arousal like "total looking time" are related to dimensions of the stimulus such as the number of elements or the amount of contour (e.g. Karmel, 1969; Kessen *et al.*, 1972); some of these effects are probably mediated by brain stem mechanisms (Bronson, 1974). In adult humans, drugs, fatigue, and inattention can lower main sequence slopes (Aschoff, 1968; Becker and Fuchs, 1969; Bahill and Stark, 1975; Abel *et al.*, 1983) to an extent similar to the difference we have observed here between stimulus types for infants. There are also data from cat and monkey linking main sequence slopes to state of arousal (Ron *et al.*, 1972; Crommelinck and Roucoux, 1975). Both the higher main sequence slopes and the higher proportion of usable data for the texture stimuli support the idea that infants were more aroused by the highly patterned texture stimuli than they were by the simpler geometric forms. Oscillations were also less frequent for textures. Lowered arousal could result in oscillations if lapses in attention can interfere with the temporal coordination of the burst and pause neurons activated during the saccade: the failure of this coordination can cause the eyes to oscillate back and forth (Dell'Osso and Daroff, 1981). Brief fluctuations in level of arousal during the experimental session may also explain the greater variability that we sometimes observed in our infants' data compared to the adult data (Ron *et al.*, 1972; Abel *et al.*, 1983). It is interesting to note that both the regular velocity-amplitude relationships, as well as the existence of slow saccades and oscillations, are all entirely compatible with Robinson's (1981) local feedback model of saccadic control. In that model, a reduction in the ability of pause neurons to inhibit the signal triggering a saccade can lead to a series of back-and-forth saccades, and simply lowering the slope and amplitude of the function determining the firing of the burst neurons (due to reduced reticular arousal) can produce slow saccades. Thus the properties of the infant saccades reported here are compatible with a mature infant saccadic generator early in life, but one which shows variability because of fluctuations in overall arousal.

Although we could not be certain in this study what the target for each saccade actually was, the fact that the mean amplitudes and distributions of saccade amplitudes for a given stimulus were similar for infants and adults suggests that the two age groups had intended targets with similar eccentricities. We rarely observed the eye movement pattern described by Aslin and Salapatek (1975) and Salapatek *et al.* (1981) in *elicited* saccade experiments with infants, namely, a series of equal amplitude steps with long inter-saccadic intervals (500 msec or more). These data were interpreted by Aslin and colleagues as reflecting immaturities in the saccade-generating system. The "step" saccades in their elicited-saccade condition may reflect deficiencies in something other than the saccadic control system. One likely candidate is the system responsible for spatial localization of the target, which presents a signal specifying desired eye position to the saccade generator (e.g. Clark and Stark, 1974; Collins, 1975; Robinson, 1981; Young, 1981). Infants lack significant experience in spatial localization, and consequently may be less able to localize small targets accurately in the absence of landmarks and contours. Alternatively, the step saccades could be the result of an inattentive or drowsy state. Multiple saccades and corrective saccades, which are larger than normal, increase with fatigue and reductions in arousal (Bahill and Stark, 1975; Abel *et al.*, 1983).

In subsequent studies of infant saccadic properties, it will be important to choose a wide range of stimuli to explore these observations more fully. Elicited saccade experiments (which emulate the most typical design for studying adult saccade properties) can sometimes record a different type of saccadic behavior from young infants than "free-scanning" paradigms do. There also appear to be striking differences in "free-scanning" studies, depending on the particular stimuli used. Experiments which systematically manipulate physical parameters of stimuli which are equated for infant attention and those which study changes in main sequence properties as infant attention lags, such as in a habituation paradigm, would be helpful in understanding the unusual properties of the infant saccadic system.

Acknowledgements—The research reported here was supported by NIH Grants HD08706 and EY03957, and awards Nos 13484, 661078, and 662199 from the PSC-CUNY Research Award Program of CUNY. We gratefully acknowledge the assistance of Max Lilling M.D., David Kliot M.D. and Downstate Medical Center of SUNY for their help in recruiting parents of infants. We also thank the parents of our infant subjects for their interest and cooperation.

REFERENCES

Abel L. A., Traccis S., Troost B. T. and Dell'Osso L. F. (1983) Saccadic variability: contributions from fatigue, inattention, and amplitude. *Invest. Ophthal. visual Sci., Suppl.* **24**, 272.

Abramov I., Gordon J., Hendrickson A., Hainline L., Dobson V. and LaBossiere E. (1982) The retina of the newborn human infant. *Science* **217**, 265–267.

Aschoff J. C. (1968) Veränderungen rascher Blickbewegungen (saccaden) beim Menschen unter Diazapam (Valium). *Archs Phychiat. Nervenkr.* **211**, 325–332.

Aslin R. N. (1981) Development of smooth pursuit in human infants. In *Eye Movements: Cognition and Visual Perception* (Edited by Fisher D. F., Monty R. A. and Senders J. W.). Lawrence Erlbaum, Hillsdale, NJ.

Aslin R. N. and Salapatek P. (1975) Saccadic localization of visual targets by the very young human infant. *Percept. Psychophys.* **17**, 293–302.

Atkinson J. and Braddick O. (1981) Development of optokinetic nystagmus in infants: an indication of cortical binocularity? In *Eye Movements: Cognition and Visual Perception* (Edited by Fisher D. F., Monty R. A. and Senders J.). Lawrence Erlbaum, Hillsdale, NJ.

Bahill A. T. and Stark L. (1975) Overlapping saccades and glissades are produced by fatigue in the saccadic eye movement system. *Expl Neurol.* **48**, 95–106.

Bahill A. T., Clark M. R. and Stark L. (1975) The main sequence: a tool for studying human eye movements. *Math. Biosci.* **24**, 191–204.

Becker W. and Fuchs A. F. (1969) Further properties of the human saccadic system: eye movements and correction saccades with and without visual fixation points. *Vision Res.* **9**, 1247–1258.

Becker W. and Jurgens R. (1979) An analysis of the saccadic system by means of double step stimuli. *Vision Res.* **19**, 967–983.

Bienfang D. C. (1974) Opsoclonus in infancy. *Archs Ophthal.* **91**, 203–205.

Boghen D., Troost B. T., Daroff R. B., Dell'Osso L. F. and Birkett J. E. (1974) Velocity characteristics of normal human saccades. *Invest. Ophthal. visual Sci.* **13**, 619–623.

Bronson G. (1974) The postnatal growth of visual capacity. *Child Devl* **45**, 873–890.

Bronson G. (1982) *The Scanning Patterns of Human Infants: Implications for Visual Learning*. Ablex, Norwood, NJ.

Carpenter R. H. S. (1977) *Movements of the Eyes*. Pion, London.

Clark M. R. and Stark L. (1974) Control of human eye movements. I. Modeling of extraocular muscles: II. A model for the extraocular plant mechanism: III. Dynamic characteristics of the eye tracking mechanism. *Math. Biosci.* **20**, 191–265.

Collins C. C. (1975) The human oculomotor control system. In *Basic Mechanisms of Ocular Motility and Their Clinical Implications* (Edited by Lennerstrand G. and Bach-y-Rita P.). Pergamon Press, Oxford.

Crommelinck M. and Roucoux A. (1975) Characteristics of cat's eye saccades in different states of alertness. *Brain Res.* **103**, 574–578.

Dayton G. O. and Jones M. H. (1964) Analysis of the characteristics of the fixation reflex in infants by use of direct current electrooculography. *Neurology* **14**, 1152–1156.

Dell'Osso L. F. and Daroff R. B. (1981) Clinical disorders of ocular movement. In *Models of Oculomotor Control and Behavior* (Edited by Zuber B. L.). CRC Press, Boca Raton, FL.

Dell'Osso L. F., Troost B. T. and Daroff R. B. (1975) Macro square wave jerks. *Neurology* **25**, 975–979.

Dixon W. J. (editor) (1981) *BMDP Statistical Software 1981*. University of California Press, Los Angeles.

Ferguson G. A. (1971) *Statistical Analysis in Psychology and Education*. McGraw-Hill, New York.

Gibson J. J. (1950) *The Perception of the Visual World*. Houghton Mifflin, Boston MA.

Hainline L. (1981) An automated eye movement system for use with human infants. *Behav. Res. Meth. Instr.* **13**, 20–24.

Hainline L. and Lemerise E. (1982) Infants' scanning of geometric forms varying in size. *J. exp. Child Psychol.* **33**, 235–256.

Hainline L., Lemerise E., Abramov I. and Turkel J. (1984) Orientational asymmetries in small-field optokinetic nystagmus in human infants. *Behav. Brain Res.* In press.

Haith M. M. (1980) *Rules That Babies Look By: the Organization of Newborn Visual Activity*. Lawrence Erlbaum, Hillsdale, NJ.

Hamann K. (1979) Verlangsamte Sakkaden bei verschiedenen neurologischen Erkrankungen. *Ophthalmologica, Basel* **178**, 357–364.

Harris C. M., Abramov I. and Hainline L. (1984) Instrument considerations in measuring fast eye movements. *Behav. Res. Meth. Instr. Comp.* In press.

Harris C. M., Hainline L. and Abramov I. (1981) A method for calibrating an eye-monitoring system for use with human infants. *Behav. Res. Meth. Instr.* **13**, 11–20.

Hollyfield J. G., Frederick J. M. and Rayborn M. E. (1983) Neurotransmitter properties of the newborn human retina. *Invest. Ophthal. visual Sci.* **24**, 893–897.

Howard I. P. (1982) *Human Visual Orientation*. Wiley, New York.

Hoyt C. S. (1977) Neonatal opsoclonus. *J. Pediat. Ophthal.* **14**, 274–277.

Hoyt C. S., Mousel D. K. and Weber A. A. (1980) Transient supranuclear disturbances of gaze in healthy neonates. *Am. J. Ophthal.* **89**, 708–713.

Karmel B. Z. (1969) The effect of age, complexity, and amount of contour on pattern preferences in human infants. *J. exp. Child Psychol.* **7**, 339–354.

Kessen W., Salapatek P. and Haith M. M. (1972) The visual response of the human infant to linear contour. *J. exp. Child Psychol.* **13**, 9–20.

Larsen J. S. (1971) The sagittal growth of the eye I. Ultrasonic measurement of the depth of the anterior chamber from birth to puberty. *Acta ophthal.* **49**, 239–262.

Mandell R. B. (1976) Corneal curvature of the human infant. *Archs Ophthal.* **77**, 345–348.

Mann I. (1964) *The Development of the Human Eye*. Br. Med. Assoc., London.

Naegele J. R. and Held R. (1982) The postnatal development of monocular optokinetic nystagmus in infants. *Vision Res.* **22**, 341–346.

Peiper A. (1963) *Cerebral Function in Infancy and Childhood*. Consultant's Bureau, New York.

Robinson D. A. (1964) The mechanics of human saccadic eye movements. *J. Physiol., Lond.* **174**, 245–264.

Robinson D. A. (1981) The use of control systems analysis in the neurophysiology of eye movements. *Ann. Rev. Neurosci.* **4**, 464–503.

Ron S., Robinson D. A. and Skavenski A. A. (1972) Saccades and the quick phase of nystagmus. *Vision Res.*, **12**, 2015–2022. **66**, 247–258.

Salapatek P. (1975) Pattern perception in early infancy. In *Infant Perception: From Sensation to Cognition* (Edited by Cohen L. B. and Salapatek P.). Vol I. Academic Press, New York.

Salapatek P., Aslin R. N., Simonson J. and Pulos E. (1980) Infant saccadic eye movements to visible and previously visible targets. *Child Devl.* **51**, 1090–1094.

Stark L. (1983) Normal and abnormal vergence. In *Vergence Eye Movements: Basic and Clinical Aspects* (Edited by Schor C. M. and Ciuffreda K. J.). Butterworth, Boston MA.

Stark L., Hoyt W., Ciuffreda K., Kenyon R. and Hsu F. (1981) Time optimal saccadic trajectory model and voluntary nystagmus. In *Models of Oculomotor Behavior and Control* (Edited by Zuber B. L.). CRC Press, Boca Raton, FL.

Vaughan J. (1983) Saccadic reaction time in visual search.

In *Eye Movements in Reading* (Edited by Rayner K.), pp. 397–411. Academic Press, New York.
Westheimer G. (1954) Mechanisms of saccadic eye movements. *A.M.A. Archs. Ophthal.* **52**, 710–724.
Yarbus A. L. (1967) *Eye Movements in Vision*. Plenum Press, New York.
Young L. R. (1981) The sampled data model and foveal dead zone for saccades. In *Models of Oculomotor Behavior and Control* (Edited by Zuber B. L.). CRC Press, Boca Raton, FL.
Young L. R. and Sheena D. (1975) Eye-movement measurement technique. *Am. Psychol.* **30**, 315–330.
Zee D. S., Optican L. M., Cook J. D., Robinson D. A. and Engel W. K. (1976) Slow saccades in spinocerebellar degeneration. *Archs. Neurol.* **33**, 243–251.
Zee D. S. and Robinson D. A. (1979) A hypothetical explanation of saccadic oscillations. *Ann. Neurol.* **5**, 405–414.

REFERENCES

Abel, L.A., Traccis, S., Troost, B.T., & Dell'Osso, L.F. (1983). Saccadic variability: contributions from fatigue, inattention and amplitude. *Investigative Ophthalmology & Visual Science* (Supplement), *24*, 272.

Abramov, I., & Gordon, J. (1977). Color vision in the peripheral retina. I. Spectral sensitivity. *Journal of the Optical Society of America, 67*, 195-202.

Abramov, I., Gordon, J., Hendrickson, A., Hainline, L., Dobson, V. & LaBossiere, E. (1982). The retina of the newborn infant. *Science, 217*, 265-267.

Alpern, M. (1962). Eye movements and accommodation. In H. Davson (Ed.) *Muscular mechanisms* (Vol. 3) of *The eye*. New York: Academic Press, 3-5.

Ankrum, C., Clavadetscher, J.E., & Teller, D.Y. (1986). Chromatic discriminations and brightness matches in infants. *Investigative Ophthalmology & Visual Science* (Supplement), *27*, 264.

Aschoff, J.C. (1968). Veranderungen rascher Blickbewegungen (saccaden) beim Menschen unter Diazapam (Valium). *Archiv fur Psychiatrie und Nervenkrankenhelten, 211*, 325-332.

Aslin, R.N. (1985). Oculomotor measures of visual development. In G. Gottlieb & N.A. Krasnegor (Eds.) *Measurement of audition and vision in the first year of life: A methodological overview.* Norwood, New Jersey: Ablex, 391-417.

Atkinson, J., Braddick, O., & Moar, K. (1977a). Contrast sensitivity of the human infant for moving and static patterns. *Vision Research, 17*, 1045-1047.

Atkinson, J., Braddick, O., & Moar, K. (1977b) Development of contrast sensitivity over the first 3 months of life in the human infant. *Vision Research, 17*, 1037-1044.

Bach, L., & Seefelder, R. (1914). *Atlas zur Entwicklungsgeschichte des menschlichen Auges.* Leipzig: Engelmann.

Bahill, A.T., Adler, D., & Stark, L. (1975). Most naturally occurring human saccades have magnitudes of 15 degrees or less. *Investigative Ophthalmology & Visual Science, 14*, 468-469.

Bahill, A.T., & Stark L. (1975). Overlapping saccades and glissades are produced by fatigue in the saccadic eye movement system.

Experimental Neurology, 48, 95-106.

Bahill, A.T., Clark, M.R., & Stark L. (1975). The main sequence: a tool for studying human eye movements. *Mathematical Biosciences, 24,* 191-204.

Banks, M.S., & Salapatek, P. (1981). Infant pattern vision: A new approach based on the contrast sensitivity function. *Journal of Experimental Child Psychology, 31,* 1-45.

Banks, M.S., Stephens, B.R., & Dannemiller, J.L. (1982). A failure to observe negative preference in infant acuity testing. *Vision Research, 22,* 1025-1031.

Batschelet, E. (1981). *Circular statistics in biology.* New York: Academic Press.

Becker, W. (1972). The control of eye movements in the saccadic system. *Bibliotheca Ophthalmologica, 82,* 233-243.

Becker, W., & Fuchs, A.F. (1969). Further properties of the human saccadic system: eye movements and correction saccades with and without fixation points. *Vision Research, 9,* 1247-1258.

Becker, W., & Jurgens, R. (1979). An analysis of the saccadic system by means of double step stimuli. *Vision Research, 19,* 967-983.

Boch, R., & Fischer, B. (1983). Saccade reaction times and activation of the prelunate cortex: parallel observations in trained rhesus monkeys. *Experimental Brain Research, 50,* 201-210.

Boch, R., Fischer, B., & Ramsperger, E. (1984). Express saccades of the monkey: reaction times versus intensity, size, duration, and eccentricity of their targets. *Experimental Brain Research, 55,* 223-231.

Boghen, D., Troost, B.T., Daroff, R.B., Dell'Osso, L.F., & Birkett, J.E. (1974). Velocity characteristics of normal human saccades. *Investigative Ophthalmology & Visual Science, 13,* 619-623.

Bronson, G. (1982). *The scanning patterns of human infants: implications for visual learning.* Norwood, New Jersey: Ablex.

Brown, J.L. (1965). Flicker and intermittent stimulation. In C.H. Graham (Ed.) *Vision and visual perception.* New York: Wiley, 251-320.

Bullinger, A., & Kaufmann, J.L. (1977). Technique d'enregistrement et d'analyse des mouvements oculaires. *Perception, 6,* 345-353.

Carmody, D.P., Kundel, H.L., & Nodine, C.F. (1980). Performance of a computer system for recording eye fixations using limbus reflection. *Behavior Research Methods & Instrumentation, 12,* 63-66.

Ciuffreda, K.J., Kenyon, R.V., & Stark, L. (1979). Abnormal saccadic substitution during small-amplitude pursuit tracking in amblyopic eyes. *Investigative Ophthalmology & Visual Science, 18,* 506-516.

Cohen, A.S. (1977). Is the duration of an eye fixation a sufficient criterion referring to information input? *Perceptual and Motor Skills, 45,* 766.

Coles, P., & Sigman, M. (1986). Infant saccadic eye movements during habituation to a geometric pattern. In J.K. O'Regan & A. Levy-Schoen (Eds.), *Eye Movements: From Physiology to Cognition.* Amsterdam: North-Holland (Elsevier).

Cox, D.R. & Oakes, D. (1984). *Analysis of survival data.* New York: Chapman & Hall.

Crommelinck, M., & Roucoux, A. (1976). Characteristics of cat's eye saccades in different states of alertness. *Brain Research, 103,* 574-578.

Cummings, M., Mayer, D.L., Hansen, R.M., & Fulton, A.B. (1986). An LED perimetric method to study peripheral vision of infants and children. *Infant Behavior & Development* (special ICIS issue), *9,* 91.

de Bie, J., & van den Brink, G. (1984). Small stimulus movements are necessary for the study of fixational eye movements. In A.G. Gale & F. Johnson (Eds.), *Theoretical and applied aspects of eye movement research.* Amsterdam: North-Holland (Elsevier), 63-70.

Dobson, V., Schwartz, T.L., & Sandstrom, D.J. (1986). The development of peripheral vision: new methods and initial findings. *Infant Behavior & Development* (special ICIS issue), *9,* 102.

Dobson, D., & Teller, D.Y. (1978). Assessment of visual acuity in infants. In J.C. Armington, J. Krauskopf, & B.R. Wooten (Eds.), *Visual psychophysics and physiology.* New York: Academic Press, 385-396.

Dodge, R., & Benedict, G.G. (1915). *Psychological effects of alcohol.* Washington, DC: Carnegie Institution of Washington.

Ellis S.R. and Smith J.D. (1985). Patterns of statistical dependency in visual scanning. In R. Groner, G.W. McConkie & C. Menz (Eds.), *Eye movements and human information processing.*

Amsterdam: North-Holland (Elsevier), 221-238.

Enoch J.M. (1959). Effect of the size of a complex display upon visual search. *Journal of the Optical Society of America, 49,* 280-286.

Feller, W. (1968). *An introduction to probability theory and its applications (3rd ed.).* New York: Wiley.

Findlay, J.M. (1980). The visual stimulus for saccadic eye movements in human observers. *Perception, 9,* 7-21.

Fischer, B., & Boch, R. (1983). Saccadic eye movements after extremely short reaction times in the monkey. *Brain Research, 260,* 21-26.

Fischer, B., & Boch, R. (1984). Express saccades of the monkey: A new type of visually guided rapid eye movement after extremely short reaction times. In A.G. Gale & F. Johnson (Eds.), *Theoretical and applied aspects of eye movement research.* Amsterdam: North-Holland (Elsevier), 403-408.

Fisher, D.F., Monty, R.A., & Senders, J.W. (Eds.) (1981). *Eye movements: Cognition and Visual Perception.* Hillsdale, New Jersey: Erlbaum.

Flom, M.C., Kirschen, D.G., & Bedell, H.E. (1980). Control of unsteady, eccentric fixation in amblyopic eyes by auditory feedback of eye position. *Investigative Ophthalmology & Visual Science, 19,* 1371-1381.

Ford, A., White, C.T., & Lichtenstein, M. (1959). Analysis of eye movements during free search. *Journal of the Optical Society of America, 49,* 287-292.

Fuchs, A.F. (1967). Saccadic and smooth pursuit eye movements in the monkey. *Journal of Physiology, London, 191,* 609-631.

Fuchs, A.F., & Binder, M.D. (1983). Fatigue resistance of human extraocular muscles. *Journal of Neurophysiology, 49,* 28-34.

Fuchs, A.F., & Luschei, E.S. (1970). Firing patterns of abducens neurons of alert monkeys in relationship to horizontal eye movements. *Journal of Neurophysiology, 33,* 382-392.

Gayl, I.E., Roberts, J.O., & Werner, J.S. (1983). Linear systems analysis of infant visual pattern preferences. *Journal of Experimental Child Psychology, 35,* 30-45.

Gibson, J.J. (1950). *The perception of the visual world.* Boston: Houghton Mifflin.

Groner, R., Menz, C., Fisher, D.F., & Monty, R.A. (Eds.) (1983). *Eye movements and psychological functions: International views.* Hillsdale, New Jersey: Erlbaum.

Hainline, L., & Lemerise, E. (1982). Infants' scanning of geometric forms varying in size. *Journal of Experimental Child Psychology, 33,* 235-256.

Hainline, L., & Lemerise, E. (1985). Corneal reflection eye-movement recording as a measure of infant pattern perception: What do we really know? *British Journal of Developmental Psychology, 3,* 229-242.

Hainline, L., Turkel, J., Abramov, I., Lemerise, E., & Harris, C.M. (1984). Characteristics of saccades in human infants. *Vision Research, 24,* 1771-1780.

Haith, M.M. (1969). Infrared television recording and measurement of ocular behavior in the human infant. *American Psychologist, 24,* 279-282.

Haith, M.M. (1980). *Rules that babies look by: the organization of newborn visual activity.* Hillsadale, New Jersey: Erlbaum.

Hallett, P.E. (1978). Primary and secondary saccades to goals defined by instructions. *Vision Research, 18,* 1279-1296.

Hallett, P.E., & Adams, B.D. (1980). The predictability of saccadic latency in a novel voluntary oculomotor task. *Vision Research, 20,* 329-339.

Harris, C.M., Hainline, L., & Abramov I. (1981). A method for calibrating an eye-monitoring system for use with human infants. *Behavior Research Methods and Instrumentation, 13,* 11-20.

Harris, P., & MacFarlane, A. (1974). The growth of the effective visual field from birth to seven weeks. *Journal of Experimental Child Psychology, 13* 340-348.

Hebb, D.O. (1949). *The organization of behavior.* New York: Wiley.

Held, R., Gwiazda, S.B., Mohindra, I., & Wolfe, J. (1979). Infant visual acuity is underestimated because near threshold gratings are not preferentially fixated. *Vision Research, 19,* 1377-1379.

Hendrickson, A.E., & Yuodelis, C. (1984). The morphological development of the human fovea. *Ophthalmology, 91,* 603-612.

Henson, D.B. (1979). Investigation into corrective saccadic eye movements for refixation amplitudes of 10 degrees and below. *Vision Research, 19,* 57-61.

Hollyfield, J.G., Frederick, J.M., & Rayborn, M.E. (1983). Neurotransmitter properties in the newborn human retina. *Investigative Ophthalmology & Visual Science, 24,* 893-897.

Hubel, D.H., & Wiesel, T.N. (1968). Receptive fields and functional architecture of monkey striate cortex. *Journal of Physiology, 195,* 215-243.

Jacobs, R.J. (1979). Visual resolution and contour interaction in the fovea and periphery. *Vision Research, 19,* 1187-1195.

Jones, L.A., & Higgins, G.C. (1947). Photographic granularity and graininess. *Journal of the Optical Society of America, 37,* 217-262.

Karmel, B.Z., & Maisel, E.G. (1975). A neuronal activity model for infant visual attention. In L.B. Cohen & P. Salapatek (Eds.), *Infant perception: From sensation to cognition, Part 1. Basic visual processes* (Vol. 1). New York: Academic Press, 78-131.

Karsh, R., & Breitenbach, F.W. (1983). Looking at looking: The amorphous fixation measure. In R. Groner, C. Menz, D.F. Fisher & R.A. Monty (Eds.), *Eye movements and psychological functions: International views.* Hillsdale, New Jersey: Erlbaum, 53-64.

Keller, E. (1977). Control of saccadic eye movements by midline brain stem neurons. In R. Baker & A. Berthoz (Eds.) *Control of gaze by brain stem neurons.* New York: North-Holland (Elsevier), 327-336.

Kelly, D.H. (1979). Motion and vision. 1. Stabilised images of stationary gratings. *Journal of the Optical Society of America, 69,* 1340-1349.

Kelly, D.H. (1985). Visual processing of moving stimuli. *Journal of the Optical Society of America A, 2,* 216-225.

Kendall, Sir M., & Stuart, A. (1977). *The advanced theory of statistics* (Vol. 1, 4th ed.). New York: Macmillan.

Kendall, Sir M., & Stuart, A. (1979). *The advanced theory of statistics* (Vol. 2, 4th ed.). New York: Macmillan.

Kliegl, R., & Olson, R.K. (1981). Reduction and calibration of eye monitor data. *Behavior Research Methods & Instrumentation, 13,* 107-111.

Kowler, E., & Steinman, R.M. (1979). The effect of expectations on slow oculomotor control - 1. Periodic steps. *Vision Research, 19,* 619-632.

Ladenheim, B., & Gordon, J. (1986). Heterochromatic flicker photometry in neonates. *Investigative Ophthalmology & Visual Science* (Supplement), *27*, 76.

Lewis, T.L., & Maurer, D. (1980). Central vision in the newborn. *Journal of Experimental Child Psychology, 29*, 475-480.

Luschei, E.S., & Fuchs, A.F. (1972). Activity of brain stem neurons during eye movements of alert monkeys. *Journal of Neurophysiology, 35*, 445-461.

Macfarlane, A., Harris, P., & Barnes, I. (1976). Central and peripheral vision in early infancy. *Journal of Experimental Child Psychology, 21*, 532-538.

Mandell, R.B. (1967). Corneal curvature of the human infant. *Archives In Ophthalmology, 77*, 345-348.

Mandell, R.B., & York, M.A. (1969). A new calibration system for photokeratoscopy. *American Journal of Optometry, 46*, 410-417.

Mann, I. (1964). *The development of the human eye.* London: British Medical Association.

Maurer, D. (1983). The scanning of compound figures by young infants. *Journal of Experimental Child Psychology, 35*, 437-448.

McConkie, G.W., Zola, D., & Wolverton, G.S. (1985). Estimating frequency and size effects due to experimental manipulations in eye movement research. In R. Groner, G.W. McConkie & C. Menz (Eds.), *Eye movements and human information processing.* Amsterdam: North-Holland (Elsevier), 137-147.

Mendelson, M.J., Haith, M.M., & Goldman-Rakic, P.S. (1981). Monitoring visual activity in infant rhesus monkeys: Method and calibration. *Behavior Research Methods & Instrumentation, 13*, 709-712.

Miles, W.R. (1924). *Alcohol and human efficiency.* Washington, DC: Carnegie Institution of Washington.

Millodot, M. (1982). Image formation in the eye. In H.B. Barlow & J.D. Mollon (Eds.), *The senses.* Cambridge: Cambridge University Press, 46-61.

Millodot, M., Johnson, C.A., Lamont, A., & Leibowitz, H.W. (1975). Effect of dioptrics on peripheral visual acuity. *Vision Research, 15*, 1357-1362.

Nelson, K., & Kessen, W. (1969). Visual scanning by human newborns: Responses to complete triangle, to sides only, and to corners only. *Proceedings of the 77th Annual Convention of the*

American Psychological Association, 4, 273-274.

Norcia, A.M., Tyler, C.W., & Allen, D. (1986). Electrophysiological assessment of contrast sensitivity in human infants. *American Journal of Optometry & Physiological Optics, 63.*

Noton, D., & Stark, L. (1971). Scanpaths in saccadic eye movements while viewing and recognizing patterns. *Vision Research, 11,* 929-941.

Papoulis, A. (1965). *Probability, random variables, and stochastic processes.* New York: McGraw-Hill.

Peiper, A. (1963). *Cerebral function in infancy and childhood.* New York: Consultant's Bureau.

Perry, V.H., & Cowey, A. (1985). The ganglion cell and cone distributions in the monkey's retina: Implications for central magnification factors. *Vision Research, 25,* 1795-1810.

Rayner, K. (Ed.) (1983). *Eye movements in reading.* New York: Academic Press.

Rayner, K., Inhoff, A.W., Morrison, R.E., Slowiaczek, M.L., & Bertera, J.H. (1981). Masking of foveal and parafoveal vision during eye fixations in reading. *Human Perception and Performance, 7,* 167-179.

Rayner, K., & McConkie, G.W. (1976). What guides a reader's eye movements? *Vision Research, 16,* 829-838.

Robinson, D.A. (1981). Control of eye movements. In V.B. Brooks (Ed.) *Handbook of Physiology,* Section 1, The nervous system, (Vol. 2). Baltimore, Maryland: Williams & Wilkins, 1275-1320.

Ron, S., Robinson, D.A., & Skavenski, A.A. (1972). Saccades and the quick phase of nystagmus. *Vision Research,* 66, *247-258.*

Salapatek, P. (1968). Visual scanning of geometric figures by the human newborn. *Journal of Comparative and Physiological Psychology, 66,* 247-258.

Salapatek, P. (1969). The visual investigation of geometric patterns by the one- and two-month-old infant. Paper presented at Meeting of the American Association for the Advancement of Science, Boston.

Salapatek, P. (1975). Pattern perception in early infancy. In L.B. Cohen & P. Salapatek (Eds.), *Infant perception from sensation to cognition,* (Vol. 1). New York: Academic Press, 133-248.

Salapatek, P., & Kessen, W. (1966). Visual scanning of triangles by

the human newborn. *Journal of Experimental Child Psychology, 3,* 155-167.

Saslow, M.G. (1967). Effects of components of displacement-step stimuli upon latency for saccadic eye movement. *Journal of the Optical Society of America, 57,* 1024-1029.

Schmidt, D., Abel, L.A., Dell'Osso, L.F., & Daroff, R.B. (1979). Saccadic velocity characteristics: intrinsic variability and fatigue. *Aviation, Space, and Environmental Medicine, 50,* 393-395.

Schoonard, J.W., Gould, J.D., & Miller, L.A. (1973). Studies of visual inspection. *Ergonomics, 16,* 365-379.

Senders, J.W., Fisher, D.F., & Monty, R.A. (Eds.) (1978). *Eye movements and the higher psychological functions.* Hillsdale, New Jersey: Erlbaum.

Siegel, S. (1956). *Non-parametric statistics.* New York: McGraw-Hill.

Skavenski, A.A., & Steinman, R.M. (1970). Control of eye position in the dark. *Vision Research, 10,* 193-204.

Skavenski, A.A., Hansen, R.M., Steinman, R.M., & Winterson, B.J. (1979). Quality of retinal image stabilization during small natural and artificial body rotations in man. *Vision Research, 19,* 675-683.

Slater, A.M., & Findlay, J.M. (1972). The measurement of fixation position in the newborn baby. *Journal of Experimental Child Psychology, 14,* 349-366.

Slater, A.M., & Findlay, J.M. (1975). The corneal reflection technique and the visual preference method: Sources of error. *Journal of Experimental Child Psychology, 20,* 240-247.

Stark, L., & Ellis, S.R. (1981). Scanpaths revisited: cognitive models direct active looking. In D.F. Fisher, R.A. Monty & J.W. Senders (Eds.), *Eye movements: Cognition and visual perception.* Hillsdale, New Jersey: Erlbaum, 193-226.

St. Cyr, G.J., & Fender, D.H. (1969). The interplay of drifts and flicks in binocular fixation. *Vision Research, 9,* 245-266.

Steinman, R.M. (1965). Effect of target size, luminance and color on monocular fixation. *Journal of the Optical Society of America, 55,* 1158-1165.

Teller, D.Y., Mayer, D.L., Makous, W.L., & Allen, J.L. (1982). Do preferential looking techniques underestimate infant visual acuity? *Vision Research, 22,* 1017-1024.

Trivedi, K.S. (1982). *Probability & statistics with reliability, queuing, and computer science applications.* Englewood Cliffs, New Jersey: Prentice-Hall.

van Hof-van Duin, J., & Mohn, G. (1986). Visual field development in fullterm and preterm infants. *Infant Behavior & Development* (special ICIS issue), *9*, 387.

Wallman J., & Pettigrew J.D. (1985). Conjugate and disjunctive saccades in two avian species with contrasting oculomotor strategies. *Journal of Neuroscience, 5,* 1418-1428.

Westheimer, G. (1954). Mechanisms of saccadic eye movements. *Archives of Ophthalmology, 52,* 710-724.

Wheeless, L.L., Boynton, R.M. and Cohen, G.H. (1966). Eye movement responses to step and pulse-step stimuli. *Journal of the Optical Society of America, 56,* 956-990.

Wolff, P.H. (1966). The causes, controls and organization of behavior in the neonate. *Psychological Issues, 5,* (Whole No. 17).

Woodhouse, J.M., & Barlow, H.B. (1982). Spatial and temporal resolution and analysis. In H.B. Barlow & J.D. Mollon (Eds.), *The senses.* Cambridge: Cambridge University Press, 133-164.

Yarbus, A.L. (1967). *Eye movements in vision.* New York: Plenum.

Young, L.R. (1981). The sampled data model and foveal dead zone for saccades. In B.L. Zuber (Ed.) *Models of oculomotor behavior and control.* Boca Raton, Florida: CRC Press.

Young, L.R., & Sheena, D. (1975). Survey of eye movement recording methods. *Behavior Research Methods & Instrumentation, 1,* 397-421.

Zee, D.S., & Robinson, D.A. (1979). A hypothetical explanation of saccadic oscillations. *Annals of Neurology, 5,* 405-414.